2021

Histologic and molecular characterization of root phellem development and suberization – from *Arabidopsis thaliana* to *Quercus suber*

Ana Rita Mendes Leal

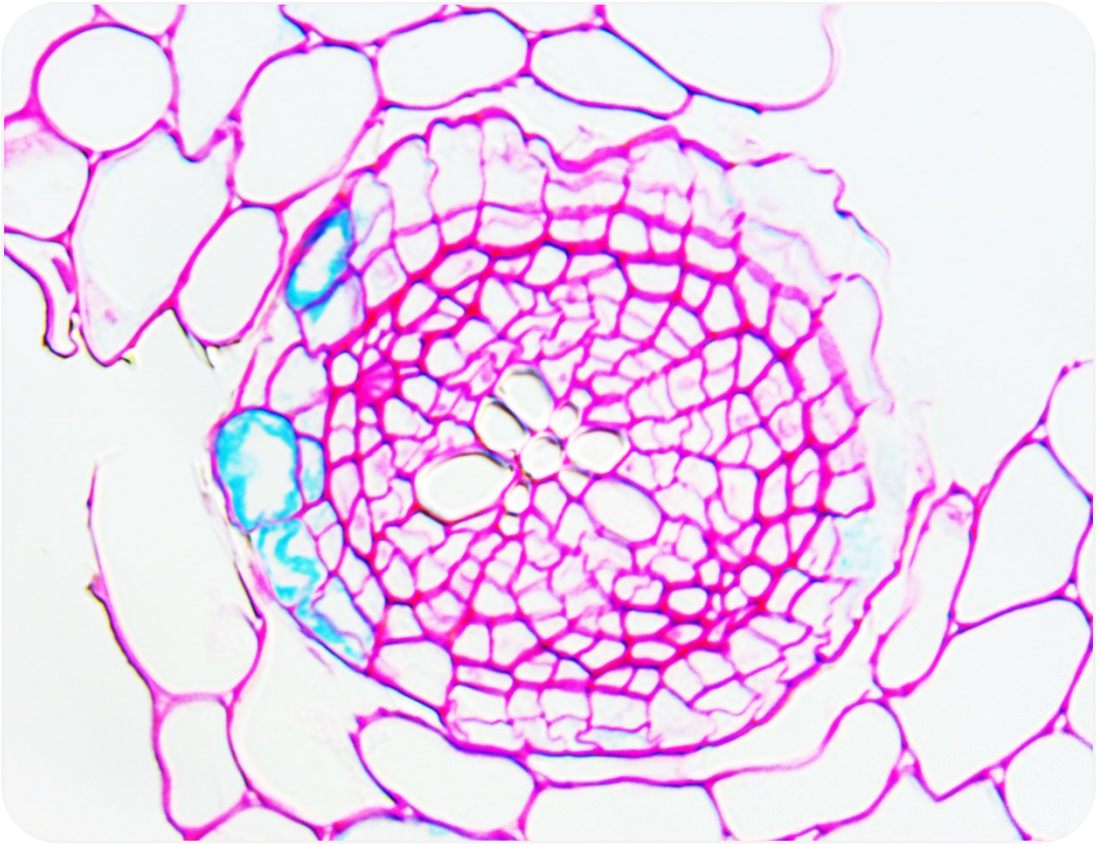

Dissertation presented to obtain the **Ph.D degree in Plant Biology**

PhD Program *Plants for Life*

Oeiras, November 2021

INSTITUTO DE TECNOLOGIA QUÍMICA E BIOLÓGICA ANTÓNIO XAVIER | UNIVERSIDADE NOVA DE LISBOA

Histologic and molecular characterization of root phellem development and suberization – from *Arabidopsis thaliana* to *Quercus suber*

Ana Rita Mendes Leal

Thesis submitted as partial fulfilment of the requirements for the degree of Doctor (Ph.D) in Plant Biology (by the Universidade Nova de Lisboa) and in Biochemistry and Biotechnology (by the University of Gent)

Oeiras, November 2021

PhD Plants for Life

itqb nova

GHENT UNIVERSITY

VIB-UGENT CENTER FOR PLANT SYSTEMS BIOLOGY

This work was performed at:

Plant Functional Genomics Laboratory

Genomic of Plant Stress Unit

Instituto de Tecnologia Química e Biológica António Xavier – Universidade Nova de Lisboa

Av. da República, Quinta do Marquês, 2780-157 Oeiras

Portugal

Root Development Laboratory

Gent University, Department of Plant Biotechnology and Bioinformatics & VIB Center for Plant Systems Biology, Technologiepark 71, 9052 Ghent, Belgium

Supervisors:

Prof. Dr. M. Margarida Oliveira - Plant Functional Genomics Laboratory

Prof. Dr. Tom Beeckman - Root Development Laboratory

This work has been financially supported by “Fundação para a Ciência e a Tecnologia” through PhD fellowship PD/BD/113472/2015 awarded to Ana Rita Leal, by the R&D Unit GREEN-IT Bioresources for Sustainability (UID/Multi/04551/2013, UID/Multi/04551/2019 and UIDB/Multi/04551/2020) and by the research project PTDC/BIA-FBT/29704/2017 “*SuberInStress - Cork formation and suberin deposition: the role of water and heat stress*”, funded by FCT/MCTES, and co-financed by FEDER in the scope of POR Lisboa 2020.

À minha família,

"Quando vier a Primavera, se eu já estiver morto,

As flores florirão da mesma maneira

E as árvores não serão menos verdes que na primavera passada.

A realidade não precisa de mim"

Alberto Caeiro

Acknowledgments

In the end of this journey, I should here thank to the kind people that, in a way or other, contributed to the development of this work:

- To Prof. Dr. Margarida, for the scientific support and for believing in my capacities to develop this work. Thanks for the guidance and nice discussions. It was always nice to feel your enthusiasm about new results!

- Prof. Dr. Tom, for introducing me to the beautiful *hidden half* of plants! Thanks for the guidance and inputs to this project. Thanks for opening the doors of your lab for me.

- To the members of my thesis committee, Dr. Jörg Becker and Dr. Cristina Silva Pereira, for the pleasant discussions and inputs to the development of this work

- To Dr. Pedro, *my* post-doc! Thanks for introducing me to the magnificent cork oak! Thanks for your patience, dedication and friendship. For the knowledge you shared with me in the preparation, execution and discussion of the experiences. For the countless corrections and improvements to this thesis. For the example of perfectionism. I owe you the development of this work!

-To Dr. Helena, for your friendship and your work. For the reassuring words, for your dedication to this cause! For the serenity with which you face the difficulties, the joy and love you put in what you do!

- To Dr. Boris, thanks for your time, support, and inputs on this work. Thanks for the help, friendship and music on the endless days sectioning and dissecting roots!

-To Joana Belo, for the help in the performance and development of cork oak and *Arabidopsis* stress assays.

- To Mafalda, Nuno, Margarida, *Sisi*, and Inês, for the daily joy at work and for the support in the not so good days.

-To André, Diego, Alicja, Natacha and Joana R., for being always there and prepared to help.

-To Rita, my dear *Rotinha*! Thanks for your friendship and support. It was a pleasure to share *cerejas*, secrets, travels and housing with you!

- To Isabel, Tiago, Nelson and Ana Paula, for the discussions and inputs to the development of this work. Thanks for the daily effort to provide us with conditions to do our science!

- To all former and present members of GPlantS.

- To Wouter, Hans, Wilson, Alaeddine, Pierre-Mathieu, Maria and Davy, for all the daily lab support and guidance.

-To Stefania, Joris and Fabian, for the amazing friendship and support during my time in Gent (and after). Thanks for all the lab guidance and sampling support! Thanks for amazing lunch talks! Thanks also to Titi, for the nights out! You all made Belgium weather more loveable! I miss you!

-To Nick and Brecht, for the kind welcome to their house! Thanks for your daily support and friendship. Best Belgium flat mates ever!

- All members of Roots and Vascular development labs, that were always supportive and ready to help me.

- À Barão de Vilar, ao Sr. Fernando, Eng. Álvaro, Dr. Rui e particularmente à Margarida, Magda e Fonseca, que nos últimos meses me introduziram e ensinaram muito acerca da bonita indústria dos Vinhos do Porto. A minha permanência e aprendizagem na Barão de Vilar aligeirou a caminhada final desta tese.

- As minhas pequenas morsas/os: a Adelaide e o *Aníbal*, a *Anita*, a *Dani* e Carlos, a *Calloira*, o *Curtinho*, a *Mini* e ao André, ao Dinis e a Nádia! Sois o meu suporte mental, a minha alegria, a família do coração! Tenho muitas saudades!

- À minha irmã, pelo seu amor incondicional. Mesmo distante está sempre no meu coração e pensamento. Por ser um modelo para mim neste mundo maravilhoso da investigação!

- À minha Avó, obrigada por cultivares em mim a simplicidade da vida, o gosto pelas plantas e tudo o que elas nos podem oferecer!

- Aos meus Pais, que de cedo me ensinaram os valores com que hoje guio a minha vida. Por todo amor e suporte incondicional. Obrigada por me darem o privilégio da educação, e pelos sacrifícios que isso implicou. São o meu modelo!

- Ao Bruno, por todo o amor e suporte! Estamos juntos a tanto tempo quanto a duração deste trabalho, e passamos por muitos altos e baixos. Mudamos de cidade, de país, moramos longe e perto, casamos e compramos a nossa casa! Tem sido um desafio encontrar o balanço entre trabalho, a escrita da tese e tempo para nós, e por isso agradeço a tua paciência e amor. Obrigada pela perseverança que me transmitiste ao longo deste trabalho, por acreditares nas minhas capacidades. A ti devo a sanidade mental que restou!

Abbreviation list

ABA	abscisic acid
ABC	ATP-binding cassette
ARK	ARBORKNOX
ATR-FTIR	attenuated total reflection Fourier transform infrared
cDNA	complementary DNA
CDS	coding sequence
CTAB	Cetyl trimethylammonium bromide
CYP	cytochrome P450
DAG	days after germination
DAS	days after sowing
DEG	differentially expressed genes
DNA	deoxyribonucleic acid
EDTA	Ethylenediamine tetraacetic acid
Em	emission
EtOH	Ethanol
Ex	excitation
FA	fatty acids
FAE	fatty acid elongase
FAR	fatty acyl reductases
FC	fold change
FY	Fluorol yellow
GO	gene ontology
GPAT	glycerol 3-phosphate acyl transferases
GUS	β-Glucuronidase
JA	jasmonic acid
LACS	long-chain acyl-CoA synthetase
LBD	LOB domain
LCFA	long chain fatty acids
LiCL	Lithium chloride
LR	lateral root
LTP	lipid transfer proteins
mRNA	messenger Ribonucleic Acid

MS	Murashige and Skoog
NaCl	Sodium cloride
NaOAc	Sodium acetate
padj	adjusted p-value
PCA	principal component analysis
PCR	polymerase chain reaction
PD	primary development
PEG	polyethylene glycol
PI	propidium iodide
PVP40	Polyvinylpyrrolidone average molecular weight 40,000
qPCR	quantitative polymerase chain reaction
RAX	Regulator of Axillary Meristems
RNA	ribonucleic acid
SA	salicylic acid
SD	secondary development
TBO	Toluidine Blue O
TF	transcription factor
TRAP-SEQ	translating ribosome affinity purification followed by mRNA sequencing
TRIS-HCl	Tris (hydroxymethyl) aminomethane hydrochloride
v	volume
VLCFA	very long chain fatty acids
w	weight
WT	wild type

Summary

During periderm differentiation, phellem cells undergo secondary cell wall thickening by suberin deposition, forming a compact barrier shielding plant organs from the environment. Development and suberization of phellem cells are tightly controlled processes, however their regulation is still poorly known. To better understand root phellem ontogeny in *Arabidopsis* and cork oak we conducted targeted histological and transcriptomic analysis. We found that phellogen activity initiates one-week after sowing in both species. A transcriptomic analysis targeting *Arabidopsis* phellem cells at the onset of suberization further revealed that the phellem transcriptome was organized in three main domains related to energy production, synthesis and transport of cell wall components, and response to stimulus. As for cork oak, a comparative transcriptomic analysis targeting the root zones undergoing primary *versus* secondary development, revealed distinct transcriptomes, with an enrichment in transcripts related to cell-wall modifications in the latter. Novel players in phellem differentiation, related to suberin monomer transport and assembly, as well as novel transcription regulators could be identified in both *Arabidopsis* and cork oak. Furthermore, we found that the application of combined heat and osmotic stress at the onset of phellem development differently influence the root suberization patterns. In *Arabidopsis*, the younger tap root zone was not affected, while the young lateral roots show ectopic suberization after the imposed combined stress. In cork oak, a positive effect of osmotic stress (over mock, heat, and combined stress) was evident by the upregulation of suberin biosynthesis genes, and subsequent increased number of suberized cells. A comparative transcriptomic analysis based on different growth conditions and root differentiation stages was performed, revealing contrasting transcriptome changes between imposed treatments. Furthermore, the integration of data

obtained from both species, allowed the identification of genes potentially involved in phellem development and in the response to environmental changes. This knowledge may further contribute to design new strategies to improve cork production in sub-optimal conditions.

Sumário

Durante a diferenciação da periderme, as células do felema sofrem espessamento da parede celular secundária pela deposição de suberina, formando uma barreira compacta que protege do ambiente os órgãos da planta. O desenvolvimento e a suberização das células de felema são processos moleculares controlados, porém a sua regulação ainda é pouco conhecida. Para compreender melhor a ontogenia do felema em raizes de *Arabidopsis* e sobreiro, conduzimos análises histológicas e transcriptómicas direcionadas. Descobrimos que a atividade do felogénio se inicia uma semana pós-sementeira, em ambas as espécies. Por outro lado, uma análise transcriptómica das células do felema de *Arabidopsis* em início da suberização revelou que o transcriptoma destas células se organiza em três domínios moleculares relacionados com a produção de energia, a síntese e o transporte de componentes da parede celular, e a resposta a estímulos. Já em sobreiro, a análise comparativa de zonas da raiz em fases contrastantes de desenvolvimento revelou transcriptomas distintos, observando-se na zona de desenvolvimento secundário o enriquecimento em transcritos relacionados com a modificações da parede celular. Nas duas espécies estudadas, foram identificados genes potencialmente envolvidos na diferenciação de felema, nomeadamente genes relacionados com o transporte e montagem de monómeros de suberina, bem como novos fatores de transcrição. Além disso, descobrimos que a imposição simultânea de calor e stress osmótico no início do desenvolvimento do felema influencia diferentemente os padrões de suberização das raizes. Em *Arabidopsis*, a zona jovem da raiz primária não foi afetada, mas as raízes laterais primárias apresentaram suberização ectópica após aplicação de calor em combinação com stress osmótico. No sobreiro, o stress osmótico teve efeito positivo na suberização, verificando-se a regulação positiva dos

genes da biossíntese da suberina e o aparecimento de maior número de células suberizadas. Foi realizada ainda uma análise transcriptómica comparativa com base em diferentes condições de crescimento de sobreiro, que revelou perfis contrastantes do transcriptoma consoante o tratamento aplicado. Da integração dos resultados obtidos para cada uma das espécies foi possível identificar genes potencialmente envolvidos no desenvolvimento do felema e na resposta às mudanças ambientais. Este conhecimento poderá contribuir para o desenho de novas estratégias de melhoria da produção de cortiça em condições ambientais sub-óptimas.

Samenvatting

Tijdens de differentiatie van de peridermis vertonen felleemcellen een verdikking van de secundaire celwand via de afzetting van suberine, waardoor er een compacte barrière wordt gevormd die plantenweefsels afschermt van de omgeving. De ontwikkeling en suberizatie van felleemcellen zijn strikt gecontroleerde processen, maar over hun regulatie is weinig geweten. Om de ontogenie van het felleem in de wortel van Arabidopsis en kurkeik beter te begrijpen werden gerichte histologische en transcriptionele analyses uitgevoerd. We hebben aangetoond dat fellogeen-activiteit in beide soorten één week na het zaaien geïnitieerd wordt. Verder heeft een transcriptionele analyse in Arabidopsis, gericht op felleemcellen bij de start van suberizatie, aangegeven dat het felleem-transcriptoom drie grote domeinen omvat, gerelateerd aan energieproductie, synthese en transport van celwandcomponenten, en reacties op stimuli. Wat kurkeik betreft, heeft een transcriptoom-analyse, gericht op de vergelijking van wortelzones tijdens primaire versus secundaire ontwikkeling, transcriptionele verschillen tussen beiden bloot gelegd, waaronder een aanrijking in genen gerelateerd met celwand-modificaties tijdens secundaire ontwikkeling. Nieuwe spelers in felleem-differentiatie, gerelateerd aan het transport en de koppeling van suberine monomeren, alsook nieuwe transcriptionele regulatoren, konden geïdentificeerd worden in zowel Arabidopsis als kurkeik. Verder hebben we ook ontdekt dat blootstelling aan een combinatie van hitte en osmotische stress bij de aanvang van felleem-ontwikkeling de suberizatie-patronen in de wortels van beide soorten beïnvloedt. In Arabidopsis wordt de jonge primaire wortel niet beïnvloed, terwijl jonge zijwortels additionele suberizatie vertonen onder gecombineerde stresscondities. In kurkeik werd een positief effect van osmotische stress (in vergelijking met de nepbehandeling, hitte, en gecombineerde stress) duidelijk aan de hand van de opregulatie van

suberine biosynthese genen en de daaropvolgende toename in het aantal gesuberizeerde cellen. Een vergelijkende transcriptoom-analyse die verschillende groeicondities en stadia van wortelontwikkeling omvatte, onthulde contrasterende transcriptionele veranderingen als gevolg van de verschillende behandelingen. Bovendien liet de integratie van de data verkregen uit beide soorten de identificatie toe van genen die potentieel betrokken zijn in felleem-ontwikkeling en reacties op omgevingsveranderingen. Deze kennis kan mogelijks bijdragen tot de ontwikkeling van nieuwe strategieën om kurkproductie in suboptimale condities te verbeteren.

Table of Contents

Chapter I

General introduction

Table of Contents

1. Plant apoplast barriers

Adaptation of land plants to the terrestrial environment required the development of several specialized structures and chemicals, namely organs for anchorage and absorption of water and mineral (roots), efficient conducting systems (xylem and phloem), as well as effective support tissues (parenchyma and collenchyma). Moreover, transition from aquatic to terrestrial environment led to an increased water potential between plant body and the environment, driving the development of protective and specialized diffusion barriers that could mitigate uncontrolled water movements and water loss. Different types of diffusion barriers are formed by the reinforcement of cell walls with additional hydrophobic materials. Lignin, cutin and suberin are complex biopolymers that can be associated with cell walls and have diverse functions as barriers. These functions are product of their own diversity in chemical compositions, structure, physical properties and specific deposition places (in certain cell types or plant organs) (Schreiber et al., 1999; Schreiber, 2010; Naseer et al., 2012). Moreover, plant apoplastic barriers are of special interest regarding strategies for plant improvement, as most of these cell wall reinforcements can be modulated by abiotic or abiotic stresses.

Lignin has been associated with mechanical support, improvement of sap conduction through the lignified vascular elements, and defence mechanisms (Lewis *et al.*, 1999). Additionally, specific and localized impregnation with lignin in the casparian strips (encircling cell walls from root endodermis), offers a primary diffusion barrier to the young roots. Given its hydrophobicity, casparian strips control the apoplast flow and provide resistance to the negative water pressure in the xylem (Doblas *et al.*, 2017).

Cutin is produced constitutively in the epidermis of the aerial surface of vascular plants (leaves, primary stems, flowers, petioles, trichomes and fruits), being integrated in a hydrophobic layer known as cuticle. The cuticle-epidermis structure forms a film that protects the plant from environmental dehydration, while gas exchanges are facilitated by the stomata (Fich *et al.*, 2016). Recently, a cuticle-like structure was also identified in underground tissues, in the root caps. This particular cuticle deposition shows to be important for root meristem protection during the critical phase of seedling establishment and promotes the efficient formation of lateral roots (Berhin et al., 2019).

Finally, suberin is found in both aerial and underground organs, and is deposited at tissue-tissue interfaces, such as the root endodermal cell walls, and at plant-environment interfaces, including periderm cell walls (Vishwanath *et al.*, 2015). Suberin is generally characterized as a barrier, especially considering endodermal depositions, where its function is well described in control of water and nutrients (Andersen *et al.*, 2015; Barberon *et al.*, 2016; Barberon, 2017). Also, suberin is important regarding stress avoidance, considering not only the barrier properties for water movement in hydric stress (Ranathunge & Schreiber, 2011; Franke *et al.*, 2012; Kreszies *et al.*, 2018), but also in resistance to pathogen penetration conferred by the accumulation of suberin in external periderm cells (Heneen *et al.*, 1994; Du *et al.*, 2011; Thangave *et al.*, 2016). Additionally, suberin is been recently observed with particular interest in plant biotechnology community. As a carbon-rich plant product, suberin has been regarded as a strategic CO_2 accumulating product relevant in the climate change combat (https://www.salk.edu/science/power-of-plants/).

2. Suberin macromolecule

2.1. Composition, structure and cellular localization

Suberin is a complex lipophilic macromolecule composed of an aliphatic domain and an aromatic domain, both including a great diversity of components (monomers) that are covalently linked by ester bounds (Bernards, 2002; Graça, 2015). Generally, but not always, suberin also contains a certain amount of soluble lipids or waxes embedded in the polymerized aliphatic domain (Bernards, 2002; Vishwanath *et al.*, 2015). The current knowledge on suberin composition derives mainly from the analysis of the monomers, released after the ester breaking reactions used to depolymerize the molecule (Kolattukudy *et al.*, 1975; Graça & Pereira, 2000; Santos & Graça, 2006).

The aliphatic domain physically spans the space between the cell wall and the plasma membrane, and it is the best characterized domain in suberin. The major components detected after depolymerization are long-chain fatty acids (Fig. **1**), that are characteristic of suberin aliphatic domain and represent around 80-90% of the total monomers identified (Holloway, 1983). Bifunctional fatty acids are largely represented by ω-hydroxyacids and α,ω-diacids (Fig. **1**), which are characterized by the presence of two linking groups at both ends of the molecules - hydroxyl or carboxylic acid. These linking groups are necessary for their integration in a polymeric structure, allowing the suberin macromolecule to grow. In addition, monofunctional fatty acids and alcohols are also found (Fig. **1**), although in comparatively smaller portions, as they only act as dead ends in the suberin macromolecule. The chain length of both ω-hydroxyacids and α,ω-diacids range typically from C16 to C26, however in some cases the monofunctional fatty acids and alcohols can reach much higher chain lengths, up to C32. Mid-chain modifications on the aliphatic monomers (double bond, epoxide ring or two vicinal hydroxyl groups) are also detected, having a significant impact on the

macromolecular structure (Santos *et al.*, 2013). The suberin aliphatic domain also includes small amounts of aromatic monomers (Fig. **1**) that are also released and solubilized after depolymerization. Among these, *p*-hydroxycinnamates, such as ferulate, *p*-coumarate, and/or sinapate, are the major phenolic constituents. Glycerol molecules are also released after suberin depolymerization and may encompass 5 to 20% of the recognized monomers (Fig. **1**). The current knowledge is that glycerol plays a particular role in the linkage of suberin monomers. It is proposed to act as a linker between successive layers of monomers within the polyaliphatic domain and also making the link between polyaliphatic and polyaromatic domains (Moire *et al.*, 1999; Graça *et al.*, 2015).

Suberin polyaromatic domain is the suberin macromolecule fraction that is directly anchored to the primary cell wall components. This domain is composed essentially of polyphenolics, hydroxycinnamic acids and their derivatives, that are directly linked to the primary cell wall carbohydrates. Suberin aromatic domain is interpreted as “non-lignin”, but this classification is controversial given the similarities to conventional lignin, as in many cases it is shown to behave analytically as typical lignin (Bernards & Razem, 2001; Mattinen *et al.*, 2009; Marques & Pereira, 2013). The monomer composition of aromatic domain of suberin were essentially described by degradative lignin technics and *in situ* studies using solid state 13C NMR, as methods used for aliphatic domain depolymerization were not able to solubilize this cell wall associated suberin domain (Bernards *et al.*, 1995; Bernards & Lewis, 1998). Ferulate, *p*-coumarate, sinapate, and caffeate are the accepted constituents on the suberin polyaromatic domain (Fig. 1). In addition, the monolignols *p*-coumaryl alcohol, coniferyl alcohol, and sinapyl alcohol are also discussed to be part of the suberin phenolic

domain (Bernards, 2002; Graça, 2015). The exact composition of the suberin polyaromatic domain remains an open question.

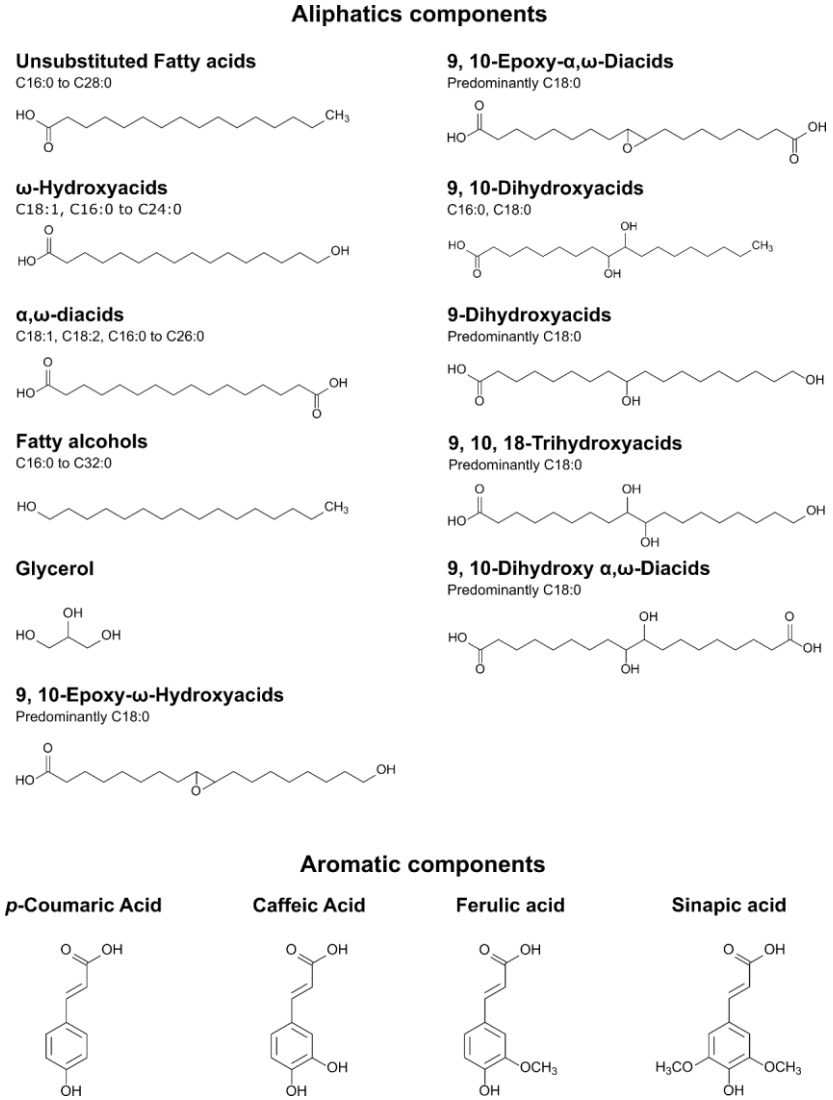

Fig. 1 *Structural formula of representative suberin monomers. For the aliphatic components, a monomer with the lower length chain is represented as example.*

Hereafter we refer suberin as the set of the chemical components of both aliphatic and aromatic domain, unless otherwise is referred

Sections of suberized cell walls frequently appear as an organized lamellar ultrastructure, with distinctive alternating light and dark bands, when observed by transmission electron microscopy (TEM), known as suberin lamellae. Yet, the overall molecular organization between suberin monomers remains to be determined (Vishwanath *et al.*, 2015).

Suberin monomers interconnection and spatial organization has been studied by incomplete suberin depolymerization, based on partial hydrolysis methods (Bernards, 2002; Graça, 2015). These methods allow the analysis of suberin fragments that still carry some of their *in situ* inter-monomer ester linkages (Graça & Pereira, 1997; Wang *et al.*, 2010; Graça *et al.*, 2015). In the proposed structural model, glycerol molecules are linked in succession to α,ω-diacids as the core backbone (glycerol – α,ω-diacids – glycerol), being able to grow as a macromolecular net, and forming a structure more or less ordered and packed (depending on its monomer composition). ω-hydroxyacids were also found esterified to ferulic acid as oligomer species, through both the acidic or ω-hydroxyl end groups. Moreover, the oligomer composed of glycerol-ω-hydroxyacid–ferulic acid plays an essential role in the macromolecule, as it can be part of the polyaliphatic domain and also in the periphery for the connection with the polyaromatic domain , (Bernards, 2002; Santos & Graça, 2006; Graça, 2015). Taken together, the available compositional, biochemical, and structural data leads to a model, represented in Fig. **2**, that integrates phenolic and aliphatic domains to form suberin macromolecule. The chemical link between the suberin molecule and primary cell wall carbohydrates is not yet very well described, and most of the discussed possibilities were made by analogy in what is known for cutin or lignin connection to the cell wall components.

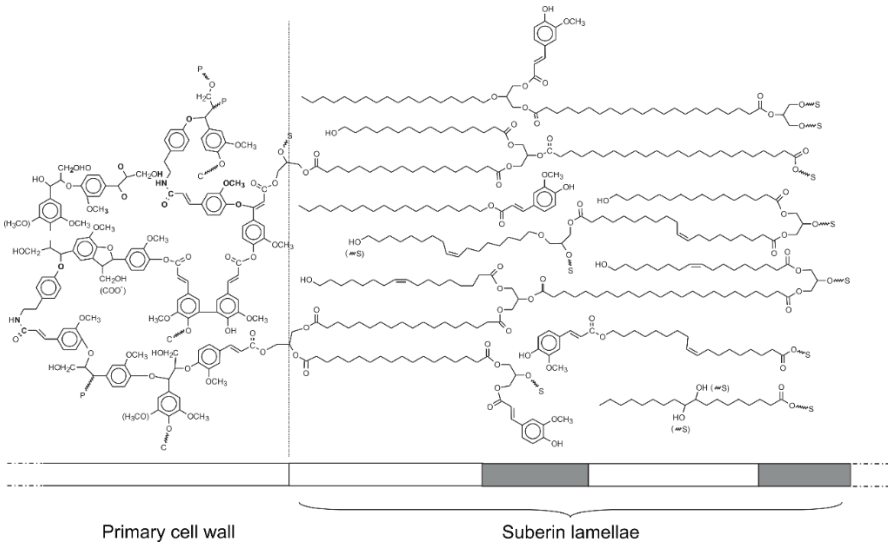

Fig. 2 *Hypothetical model for potato suberin structure (Bernards, 2002). The phenolic domain is restricted to the primary cell wall and covalently attached to carbohydrate units of cell walls (C). Attachments of the structure to other suberin components as well as the cell wall itself are shown with wavy lines. Connections are to the following: C, carbohydrate; P, phenolic; S, suberin (phenolic or aliphatic). Suberin associated waxes are not represented in this structure, but they likely span successive lamellar bands or intercalate within the macromolecular network. (Adapted from Bernards, 2002).*

Mostly, the suberin phenolic domain components are assumed to be covalently linked by ester or ether linkages, to the cellulose, hemicellulose or pectin molecules that integrate the primary cell wall (Negrel *et al.*, 1996; Yan & Stark, 2000; Lopes *et al.*, 2000; Bernards, 2002).

The proposed structural model may explain the above-mentioned light and dark lamellar structure of suberized cell walls, visible in TEM. This alternating structure could be generated by stacking successive layers of aliphatic monomers (light bands) with esterified phenolics (dark band) within the polyaliphatic domain. However, several studies with suberin biosynthesis mutants contradict these assumptions. In fact,

reduction of phenolic or aliphatic components caused by targeting different biosynthesis genes revealed no defects on the lamellar structure observed by TEM, showing that the basis of the lamellar appearance is still not fully understood (Molina *et al.*, 2009; Vishwanath *et al.*, 2013). Moreover, the relative proportion of the different families of suberin monomers and mid-chain substitutions is highly variable within plant species or tissue location and may influence the overall structure. The reasons for suberin composition variability are not clear, although it is hypothesized that such variability may be related to the ontogeny of the tissue, the physiological characteristic of the tissue or even the genetics related to phylogeny.

2.2. Tissue-specific deposition and functional role

Suberin is deposited on the inner side of the cell wall, against plasma membrane at both tissue-tissue or plant-environment interfaces (Vishwanath *et al.*, 2015). During plant development suberin is deposited in specialized cells, including: root endodermis and exodermis; periderm of shoots (outer barks), roots and tubers; seed coat; bundle sheath cells; and abscission zones. In addition, suberin is also detected in response to several stimulus in cells that normally are not suberized, such as wound sites (Zeier & Schreiber, 1999; Schreiber, 2010), or in root cortex cells in response to ABA treatments (Barberon *et al.*, 2016). The physiological role of suberin is specialized and can be correlated with its cell-specific location, pattern of deposition and composition, however, in a general overview, suberin mainly acts as a physical barrier (Schreiber *et al.*, 1999). The tissue distribution of suberization suggests also that plants synthesize and deposit suberin whenever a persistent barrier is needed (Franke & Schreiber, 2007).

Suberin deposition in root tissues, namely in the endodermis and exodermis, is described to contribute to prevent the uncontrolled and non-specific transport of water and solutes, from the environment to the

stele, and *vice-versa*, working as a bidirectional barrier (Hose *et al.*, 2001; Enstone *et al.*, 2002; Baxter *et al.*, 2009; Doblas *et al.*, 2017). Studies with Arabidopsis loss of function *horst/cyp86a1* mutants, that produce 33% less aliphatic suberin monomers than WT plants, observed an increase in permeability to water and ions at the root endodermal level (Höfer *et al.*, 2008; Ranathunge & Schreiber, 2011). However, the *esb-1* mutant, characterized by its high aliphatic suberin content, showed no changes in permeability, when compared to WT plants (Ranathunge & Schreiber, 2011). These studies have shown that the simple assumption that the amount of root suberin negatively correlates with permeability may not always be true. The aliphatic monomer arrangement in the suberin layer and its overall polymeric structure may play a relevant role in the suberin barrier (Kreszies *et al.*, 2018). Also, caution must be taken when correlating suberin barrier properties in different mutants, since many times suberin occurs together with other apoplastic barriers, such as Casparian bands (in endodermis). Observed phenotypes can be influenced by compensation of these other barriers or even other molecular mechanisms (Wang *et al.*, 2019). Is has been proposed that synthesis and degradation of suberin in endodermis is a dynamic process that can be modulated in response to environmental conditions. Recent publications using *Arabidopsis* showed that the nutritional deficiencies of elements, such as K, Fe, or S, can lead to changes in endodermal suberization, by induction of suberin synthesis or even degradation of suberin. This plasticity of root suberization highlighting the role of suberin, not only as an obstructive barrier, but also as a selective barrier controlling the uptake of ions (Barberon *et al.*, 2016; Doblas *et al.*, 2017).

Suberin deposition in the parenchymatous bundle sheath cell wall is a characteristic feature of the C4-photosynthesis plants. Much remains to be understood about the physiological role of bundle sheath

suberization in leaf, mostly by the lack of genetic resources in model grasses. However it is hypothesized that suberin can prevent the apoplastic diffusion of CO_2 and sucrose from bundle sheath cells to mesophyll cells, functioning as a gas exchange barrier (Mertz & Brutnell, 2014).

Considering suberin properties in boundary plant tissues, such as the seed coat and periderm, it is accepted that it functions almost as an impermeable barrier to water and dissolved compounds. In mature seeds, suberin is found in seed coat layers, sealing off the chalazal micropyle region after abscission. *Arabidopsis* mutants *awake-1* or *gpat5,* with reduced amounts of suberin in seed coat, showed reduced dormancy as well as high permeability to dyes, water and oxygen (Beisson *et al.*, 2007; Yadav *et al.*, 2014; Fedi *et al.*, 2017). This suggests that suberin is involved in the establishment of primary dormancy during seed maturation or its maintenance during seed imbibition. Regarding periderm, suberization occurs specifically on the phellem cells, which constitute the outermost cell layer(s) developed during secondary growth of roots, stems and branches (Campilho *et al.*, 2020). Several studies in woody species periderm have shown that suberin in phellem cells may work as a primary barrier against desiccation of plant body, as isolated phellem cell walls are low permeable to water and gases. Interestingly, phellems isolated from different species shown different permeabilities, that can be a direct result of differences in chemical composition of the cell walls. Moreover, the waxes also present as non-structural cell wall components, largely contribute to decrease the water permeability (Groh *et al.*, 2002; Lendzian, 2006). In the same way, in potato tubers, suberin and the associated waxes from phellem cells can provide the isolation necessary for tuber conservation, avoiding dehydration, physical injuries

and protection from pathogen attacks (Vaughn & Lulai, 1991; Schreiber *et al.*, 2005a; Thangave *et al.*, 2016; Tanios *et al.*, 2020).

Suberin can also be developed as a plant protection response, since environmental cues may also induce the increase of suberin-reinforced cell walls, not only in tissues that are normally suberized, but also in cells where suberization is not detected under non-stress conditions. The waterlogged adapted rice plants (*Oryza sativa*) can produce more suberin on exodermis when growing under stagnant deoxygenated conditions. In these cells, suberization act as a strong barrier to prevent radial oxygen loss from root aerenchyma to the substrate and prevent the uncontrollable penetration of water and toxic solutes (Watanabe *et al.*, 2013; Kreszies *et al.*, 2018). In barley, osmotic stress leads to significantly enhanced root suberization in modern cultivars, whereas this response is much weaker in the wild accessions. In this situation wild accessions kept their water transport constant, but the enhanced suberization observed in modern cultivars significantly reduced the radial water transport, leading to less beneficial trait regarding adaptation to osmotic stress (Ranathunge *et al.*, 2017; Kreszies *et al.*, 2020). Salt stress can induce the accumulation of suberin in endodermal and exodermal root zone of castor bean (Schreiber *et al.*, 2005b). Moreover, in *Arabidopsis* its well described that also salt stress induces the accumulation of suberin biosynthesis genes and suberin monomers, not only earlier in endodermis development, but also in surrounding cortex cells (Franke *et al.*, 2009; Barberon *et al.*, 2016). This adaptive response leads to the formation of a barrier that may minimize the salt penetration in root tissues in toxic concentrations.

Suberized cells can also be produced in response to wounding, in diverse plant tissues ,such as potato tubers, carrot roots, *Arabidopsis* leaves and roots, sour cherry leaves and others (Rittinger *et al.*, 1987;

Schreiber *et al.*, 2005a; Domergue *et al.*, 2010; Holbein *et al.*, 2019). Although wound healing process may differ among plant species and organs, there is a similar pattern described. The first layer of intact cells adjacent to the wound is modified by the accumulation of various antimicrobial and water-impermeable substances, including lignin and suberin, forming a sealing layer. The production of additional suberized periderm cells may further occur, minimizing pathogen invasion and loss of fluids from plant organs (Lulai & Freeman, 2001; Schreiber *et al.*, 2005a; Ginzberg, 2008).

2.3. Suberin biosynthesis and assembly

Suberin deposition requires the specific synthesis of its aliphatic, aromatic and glycerol components, a transportation system of these monomers across the cell membrane, followed by an organized assembly and polymerization in the cell wall. Globally, genes associated with the suberin biosynthesis and monomer transportation have been uncovered by transcriptomic studies on various suberin-rich tissues, such as cork oak, potato, poplar and birch periderms or even in apple russeting and melon skin (Soler *et al.*, 2007; Legay *et al.*, 2015; Vulavala *et al.*, 2017; Cohen *et al.*, 2019; Alonso-Serra *et al.*, 2019; Lopes *et al.*, 2019). Forward and reverse genetic studies have been used for functional characterization of individual genes, with isolation of numerous mutant and marker lines, mainly in *Arabidopsis* and potato. Moreover, despite the variability found in monomeric composition of suberin between different plant species and/or tissues, the molecular mechanisms underlying monomer biosynthesis are somewhat conserved. Thus, studies in different model systems may be relevant and transferable to other plants species (Beisson *et al.*, 2007; Molina *et al.*, 2009; Domergue *et al.*, 2010; Boher *et al.*, 2013; Yadav *et al.*, 2014; Kosma *et al.*, 2014).

The monomeric composition of suberin biopolymer is known for a wide variety of plants, although, numerous processes underlying suberin biosynthesis, such as the sequence of biosynthetic reactions, transport mechanism of monomers, and controlled polymerization, remain poorly described.

2.3.1. Biosynthesis of phenolic monomers

Phenolic components of suberin are mainly produced through the phenylpropanoid pathway (Fig. **3**). This pathway is highly conserved across the plant kingdom and is involved in preliminary steps towards the biosynthesis of different secondary metabolites, including mostly monomers specific to lignin and suberin (Vogt, 2010). Because this pathway is common to many chemical components in plant cells, it is difficult to attribute and categorize the enzymes as belonging to suberin biosynthesis. Most of the reactions described are common to lignin biosynthesis.

The biosynthetic pathway of the aromatic components present in suberin starts from phenylalanine, a derivate from the shikimate pathway. This aminoacid is converted to cinnamate by phenylalanine ammonia lyase (PAL), followed by the production of *p*-coumaric acid (4-hydroxycinnamic acid) through *para*-hydroxylation with the cinnamic acid 4- hydroxylase (C4H) enzyme. PAL and C4H enzymes are mostly described to be involved in lignification processes, however, they are commonly found in transcriptomic studies of suberin-rich tissues, such as periderms (Soler *et al.*, 2007, 2011; Rains *et al.*, 2018; Wei *et al.*, 2019) or as a result of overexpression of suberin related transcription factors (Kosma *et al.*, 2014; Legay *et al.*, 2016). *p*-coumaric acid has several possible metabolic fates, including conversion to caffeic acid, ferulic acid, 5-OH-ferulic acid and sinapic acid, all likely to be found in the final suberin polymer.

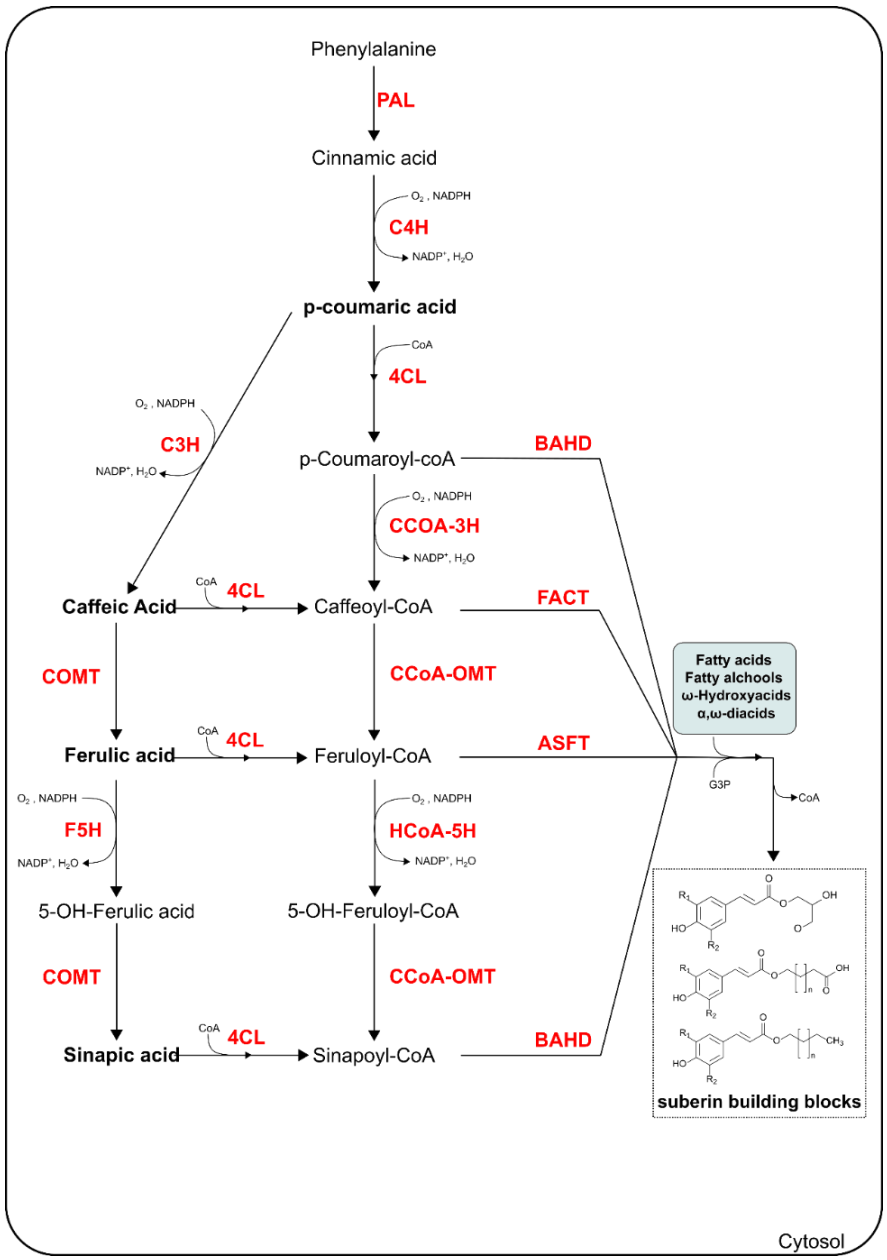

Fig. 3 *Proposed pathways for synthesis of aromatic suberin monomers. Example of suberin building blocks are represented by the result conjugation of hydroxycinnamic acids with glycerol, ω-hydroxyacids and fatty alcohols. 4CL: 4-coumarate-CoA ligase; ASFT: aliphatic suberin feruloyl transferase; BAHD: BEAT, AHCTs, HCBT and DAT family of acyl transferases; C3H: p-coumarate 3- hydroxylase; C4H: cinnamic acid 4- hydroxylase; CCoA-3H: p-coumaroyl Co-A 3- hydroxylase; HCoA-5H: hydroxycinnamoyl-CoA-5-hydroxylase; CCoA-OMT: caffeoyl CoA 3-O-methyltransferase; COMT: caffeic acid O-methyltransferase; F5H: ferulate 5- hydroxylase; FACT: fatty alcohol:caffeoyl-*

CoA caffeoyl transferase; PAL: phenylalanine ammonia lyase. In the suberin building blocks structures R_1=R_2=H: p-coumaric acid; R_1=OH and R_2=H: Caffeic acid; R_1=OCH_3 and R_2=H: Ferulic acid; R_1=R_2=OCH_3: Sinapic acid.

Hydroxylation and methyl-transfer reactions to retrieve these products are described to be carried out by p-coumarate 3- hydroxylase (C3H), caffeic acid O-methyltransferase (COMT) and ferulate 5- hydroxylase (F5H) (Meyer *et al.*, 1996; Schoch *et al.*, 2001). COMT can utilize both caffeic acid and 5-OH-ferulic acid as substrates in this pathway. The produced hydroxycinnamic acids can than converted by hydroxycinnamate CoA hydroxylase to caffeoyl-CoA, feruloyl-CoA, 5-OH-feruloyl-CoA and sinapoyl-CoA (Bernards, 2002). In parallel *p*-coumaric acid also can be converted to *p*-coumaroyl-CoA by 4-coumarate-CoA ligase (4CL) (Schneider *et al.*, 2003). Further conversion of *p*-coumaroyl-CoA to the caffeoyl-CoA, feruloyl-CoA, 5-OH-feruloyl-CoA and sinapoyl-CoA is possible through p-coumaroyl Co-A 3- hydroxylase (CCoA-3H), caffeoyl CoA 3-O-methyltransferase (CCoA-OMT) and hydroxycinnamoyl-CoA-5-hydroxylase (HCoA-5H) (Bernards, 2002). CoA activation is hypothesized as a necessary step for conjugation of hydroxycinnamates with other suberin aliphatic components that can then be incorporated in suberin polymer (Bernards, 2002).

2.3.1. Biosynthesis of aliphatic monomers

Suberin aliphatic monomer production begins with the plastidic synthesis of C16 and C18 fatty acids driven by the fatty acid synthase multienzyme complex. Several downstream modifications of fatty acid precursors yield the final aliphatic suberin monomers. These reactions, represented in Fig. **4**, include activation of fatty acids to fatty acyl-CoA thioesters, elongation to long and very long chain fatty acids (LCFA and VLCFA), reduction of LCFAs and VLCFAs to primary fatty alcohols, and

to ω-hydroxylation, and further oxidation to α,ω-dioic acid of ω-hydroxy fatty acids (Vishwanath *et al.*, 2015).

Acyl activation

Fatty acid activation through conversion of free fatty acids to fatty thioesters is a required step for downstream production of suberin aliphatic monomers. These reactions are carried out by long-chain acyl-CoA synthetases (LACS), that were initially characterized as being involved in cutin and cuticular wax biosynthesis(Lu *et al.*, 2009). LACS genes are not reported to be directly involved in suberin biosynthesis pathway, however, the knockdown of the suberin-specific transcription factor MYB107 lead to a general suppression of genes related to suberin biosynthesis, including LACS2 as opposed to other LACS genes (Gou *et al.*, 2017). This is in agreement with the proposed additional roles of particular LACS enzymes in suberin biosynthesis, by producing the fatty-CoAs precursors (Li-Beisson *et al.*, 2013).

Acyl elongation

Elongation of fatty-CoAs are performed by the complex fatty acid elongase (FAE) in the endoplasmic reticulum (Joubès et al., 2008; Li-Beisson et al., 2013). Specific enzymes in the FAE complex, involved in the synthesis of LCFAs and VLCFAs, are not specifically described to be involved in the production of suberin monomers. In fact, it is acknowledged that these molecules are the precursors for various lipidic compounds, which can be incorporated in several structures, such as triacylglycerols (stored in seeds), cuticular waxes, sphingolipids and suberin (Li-Beisson et al., 2013). For that reason, assessing the specific function of the enzymes is difficult as they function in a partial redundant way and are common to many other biosynthetic pathways.

Reactions on the FAE complex are performed in four steps, being the specificity of monomer of elongation controlled in the first step by β-

ketoacyl-CoA synthases (KCS) (Millar & Kunst, 1997; Blacklock & Jaworski, 2006). In *Arabidopsis*, the KCS2/DAISY and KCS20 enzymes participate specifically in the elongation of C20 monomer suberin precursors. The individual loss of function of these genes in *Arabidopsis* affected specifically the quantity of C22 and C24 monomers, although not affecting the total amount of suberin (Franke *et al.*, 2009; Lee *et al.*, 2009). Also, these enzymes showed some functional redundancy, as the double mutant *kcs20 kcs2/daisy-1* shows a higher reduction of C22 and C24 and an accumulation of C20 aliphatic derivates in suberin (Lee *et al.*, 2009).

In contrast to the KCS enzymes that have strict substrate and tissue specificities, the following steps of FAE are believed to be common to all VLCFA biosynthetic reactions, through enzymes with (presumed) broad substrate specificities (Millar & Kunst, 1997). These includes the β-ketoacyl reductase (KCR) enzyme that converts the generated β-ketoacyl-CoA to hydroxyacyl-CoA (Beaudoin *et al.*, 2009). Next, the 3-hydroxyacyl-CoA dehydratase (HCD) dehydrates the 3-hydroxyacyl-CoA in trans-2,3-enoyl-CoA (Bach *et al.*, 2008). Finally the enoyl-CoA reductase (ECR) may reduce its substrate into the elongated chain with two additional carbons (Zheng *et al.*, 2005). The acyl-CoA elongated by two carbons can re-enter an elongation cycle to eventually produce VLCFAs ranging from C18 to C32 in *Arabidopsis*.

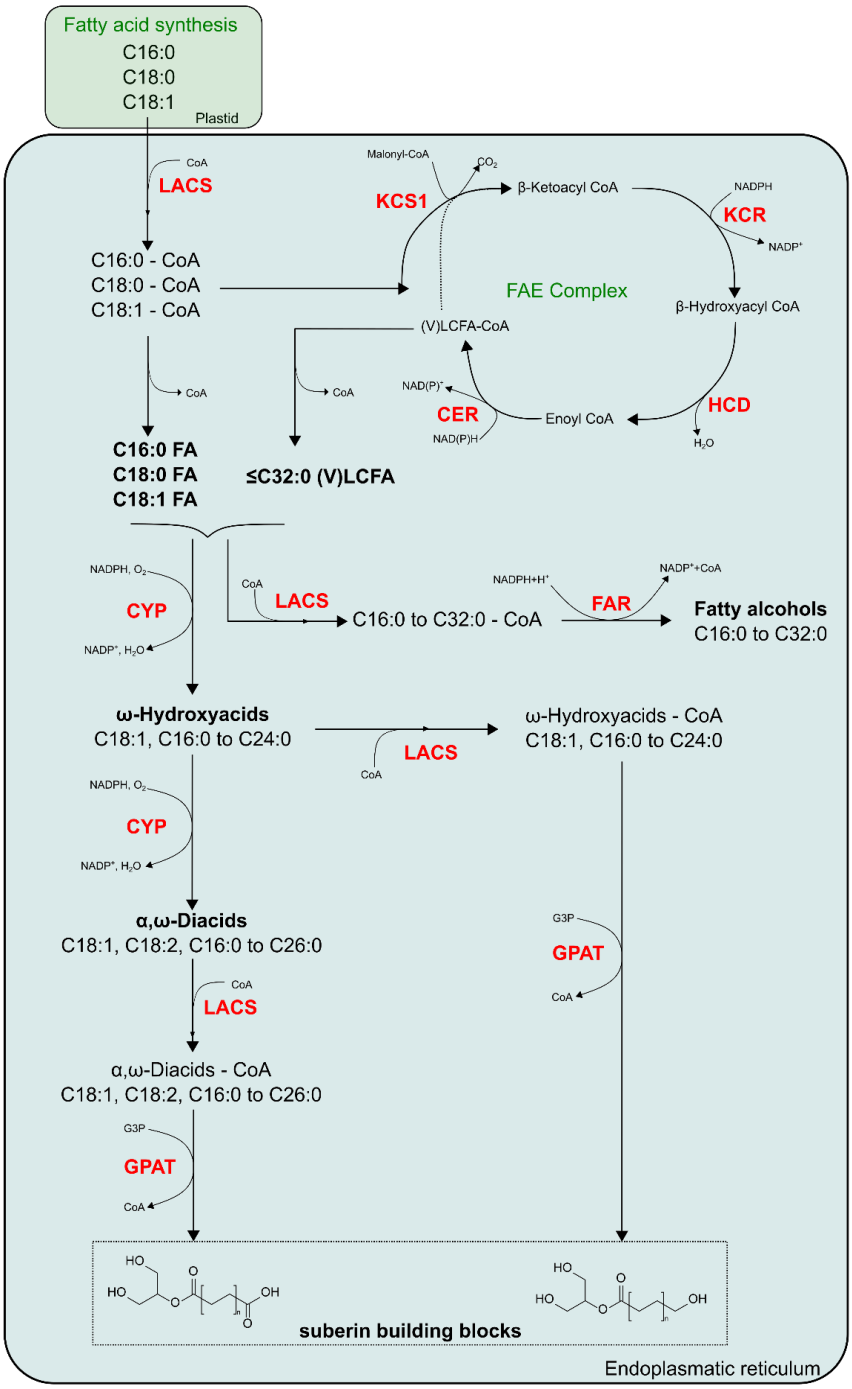

Fig. 4 *Proposed pathways for the synthesis of suberin aliphatic monomers. Example of suberin building blocks are represented by the result conjugation of α,ω-diacid and ω-hydroxyacids with glycerol.CYP: cytochrome P450 oxygenases; . ECR: enoyl-CoA reductase; FAR: fatty acyl reductases ;GPAT:*

glycerol 3-phosphate acyl transferases; HCD: 3-hydroxyacyl-CoA dehydratase; KCS1: ketoacyl-CoA synthases ; KCR: β-ketoacyl reductase; LACS: long-chain acyl-CoA synthetases.

Acyl oxidation

Production of the suberin bifunctional fatty acids monomers, ω-hydroxyacids, α,ω-diacids, as well as mid-chain modifications of these bifunctional fatty acids, are yielded by oxidation reactions of fatty acids (LCFA and VLCFA) (Bernards, 2002; Vishwanath *et al.*, 2015). The ω-hydroxylation is mediated by cytochrome P450 monooxygenases, and a proportion of the produced ω-hydroxyacids can be further oxidized to α,ω-diacids by a fatty acid dehydrogenase. An alternative enzymatic route proposes that P450 monooxygenases are multifunctional and can catalyse all ω-oxidation steps to form α,ω-diacids (Pinot & Beisson, 2011).

In *Arabidopsis*, CYP86A1 and CYP86B1 are cytochrome P450-dependent fatty acid oxidases described to be involved in the synthesis of root suberin ω-hydroxyacids and α,ω-diacids. (Höfer *et al.*, 2008; Compagnon *et al.*, 2009; Li-Beisson *et al.*, 2013). Loss-of-function mutants of CYP86A1 (*horst*) exhibited a 60% reduced amount of total aliphatic suberin, mainly due to a strong reduction in long chain ω-hydroxyacids and α,ω-diacids, specifically C16 and C18 (Höfer *et al.*, 2008). On the other hand, CYP86B1 (*ralph*) mutants have a specific impact on VLCFA monomers, with almost complete absence of C22 and C24 ω-hydroxyacids and α,ω-diacids. However, these changes did not affect the total amount of aliphatic suberin due the correspondent accumulation of unsubstituted/monofunctional C22 and C24 VLCFA (Compagnon *et al.*, 2009). Similarly, orthologues of these cytochrome P450-dependent fatty acid oxidases have been found in several transcriptomic studies to be associated to suberin biosynthesis (Soler *et al.*, 2007, 2011; Teixeira *et al.*, 2014, 2018; Vulavala *et al.*, 2017; Rains

et al., 2018; Alonso-Serra *et al.*, 2019; Lopes *et al.*, 2019). One of these is CYP86A33 from potato that was later characterized to be necessary for production of ω-hydroxyacids and α,ω-diacids in tuber periderm (Serra *et al.*, 2009; Bjelica *et al.*, 2016).

Mid-chain hydroxylation and epoxidation specific enzymes have not yet been characterized, but these reactions are proposed to be also catalysed by P450 enzymes (Graça, 2015). Only *in vitro* epoxidation of the C-9 double bond of the C18:1(oleic) acid by the *Vicia sativa* CYP94A1 oxygenase was described to be involved in the production of mid-chain modified monomers for suberin polymer (Durst *et al.*, 1998).

Acyl reduction

Fatty acyl reductases (FARs) reduce the activated fatty acids to deliver suberin primary alcohols. Several FARs have been identified and characterized in *Arabidopsis* (Rowland & Domergue, 2012), of which only three were confirmed to be specifically involved in suberin monomer production – FAR1, FAR4 and FAR5 (Domergue *et al.*, 2010). These enzymes are described to be not only involved in production of the primary fatty alcohols present in the suberin polymeric fraction, but also non-polymeric (soluble) fraction, the suberin-associated waxes (Kosma *et al.*, 2012). Triple mutant lines *far1 far4 far5* show a reduction of 70-80% in total alcohols, and no impact on the other suberin monomers, suggesting that polymerization process is not affected. This can be explained by the fact that fatty alcohols have a limited ability to be incorporated into polymers when compared with bifunctional monomers (Vishwanath *et al.*, 2013). Moreover, individual FAR enzymes have shown chain length specificity for activated fatty acids. Individual loss-of-function mutants may impact different length fatty alcohols, namely C22 alcohols, C20 fatty alcohols and C18 alkanols, which showed reduced levels in *far1*, *far4* and *far5* mutants, respectively (Domergue *et al.*, 2010).

2.3.2. Esterification, transport and assembly

Acyl esterification of suberin monomers, such as ω-hydroxy acids and α,ω-diacids, can be considered the first step of suberin assembly, as the produced monoacylglycerols are thought to constitute the initial suberin building blocks (Beisson *et al.*, 2007; Yang *et al.*, 2012). In this step, the glycerol 3-phosphate acyl transferases (GPATs) catalyse the transfer of the fatty acid unit from the CoA to glycerol 3-phosphate, forming the first ester bound of the suberin polymer. In *Arabidopsis*, several GPATs have been characterized, and functionally linked to cutin or suberin biosynthesis (Yang *et al.*, 2010, 2012). GPAT5 is mostly studied in *Arabidopsis* with gain and loss-of-function approaches and is known to be involved in the transfer of VLCFA to the glycerol-based acceptor. The *gpat5* plants showed a 50% decrease in aliphatic suberin in young roots and produced seed coats with reduction in C20-C24 ω-hydroxyacids and α,ω-diacids (Beisson *et al.*, 2007). Another member of this family, *GPAT7*, is only described to be expressed after wounding, yet, when overexpressed it can induce the production of soluble extractable suberin-like monomers in seeds and stems (Yang *et al.*, 2012).

Conjugation of hydroxycinnamic acids with modified fatty acids of aliphatic suberin monomers have been described mostly in *Arabidopsis* and potato (Gou *et al.*, 2009; Molina *et al.*, 2009; Serra *et al.*, 2010a; Boher *et al.*, 2013). Feruloyl-CoA transferases catalyse the reaction where feruloyl-CoA acts as an acyl donor for fatty acid acceptor to yield ferulate esters (alkyl ferulates), which constitute a point of convergence between the two major suberin-related biosynthetic pathways (phenolic and aliphatic). These ferulate esters are part of the aliphatic domain but also the point of connection between aromatic and aliphatic domains, as well as between the aromatic domain and the cell wall (Bernards & Lewis, 1998; Bernards & Razem, 2001; Graça, 2015). In *Arabidopsis*,

there are two described feruloyl-CoA transferases, ASFT/HHT (aliphatic suberin feruloyl transferase/fatty alcohol hydroxycinnamoyl transferase) and FACT (fatty alcohol:caffeoyl-CoA caffeoyl transferase), that belong to the BAHD (BEAT, AHCTs, HCBT and DAT) family of acyl transferases. The *Arabidopsis* ASFT/HHT, and the homologue in potato FHT, catalyse an acyl transfer between feruloyl-CoA and ω-hydroxyacids or primary alcohols, and have a demonstrated preference for primary fatty alcohols that will be incorporated in the aliphatic suberin (Gou *et al.*, 2009; Molina *et al.*, 2009; Boher *et al.*, 2013). On the other hand FACT is described to have preference for caffeoyl-CoA donor, to produce specific alkyl caffeates that are typically incorporated in soluble root suberin associated wax, although coumaroyl and feruoyl-CoAs could also be used as substrates (Kosma *et al.*, 2012; Domergue & Kosma, 2017).

After all these steps, the end products of the suberin monomer biosynthetic pathways need to be exported from the endoplasmic reticulum to and across the plasma membrane, and then polymerized in the apoplast. Current models for transport of suberin precursors to the cell wall include the secretory pathway, passive transport via oleophilic bodies, or through transporters (Fig. **5**) (Vishwanath *et al.*, 2015).

Several plasma membrane-localized ATP-binding cassette (ABC) transporters have been proposed to be associated with suberization of diverse tissues. The ABCG subfamily forms the largest subfamily of ABC transporters, and notably the majority of the described members of this family have been shown to be necessary for diffusion barrier formation, such as cutin or suberin (Nawrath *et al.*, 2013). ABCG transporters associated with suberin monomer transport have been mostly described in *Arabidopsis*, and presently constitute the most studied and better characterized players in suberin monomers transport. All *Arabidopsis* ABCG proteins belong to the same phylogenetic clade,

and in some cases, they may work in a redundant way in the suberization process, as single mutants show no strong phenotypes. Suberin deposited in the triple mutant *abcg2 abcg6 abcg20* showed a distorted lamellar structure and reduced proportions of aliphatic components, which negatively affected the barrier properties of suberin in seed coat and roots. This effect was not detected for *abcg2* and *abcg6* single or double mutants (Yadav *et al.*, 2014), but a closer observation of *abcg20* single mutant, *awak-1*, highlighted a suberization deficient phenotype specifically on seed coat, that resulted on seed dormancy defects (Fedi *et al.*, 2017). ABCG transporters have been shown to perform transport of suberin moieties in a monomer specific way, considering chain-length and fatty acid transformation (Landgraf *et al.*, 2014; Shanmugarajah *et al.*, 2019). Furthermore, transcripts of *ABCG* transporters are highly represented in recent transcriptome analysis targeting suberized tissues (Vulavala *et al.*, 2017, 2019; Rains *et al.*, 2018).

It has been suggested that lipid transfer proteins (LTPs) are also important for transfer of the precursors of lipid barriers such as cuticular wax, suberin and sporopollenin (Debono *et al.*, 2009; Edqvist *et al.*, 2018). *LPTI-4* is specifically expressed in suberized periderm of crown gall tumours of *Arabidopsis*, that develops after infection of virulent *Agrobacterium tumefaciens* strains (Deeken *et al.*, 2016). *ltpI-4* loss of function mutant reveals a specific reduction of long-chain fatty acids in crown gall tumours, and the ectopic expression of this protein in epidermis (where normally it is not detected) resulted in altered composition in the cuticular wax (Deeken *et al.*, 2016). Also *LTPG15* was shown to be expressed specifically in seed coat, and the loss-of-function mutant lead to defects on seed coat properties, due to a reduction on VLCFAs, primary alcohols, ω-hydroxyacids and α,ω-diacids from suberin components (Lee & Suh, 2018). Moreover, several

LTP genes were overrepresented together with suberin biosynthetic genes and *ABCG* transporters in specific transcriptomic analysis of cells with strong suberization profile (Legay *et al.*, 2016; Teixeira *et al.*, 2018; Cohen *et al.*, 2019), suggesting that that LTP proteins may enhance the extracellular delivery of fatty acyl precursors for suberin deposition.

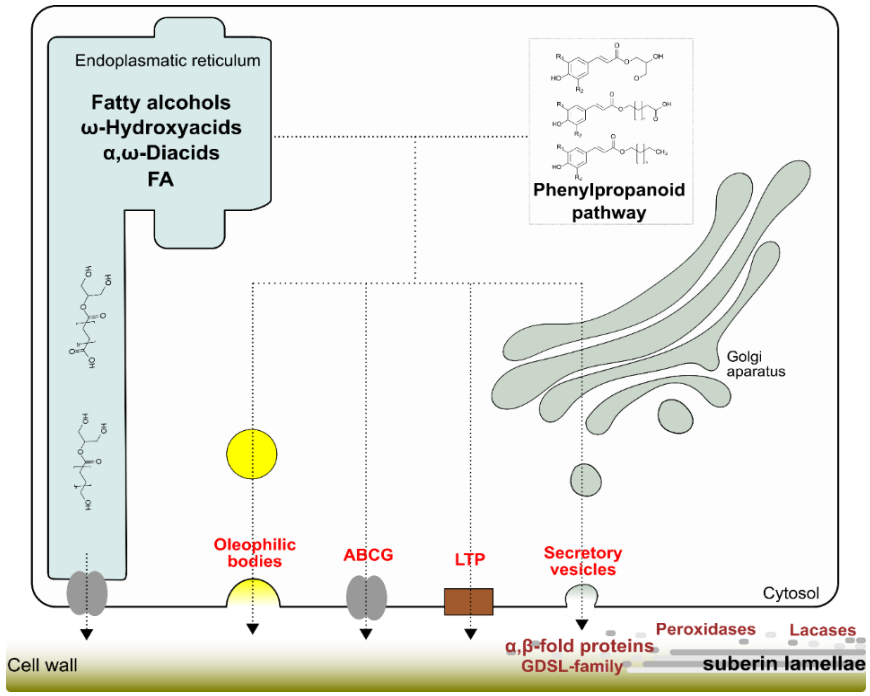

Fig. 5 *Potential mechanisms involved in the transport of suberin monomers and posterior polymerization of suberin in cell wall. ABCG: ATP-binding cassette G-family transporters; LTP: lipid transfer proteins. (Adapted from Li-Beisson et al., 2013).*

Export mechanisms involving secretory vesicles or oleophilic bodies have been also hypothesized, in the same way as it is described for transport of cuticular waxes to the apoplast (Mcfarlane *et al.*, 2014). However, these processes have not yet been confirmed for suberin monomers transport.

Molecular mechanisms describing the polymerization and organization of suberin macromolecule in the apoplast remain unknown, however, some hypotheses have been proposed, based on the suberin structural similarity to cutin and lignin.

Extracellular GDSL-motif esterase/acyltransferase/lipase proteins and α,β-fold protein hydrolases Have been hypothesized to be involved in the polymerisation of suberin aliphatic monomers. These proteins are described to be involved directly in cutin polymerization, catalysing the acyl esterification and cross-linking between cutin monoacylglycerols precursors (Kurdyukov *et al.*, 2006; Yeats *et al.*, 2012, 2014; Jakobson *et al.*, 2016). Several *GDSL* genes were upregulated in specific suberized tissues, such as cork and poplar outer barks as well as potato, apple and melon skins (Soler *et al.*, 2007; Legay *et al.*, 2015; Vulavala *et al.*, 2017; Rains *et al.*, 2018; Cohen *et al.*, 2019). Also, protein-protein co-expression analysis showed strong interactions between some GDSL-esterase/lipases, α,β-fold protein hydrolases, and suberin biosynthetic gene clusters (Legay *et al.*, 2016). Recently, GDSL proteins were reported to be involved specifically in the suberization process. Interestingly, while some GDSL are associated with the suberin degradation process (as *GELP12*, *GELP55*, *GELP72*, *GELP73* and *GELP81*), others have a strong correlation with the suberin biosynthesis (*GELP38*, *GELP51* and *GELP96*), demonstrating the importance of these enzymes in the suberization plasticity (Ursache *et al.*, 2021).

The phenolic domain of suberin is assumed to undergo polymerization by O_2-dependent laccases and H_2O_2-dependent laccases (Kolattukudy *et al.*, 1975; Nawrath, 2002), in a similar process to what is described for the oxidative cross-linking model for lignification (Tobimatsu & Schuetz, 2019). One evidence for this is the identified anionic peroxidase isoform of potato skin, that is expressed during wound-induced suberization. This peroxidase was essentially

associated to suberin due its preference specificity for suberin hydroxycinnamates that accumulate in tuber skin after wounding (Espelie & Kolattukudy, 1985; Bernards *et al.*, 1999). In agreement with this data, several peroxidases together with laccases were identified in transcriptomic studies of suberized tissues making the mediated lignin-like polymerization a stronger hypothesis for suberin phenolics polymerisation (Rains *et al.*, 2018; Cohen *et al.*, 2019; Vulavala *et al.*, 2019). Recently, it was also speculated that CASP and CASP-like proteins can be involved in polymerisation of suberin, being the mediators that coordinate mechanisms required for the targeted suberin phenolic domain polymerization. CASP proteins are known to be involved in the precise polymerisation of lignin present in the Casparian strip, by acting as membrane scaffolds and mediating the recruitment of machinery involved in the polymerization of phenolics (Roppolo *et al.*, 2011; Li *et al.*, 2018). CASPs have also been identified in suberizing tissues of apple fruit skins, potato tuber periderm, as well as the *Arabidopsis* seed coat, that contain suberin but do not contain Casparian bands. This hints may point to a role for CASP family proteins in suberin polymerization (Lashbrooke *et al.*, 2016; Legay *et al.*, 2016; Vulavala *et al.*, 2017).

2.4. Regulation of suberin deposition

Suberization process, including synthesis, transport and polymerization of monomers must be fine-tuned regulated in order to guarantee suberin deposition in a cell type specific manner, varying in composition and structure, during normal development or upon stress exposure. The molecular mechanisms controlling suberization are still not fully understood, however, in the past years some aspects of regulation have been revealed by the most recent molecular techniques targeting different suberized tissues in diverse plants. Transcription factors belonging to the MYB and NAC families together with the ABA

an ethylene phytohormones, have been regarded with special interest for suberization process.

2.4.1. Hormone regulation

Consistent with the physiological function of suberin in protection against water loss and infection, ABA was soon considered as a possible phytohormone controlling suberization in plant tissues, due to its known contribution to plant adaptation through environmental stresses (Mauch-Mani & Mauch, 2005; Vishwakarma *et al.*, 2017). The first clues linking ABA hormone to suberization were shown in potato tubers. The suberization process occurring during wound periderm formation was shown to be linked to the production of ABA, and additional treatments with this phytohormone were shown to increase the activity of enzymes related to suberin monomers synthesis as well as suberin amount (Soliday *et al.*, 1978; Cottle & Kolattukudy, 1982). Application of a *de novo* ABA biosynthesis inhibitor reduced the accumulation of suberin aromatic and aliphatic components, as well as the transcription of suberin related enzymes in wound healing tubers. On the opposite, exogenous application of ABA was sufficient to induce suberin biosynthesis genes as well detectable increase in suberization (Lulai *et al.*, 2008). In potato periderm, *CYP86A33* and *FHT* were induced by external application of ABA, and detailed in silico analyses of the promoter regions of these genes showed the presence of ABA-linked response elements (Boher et al., 2013; Bjelica et al., 2016). In *Arabidopsis*, several genes described for suberin biosynthesis and transport have been shown to be regulated by ABA, including *DAISY/ KCS2*, *GPAT5* and *ABCG6*, *ABCG16* (Lee et al., 2009; Yadav et al., 2014; Barberon et al., 2016). Actually, in *Arabidopsis*, ABA was described as required for endodermal suberization, where the endoderm specific suppression of ABA signalling induced a strong delay on the suberization process in non-stress conditions (Barberon et al.,

2016). Also, several TFs involved specifically in suberization processes, such as *Arabidopsis* MYB41 and MYB107 and potato NAC103, were shown to be induced by ABA (Kosma et al., 2014; Verdaguer et al., 2016; Gou et al., 2017). Furthermore, accumulating evidences show that ABA plays a positive and crucial role in suberization processes in diverse species and tissues. In cork oak periderm ABA associated genes were described to be more expressed in tissues with more abundant suberization (Soler et al., 2007; Teixeira et al., 2018). In fruit species, such as kiwi and tomato, scar healing tissues showed upregulation of suberin biosynthetic genes concomitant with increased accumulation of suberin, increased expression of ABA related genes and ABA accumulation (Leide et al., 2012; Han et al., 2018). Moreover, recently two Kiwi TFs (AchnbZIP12 and AchnABF2) were described to be directly triggered by ABA, being able then to interact with promoters and induce the transcription of suberin biosynthesis genes and other suberin described TFs (Wei et al., 2019; Han et al., 2019).

When studying the decrease in suberin deposition in response to ion deficiency, such as Fe, Zn and Mn (Barberon et al., 2016), ethylene was proposed as probable suberization regulator. Application of ethylene precursor ACC (1-aminocyclopropane-1-carboxylic acid) in *Arabidopsis* negatively impacts endodermal suberization, causing a strong reduction of suberin accumulation in newly formed parts of the root. A similar phenotype was also detected in ethylene signalling mutants (Barberon et al., 2016). In addition to this effect on *de novo* suberization, ethylene was also able to induce the degradation of pre-existing suberin lamellae. Interestingly, ABA application on ethylene signalling mutants lead to an almost normal suberization pattern in *Arabidopsis* endoderm, showing that ABA and ethylene can work in a opposite manner regulating suberization (Barberon *et al.*, 2016; Doblas *et al.*, 2017). However, caution should be taken regarding ethylene

suberization regulation, as previous reports have shown that ethylene was not involved directly in suberization process in potato periderm. In fact neither ethylene external application nor ethylene antagonists have blocked the suberization in potato phellem cells (Lulai & Suttle, 2004, 2009). This highlights some variability in the regulatory pathways of suberization that could be dependent on tissue, developmental stage or even species.

2.4.2. Transcription factors

Considering plant specialized metabolism to produce apoplastic barriers, a variety of TFs has been identified and characterized as being able to control entire pathways, or specific branches of the pathway, under control or stress conditions. Regarding suberization, several TFs have been identified and functionally attributed to suberization processes in *Arabidopsis*, potato, apple and cork oak.

Arabidopsis MYB41 was the first TF to be described in suberization regulation. MYB41 was previously described as a regulator of accumulation of cuticle lipid, based primarily on the observation that overexpression lines exhibited phenotypes associated with a malformed cuticle (Cominelli et al., 2008). However, detailed observation showed that the overexpression of *MYB41* was activating ectopic production of aliphatic suberin by activation of specific suberin biosynthesis genes and consequently inducing the deposition of suberin-like lamellae in leaf epidermal and mesophyll cells (Kosma et al., 2014). Curiously, *MYB41* was found to be expressed in response to stress treatments (salt, drought and cold), and in response to ABA, but not under control conditions in normal suberized tissues of *Arabidopsis* such as endodermis (Cominelli et al., 2008; Kosma et al., 2014). Interestingly, homologues of this TF were not found in transcriptomic studies targeting diverse suberized tissues in control conditions (Rains *et al.*, 2018; Teixeira *et al.*, 2018; Cohen *et al.*, 2019; Vulavala *et al.*, 2019; Alonso-

Serra *et al.*, 2019), supporting the idea of MYB41 as central role in suberin deposition regulation only under stress conditions.

The recent emergence of transcriptomic data sets targeting diverse tissues with strongly suberized structures have been delivering others TF candidates specifically involved in suberization processes. Comparative transcriptome analysis of diverse suberin rich tissues, in different plants and tissues, including suberized healing tomato skin and other tomato organs (Sato *et al.*, 2012; Lashbrooke *et al.*, 2016), russeted apple (Legay et al., 2015; Lashbrooke et al., 2016), *Arabidopsis* seeds (Le et al., 2010), diverse organs of grapevine (Fasoli et al., 2012), potato tuber (Xu et al., 2011) and rice roots (Shiono et al., 2014), revealed a conserved multispecies gene expression signature for suberin biosynthesis, including several genes in suberin formation as well as conserved TFs (Lashbrooke et al., 2016). Central elements in this gene expression signature were the *Arabidopsis* homologues of the TFs MYB107, MYB9 as well as MYB39. MYB9 and MYB107 where confirmed as TFs positively regulating suberization in *Arabidopsis* seed coat. *myb107* and *myb9* mutants exhibited a down regulation of most of suberin biosynthesis genes together with a detected reduction in suberin monomers in seed coat, leading to an increased permeability and lower germination capacities under osmotic and salt stress (Lashbrooke et al., 2016). MYB107 alone was further characterized in *Arabidopsis* as specifically involved in seed coat suberization, with no expression detected in other suberized tissues. Additionally, MYB107 was prove to be able to directly bind to the promoters of suberin biosynthetic genes, validating its role in direct regulation of their expression (Gou et al., 2017). Regarding *MYB93*, no effect was detected in the suberization profile of *Arabidopsis* seed coat in the loss of function mutant plants, however no other *Arabidopsis* suberized tissue was studied (Lashbrooke et al., 2016). In other studies, *MYB93* is characterized to

be specifically expressed in endodermal cells, negatively regulating lateral root development (Gibbs et al., 2014). Yet, so far, no putative involvement of *MYB93* in endoderm suberization has been demonstrated for *Arabidopsis*. On the opposite, the apple orthologue *MYB93* was first identified as important in apple russeting and with a strong gene expression correlation with suberin biosynthesis genes (Legay et al., 2015). Furthermore, the transient expression in *Nicotiana benthamiana* leaves of the apple *MYB93* lead to a massive accumulation of suberin precursors as result of increase expression of suberin biosynthetic genes. These results demonstrated that the predicted apple ortholog of *MYB93* is able to orchestrate the synthesis and organization of suberin (Legay et al., 2016).

Another member of MYB family, the *Quercus suber* MYB1, identified as candidate regulator of cork formation (Almeida et al., 2013), was also recently proposed as a specific regulator of suberization in cork oak periderm (Capote et al., 2018). In these studies, ChIP-Seq (Chromatin Immunoprecipitation coupled with next-generation DNA sequencing) analysis of embryogenic callus tissue overexpressing this TF, revealed genes involved in suberin biosynthesis as candidate targets of MYB1. These included genes involved in monomer synthesis, as well as genes encoding *ABCG* and *LTPs*, involved in the transport of monomeric suberin units across the cellular membrane (Capote et al., 2018). Also, the expression of the closest *Arabidopsis* orthologue *MYB84/RAX3* was found specifically in cells undergoing suberization in *Arabidopsis* roots (endodermis and periderm) (Wunderling *et al.*, 2018) and induced upon drought and heat treatment (Feng *et al.*, 2004), however no targeted correlation with suberization process was proved experimentally in *Arabidopsis*.

Recently, members of NAC family of transcription factors were also associated with suberization processes in diverse plant models and

tissues. *ANAC046* was previously characterized to be a positive regulator of cell death and senescence in *Arabidopsis* (Oda-Yamamizo et al., 2016; Huysmans et al., 2018). This gene was also found to be co-expressed with a number of genes involved in suberin biosynthesis such as *CYP86B1*, *FAR4*, *FAR5* and *GPAT5* (Mahmood et al., 2019). In *Arabidopsis* roots, *ANAC046* promoter is predominantly active in the endodermis and periderm and its overexpression leads to an increased expression of suberin biosynthesis genes, which resulted in suberin accumulation in roots (Mahmood et al., 2019).

Contrastingly, other NAC family member, NAC103 was reported as a repressor of suberin and associated waxes in potato skin, being the first gene identified as negative regulator of suberization (Verdaguer et al., 2016). Interestingly, the putative orthologue of this TF was previously highlighted in cork oak phellem (Soler *et al.*, 2007) and the expression pattern throughout the cork growing season shows to be similar to suberin biosynthesis genes (Soler *et al.*, 2008). In potato, *NAC103* is only expressed in suberizing tissues and its silencing (NAC103i) leads to an accumulation in suberin and wax compounds, as well as upregulation of biosynthesis genes (Verdaguer et al., 2016).

Also, in a recent strategy of silencing the conserved NAC103 domain, several other potato NAC genes were identified as possible regulators of suberin deposition (Soler *et al.*, 2020). The conserved silencing line mainly revealed an expected decrease of *NAC103* expression together with the strong decrease of *NAC101* gene expression, indicating *NAC101* as strong candidate involved in suberization. Globally, the increase in suberin monomers is detected and supported by the accumulation of suberin biosynthesis transcripts. Also, an increased load of associated waxes in tuber phellem was detected for a conserved silencing line (on contrary to the NAC103i

alone and WT) indicating that potato NAC101 acts as a specific repressor of suberin-associated waxes (Soler *et al.*, 2020).

3. Phellem – the plant boundary

During secondary growth the epidermis is replaced in the stems and roots by the periderm, contributing for the increased thickness of these organs. Periderm is organized in layers that are composed by the phellogen or cork cambium, phellem (also known as cork), and phelloderm. The organized structure is also found in other specialized tissues such as fruit and tuber skin or wound sealing periderm. Phellem cells are the outermost barrier of those organs, having a significant function in plant protection against pathogens and environmental conditions as well as influencing the exchange of vital gases such as CO_2, O_2, and water vapour (Lendzian, 2006; Evert, 2006; Crang *et al.*, 2018).

Cork was the first cellular structure to be observed and described under the microscope by Robert Hooke (1635–1703), who made rigorous drawings of thin slices of cork as he saw them at the microscope. Since then and with the evolution of imaging techniques, the structure of different phellem cells has been analysed with greater accuracy over time. The shape of phellem cells varies according to the observation plane, with phellem cells from cork oak and potato being the most described (Graça, 2015; Crouvisier-Urion et al., 2019). Most commonly, phellem cells are rectangular prisms but when observed at a tangential plane can be irregular, and can be elongated at a vertical, radial or tangential plane of the plant organ analysed (Pereira, 2007).

The most predominant characteristic of phellem tissues is the structural arrangement of cells in a multi-layered tissue, compact and with no intercellular spaces. At maturity, phellem cells are non-living,

filled with air, dark resins or tannins and its cell walls have a high degree of suberization. The cellular structure of phellem cell wall consists of a thin, lignin-rich middle lamellae (internal primary wall), a thick secondary wall of suberin lamellae and in some cases a thin tertiary wall of polysaccharides and waxes. Some studies suggest that the secondary wall may be lignified and therefore may not consist exclusively of suberin. Nevertheless, suberin is the most abundant component of phellem cells, constituting approximately 40% of its total composition (Bernards & Lewis, 1998; Evert, 2006; Pereira, 2007; Pinheiro *et al.*, 2019). Phellem cells may have evenly or unevenly thickened walls, as in some species it is possible to observe U-shaped wall thickenings, with either the inner or outer tangential wall together with adjoining parts of the radial walls being thickened (Evert, 2006). Also, phellem cells may be enriched with diverse metabolites, that can be correlated with defensive functions, such as alkanoids, terpenes, phenolics and other bioactive compounds (Silva *et al.*, 2005; Carranza *et al.*, 2015; Ferreira *et al.*, 2017). Most of the metabolites are often species-specific, like the betulin, which is a triterpene metabolite abundantly found in birch phellem, but not so abundant in other phellems, even in closely related-species such as the black alder (Alonso-Serra *et al.*, 2019).

The number of phellem layers and their cell wall thickness (mostly considering suberin deposition) also vary among species, and despite the unclear reason of these differences it is suggested that these traits correlate with specialized functions of the different phellem tissues (Lendzian, 2006). Some species have an extensive production of phellem cells, as it is the case of *Quercus suber* (Fig. **6**) that can continuously produce phellem at rates of 10-20 cell layers per year (Graça & Pereira, 2004; Leite & Pereira, 2017). Other species, including poplar and potato have a constant and much smaller number of phellem cell layers, independently of the plant age (Kaufert, 1937).

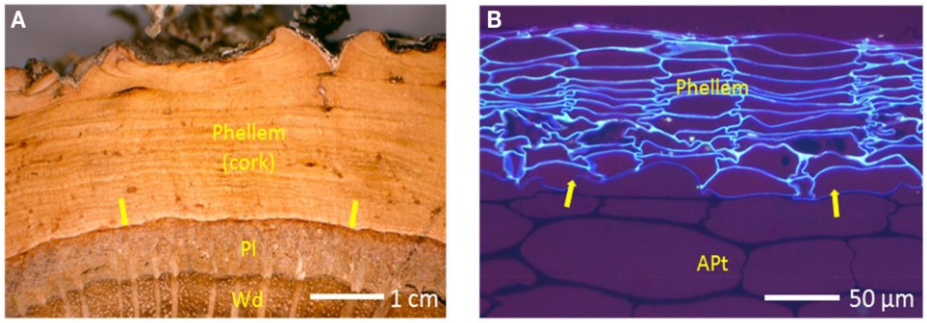

Fig. 6 *Periderm and suberized cells in cork (Quercus suber) and potato tubers (Solanum tuberosum). (A) Q. suber trunk outer tissues, showing the periderm, made of high accumulation of phellem (suberized tissue, the cork), phellogen (the meristem layer, arrows), and phelloderm (not highlighted); Pl, phloem; Wd, xylem (wood). (B) Potato tuber outer tissues, showing the periderm, made of phellem (suberized tissue, light blue), phellogen (arrows), and phelloderm (not highlighted); Apt, amylaceous parenchyma tissue. (Adapted from Graça 2015).*

Another characteristic of phellem tissue is the presence of specialized structures with mostly non-suberized cells, the lenticels or lenticular channels. In contrast to the surrounding phellem cells, the lenticels have a relatively open arrangement, being regarded as structures that allow air entry and circulation in phellem tissues similarly to stomata in the epidermis (Groh *et al.*, 2002; Lendzian, 2006). The density of lenticels in phellem as well as the chemical composition of the complementary tissue of lenticels is species-specific (Evert, 2006; Pereira, 2007).

3.1. Phellem origin and differentiation

The phellem cells differentiate after cell division in the phellogen, the meristematic cell layer also known as cork cambium. The first cork cambium/phellogen cell develops only in particular moments of post-embryonic plant development, by dedifferentiation of a parenchymatous cell (i.e., return to a meristematic function) (Evert, 2006). It is assumed that phellogen dedifferentiation is initiated by the necessity of a new

protective tissue in the plant body, namely during secondary growth in roots and stems, when the excessive growth of the vascular cambium damages the epidermis (Pereira, 2007; Wunderling *et al.*, 2018). Phellogen also occurs in tuber-forming species, when the original epidermis is replaced by the protective phellem (Lulai & Freeman, 2001), and is also described in tuber wound healing (Sabba & Lulai, 2002). In stems, phellogen cells always dedifferentiate outside the vascular cambium and, depending on the species, they can appear at different depths. In some cases they dedifferentiate in the sub-epidermis or in the underneath cell layer by a periclinal cell division, while in other cases they can arise close to the vascular region (Pereira, 2007). In most roots, however, the phellogen originates deep in the axis, usually in the pericycle (Dolan *et al.*, 1993; Wunderling *et al.*, 2018; Smetana *et al.*, 2019). The first phellogen is always initiated by periclinal divisions in a local area and it became continuous by lateral spread of the meristem activity (anticlinal divisions), both in stems and roots. After dedifferentiation, the phellogen cell starts meristematic activity, with periclinal divisions in two directions: towards inside, forming the phelloderm, and towards outside forming the phellem. Occasionally cells also divide in anticlinal direction to cope with the organ radial growth (Evert, 2006; Crang *et al.*, 2018).

Recent studies have advanced the mechanics of phellem development in *Arabidopsis* through morphodynamic analyses (Wunderling *et al.*, 2018) and lineage-tracing (Smetana *et al.*, 2019), which confirmed the pericycle origin of root phellogen. For *Arabidopsis*, periderm origin and development were categorised in six different stages of differentiation. The defined developmental stages are represented in Fig. **7**. This model describes development from the first cell division in the pericycle, to the shedding of cortex and epidermis,

ending with a complete ring of outer suberized phellem cells (Wunderling *et al.*, 2018; Campilho *et al.*, 2020).

In general, the meristematic activity of phellogen is asymmetrical, producing more cell layers outwards than inwards. In most cases there is only one layer of phelloderm and several layers of phellem, although in a few species the phelloderm may be thicker. In *Ginkgo* about 40 cell layers of phelloderm could be counted, and, in some tropical trees, as in *Ficus* spp. and *Brosimum* spp. a thicker phelloderm is observed, contributing with at least one third of the total outer bark width (Evert, 2006; Pereira, 2007; Leite & Pereira, 2017).

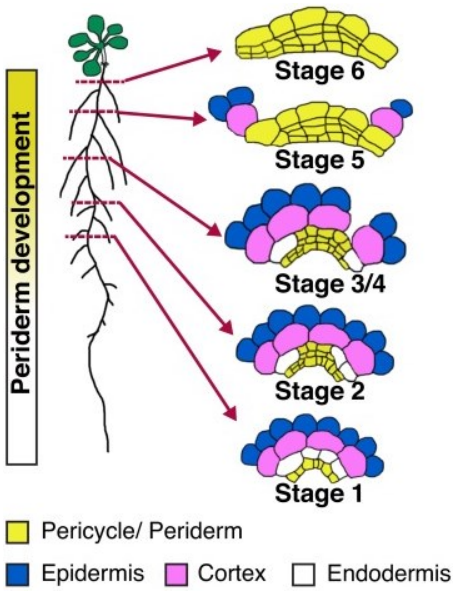

Fig. 7 Periderm development in Arabidopsis root represented schematically to show different stages of periderm development in cross sections (Campilho et al., 2020). The periderm arises from an inner tissue, the pericycle (yellow; stage1), which is surrounded by the endodermis (white), the cortex (pink) and the epidermis (blue). Notably, the endodermis is absent in stage 4, whereas the epidermis and cortex break at stage 3/4, when the first phellem cells are visible. In stage 5 there is a clear ring of suberized phellem cells.

After cell division from phellogen, phellem cells undergo several differentiation steps until they reach maturity. The sequential differentiation steps for phellem maturation include extensive deposition of suberin and waxes, cell expansion and an irreversible program of senescence, ending in cell death. The establishment of phellem as a

barrier starts with the processes of suberization that includes the activation of enzymes for the process of biosynthesis, transport and deposition of suberin monomers.

The molecular signature of phellem cells has been mainly described in the increasing transcriptomic studies targeting suberized periderms. Suberization-related transcripts, including those involved in synthesis, transport and assembly associated transcripts, are commonly found in the diverse analysed phellems, such as cork barks (Soler *et al.*, 2007; Leite & Pereira, 2017; Boher *et al.*, 2018), potato skin (Ginzberg et al., 2009; Vulavala et al., 2017), *Arabidopsis* roots (Wunderling *et al.*, 2018), and stem outer barks of poplar (Rains *et al.*, 2018) and birch (Alonso-Serra *et al.*, 2019), indicating that this is a conserved process in periderm development. Interestingly, when phellogen cells are specifically targeted for transcriptomic studies, it is already possible to identify some transcripts related to the suberization process, indicating that suberization is initiated early in phellem differentiation. In cork oak, non-suberized cells, positioned right beneath the phellem suberized cells, were selected as a phellogen-like meristematic region and targeted for RNA-seq (Teixeira et al., 2018). In tree samples that were characterized as producing highly suberized cork cells, the data, analysed in comparison with samples producing low suberized cork cells, showed an over-representation of genes related to fatty-acid synthesis and fatty-acid elongation (Teixeira et al., 2018). Also, RNA-seq of laser microdissected potato phellogen tissues, highlighted a number of transcripts related to cell wall modification, many of them related to the initial steps of production of suberin monomers (Vulavala et al., 2019). Altogether these data suggest that the suberization process is induced early after phellogen division and before suberin is detected. After the initiation of the suberization process, immature phellem cells start to expand, increasing the cell volume. In *Arabidopsis*,

although phellem cell volume is highly variable, larger cells are identified mostly in the older and mature part of the root containing older phellem cells (Wunderling *et al.*, 2018). In agreement with morphological observations, the gene expression profiles of phellem cells in multiple species also include genes involved in cell division, differentiation and cell wall organization. This is the case of *Cellulose Synthase-like D* (*CSLD*) and several expansins, which corroborates the ongoing cell expansion and suberization of cell walls for phellem maturation (Soler *et al.*, 2007; Vulavala *et al.*, 2017; Boher *et al.*, 2018; Wunderling *et al.*, 2018).

When suberization and cell expansion are complete, the final step of phellem maturation is cell death and complete emptying of the cellular content (Pereira, 2007; Campilho *et al.*, 2020). Programmed cell death markers are found in diverse plant species when mature phellem cells are analysed. Transcripts encoding oxylipins, that relate to jasmonic acid accumulation and programmed cell death or senescence, are commonly found in outer bark tissues of cork oak and poplar (Soler *et al.*, 2007; Rains *et al.*, 2018; Boher *et al.*, 2018). Also, regulated proteolysis-related transcripts known to be required for programmed cell death (Moreau et al., 2005), such as a *Cys protease* and a *Ub/26S proteasome system*, were found highly induced in phellem tissues of cork oak and potato (Soler et al., 2007, 2011; Vulavala et al., 2017). More specifically, marker genes related to programmed cell death, including RNS3, EXI1 and DPM4 are active specifically in some *Arabidopsis* phellem cells. Also in *Arabidopsis*, cell viability testes showed that the larger death cells were from phellem in the root, revealing that cell expansion anticipates cell death in the process of phellem maturation (Wunderling *et al.*, 2018).

3.2. Molecular regulation of phellem cell fate

In the last years, the molecular signatures of phellem cells have been addressed in transcriptomic studies, aiming to elucidate possible transcription factors and related hormonal pathways regulating the final fate of a phellogen cell in an mature phellem cell (Soler *et al.*, 2007, 2011; Ginzberg *et al.*, 2009; Vulavala *et al.*, 2017; Rains *et al.*, 2018; Boher *et al.*, 2018; Alonso-Serra *et al.*, 2019; Lopes *et al.*, 2019).

3.2.1. Hormonal control of phellem differentiation

Regarding hormonal control of phellem differentiation, very limited knowledge is available, however, several transcripts assigned to hormone metabolism and hormone responsive processes have been detected in several studies.

Auxin is discussed to be involved in the early differentiation of phellem, with auxin associated transcripts commonly found not only in differentiating phellem but also in the phellogen containing samples. Using laser dissected phellogen cells from cork oak Teixeira *et al.* (2018) could identify several transcripts associated with auxin. Using another sampling approach that joined differentiating phellem and a few phellogen cells from harvested cork oak outer barks (Lopes et al., 2019), several regulators related to auxin were detected, including the auxin responsive protein AUXIN/INDOLE ACETIC ACID (IAA) 31, IAA33, AUXIN RESPONSE FACTOR (ARF)18, as well as a TF reported as activator of auxin-mediated transcription, bZIP11. In potato, transcription of HOMEOBOX ARABIDOPSIS THALIANA3 (*HAT3*) was strongly expressed in phellogen sections (Vulavala et al., 2019). Interestingly, this TF was previously characterized to be involved in the control of meristematic activity through changes in auxin distribution and response (Turchi et al., 2013).

On the opposite, ethylene related transcripts are mostly found in mature phellem samples. In cork oak, when relating phellem with xylem transcripts, an overrepresentation of genes related to ethylene metabolism showed up in phellem tissues (Soler et al., 2007; Lopes et al., 2019). In potato tuber skin, ethylene has been shown to be involved in phellem differentiation, not only during normal phellem development, where Ethylene Responsive Factors (ERF) were identified (Vulavala et al., 2017), but also in heal wounding phellem formation, where production of ethylene is increased (Lulai & Suttle, 2009). Although in less extent, transcripts of ERFs, such as ethylene insensitive 3 (EIN3) and ethylene receptors (ETR1/ETR2) were also detected specifically in laser dissected phellogen tissues of *Q. suber* and potato, indicating that ethylene may be involved in the later steps of cell differentiation from phellogen into phellem (Teixeira et al., 2018; Vulavala et al., 2019). The ethylene is proposed to play a similar role in phellem as in xylem formation, where it leads the transcriptional reprogramming of vascular meristematic cells for xylem differentiation and expansion (Soler et al., 2007; Seyfferth et al., 2018; Lopes et al., 2019). However, ethylene function in developing phellem cells is still unclear.

Jasmonic acid associated transcripts were equally detected in phellem in diverse studies. In cork oak and in poplar outer barks, phellem transcriptome revealed the presence of lipoxygenases (*LOXs)* and putative lipase transcripts, that are described to be involved in the synthesis of jasmonic acid (Soler *et al.*, 2007; Rains *et al.*, 2018). Also, *CYP82D*, that has been reported as a modulator of the octadecanoid pathway through which jasmonic acid is produced (Sun et al., 2014), was recently detected in cork oak phellem (Lopes et al., 2019). Moreover, genes related to oxylipin metabolism are also strongly enriched in cork accumulating barks (Boher et al., 2018), which could be related to jasmonic acid accumulation and its role in programmed cell

death or senescence (Reinbothe et al., 2009). Common detection of ethylene and jasmonate related genes can be considered relevant for phellem differentiation (Lulai & Suttle, 2009; Lopes *et al.*, 2019) as the cross-talk between the two is described to be required and can coordinate plant growth and developmental events (Zhu, 2014).

Experimental determination of hormone levels on the different periderm tissues is not yet described, although it would be an important step to understand periderm development process. Nevertheless, the current results indicate that hormonal control could work in periderm tissues, in an model likely analogous to that proposed for wood formation, with hormonal and corresponding gene transcriptional gradients of different hormones across the different developing tissues of phellem, phellogen and phelloderm (Immanen et al., 2016; Alonso-Serra et al., 2019).

3.2.2. Transcription factors regulating meristem maintenance and phellem differentiation

Several lines of evidence have indicated that although the structure of the plant meristems differs, there are commonalities in the molecular mechanisms underlying their function. Comparisons between lateral meristems and/or apical meristems have identified not only many common regulatory components, such as TFs, cyclins, or receptor-like-kinases, but also characteristics that are specific for each of the meristems (Schrader et al., 2004; Baucher et al., 2007; Du et al., 2010; Fischer et al., 2019).

The *Arabidopsis* SHORT ROOT (SHR) characterized as key regulator of radial patterning and stem cell niche specification in the root apical meristem (Helariutta et al., 2000; Nakajima et al., 2001), was also identified in woody species with a suggested role in root vascular meristem formation and maintenance (Solé et al., 2008; Gaboreanu et

al., 2011; Miguel et al., 2011). Contrastingly, a poplar orthologue, SHORT-ROOT 2B (SHR2B), was shown as specifically expressed in the stem phellogen, and its ectopic expression lead to an increased proportion of outer bark relative to wood (Miguel et al., 2016). The constitutive expression of SHR2B also lead to increased transcript levels of cytokinin metabolism and response-related genes, as well as to an increase in total cytokinin levels. The work by Miguel et al. (2016) provided the first functional validation of a TF specifically involved in phellem differentiation, possibly through modulation of cytokinin homeostasis. In fact, *Arabidopsis* mutants defective in cytokinin biosynthesis develop thinner roots, a phenotype that can be rescued by exogenous cytokinin application (Matsumoto-Kitano et al., 2008). These evidences highlight the involvement of cytokinin in the regulation of secondary growth in plants. Some authors already reported expression of cytokinin-regulated transcripts in cambium cells, including the ARR5, specifically expressed in potato phellogen cells (Vulavala et al., 2019), and ARR15, expressed in both lateral cambium cells of *Arabidopsis* roots (Zhang et al., 2019).

Cytokinins can induce the CYCD3;1, a conserved regulatory sub-unit of the cyclin D-cyclin-dependent kinase (CYCD-CDK) complex that promote cell cycle progression, and is expressed, not only in vascular cambium, but also in phellogen (Randall et al., 2015). In vascular cambium, CYCD3;1 is activated by AINTEGUMENTA (ANT) in a cytokinin-dependent manner (Randall et al., 2015). While expression of *ANT* has been only detected once in phellogen tissues (Alonso-Serra *et al.*, 2019), it is tempting to speculate that in the cork cambium there is an analogous ANT-mediated regulation of CYCD3;1 (Campilho *et al.*, 2020). Contradictory to these observation, cytokinin signalling-related genes are not over-represented in phellogen or phellem tissues analysed by RNA-sequencing, including in poplar outer barks, where

SHR2B was implied to act in phellem determination through cytokinin management.

Other genes putatively related to meristem function, also identified in phellem, include the WUSCHEL-related homeobox (WOX) family of TFs. These TFs have been shown to be involved in the induction of cell division and/or prevention of premature cell differentiation in diverse processes of tissue differentiation (Gaillochet & Lohmann, 2015). *WOX4*, that was associated to vascular cambium activity (Nieminen et al., 2015; Zhang et al., 2019), was identified in phellogen and phellem transcriptomic studies (Boher *et al.*, 2018; Alonso-Serra *et al.*, 2019). In birch, *WOX4* transcription was detected at both vascular cambium and phellogen fractions, when compared to xylem fraction (Alonso-Serra *et al.*, 2019). In a comparison of phellem transcriptomes from *Quercus suber* and *Quercus ilex* species, *WOX4* expression was strongly detected in *Quercus suber* bark (Boher et al., 2018) and this was also the case of the orthologue of SHOOT-MERISTEMLESS (*STM*). While *WOX4* has been shown to trigger cambial proliferation (Ji et al., 2010), *STM* was described to promote cell differentiation in secondary growth (Liebsch *et al.*, 2014). This suggests that the higher expression of these TFs in *Q. suber* may be required to maintain a stronger meristematic activity for a longer period, thus allowing the formation of more phellem daughter cells in this species (Boher et al., 2018). In addition to *WOX4*, other *WOX* orthologues were also found exclusively represented in phellem tissues (when compared to xylem), as WOX9 in phellem of *Quercus suber* (Lopes et al., 2019) and WOX9 and WOX1 in different stages of development of poplar phellem (Rains *et al.*, 2018). Previous reports describe WOX1 as confined to the initiating vascular primordium of the cotyledons during heart and torpedo stages (Haecker et al., 2004; Zhang et al., 2011). Additionally, WOX9 is associated to post-embryonic development, acting in promoting cell proliferation and preventing

premature differentiation in meristematic tissues of *Arabidopsis* (Wu *et al.*, 2007). The exclusive presence of WOX1 and WOX9 transcripts in phellem tissues may indicate an additional role of these TFs in secondary development, specifically in phellem cell fate.

The LATERAL ORGAN BOUNDARIES DOMAIN (LBD) family displays high functional diversity in regulating a large number of developmental and metabolic processes in higher plants, including meristem programming and vascular patterning (Xu *et al.*, 2016). In poplar vascular cambium, LBD1 promotes the expression of ALTERED PHLOEM DEVELOPMENT (APL) and restricts the expression of ARK1 and ARK2, which are involved in maintaining the cambium meristems (Yordanov *et al.*, 2010). In addition to other LBD genes, the expression of a *Lateral Organ Boundaries 1* (*LOB1)* orthologue was reported in phellem tissues from cork oak, birch and poplar (Rains *et al.*, 2018; Alonso-Serra *et al.*, 2019; Lopes *et al.*, 2019). This suggests that LBD may also play a role in cambium and/or in promoting tissue differentiation in periderm, in a similar way as proposed for poplar wood formation (Yordanov *et al.*, 2010; Lopes *et al.*, 2019).

Among the TFs commonly identified in transcriptomic analysis of phellogen and phellem there are several TF from the MYB, NAC and WRKY families. Many of these TFs lack a direct association with meristematic functions, however many have been associated with suberin accumulation, being in this way considered regulators of phellem differentiation. Examples of such genes are the *RAX3/MYB84* (*QsMYB1*), *MYB9*, *MYB107*, *MYB41* and potato NAC101 and *NAC103* (Almeida *et al.*, 2013; Kosma *et al.*, 2014; Lashbrooke *et al.*, 2016; Verdaguer *et al.*, 2016; Soler *et al.*, 2020), which were already described in section 2.4.

One of the most studied TFs associated with suberization in phellem cells is the RAX3/MYB84 (QsMYB1), that was found to be expressed in cork oak (Lopes et al., 2019), birch (Alonso-Serra *et al.*, 2019), poplar (Rains *et al.*, 2018), and *Arabidopsis* (Wunderling *et al.*, 2018) periderms. In *Arabidopsis*, RAX3/MYB84 was previously reported as expressed in the pericycle dividing for periderm formation (Wunderling *et al.*, 2018). This gene is partially redundant with other two RAX genes (RAX1 and RAX2) that have been associated with the control of lateral meristem initiation, through the regulation of axillary meristems (Feng *et al.*, 2004; Müller *et al.*, 2006).

Collectively, the several studies already conducted across different plant species highlighted a set of common regulators operating in phellem differentiation. However, despite all these clues, further functional analysis of the candidate phellem fate regulators should be considered, specially aiming to clarify the function of common regulators between meristems, or other differentiated tissues.

3.3. Plant models for molecular phellem differentiation studies

Different plant models have been used with different approaches to study phellem development. These models range from herbaceous to woody species and include not only secondary growth, but also phellem tissues of other origins such as potato and fruit skin or wound healing periderms.

The technical difficulties of harvesting isolated phellem tissues encourage the selection of tree models with high accumulation of phellem cells and easy debarking processes, to facilitate studying almost pure phellem cells. Also, availability of genome information and possibility of genetic transformation for further functional studies are attractive characteristics for developmental studies of phellem. Recently, several high-quality transcriptomic studies targeting phellem

tissues of trees have been released, including cork oak, birch, and poplar (Rains *et al.*, 2018; Boher *et al.*, 2018; Alonso-Serra *et al.*, 2019; Lopes *et al.*, 2019). Despite the time required for the development of a suberized outer bark, these tree models show phellem accumulation and easy access of phellem cells in outer barks, besides the availability of a sequenced genome.

Cork oak is the paradigm for phellem development because each year it produces about 60 layers of almost pure cork cells containing high amounts of suberin (Pereira, 2007). In addition, the chemical and physical properties of commercial cork are well known, as they justify the economic importance of this species. Historically it was the first model to have a molecular fingerprint of phellem cells, with the release of the first markers for phellem development and suberization (Soler et al., 2007). Since then, and with the recent release of the cork oak genome (Ramos et al., 2018), several other transcriptomic analyses targeting periderm tissues also came out, including targeted analysis of phellem (Alonso-Serra *et al.*, 2019; Lopes *et al.*, 2019) and phellogen tissues (Teixeira *et al.*, 2018; Alonso-Serra *et al.*, 2019). Poplar (such as *Populus tremula* x *P. alba* hybrid and *Populus tremula L*. × *Populus tremuloides* hybrid) has long been used as model tree to study secondary growth, mainly because of its high annual growth rate and efficient tools for genetic manipulation (as compared to other woody species). Adding to the extensive transcriptomic analysis of phellem developmental stages (Rains *et al.*, 2018), it was possible to use poplar to functionally characterize TF SHR2B in phellem formation (Miguel et al., 2016). Birch species (*Betula pendula*, *Alnus glutinosa*) have been also used to study phellem development, mainly due to the striking contrast of outer bark phenotypes within the same family, thus providing a good comparative system to study phellem development (Alonso-Serra *et al.*, 2019). Despite all these high informative studies, the

functional assessment of phellem molecular regulators is still difficult to perform in trees, due to their size, long life cycle, very long regeneration times to obtain genetically modified plants for functional validations, and even low transformation rates. On the other hand, potato phellem development has been extensively studied, as periderm cells can be easily isolated from the tuber in sufficient amounts for diverse analyses. Potato plants are easy to grow and to manipulate in laboratory, and its efficient genetic transformation have allowed several functional studies of different regulators and enzymes related to phellem development and suberization (Serra *et al.*, 2010b; Boher *et al.*, 2013; Bjelica *et al.*, 2016). Also, transcriptomic studies in periderm tissues of potato, including approaches directly targeting the phellogen, have revealed important molecular players in the phellem differentiation process (Ginzberg et al., 2009; Soler et al., 2011; Vulavala et al., 2017).

With the increasing interest in the study of phellem development and suberization, the use of *Arabidopsis thaliana* has also proved as an excellent model system, given the comprehensive knowledge on its genome structure, small size and short life cycle, easy manipulation, and large collection of knock-out mutants. Recently, a framework of root periderm development was presented (Wunderling *et al.*, 2018), from the initial pericycle cell division to the full ring of differentiated and outer phellem cells. This study also showed that *Arabidopsis* periderm shares basic structural characteristics with that of woody plants, and the role of some identified specific regulators, such as *MYB84,* is also conserved in *Arabidopsis*.

4. Objectives and thesis outline [1]

Currently, the molecular regulation of phellem differentiation is not very well understood, mostly because functional studies on a secondary developmental process are not easy to undertake. This thesis work was designed to gather data to better understand, at morphologic and molecular levels, the phellem development, with particular focus on suberization. Q. suber (cork oak) was selected as model of interest, mostly because its cork bark has added economic value for a wide range of applications, and its suberin content is the major determinant of its unique physical properties. The fact that cork bark extraction is performed in conditions of drought and heat, and the subsequent phellem development is initiated in these conditions, raised our interest to study how the phellem development, and particularly suberization, are modulated by these environmental cues.

As secondary development on cork oak takes too long to initiate, we used the root as proxy model to study the phellem development. In complementation, and because of the shortage of molecular tools and technical difficulties associated to the study of a secondary development process in cork oak, we used Arabidopsis thaliana roots for a deeper and targeted study of phellem differentiation.

With the use of both models, this PhD research aims to address the following questions:

- What is the morphology and timeline of root phellem differentiation and suberization?
- What are the molecular mechanisms controlling initial root phellem development?
- What is the impact of heat and osmotic stress on root phellem development and suberization?

We started with a spatial and temporal histological analysis of the suberization (using suberin staining and gene expression studies) of

Arabidopsis and cork oak roots (Chapters II and IV, respectively). In Arabidopsis, we further described the translatome of initial phellem cells, obtained by Translating Ribosome Affinity Purification followed by mRNA sequencing (TRAP-SEQ). In turn, for cork oak, we performed a comparative transcriptomic analysis of root segments undergoing secondary and primary development.

To study how phellem suberization and development can be affected by heat and osmotic stresses, we applied these conditions targeting the moment of initial phellem development (previously defined) in both Arabidopsis and cork oak. To get an insight on the stress impact, we applied a combination of heat and osmotic stress on Arabidopsis, and described the effect on the overall root suberization, studied by the suberin specific staining and gene expression (Chapter III). In parallel, cork oak root development and suberization were monitored, particularly in the secondary development zone, throughout independent and combined osmotic and heat stress treatments. In addition, these cork oak secondary developed root segments were targeted in a transcriptomic analysis (Chapter V). Lastly, we highlight the significance of the results presented and how further studies will deepen the knowledge created in phellem development and suberization

[1] In the Chapter organization, the numbering of Figures and Tables is always made referring to that specific chapter, unless otherwise indicated.

5. Bibliography

Almeida T, Menéndez E, Capote T, Ribeiro T, Santos C, Gonçalves S. **2013**. Molecular characterization of Quercus suber MYB1, a transcription factor up-regulated in cork tissues. *Journal of Plant Physiology* **170**: 172–178.

Alonso-Serra J, Safronov O, Lim K, Fraser-Miller SJ, Blokhina OB, Campilho A, Chong S, Fagerstedt K, Haavikko R, Helariutta Y, *et al.* 2019. Tissue-specific study across the stem reveals the chemistry and transcriptome dynamics of birch bark. *New Phytologist* **222**: 1816–1831.

Andersen TG, Barberon M, Geldner N. **2015**. Suberization-the second life of an endodermal cell. *Current Opinion in Plant Biology* **28**: 9–15.

Bach L, Michaelson L V., Haslam R, Bellec Y, Gissot L, Marion J, Da Costa M, Boutin

J-P, Miquel M, Tellier F, *et al.* 2008. The very-long-chain hydroxy fatty acyl-CoA dehydratase PASTICCINO2 is essential and limiting for plant development. *Proceedings of the National Academy of Sciences* **105**: 14727–14731.

Barberon M. **2017**. The endodermis as a checkpoint for nutrients. *New Phytologist* **213**: 1604–1610.

Barberon M, Vermeer JEM, De Bellis D, Wang P, Naseer S, Andersen TG, Humbel BM, Nawrath C, Takano J, Salt DE, *et al.* 2016. Adaptation of Root Function by Nutrient-Induced Plasticity of Endodermal Differentiation. *Cell* **164**: 447–459.

Baucher M, Jaziri M El, Vandeputte O. **2007**. From primary to secondary growth : origin and development of the vascular system. **58**: 3485–3501.

Baxter I, Hosmani PS, Rus A, Lahner B, Borevitz JO, Balasubramaniam M, Mickelbart M V., Schreiber L, Franke RB, Salt DE. **2009**. Root suberin forms an extracellular barrier that affects water relations and mineral nutrition in Arabidopsis. *PLoS Genetics* **5**.

Beaudoin F, Wu X, Li F, Haslam RP, Markham JE, Zheng H, Napier JA, Kunst L. **2009**. Functional Characterization of the Arabidopsis β -Ketoacyl-Coenzyme A Reductase Candidates of the Fatty Acid Elongase. *Plant Physiology* **150**: 1174–1191.

Beisson F, Li Y, Bonaventure G, Pollard M, Ohlrogge JB. **2007**. The acyltransferase GPAT5 is required for the synthesis of suberin in seed coat and root of Arabidopsis. *The Plant cell* **19**: 351–368.

Berhin A, de Bellis D, Franke RB, Buono RA, Nowack MK, Nawrath C. **2019**. The Root Cap Cuticle: A Cell Wall Structure for Seedling Establishment and Lateral Root Formation. *Cell* **176**: 1367-1378.e8.

Bernards MA. **2002**. Demystifying suberin. *Canadian Journal of Botany* **80**: 227–240.

Bernards MA, Fleming WD, Llewellyn DB, Priefer R, Yang X, Sabatino A, Plourde GL. **1999**. Biochemical characterization of the suberization-associated anionic peroxidase of potato. *Plant Physiology* **121**: 135–145.

Bernards MA, Lewis NG. **1998**. The macromolecular aromatic domain in suberized tissue: A changing paradigm. *Phytochemistry* **47**: 915–933.

Bernards MA, Lopez ML, Zajicek J, Lewis NG. **1995**. Hydroxycinnamic Acid-derived Polymers Constitute the Polyaromatic Domain of Suberin. *Journal of Biological Chemistry* **270**: 7382–7386.

Bernards M a, Razem F a. **2001**. The poly(phenolic) domain of potato suberin: a non-lignin cell wall bio-polymer. *Phytochemistry* **57**: 1115–1122.

Bjelica A, Haggitt ML, Woolfson KN, Lee DPN, Makhzoum AB, Bernards MA. **2016**. Fatty acid ω-hydroxylases from Solanum tuberosum. *Plant Cell Reports* **35**: 2435–2448.

Blacklock BJ, Jaworski JG. **2006**. Substrate specificity of Arabidopsis 3-ketoacyl-CoA synthases. *Biochemical and Biophysical Research Communications* **346**: 583–590.

Boher P, Serra O, Soler M, Molinas M, Figueras M. **2013**. The potato suberin feruloyl transferase FHT which accumulates in the phellogen is induced by wounding and regulated by abscisic and salicylic acids. *Journal of Experimental Botany* **64**: 3225–3236.

Boher P, Soler M, Sánchez A, Hoede C, Noirot C, Paiva JAP, Serra O, Figueras M. **2018**. A comparative transcriptomic approach to understanding the formation of cork. *Plant Molecular Biology* **96**: 103–118.

Campilho A, Nieminen K, Ragni L. **2020**. The development of the periderm: the final frontier between a plant and its environment. *Current Opinion in Plant Biology* **53**: 10–14.

Capote T, Barbosa P, Usié A, Ramos AM, Inácio V, Ordás R, Gonçalves S, Morais-Cecílio L. **2018**. ChIP-Seq reveals that QsMYB1 directly targets genes involved in lignin and suberin biosynthesis pathways in cork oak (Quercus suber). *BMC Plant Biology* **18**: 1–19.

Carranza MG, Sevigny MB, Banerjee D, Fox-Cubley L. **2015**. Antibacterial activity of native California medicinal plant extracts isolated from Rhamnus californica and Umbellularia californica. *Annals of Clinical Microbiology and Antimicrobials* **14**: 29.

Cohen H, Dong Y, Szymanski J, Lashbrooke J, Meir S, Almekias-Siegl E, Zeisler-Diehl

VV, Schreiber L, Aharoni A. **2019**. A multilevel study of melon fruit reticulation provides insight into skin ligno-suberization hallmarks. *Plant Physiology* **179**: 1486–1501.

Cominelli E, Sala T, Calvi D, Gusmaroli G, Tonelli C. **2008**. Over-expression of the Arabidopsis AtMYB41 gene alters cell expansion and leaf surface permeability. *Plant Journal* **53**: 53–64.

Compagnon V, Diehl P, Benveniste I, Meyer D, Schaller H, Schreiber L, Franke R, Pinot F. **2009**. CYP86B1 Is Required for Very Long Chain ω -Hydroxyacid and α , ω -Dicarboxylic Acid Synthesis in Root and Seed Suberin Polyester. *Plant Physiology* **150**: 1831–1843.

Cottle W, Kolattukudy PE. **1982**. Abscisic Acid Stimulation of Suberization. *Plant Physiology* **70**: 775–780.

Crang R, Lyons-Sobaski S, Wise R. **2018**. *Plant Anatomy*. Cham: Springer International Publishing.

Crouvisier-Urion K, Chanut J, Lagorce A, Winckler P, Wang Z, Verboven P, Nicolai B, Lherminier J, Ferret E, Gougeon RD, *et al.* 2019. Four hundred years of cork imaging: New advances in the characterization of the cork structure. *Scientific Reports* **9**: 1–10.

Debono A, Yeats TH, Rose JKC, Bird D, Jetter R, Kunst L, Samuels L. **2009**. Arabidopsis LTPG Is a Glycosylphosphatidylinositol-Anchored Lipid Transfer Protein Required for Export of Lipids to the. **21**: 1230–1238.

Deeken R, Saupe S, Klinkenberg J, Riedel M, Leide J, Hedrich R, Mueller TD. **2016**. The Nonspecific Lipid Transfer Protein AtLtpI-4 Is Involved in Suberin Formation of Arabidopsis thaliana Crown Galls. *Plant Physiology* **172**: 1911–1927.

Doblas VG, Geldner N, Barberon M. **2017**. The endodermis, a tightly controlled barrier for nutrients. *Current Opinion in Plant Biology* **39**: 136–143.

Dolan L, Janmaat K, Willemsen V, Linstead P, Poethig S, Roberts K, Scheres B. **1993**. Cellular organisation of the Arabidopsis thaliana root. *Development* **119**: 71–84.

Domergue F, Kosma DK. **2017**. Occurrence and Biosynthesis of Alkyl Hydroxycinnamates in Plant Lipid Barriers. : 1–17.

Domergue F, Vishwanath SJ, Joubès J, Ono J, Lee JA, Bourdon M, Alhattab R, Lowe C, Pascal S, Lessire R, *et al.* 2010. Three Arabidopsis fatty acyl-coenzyme A reductases, FAR1, FAR4, and FAR5, generate primary fatty alcohols associated with suberin deposition. *Plant physiology* **153**: 1539–54.

Du J, Groover A, Groover A. **2010**. Transcriptional Regulation of Secondary Growth and Wood Formation. **52**: 17–27.

Du YP, Wang ZS, Zhai H. **2011**. Grape root cell features related to phylloxera resistance and changes of anatomy and endogenous hormones during nodosity and tuberosity formation. *Australian Journal of Grape and Wine Research* **17**: 291–297.

Durst F, Salau J, Tijet N, Helvig C, Pinot F, Bouquin RLE. **1998**. plant cytochrome P - 450 (CYP94A1) involved in cutin monomers synthesis. **589**: 583–589.

Edqvist J, Blomqvist K, Nieuwland J, Salminen TA. **2018**. Plant lipid transfer proteins : are we finally closing in on the roles of these enigmatic proteins ? **59**.

Enstone DE, Peterson C a., Ma F. **2002**. Root endodermis and exodermis: Structure, function, and responses to the environment. *Journal of Plant Growth Regulation* **21**: 335–351.

Espelie KE, Kolattukudy PE. **1985**. Purification and characterization of an abscisic acid-inducible anionic peroxidase associated with suberization in potato (Solanum tuberosum). *Archives of Biochemistry and Biophysics* **240**: 539–545.

Evert RF. **2006**. *Esau's Plant Anatomy*. Hoboken, NJ, USA: John Wiley & Sons, Inc.

Fasoli M, Dal Santo S, Zenoni S, Tornielli GB, Farina L, Zamboni A, Porceddu A, Venturini L, Bicego M, Murino V, *et al.* 2012. The grapevine expression atlas reveals a deep transcriptome shift driving the entire plant into a maturation program. *Plant Cell* **24**: 3489–3505.

Fedi F, Neill CMO, Menard G, Trick M, Dechirico S, Corbineau F, Bailly C, Eastmond PJ, Pen S. **2017**. Awake1 , an ABC-Type Transporter , Reveals an Essential Role for Suberin in the Control of Seed Dormancy [OPEN]. **174**: 276–283.

Feng C, Andreasson E, Maslak A, Mock HP, Mattsson O, Mundy J. **2004**. Arabidopsis

MYB68 in development and responses to environmental cues. *Plant Science* **167**: 1099–1107.

Ferreira JPA, Quilhó T, Pereira H. **2017**. Characterization of Betula pendula Outer Bark Regarding Cork and Phloem Components at Chemical and Structural Levels in View of Biorefinery Integration. *Journal of Wood Chemistry and Technology* **37**: 10–25.

Fich EA, Segerson NA, Rose JKC. **2016**. The Plant Polyester Cutin: Biosynthesis, Structure, and Biological Roles. *Annual Review of Plant Biology* **67**: 207–233.

Fischer U, Kucukoglu M, Helariutta Y, Bhalerao RP. **2019**. The Dynamics of Cambial Stem Cell Activity. *Annual Review of Plant Biology* **70**: annurev-arplant-050718-100402.

Franke RB, Dombrink I, Schreiber L. **2012**. Suberin Goes Genomics: Use of a Short Living Plant to Investigate a Long Lasting Polymer. *Frontiers in Plant Science* **3**: 1–8.

Franke R, Höfer R, Briesen I, Emsermann M, Efremova N, Yephremov A, Schreiber L. **2009**. The DAISY gene from Arabidopsis encodes a fatty acid elongase condensing enzyme involved in the biosynthesis of aliphatic suberin in roots and the chalaza-micropyle region of seeds. *Plant Journal* **57**: 80–95.

Franke R, Schreiber L. **2007**. Suberin - a biopolyester forming apoplastic plant interfaces. *Current Opinion in Plant Biology* **10**: 252–259.

Gaboreanu I, Hertzberg M, Matthew R, Wang J, Andersson-gunnera S, Mellerowicz EJ, Laux T, Zheng B, Les J. **2011**. Reduced Expression of the SHORT-ROOT Gene Increases the Rates of Growth and Development in Hybrid Poplar and Arabidopsis. **6**: 1–9.

Gaillochet C, Lohmann JU. **2015**. The never-ending story: From pluripotency to plant developmental plasticity. *Development (Cambridge)* **142**: 2237–2249.

Gibbs DJ, Voß U, Harding SA, Fannon J, Moody LA, Yamada E, Swarup K, Nibau C, Bassel GW, Choudhary A, *et al.* 2014. At MYB93 is a novel negative regulator of lateral root development in Arabidopsis. *New Phytologist* **203**: 1194–1207.

Ginzberg I. **2008**. Wound-Periderm Formation. In: Induced Plant Resistance to Herbivory. Dordrecht: Springer Netherlands, 131–146.

Ginzberg I, Barel G, Ophir R, Tzin E, Tanami Z, Muddarangappa T, De Jong W, Fogelman E. **2009**. Transcriptomic profiling of heat-stress response in potato periderm. *Journal of Experimental Botany* **60**: 4411–4421.

Gou M, Hou G, Yang H, Zhang X, Cai Y, Kai G, Liu C-J. **2017**. The MYB107 Transcription Factor Positively Regulates Suberin Biosynthesis. *Plant Physiology* **173**: 1045–1058.

Gou JY, Yu XH, Liu CJ. **2009**. A hydroxycinnamoyltransferase responsible for synthesizing suberin aromatics in Arabidopsis. *Proceedings of the National Academy of Sciences of the United States of America* **106**: 18855–18860.

Graça J. **2015**. Suberin: the biopolyester at the frontier of plants. *Frontiers in Chemistry* **3**: 1–11.

Graça J, Cabral V, Santos S, Lamosa P, Serra O, Molinas M, Schreiber L, Kauder F, Franke R. **2015**. Partial depolymerization of genetically modified potato tuber periderm reveals intermolecular linkages in suberin polyester. *Phytochemistry* **117**: 209–219.

Graça J, Pereira H. **1997**. Cork Suberin: A Glyceryl Based Polyester. *Holzforschung* **51**: 225–234.

Graça J, Pereira H. **2000**. Suberin structure in potato periderm: Glycerol, long-chain monomers, and glyceryl and feruloyl dimers. *Journal of Agricultural and Food Chemistry* **48**: 5476–5483.

Graça J, Pereira H. **2004**. The periderm development in Quercus suber. *IAWA Journal* **25**: 325–335.

Groh B, Hübner C, Lendzian KJ. **2002**. Water and oxygen permeance of phellems isolated from trees: The role of waxes and lenticels. *Planta* **215**: 794–801.

Groover AT, Mansfield SD, DiFazio SP, Dupper G, Fontana JR, Millar R, Wang Y. **2006**. The Populus homeobox gene ARBORKNOX1 reveals overlapping mechanisms regulating the shoot apical meristem and the vascular cambium. *Plant Molecular Biology* **61**: 917–932.

Haecker A, Groß-Hardt R, Geiges B, Sarkar A, Breuninger H, Herrmann M, Laux T. **2004**. Expression dynamics of WOX genes mark cell fate decisions during early

embryonic patterning in Arabidopsis thaliana. *Development* **131**: 657–668.
Han X, Lu W, Wei X, Li L, Mao L, Zhao Y. **2018**. Proteomics analysis to understand the ABA stimulation of wound suberization in kiwifruit. *Journal of Proteomics* **173**: 42–51.
Han X, Mao L, Lu W, Wei X, Ying T, Luo Z. **2019**. Positive Regulation of the Transcription of AchnKCS by a bZIP Transcription Factor in Response to ABA-Stimulated Suberization of Kiwifruit. *Journal of Agricultural and Food Chemistry* **67**: 7390–7398.
Helariutta Y, Fukaki H, Wysocka-Diller J, Nakajima K, Jung J, Sena G, Hauser MT, Benfey PN. **2000**. The SHORT-ROOT gene controls radial patterning of the Arabidopsis root through radial signaling. *Cell* **101**: 555–567.
Heneen WK, Gustafsson M, Brismar K, Karlsson G. **1994**. Interactions between Norway spruce (Picea abies) and Heterobasidion annosum. II. Infection of woody roots. *Canadian Journal of Botany* **72**: 884–889.
Höfer R, Briesen I, Beck M, Pinot F, Schreiber L, Franke R. **2008**. The Arabidopsis cytochrome P450 CYP86A1 encodes a fatty acid ω-hydroxylase involved in suberin monomer biosynthesis. *Journal of Experimental Botany* **59**: 2347–2360.
Holbein J, Franke RB, Marhavý P, Fujita S, Górecka M, Sobczak M, Geldner N, Schreiber L, Grundler FMW, Siddique S. **2019**. Root endodermal barrier system contributes to defence against plant-parasitic cyst and root-knot nematodes. *The Plant Journal* **100**: 221–236.
Holloway PJ. **1983**. Some variations in the composition of suberin from the cork layers of higher plants. *Phytochemistry* **22**: 495–502.
Hose E, Clarkson DT, Steudle E, Schreiber L, Hartung W. **2001**. The exodermis: a variable apoplastic barrier. *Journal of experimental botany* **52**: 2245–2264.
Huysmans M, Buono RA, Skorzinski N, Radio MC, De Winter F, Parizot B, Mertens J, Karimi M, Fendrych M, Nowack MK. **2018**. NAC Transcription Factors ANAC087 and ANAC046 Control Distinct Aspects of Programmed Cell Death in the Arabidopsis Columella and Lateral Root Cap. *The Plant Cell* **30**: 2197–2213.
Jakobson L, Lindgren LO, Verdier G, Laanemets K, Brosché M, Beisson F, Kollist H. **2016**. BODYGUARD is required for the biosynthesis of cutin in Arabidopsis. *The New phytologist* **211**: 614–626.
Ji J, Strable J, Shimizu R, Koenig D, Sinha N, Scanlon MJ. **2010**. WOX4 Promotes Procambial Development. *Plant Physiology* **152**: 1346–1356.
Joubès J, Raffaele S, Bourdenx B, Garcia C, Laroche-Traineau J, Moreau P, Domergue F, Lessire R. **2008**. The VLCFA elongase gene family in Arabidopsis thaliana: phylogenetic analysis, 3D modelling and expression profiling. *Plant Molecular Biology* **67**: 547–566.
Kaufert F. **1937**. Factors Influencing the Formation of Periderm in Aspen. *American Journal of Botany* **24**: 24.
Kolattukudy PE, Kronman K, Poulose AJ. **1975**. Determination of Structure and Composition of Suberin from the Roots of Carrot, Parsnip, Rutabaga, Turnip, Red Beet, and Sweet Potato by Combined Gas-Liquid Chromatography and Mass Spectrometry. *Plant Physiology* **55**: 567–573.
Kosma DK, Molina I, Ohlrogge JB, Pollard M. **2012**. Identification of an Arabidopsis Fatty Alcohol:Caffeoyl-Coenzyme A Acyltransferase Required for the Synthesis of Alkyl Hydroxycinnamates in Root Waxes. *Plant Physiology* **160**: 237–248.
Kosma DK, Murmu J, Razeq FM, Santos P, Bourgault R, Molina I, Rowland O. **2014**. At <scp>MYB</scp> 41 activates ectopic suberin synthesis and assembly in multiple plant species and cell types. *The Plant Journal* **80**: 216–229.
Kreszies T, Eggels S, Kreszies V, Osthoff A, Shellakkutti N, Baldauf JA, Zeisler-Diehl V V., Hochholdinger F, Ranathunge K, Schreiber L. **2020**. Seminal roots of wild and cultivated barley differentially respond to osmotic stress in gene expression, suberization, and hydraulic conductivity. *Plant, Cell & Environment* **43**: 344–357.
Kreszies T, Schreiber L, Ranathunge K. **2018**. Suberized transport barriers in Arabidopsis, barley and rice roots: From the model plant to crop species. *Journal of Plant Physiology* **227**: 75–83.
Kurdyukov S, Faust A, Nawrath C, Bär S, Voisin D, Efremova N, Franke R, Schreiber

L, Saedler H, Métraux JP, *et al.* 2006. The epidermis-specific extracellular BODYGUARD controls cuticle development and morphogenesis in Arabidopsis. *Plant Cell* **18**: 321–339.

Landgraf R, Smolka U, Altmann S, Eschen-Lippold L, Senning M, Sonnewald S, Weigel B, Frolova N, Strehmel N, Hause G, *et al.* 2014. The ABC transporter ABCG1 is required for suberin formation in potato tuber periderm. *Plant Cell* **26**: 3403–3415.

Lashbrooke J, Cohen H, Levy-Samocha D, Tzfadia O, Panizel I, Zeisler V, Massalha H, Stern A, Trainotti L, Schreiber L, *et al.* 2016. MYB107 and MYB9 Homologs Regulate Suberin Deposition in Angiosperms. *The Plant Cell* **28**: 2097–2116.

Le BH, Cheng C, Bui AQ, Wagmaister JA, Henry KF, Pelletier J, Kwong L, Belmonte M, Kirkbride R, Horvath S, *et al.* 2010. Global analysis of gene activity during Arabidopsis seed development and identification of seed-specific transcription factors. *Proceedings of the National Academy of Sciences of the United States of America* **107**: 8063–8070.

Lee SB, Jung SJ, Go YS, Kim HU, Kim JK, Cho HJ, Park OK, Suh MC. **2009**. Two Arabidopsis 3-ketoacyl CoA synthase genes, KCS20 and KCS2/DAISY, are functionally redundant in cuticular wax and root suberin biosynthesis, but differentially controlled by osmotic stress. *Plant Journal* **60**: 462–475.

Lee SB, Suh MC. **2018**. Disruption of glycosylphosphatidylinositol-anchored lipid transfer protein 15 affects seed coat permeability in Arabidopsis. *Plant Journal* **96**: 1206–1217.

Legay S, Guerriero G, André C, Guignard C, Cocco E, Charton S, Boutry M, Rowland O, Hausman J-F. **2016**. MdMyb93 is a regulator of suberin deposition in russeted apple fruit skins. *New Phytologist* **212**: 977–991.

Legay S, Guerriero G, Deleruelle A, Lateur M, Evers D, André CM, Hausman JF. **2015**. Apple russeting as seen through the RNA-seq lens: strong alterations in the exocarp cell wall. *Plant Molecular Biology* **88**: 21–40.

Leide J, Hildebrandt U, Hartung W, Riederer M, Vogg G. **2012**. Abscisic acid mediates the formation of a suberized stem scar tissue in tomato fruits. *New Phytologist* **194**: 402–415.

Leite C, Pereira H. **2017**. Cork-Containing Barks—A Review. *Frontiers in Materials* **3**: 1–19.

Lendzian KJ. **2006**. Survival strategies of plants during secondary growth : barrier properties of phellems and lenticels towards water , oxygen , and carbon dioxide. **57**: 2535–2546.

Lewis NG, Davin LB, Sarkanen S. **1999**. The Nature and Function of Lignins. In: Comprehensive Natural Products Chemistry. Elsevier, 617–745.

Li-Beisson Y, Shorrosh B, Beisson F, Andersson MX, Arondel V, Bates PD, Baud S, Bird D, DeBono A, Durrett TP, *et al.* 2013. Acyl-Lipid Metabolism. *The Arabidopsis Book* **11**: e0161.

Li P, Yu Q, Gu X, Xu C, Qi S, Wang H, Zhong F, Baskin TI, Rahman A, Wu S. **2018**. Construction of a Functional Casparian Strip in Non-endodermal Lineages Is Orchestrated by Two Parallel Signaling Systems in Arabidopsis thaliana. *Current Biology* **28**: 2777-2786.e2.

Lopes MH, Gil AM, Silvestre AJD, Neto CP. **2000**. Composition of Suberin Extracted upon Gradual Alkaline Methanolysis of Quercus suber L. Cork. *Journal of Agricultural and Food Chemistry* **48**: 383–391.

Lopes ST, Sobral D, Costa B, Perdiguero P, Chaves I, Costa A, Miguel CM. **2019**. Phellem versus xylem: genome-wide transcriptomic analysis reveals novel regulators of cork formation in cork oak. *Tree Physiology*: 1–39.

Lu S, Song T, Kosma DK, Parsons EP, Rowland O, Jenks MA. **2009**. Arabidopsis CER8 encodes LONG-CHAIN ACYL-COA SYNTHETASE 1 (LACS1) that has overlapping functions with LACS2 in plant wax and cutin synthesis. **1**: 553–564.

Lulai EC, Freeman TP. **2001**. The importance of phellogen cells and their structural characteristics in susceptibility and resistance to excoriation in immature and mature potato tuber (Solanum tuberosum L.) Periderm. *Annals of Botany* **88**: 555–561.

Lulai EC, Suttle JC. **2004**. The involvement of ethylene in wound-induced suberization of

potato tuber (Solanum tuberosum L.): A critical assessment. *Postharvest Biology and Technology* **34**: 105–112.

Lulai EC, Suttle JC. **2009**. Signals involved in tuber wound-healing. *Plant Signaling and Behavior* **4**: 620–622.

Lulai EC, Suttle JC, Pederson SM. **2008**. Regulatory involvement of abscisic acid in potato tuber wound-healing. *Journal of Experimental Botany* **59**: 1175–1186.

Mahmood K, Zeisler-Diehl VV, Schreiber L, Bi Y, Rothstein SJ, Ranathunge K. **2019**. Overexpression of ANAC046 Promotes Suberin Biosynthesis in Roots of Arabidopsis thaliana. *International Journal of Molecular Sciences* **20**: 6117.

Marques AV, Pereira H. **2013**. Lignin monomeric composition of corks from the barks of Betula pendula, Quercus suber and Quercus cerris determined by Py-GC-MS/FID. *Journal of Analytical and Applied Pyrolysis* **100**: 88–94.

Matsumoto-Kitano M, Kusumoto T, Tarkowski P, Kinoshita-Tsujimura K, Václavíková KK, Miyawaki K, Kakimoto T. **2008**. Cytokinins are central regulators of cambial activity. *Proceedings of the National Academy of Sciences of the United States of America* **105**: 20027–31.

Mattinen ML, Filpponen I, Järvinen R, Li B, Kallio H, Lektinen P, Argyropoulos D. **2009**. Structure of the polyphenolic component of suberin isolated from potato (Solanum tuberosum war. Nikola). *Journal of Agricultural and Food Chemistry* **57**: 9747–9753.

Mauch-Mani B, Mauch F. **2005**. The role of abscisic acid in plant-pathogen interactions. *Current Opinion in Plant Biology* **8**: 409–414.

Mcfarlane HE, Watanabe Y, Yang W, Huang Y, Ohlrogge J, Samuels AL, H MSLY. **2014**. Golgi- and Trans-Golgi Network-Mediated Vesicle Trafficking Is Required for Wax Secretion from. **164**: 1250–1260.

Mertz R a, Brutnell TP. **2014**. Bundle sheath suberization in grass leaves: multiple barriers to characterization. *Journal of experimental botany* **65**: 3371–3380.

Meyer K, Cusumano JC, Somerville C, Chapple CCS. **1996**. Ferulate-5-hydroxylase from Arabidopsis thaliana defines a new family of cytochrome P450-dependent monooxygenases. *Proceedings of the National Academy of Sciences of the United States of America* **93**: 6869–6874.

Miguel A, Milhinhos A, Novák O, Jones B, Miguel CM. **2016**. The SHORT-ROOT -like gene PtSHR2B is involved in Populus phellogen activity. *Journal of Experimental Botany* **67**: 1545–1555.

Miguel A, Ricardo PC, Jones B, Miguel C. **2011**. Identification of a putative molecular regulator of cork cambium. *BMC Proceedings* **5**: P70.

Millar AA, Kunst L. **1997**. Very-long-chain fatty acid biosynthesis is controlled through the expression and specificity of the condensing enzyme. **12**: 121–131.

Moire L, Schmutz A, Buchala A, Yan B, Stark RE, Ryser U. **1999**. Glycerol is a suberin monomer. New experimental evidence for an old hypothesis. *Plant Physiology* **119**: 1137–1146.

Molina I, Li-Beisson Y, Beisson F, Ohlrogge JB, Pollard M. **2009**. Identification of an Arabidopsis feruloyl-coenzyme a transferase required for suberin synthesis. *Plant Physiology* **151**: 1317–1328.

Moreau C, Aksenov N, Lorenzo MG, Segerman B, Funk C, Nilsson P, Jansson S, Tuominen H. **2005**. A genomic approach to investigate developmental cell death in woody tissues of Populus trees. *Genome biology* **6**.

Müller D, Schmitz G, Theres K. **2006**. Blind Homologous R2R3 Myb Genes Control the Pattern of Lateral Meristem Initiation in Arabidopsis . *The Plant Cell* **18**: 586–597.

Nakajima K, Sena G, Nawy T, Benfey PN. **2001**. Intercellular movement of the putative transcription factor SHR in root patterning. *Nature* **413**: 307–311.

Naseer S, Lee Y, Lapierre C, Franke R, Nawrath C, Geldner N. **2012**. Casparian strip diffusion barrier in Arabidopsis is made of a lignin polymer without suberin. *Proceedings of the National Academy of Sciences* **109**: 10101–10106.

Nawrath C. **2002**. The Biopolymers Cutin and Suberin. *The Arabidopsis Book* **1**: e0021.

Nawrath C, Schreiber L, Franke RB, Geldner N, Reina-Pinto JJ, Kunst L. **2013**. Apoplastic diffusion barriers in Arabidopsis. *The Arabidopsis book / American Society of*

Plant Biologists **11**: e0167.
Negrel J, Pollet B, Lapierre C. **1996**. Ether-linked ferulic acid amides in natural and wound periderms of potato tuber. *Phytochemistry* **43**: 1195–1199.
Nieminen K, Blomster T, Helariutta Y, Mähönen AP. **2015**. Vascular Cambium Development. *The Arabidopsis Book* **13**: e0177.
Oda-Yamamizo C, Mitsuda N, Sakamoto S, Ogawa D, Ohme-Takagi M, Ohmiya A. **2016**. The NAC transcription factor ANAC046 is a positive regulator of chlorophyll degradation and senescence in Arabidopsis leaves. *Scientific Reports* **6**: 23609.
Pereira H. **2007**. *Cork: Biology, Production and Uses*. Elsevier.
Pinheiro C, Wienkoop S, de Almeida JF, Brunetti C, Zarrouk O, Planchon S, Gori A, Tattini M, Ricardo CP, Renaut J, *et al.* 2019. Phellem Cell-Wall Components Are Discriminants of Cork Quality in Quercus suber. *Frontiers in Plant Science* **10**: 1–15.
Pinot F, Beisson F. **2011**. Cytochrome P450 metabolizing fatty acids in plants: Characterization and physiological roles. *FEBS Journal* **278**: 195–205.
Rains MK, De Silva NDG, Molina I. **2018**. Reconstructing the suberin pathway in poplar by chemical and transcriptomic analysis of bark tissues. *Tree Physiology* **38**: 340–361.
Ramos AM, Usié A, Barbosa P, Barros PM, Capote T, Chaves I, Simões F, Abreu I, Carrasquinho I, Faro C, *et al.* 2018. The draft genome sequence of cork oak. *Scientific Data* **5**: 1–12.
Ranathunge K, Kim YX, Wassmann F, Kreszies T, Zeisler V, Schreiber L. **2017**. The composite water and solute transport of barley (Hordeum vulgare) roots: effect of suberized barriers. *Annals of botany* **119**: 629–643.
Ranathunge K, Schreiber L. **2011**. Water and solute permeabilities of Arabidopsis roots in relation to the amount and composition of aliphatic suberin. *Journal of Experimental Botany* **62**: 1961–1974.
Randall RS, Miyashima S, Blomster T, Zhang J, Elo A, Karlberg A, Immanen J, Nieminen K, Lee J-Y, Kakimoto T, *et al.* 2015. AINTEGUMENTA and the D-type cyclin CYCD3;1 regulate root secondary growth and respond to cytokinins. *Biology open*: 1–8.
Reinbothe C, Springer A, Samol I, Reinbothe S. **2009**. Plant oxylipins: Role of jasmonic acid during programmed cell death, defence and leaf senescence. *FEBS Journal* **276**: 4666–4681.
Rittinger PA, Biggs AR, Peirson DR. **1987**. Histochemistry of lignin and suberin deposition in boundary layers formed after wounding in various plant species and organs. *Canadian Journal of Botany* **65**: 1886–1892.
Roppolo D, De Rybel B, Tendon VD, Pfister A, Alassimone J, Vermeer JEM, Yamazaki M, Stierhof Y-D, Beeckman T, Geldner N. **2011**. A novel protein family mediates Casparian strip formation in the endodermis. *Nature* **473**: 380–383.
Rowland O, Domergue F. **2012**. Plant fatty acyl reductases: Enzymes generating fatty alcohols for protective layers with potential for industrial applications. *Plant Science* **193–194**: 28–38.
Sabba RP, Lulai EC. **2002**. Histological Analysis of the Maturation of Native and Wound Periderm in Potato (Solanum tuberosum L.) Tuber. *Annals of Botany* **90**: 1–10.
Santos S, Cabral V, Graça J. **2013**. Cork suberin molecular structure: Stereochemistry of the C18 epoxy and vic-diol ω-hydroxyacids and α,ω-diacids analyzed by nmr. *Journal of Agricultural and Food Chemistry* **61**: 7038–7047.
Santos S, Graça J. **2006**. Glycerol-ω-hydroxyacid-ferulic acid oligomers in cork suberin structure. *Holzforschung* **60**: 171–177.
Sato S, Tabata S, Hirakawa H, Asamizu E, Shirasawa K, Isobe S, Kaneko T, Nakamura Y, Shibata D, Aoki K, *et al.* 2012. The tomato genome sequence provides insights into fleshy fruit evolution. *Nature* **485**: 635–641.
Schneider K, Hövel K, Witzel K, Hamberger B, Schomburg D, Kombrink E, Stuible H-P. **2003**. The substrate specificity-determining amino acid code of 4-coumarate:CoA ligase. *Proceedings of the National Academy of Sciences* **100**: 8601–8606.
Schoch G, Goepfert S, Morant M, Hehn A, Meyer D, Ullmann P, Werck-Reichhart D. **2001**. CYP98A3 from Arabidopsis thaliana Is a 3′-Hydroxylase of Phenolic Esters, a

Missing Link in the Phenylpropanoid Pathway. *Journal of Biological Chemistry* **276**: 36566–36574.

Schrader J, Nilsson J, Mellerowicz E, Berglund A, Nilsson P, Hertzberg M. **2004**. A High-Resolution Transcript Profile across the Wood-Forming Meristem of Poplar Identifies Potential Regulators of Cambial Stem Cell Identity. **16**: 2278–2292.

Schreiber L. **2010**. Transport barriers made of cutin, suberin and associated waxes. *Trends in Plant Science* **15**: 546–553.

Schreiber L, Franke R, Hartmann K. **2005a**. Wax and suberin development of native and wound periderm of potato (Solanum tuberosum L.) and its relation to peridermal transpiration. *Planta* **220**: 520–530.

Schreiber L, Franke R, Hartmann K. **2005b**. Effects of NO 3 deficiency and NaCl stress on suberin deposition in rhizo- and hypodermal (RHCW) and endodermal cell walls (ECW) of castor bean (Ricinus communis L.) roots. *Plant and Soil* **269**: 333–339.

Schreiber L, Hartmann K, Skrabs M, Zeier J. **1999**. Apoplastic barriers in roots: chemical composition of endodermal and hypodermal cell walls. *Journal of Experimental Botany* **50**: 1267–1280.

Serra O, Figueras M, Franke R, Prat S, Molinas M. **2010a**. Unraveling ferulate role in suberin and periderm biology by reverse genetics. *Plant Signaling and Behavior* **5**: 953–958.

Serra O, Hohn C, Franke R, Prat S, Molinas M, Figueras M. **2010b**. A feruloyl transferase involved in the biosynthesis of suberin and suberin-associated wax is required for maturation and sealing properties of potato periderm. *The Plant Journal* **62**: 277–290.

Serra O, Soler M, Hohn C, Sauveplane V, Pinot F, Franke R, Schreiber L, Prat S, Molinas M, Figueras M. **2009**. CYP86A33 -Targeted Gene Silencing in Potato Tuber Alters Suberin Composition, Distorts Suberin Lamellae, and Impairs the Periderm's Water Barrier Function. *Plant Physiology* **149**: 1050–1060.

Seyfferth C, Wessels B, Jokipii-Lukkari S, Sundberg B, Delhomme N, Felten J, Tuominen H. **2018**. Ethylene-related gene expression networks in wood formation. *Frontiers in Plant Science* **9**: 1–17.

Shanmugarajah K, Linka N, Gräfe K, Smits SHJ, Weber APM, Zeier J, Schmitt L. **2019**. ABCG1 contributes to suberin formation in Arabidopsis thaliana roots. *Scientific Reports* **9**: 11381.

Shiono K, Yamauchi T, Yamazaki S, Mohanty B, Imran Malik A, Nagamura Y, Nishizawa NK, Tsutsumi N, Colmer TD, Nakazono M. **2014**. Microarray analysis of laser-microdissected tissues indicates the biosynthesis of suberin in the outer part of roots during formation of a barrier to radial oxygen loss in rice (Oryza sativa). *Journal of Experimental Botany* **65**: 4795–4806.

Silva SP, Sabino MA, Fernandes EM, Correlo VM, Boesel LF, Reis RL. **2005**. Cork: properties, capabilities and applications. *International Materials Reviews* **50**: 345–365.

Smetana O, Mäkilä R, Lyu M, Amiryousefi A, Sánchez Rodríguez F, Wu MF, Solé-Gil A, Leal Gavarrón M, Siligato R, Miyashima S, *et al.* 2019. High levels of auxin signalling define the stem-cell organizer of the vascular cambium. *Nature* **565**: 485–489.

Solé A, Sánchez C, Vielba JM, Valladares S, Abarca D, Díaz-sala C. **2008**. Characterization and expression of a Pinus radiata putative ortholog to the Arabidopsis SHORT-ROOT gene. : 1629–1639.

Soler M, Serra O, Fluch S, Molinas M, Figueras M. **2011**. A potato skin SSH library yields new candidate genes for suberin biosynthesis and periderm formation. *Planta* **233**: 933–945.

Soler M, Serra O, Molinas M, García-Berthou E, Caritat A, Figueras M. **2008**. Seasonal variation in transcript abundance in cork tissue analyzed by real time RT-PCR. *Tree physiology* **28**: 743–751.

Soler M, Serra O, Molinas M, Huguet G, Fluch S, Figueras M. **2007**. A Genomic Approach to Suberin Biosynthesis and Cork Differentiation. *Plant Physiology* **144**: 419–431.

Soler M, Verdaguer R, Fernández-Piñán S, Company-Arumí D, Boher P, Góngora-Castillo E, Valls M, Anticó E, Molinas M, Serra O, *et al.* 2020. Silencing against the

conserved NAC domain of the potato StNAC103 reveals new NAC candidates to repress the suberin associated waxes in phellem. *Plant Science* **291**: 110360.

Soliday CL, Dean BB, Kolattukudy PE. **1978**. Suberization: Inhibition by Washing and Stimulation by Abscisic Acid in Potato Disks and Tissue Culture. *Plant Physiology* **61**: 170–174.

Sun L, Zhu L, Xu L, Yuan D, Min L, Zhang X. **2014**. Cotton cytochrome P450 CYP82D regulates systemic cell death by modulating the octadecanoid pathway. *Nature Communications* **5**.

Tanios S, Thangavel T, Eyles A, Tegg RS, Nichols DS, Corkrey R, Wilson CR. **2020**. Suberin deposition in potato periderm: a novel resistance mechanism against tuber greening. *New Phytologist* **225**: 1273–1284.

Teixeira RT, Fortes AM, Bai H, Pinheiro C, Pereira H. **2018**. Transcriptional profiling of cork oak phellogenic cells isolated by laser microdissection. *Planta* **247**: 317–338.

Teixeira RT, Fortes AM, Pinheiro C, Pereira H. **2014**. Comparison of good- and bad-quality cork: Application of high-throughput sequencing of phellogenic tissue. *Journal of Experimental Botany* **65**: 4887–4905.

Thangave T, Tegg RS, Wilson CR. **2016**. Toughing it out-disease-resistant potato mutants have enhanced tuber skin defenses. *Phytopathology* **106**: 474–483.

Tobimatsu Y, Schuetz M. **2019**. Lignin polymerization: how do plants manage the chemistry so well? *Current Opinion in Biotechnology* **56**: 75–81.

Turchi L, Carabelli M, Ruzza V, Possenti M, Sassi M, Peñalosa A, Sessa G, Salvi S, Forte V, Morelli G, *et al.* 2013. Arabidopsis HD-Zip II transcription factors control apical embryo development and meristem function. **2129**: 2118–2129.

Ursache R, De Jesus Vieira Teixeira C, Dénervaud Tendon V, Gully K, De Bellis D, Schmid-Siegert E, Grube Andersen T, Shekhar V, Calderon S, Pradervand S, *et al.* 2021. GDSL-domain proteins have key roles in suberin polymerization and degradation. *Nature Plants* **7**: 353–364.

Vaughn SF, Lulai EC. **1991**. The involvement of mechanical barriers in the resistance response of a field-resistant and a field-susceptible potato cultivar to Verticillium dahliae. *Physiological and Molecular Plant Pathology* **38**: 455–465.

Verdaguer R, Soler M, Serra O, Garrote A, Fernández S, Company-Arumí D, Anticó E, Molinas M, Figueras M. **2016**. Silencing of the potato StNAC103 gene enhances the accumulation of suberin polyester and associated wax in tuber skin. *Journal of Experimental Botany* **67**: 5415–5427.

Vishwakarma K, Upadhyay N, Kumar N, Yadav G, Singh J, Mishra RK, Kumar V, Verma R, Upadhyay RG, Pandey M, *et al.* 2017. Abscisic acid signaling and abiotic stress tolerance in plants: A review on current knowledge and future prospects. *Frontiers in Plant Science* **8**: 1–12.

Vishwanath SJ, Delude C, Domergue F, Rowland O. **2015**. Suberin: biosynthesis, regulation, and polymer assembly of a protective extracellular barrier. *Plant Cell Reports* **34**: 573–586.

Vishwanath SJ, Kosma DK, Pulsifer IP, Scandola S, Pascal S, Joubès J, Dittrich-Domergue F, Lessire R, Rowland O, Domergue F. **2013**. Suberin-Associated Fatty Alcohols in Arabidopsis: Distributions in Roots and Contributions to Seed Coat Barrier Properties. *Plant Physiology* **163**: 1118–1132.

Vogt T. **2010**. Phenylpropanoid Biosynthesis. *Molecular Plant* **3**: 2–20.

Vulavala VKR, Fogelman E, Faigenboim A, Shoseyov O, Ginzberg I. **2019**. The transcriptome of potato tuber phellogen reveals cellular functions of cork cambium and genes involved in periderm formation and maturation. *Scientific Reports* **9**: 10216.

Vulavala VKR, Fogelman E, Rozental L, Faigenboim A, Tanami Z, Shoseyov O, Ginzberg I. **2017**. Identification of genes related to skin development in potato. *Plant Molecular Biology* **94**: 481–494.

Wang P, Calvo-Polanco M, Reyt G, Barberon M, Champeyroux C, Santoni V, Maurel C, Franke RB, Ljung K, Novak O, *et al.* 2019. Surveillance of cell wall diffusion barrier integrity modulates water and solute transport in plants. *Scientific Reports* **9**: 4227.

Wang W, Tian S, Stark RE. **2010**. Isolation and Identification of Triglycerides and Ester

Oligomers from Partial Degradation of Potato Suberin. *Journal of Agricultural and Food Chemistry* **58**: 1040–1045.

Watanabe K, Nishiuchi S, Kulichikhin K, Nakazono M. **2013**. Does suberin accumulation in plant roots contribute to waterlogging tolerance? *Frontiers in Plant Science* **4**: 1–7.

Wei X, Lu W, Mao L, Han X, Wei X, Zhao X, Xia M, Xu C. **2019**. ABF2 and MYB transcription factors dominate feruloyl transferase FHT gene involved in ABA-mediated wound suberization of kiwifruit. *Journal of Experimental Botany*.

Wu X, Chory J, Weigel D. **2007**. Combinations of WOX activities regulate tissue proliferation during Arabidopsis embryonic development. *Developmental Biology* **309**: 306–316.

Wunderling A, Ripper D, Barra-Jimenez A, Mahn S, Sajak K, Targem M Ben, Ragni L. **2018**. A molecular framework to study periderm formation in Arabidopsis. *New Phytologist* **219**: 216–229.

Xu C, Luo F, Hochholdinger F. **2016**. LOB Domain Proteins: Beyond Lateral Organ Boundaries. *Trends in Plant Science* **21**: 159–167.

Xu X, Pan S, Cheng S, Zhang B, Mu D, Ni P, Zhang G, Yang S, Li R, Wang J, *et al.* 2011. Genome sequence and analysis of the tuber crop potato. *Nature* **475**: 189–195.

Yadav V, Molina I, Ranathunge K, Castillo IQ, Rothstein SJ, Reed JW. **2014**. ABCG Transporters Are Required for Suberin and Pollen Wall Extracellular Barriers in Arabidopsis. *The Plant Cell* **26**: 3569–3588.

Yan B, Stark RE. **2000**. Biosynthesis, molecular structure and domain architecture of potato suberin: A solid-state 13 C NMR study using 13 C-enriched precursors. *J.Agric.Food Chem* **48**: 3298–3304.

Yang W, Pollard M, Li-Beisson Y, Beisson F, Feig M, Ohlrogge J. **2010**. A distinct type of glycerol-3-phosphate acyltransferase with sn-2 preference and phosphatase activity producing 2-monoacylglycerol. *Proceedings of the National Academy of Sciences of the United States of America* **107**: 12040–12045.

Yang W, Simpson JP, Li-Beisson Y, Beisson F, Pollard M, Ohlrogge JB. **2012**. A land-plant-specific glycerol-3-phosphate acyltransferase family in arabidopsis: Substrate specificity, sn-2 preference, and evolution. *Plant Physiology* **160**: 638–652.

Yeats TH, Huang W, Chatterjee S, Viart HM-F, Clausen MH, Stark RE, Rose JKC. **2014**. Tomato Cutin Deficient 1 (CD1) and putative orthologs comprise an ancient family of cutin synthase-like (CUS) proteins that are conserved among land plants. *The Plant Journal* **77**: 667–675.

Yeats TH, Martin LBB, Viart HM-F, Isaacson T, He Y, Zhao L, Matas AJ, Buda GJ, Domozych DS, Clausen MH, *et al.* 2012. The identification of cutin synthase: formation of the plant polyester cutin. *Nature Chemical Biology* **8**: 609–611.

Yordanov YS, Regan S, Busov V. **2010**. Members of the LATERAL ORGAN BOUNDARIES DOMAIN transcription factor family are involved in the regulation of secondary growth in populus. *Plant Cell* **22**: 3662–3677.

Zeier J, Schreiber L. **1999**. Fourier transform infrared-spectroscopic characterisation of isolated endodermal cell walls from plant roots: Chemical nature in relation to anatomical development. *Planta* **209**: 537–542.

Zhang J, Eswaran G, Alonso-Serra J, Kucukoglu M, Xiang J, Yang W, Elo A, Nieminen K, Damén T, Joung JG, *et al.* 2019. Transcriptional regulatory framework for vascular cambium development in Arabidopsis roots. *Nature Plants* **5**: 1033–1042.

Zhang Y, Wu R, Qin G, Chen Z, Gu H, Qu LJ. **2011**. Over-expression of WOX1 Leads to Defects in Meristem Development and Polyamine Homeostasis in Arabidopsis. *Journal of Integrative Plant Biology* **53**: 493–506.

Zheng H, Rowland O, Kunst L. **2005**. Disruptions of the Arabidopsis Enoyl-CoA Reductase Gene Reveal an Essential Role for Very-Long-Chain Fatty Acid Synthesis in Cell Expansion during Plant Morphogenesis. *The Plant Cell* **17**: 1467–1481.

Zhu Z. **2014**. Molecular basis for jasmonate and ethylene signal interactions in Arabidopsis. *Journal of Experimental Botany* **65**: 5743–5748.

Chapter II

Phellem translational landscape active during secondary development in *Arabidopsis* roots

Ana Rita Leal [1,2,3], Pedro Barros[1], Boris Parizot[2,3], Helena Sapeta[1], Nick Vangheluwe[2,3], Tonni Grube Andersen[4,5], Tom Beeckman[2,3*] & M. Margarida Oliveira[1*]

[1] Instituto de Tecnologia Química e Biológica António Xavier, Universidade Nova de Lisboa (ITQB NOVA), GPlantS, Av. da República, 2780-157 Oeiras, Portugal;

[2] Ghent University, Department of Plant Biotechnology and Bioinformatics, Technologiepark 71, 9052 Ghent, Belgium

[3] VIB Center for Plant Systems Biology, Technologiepark 71, 9052 Ghent, Belgium

[4] University of Lausanne, Department of Plant Molecular Biology, Biophore, CH-1015, Lausanne, Switzerland

[5] Current address: Max Planck Institute for Plant Breeding Research, Carl-von-Linné-Weg 10, D-50829 Cologne, Germany

* co-corresponding authors

Table of Contents

1. Summary

The phellem is a specialized boundary tissue providing the first line of defense against abiotic and biotic stresses in organs undergoing secondary growth. Phellem cells undergo several differentiation steps, which include cell wall suberization, cell expansion and programmed cell death. Yet, the molecular players acting particularly in phellem cell differentiation remain poorly described, particularly in the widely used model plant *Arabidopsis thaliana*. Using specific marker lines we followed the onset and progression of phellem differentiation in *A. thaliana* roots, and further targeted the translatome of new developed phellem cells using Translating Ribosome Affinity Purification followed by mRNA sequencing (TRAP-SEQ).We showed that phellem suberization is initiated early after phellogen (cork cambium) division. The specific translational landscape was organized in three main domains related to energy production, synthesis and transport of cell wall components, and response to stimulus. Novel players in phellem differentiation, related to suberin monomer transport and assembly, as well as novel transcription regulators were identified. This strategy provided an unprecedented resolution of the translatome of developing phellem cells, giving a detailed and specific view on the molecular mechanisms controlling cell differentiation in periderm tissues of the model plant *Arabidopsis*.

2. Introduction

Adaptation and evolution of plants to the terrestrial environment was made possible by the development of specialized lipid and phenolic barriers that improved resistance to dehydration and protection against other environmental threats. In mature stems and roots undergoing secondary development, as well as in tubers and fruits, this protection is mostly provided by a suberized periderm (Ragni and Greb, 2018;

Evert, 2006). The periderm is a complex structure, organized in three specialized layers: phellogen, phelloderm, and phellem. The phellogen (or cork cambium), is the meristematic layer that dedifferentiates from parenchymatous cells during secondary development. Periderm development occurs through phellogen activity, producing phelloderm cells towards the inside, and phellem cells towards the outside (Evert, 2006; Pereira, 2007). While phelloderm cells differentiate into parenchyma, phellem cells undergo several differentiation steps, which include cell wall suberization, cell expansion and programmed cell death (Evert, 2006; Crang *et al.*, 2018). As the outermost layer, phellem provides the ultimate protection in diverse plant organs.

The molecular regulation of periderm development has been studied in several plant species through transcriptomic analyses (Vulavala *et al.*, 2017; Soler *et al.*, 2011; Ginzberg *et al.*, 2009; Soler *et al.*, 2007; Rains *et al.*, 2018; Boher *et al.*, 2018; Alonso-Serra *et al.*, 2019; Lopes *et al.*, 2019). Collectively, these studies highlighted multiple genes related to phellem differentiation and more particularly to the suberization process, which is shown to be highly conserved across different species. Suberin is a complex lipophilic macromolecule composed of a diversity of aliphatic and aromatic components (monomers) that are covalently linked by primarily ester bounds (Bernards, 2002; Graça, 2015). Core pathways required for suberization retrieved in those transcriptomic studies include genes involved in the synthesis of specific aliphatic (*Long-Chain acyl-CoA Synthetase 2 - LACS2*, *Fatty acyl-coenzyme A reductase 1/4/5 - FAR1/4/5*, Cytochrome P450 86A1 - *CYP86A1* and *CYP86B1*) and aromatic components (*phenylalanine ammonia lyase - PAL*, *Cinnamate-4-hydroxylase - C4H* and *Ferulate 5-hydroxylase - F5H*), assembly (*Glycerol-3-phosphate Acyl- Transferase 5/7 - GPAT5/7* , *Aliphatic suberin feruloyl transferase - ASFT* and Fatty alchol:caffeoyl-CoA transferase- *FACT*) and transport (*ATP-binding cassette G2/6/20 - ABCG2/6/20*) of monomers (Vishwanath *et al.*, 2015;

Graça, 2015; Philippe *et al.*, 2020). Previous transcriptomic studies on cork oak (Teixeira *et al.*, 2018) and potato (Vulavala *et al.*, 2019) using micro-dissected periderm samples (including phellogen and early-developed phellem) detected expression of suberization-related genes, suggesting that this process occurs at an early stage of periderm development. Expression activity of multiple transcription factors (TFs), including members of the MYB, NAC and WOX families, was also detected across targeted phellem transcriptomes, suggesting a conserved regulatory landscape acting during phellem development. Overall, these genome-wide transcriptomic studies greatly improved the understanding of the genetic mechanisms contributing to phellem differentiation.

Recently, the model plant *Arabidopsis thaliana* was proposed as a suitable model to study periderm development and differentiation (Wunderling *et al.*, 2018; Campilho *et al.*, 2020). As in woody stems, secondary development in *Arabidopsis* roots is organized in two concentric meristems: the inner vascular cambium and the outer phellogen. Morphological analysis of root development (Wunderling *et al.*, 2018), together with lineage tracing studies (Smetana *et al.*, 2019), confirmed periderm ontogeny from pericycle cells, that divide to give origin to the root phellogen. Initial pericycle cell divisions were reported already at 6 days after germination (DAG) in primary roots below hypocotyl-root junction, resulting in phellogen establishment (Smetana *et al.*, 2019). Core genes related to suberization are also strongly expressed in emerging phellem cells from *Arabidopsis* roots. Moreover, putative transcriptional regulators of phellem detected in woody species are also found in *Arabidopsis* phellem (Wunderling *et al.*, 2018), demonstrating once more the conservation of the developmental process of phellem between diverse species. In the present study we aimed to obtain a detailed view on the translatome of *Arabidopsis* phellem at initial stages of differentiation. After establishing a timeline

for the onset of suberization in the root periderm, we performed Translating Ribosome Affinity Purification followed by mRNA sequencing (TRAP-SEQ) of newly formed phellem cells. TRAP-SEQ enabled for the first time the isolation of an mRNA pool from young phellem cells, avoiding the manual dissection of the tissue. The specific translational landscape of phellem cells revealed, not only previously described phellem molecular profiles, but also novel candidates related to synthesis and transport of suberin, as well as hormonal and transcriptional components putatively involved in phellem development. This strategy provided an unprecedented resolution of the translatome of developing phellem cells, giving a detailed and specific view on the molecular mechanisms controlling cell differentiation in periderm tissues of the model plant *Arabidopsis*. This study represents a starting point for in-depth analysis of the molecular regulation of phellem differentiation.

3. Material and Methods

Plant growth conditions:

For *in vitro* assays, seeds were surface sterilized with 70% (v/v) ethanol for 5 min., 20% (v/v) bleach for 5 min. and rinsed 5x with sterile water. Thereafter, seeds were sown on square plates containing sterile half-strength Murashige and Skoog (1/2 MS) medium [0.5 x MS salts, 1% (w/v) sucrose, 0.5 g/L 2-(*N*-morpholino) ethanesulfonic acid MES, 0.1g/L Myo-Inositol, pH 5.7, and 1% (w/v) agar] and stratified at 4 °C for 3 days in the dark. Seeds were germinated on vertically positioned square plates in a growth chamber at 21 °C under continuous light (100 µmol m^{-2} s^{-1}).

Plant material and constructs:

Arabidopsis thaliana ecotype Columbia (Col-0) was used as wild type and for the transgenic lines used. The lines *pGPAT5::mCITRINE-*

SYP122, *pFAR4::GUS* and *pNF-YC12::GUS* were previously described (Barberon *et al.*, 2016; Domergue *et al.*, 2010; Siefers *et al.*, 2009).
Constructs used for TRAP were generated by Gateway cloning in the pH7m24GW,3 vector (Karimi *et al.*, 2007). The BLRP-FLAG-GFP-RPL18 entry vector was made by overlapping PCR. attB1-BLRP-FLAG-GFP and the RPL18-attB2 sequences were PCR amplified using the primer pairs B1-BLRP-FLAG-GFP_F/ GFP-RPL18_R (with GFP sequence as template) and GFP-RPL18_F/ B2-RPL18_R (*Arabidopsis* gDNA template) (Table S**1**). The final overlapping PCR was performed using the primer pair B1-BLRP-FLAG-GFP_F/ B2-RPL18_R (with previous fragments as template) (Table S1). The BLRP-FLAG-GFP-RPL18 construct was subsequently cloned into a PDONR221 entry vector using BP clonase II (Invitrogen) according to manufactures description. Consecutive expression vectors (*pGPAT5* (2,148 bp before ATG) and *pUBQ10* (1,989 before ATG)-driven) were made by LR-cloning using the LR clonase II enzyme mix (Invitrogen) into a Fasted selection containing R4R2 in destination vector as previously described (Barberon *et al.*, 2016). The corresponding gene identifiers are: *GPAT5*, AT3G11430; *UBQ10*, AT4G05320; *FAR4*, AT3G44540.

Light microscopy:

Histochemical GUS staining was performed on fresh *pFAR4::GUS and pNF-YC12:: GUS* roots as previously described (Beeckman and Engler, 1994). Roots were fixed in a 4% formaldehyde and 1% glutaraldehyde solution in 0.1 M phosphate buffer (pH 7.2), dehydrated and embedded in Technovit 7100 resin (Heraeus Kulzer, Wehrheim, Germany), properly oriented, as previously described (Beeckman and Viane, 2000). Sections were obtained (5 µm), placed on glass slides and stained with 0.05% (w/v) ruthenium red solution. Stained sections were subsequently mounted in DePeX (Sigma – Aldrich) and photographed

using a Leica DM6 B upright light microscope. A minimum of 8 plants where analysed for each marker line.

Confocal microscopy:

Confocal laser scanning microscopy imaging was performed either on a Leica SP5 or a Zeiss LSM 710 microscope. Excitation and detection windows were set as follows: Propidium iodide (PI): Ex: 514nm and Em: 650-700 nm; mCITRINE: Ex: 488 nm and Em: 500-550 nm; Fluorol Yellow (FY) and GFP: Ex: 488 nm and Em: 500-550 nm; Nile Red: Ex: 561 nm and Em: 600-700 nm; Calcofluor white: Ex: 405 nm and Em: 430-470 nm.

For FY staining (Brundrett *et al.*, 1991), whole plants were incubated in a freshly prepared solution of 0.01% (w/v) FY (Santa Cruz Biotechnologies) in lactic acid (80%) at 70 °C for 30 min. The samples were washed 3x (5 min. in water) and counter-stained with aniline blue (0.5% (w/v), in water) at room temperature in darkness for 30 min. After staining, plants were washed 3x (10 min. in water) and mounted on 50% glycerol.

For PI staining, plants were incubated for 5 min. in a fresh solution of 15 mM PI, rinsed twice in water and mounted in 50% glycerol.

To image TRAP-lines, plants were cleared using ClearSee protocol (Kurihara *et al.*, 2015), and GFP was detected in combination with two histochemical stainings: Calcofluor White M2R (Sigma-Aldrich) for general cell wall staining, and Nile Red (Sigma-Aldrich) to stain suberin (Ursache *et al.*, 2018). To circumvent the difficulty of the periderm development staging associated to the gradient of secondary growth along the same root, morphological observations were confined to a region of 0.5 cm bellow the hypocotyl-root junction through a time-course experiments from 6 to 10 DAG. A minimum of 10 plants where analysed for all the lines and/or staining described.

Translating Ribosome Affinity Purification and RNA extraction:

Seedlings grown on 1/2 MS agar plates with 1% (w/v) sucrose were sampled at 8 DAG. For translatome profiling, root fragments from the hypocotyl base until the first emerged lateral root were pooled and frozen in liquid nitrogen for three biological replicates per line. Frozen root segments were grinded and homogenized in ice-cold polysome extraction buffer (200 mM Tris-HCl (pH 9.0), 200 mM KCl, 36 mM $MgCl_2$, 25 mM ethylene glycol tetraacetic acid, 1 mM dithiothreitol, 50 µg/ml cycloheximide, 50 µg/ml chloramphenicol, 1% Igepal CA-630, 1% Brig-35, 1% Triton X-100, 1% Tween-20, 2% polyoxyethylene (10) tridecyl ether, 1% sodium deoxycholate). After incubation for 10 min. on ice, homogenates were centrifuged at 16,000 × g at 4 °C for 10 min. to pellet insoluble cell debris. Affinity purification of tagged RPL18-containing polysomes was carried out using anti-FLAG beads (Sigma-Aldrich) incubated with the supernatant at 4 °C for 3 hours. Gels were subsequently collected by centrifugation and washed 4 times with polysome wash buffer (200 mM Tris-HCl, pH 9.0, 200 mM KCl, 36 mM $MgCl_2$, 25 mM ethylene glycol tetraacetic acid, 5 mM dithiothreitol, 50 µg/ml cycloheximide, 50 µg/ml chloramphenicol). Polysomes were eluted by resuspension of the washed gel in polysome wash buffer containing 3×FLAG peptide (Sigma-Aldrich). Total RNA was extracted from the final elution using Direct-zol RNA kit (Zymo research). In column DNAse I treatment was performed according to the manufacturer instructions.

Library preparation and RNA-sequencing

RNA concentration and purity were determined spectrophotometrically using the Nanodrop ND-1000 (Nanodrop Technologies) and RNA integrity was assessed using a Bioanalyser 2100 (Agilent). Per sample, 1 ng of total RNA was used as input for cDNA synthesis using the SMART-Seq v4 Ultra Low Input RNA protocol (version "091817") from

Takara Bio USA, Inc. One ng of purified cDNA was sheared to 300 bp using the Covaris M220 and libraries were prepared with the NEBNext Ultra DNA Library Prep Kit for Illumina (version 7.0 - 3/18), according to the manufacturer's protocol, and selecting for 250 bp insert size. cDNA-libraries from each sample were equimolarly pooled and sequenced on Illumina NextSeq 500 instrument (v2.5, High Output, 75 bp, Single Reads) at the VIB Nucleomics core (www.nucleomics.be).

Gene expression analysis

For quantitative PCR analysis, first strand cDNA synthesis was performed using mRNA with an oligo-dT primer using Transcriptor High Fidelity cDNA Synthesis Kit (Roche), according to the manufacturer's instructions. The cDNA was used as template for amplification by qPCR using gene-specific primers (listed on Table S1). Ubiquitin-conjugating enzyme E2 (At5g25760) was used as internal control. Real Time qPCR was done in a Lightcycler 480 (Roche), using Lightcycler 480 Master I Mix (Roche). Amplification reactions were performed in triplicate for each cDNA sample. Target transcript abundance was calculated according to Pfaffl (2001).

Sequence data processing and differential expression analysis.

After RNA-sequencing, the resulting FASTQ files were imported into the Galaxy Workflow Environment (Afgan *et al.*, 2018). Quality control of the single strand reads was assessed before and after trimming using FastQC. Trimming of adapters and low quality bases was performed using Trimmomatic with “TruSeq3 (single-ended, for MiSeq and HiSeq)” setting for the adapter sequences to use, and all other parameters by default. Reads were mapped on the *A. thaliana* CDS reference from Araport11 using Salmon (Patro *et al.*, 2017) with default parameters. Finally, tximport was used to summarize transcript-level estimates. To identify differentially expressed genes (DEGs) between tissues, statistical analysis was carried out using the DESeq2 package (Love *et*

al., 2014) in Rstudio 1.1 (http://www.rstudio.com/) with R version 3.5.2 (R Foundation for Statistical Computing., 2018). Expression values were normalized by the "Relative Log Expression" (RLE) normalization. Gene expression was pre-filtered with a threshold of ≥10 counts in at least three samples, and in at least one of the two tissues. Differential expression analysis was performed between *GPAT5*-associated and *UBQ10*-associated samples and DEGs were filtered based on a fold change (FC) ≥ 2 and an adjusted p-value ≤ 0.01 (p-values were corrected using the Benjamini-Hochberg method). DEGs were annotated using Araport11 annotation. The RNA-sequencing data set was deposited in ArrayExpress (http://www.ebi.ac.uk/arrayexpress/experiments/E-MTAB-8949).

Gene Ontology (GO) functional enrichment was performed using BiNGO plugin for Cytoscape version 3.7.1 (Maere *et al.*, 2005). The significant GO terms related to cellular component, biological processes and molecular function were retrieved by applying hypergeometric distribution and adjusted p-value < 0.05.

Functional associations between DEGs in phellem (FC > 4) were predicted using STRING v.11.0 database (Szklarczyk *et al.*, 2019). Confidence score for interactions was set for medium score (above 0.4), taking into account co-expression data and protein-protein interaction evidences. The gene network obtained from STRING v.11 was imported into Cytoscape version 3.7.1 for further analysis and display.

Sequence Alignment and Phylogenetic analysis

The MYB, NAC and WOX protein sequences were aligned using ClustalW. Phylogenetic analysis was performed using Maximum Likelihood inference with a JTT substitution model, with 500 bootstrap replicates. Both alignment and phylogenetic analysis were conducted with MEGA X (Kumar *et al.*, 2018).

4. Results

Suberization timeline in phellem differentiation of the Arabidopsis root

To follow the establishment of new phellem cells, we performed a detailed morphological and spatio-temporal characterization of suberization during secondary development of *Arabidopsis* roots. To faster study this development process, we supplemented the used growth medium with sucrose, which was previously demonstrated to positively influence the secondary development of Arabidopsis roots (Wunderling *et al.*, 2018). We used previously established *Arabidopsis* suberin gene marker lines together with histological suberin staining to follow up phellem differentiation in transverse and longitudinal planes of roots. Promoter reporter lines for two suberin biosynthesis genes - *FAR4* (Domergue *et al.*, 2010) and *GPAT5* (Barberon *et al.*, 2016; Beisson *et al.*, 2007) - were used to monitor activation of suberin biosynthesis, while Nile Red and Fluorol Yellow (FY) were used for suberin detection in cell walls. FY (Brundrett *et al.*, 1991) and Nile Red (Ursache *et al.*, 2018) are highly sensitive fluorescent stains that can label suberin-enriched cell walls in fresh or ClearSee treated roots, respectively. Despite the unknown interactions of FY and Nile Red with the suberin, these stainings are widely used and accepted in the community as specific for suberized cells walls. Observations were always conducted below root-hypocotyl junction, where secondary development is initiated (Smetana *et al.*, 2019), on time-course experiments starting 6 DAG to 11 DAG. At the earliest time-point, cross sections revealed cell divisions at procambium and at pericycle level (xylem and phloem pole) (Fig. **1a** – 6 DAG, arrows), confirming the onset of secondary growth and more particularly phellogen development. However, on these sections *FAR4* promoter activity was not detected in pericycle daughter cells nor in endodermal cells. Longitudinal imaging

of the same root zone with the *pGPAT5::BLRP-FLAG-GFP-RPL18* marker line stained with Nile Red, revealed that suberin is present only in the endodermis cell walls (Fig. **1b**, S**1a**). As observed for *FAR4*, *GPAT5* expression was also not detected at this developmental stage (Fig. **1b**, S**1b**). Together, these observations indicate that suberin biosynthesis in the endodermis may be reduced, due the absence of the activity of the analysed markers. At 7 DAG we observed an increase in cell proliferation in the stele, including both in the procambium and the pericycle, likely imposing pressure on the overlying endodermis layer (Fig. **1a** – 7 DAG arrow), while cortex and epidermis maintained their normal cell shape. Punctual expression of *FAR4* was also detected in some cortex cells (Fig. **1a** – 7 DAG), in agreement with stochastic suberin staining detected in longitudinal imaging (Fig. **1b** – 7 DAG). At this stage suberin was no longer detected in the endodermis using Nile Red staining, which, however, was possible using FY staining in Col-0 roots (Fig. **S1a** – 7 DAG). At this time point, *GPAT5* reporter activity was detected in the stele region of root, however, cell specificity could not be determined due to the low signal penetration across cell walls (Fig. **1b**, **S1b**). At 8 DAG, *FAR4* expression was detected specifically in pericycle-derived cells (Fig. **1a**). At the same time point, the *GPAT5* was detected in more cells and some of which were suberized, as revealed by Nile Red staining (Fig. **1b**). The appearance of these suberizing cells, with marker activation and suberin being detected, indicates that phellogen is active and phellem cells are being produced. The early activation of *GPAT5* promoter at 7 DAG, prior to suberin detection, suggests that this gene is a suitable marker for early stages of phellem development. Further, at 9 DAG, the number of differentiated phellem cells increased, as expression of both markers and suberization were detected in more cells (Fig. **1a, 1b, S1a**, **S1b**). After the initiation of phellem suberization, expansion of phellem cells was detected, together with abscission of cortex and epidermis layers, while the endodermis cells were no longer

observed (Fig. **1a - 9DAG, S1c**). The number of circumference cells limiting the stele region, originated from pericycle cells (Fig. **1a** – 6DAG arrows), increased only till 7 DAG and this cell number was maintained in further analysed days (Fig. **S1c**), after detection of phellem as the limiting tissue. This demonstrates that phellem cell expansion starts in parallel with suberization.

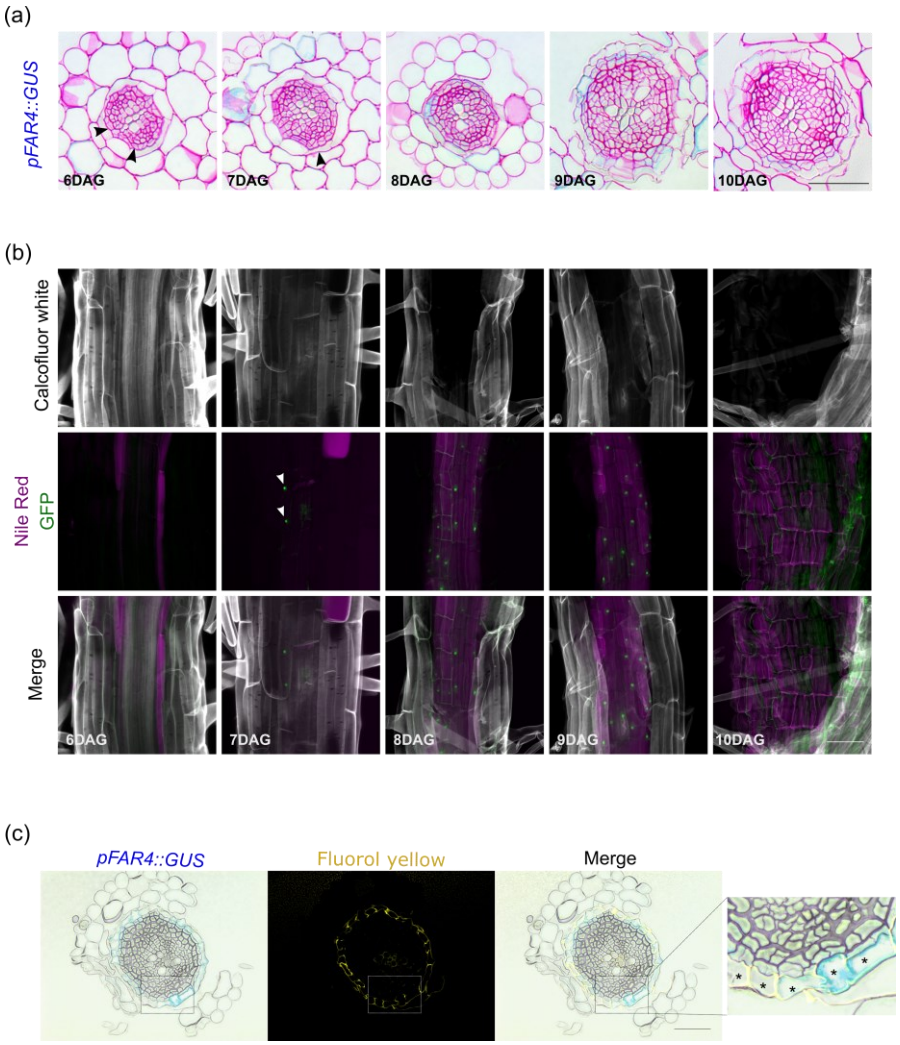

Fig. 1 *Activation of specific suberin biosynthesis markers during periderm development of Arabidopsis thaliana roots. (a) Plastic embedded cross-sections of FAR4::GUS taken below the hypocotyl-root junction, between 6 and 10 DAG. Arrowheads indicate new cell divisions in pericycle cells (6 DAG) and endodermis deformation (7 DAG). (b) GPAT5::BLRP-FLAG-GFP-RPL18*

expression (green) in the phellem differentiation zone, below the root-hypocotyl junction, between 6 and 10 DAG. Cell walls (grey) visualized by calcofluor white and suberin (purple) using Nile red staining, after ClearSee treatment. Arrowheads indicate GPAT5::BLRP-FLAG-GFP-RPL18 expression. The 3D maximum projection figures were obtained by confocal laser scanning with Z-stack images. (c) Plastic embedded cross-sections of 11 DAG plants of FAR4::GUS taken below hypocotyl-root junction and stained with Fluorol Yellow for suberin. Asterisks (*) show suberized phellem cells. Scale bars: 50 µm. Images are representative of all analysed samples.

Finally, at 10 DAG, while *FAR4* and *GPAT5* expression was reduced, a continuous layer of suberized phellem cells could be identified (Fig. **1**, **S1a**, **S1b**). At this later stage, phellem is displayed as a continuous layer of suberized cells surrounding the root stele (Fig. **1c**) and in the longitudinal view, suberized phellem appears as a tissue covering the external part of the root, with cells organized in a compact and regular arrangement (Fig. **1 b**; **S1a**).

Collectively, this chronological study framed the onset of root phellem development between 7 to 8 DAG, just below the root-hypocotyl junction, closely followed by cell wall suberization of these newly formed cells.

Isolation of phellem translatome

To identify the pathways mediating the early stages of phellem differentiation we performed a transcriptomic analysis at the onset of phellem suberization, which occurs, based on our microscopic study, at 8 DAG in the mature region of the root. We used the *pGPAT5::BLRP-FLAG-GFP-RPL18* line, where *pGPAT5* driven expression of the tagged Ribosomal Protein L18 (*RPL18*) allowed immunopurification and sequencing of the phellem-associated translatome (TRAP-SEQ). As a control, we used plants expressing the same construct under control of a near-constitutive promoter (*pUBQ10::BLRP-FLAG-GFP-RPL18*), to obtain a representative translatome of all root cell types of the same root

region and developmental stage (Fig. **2a**). Using Illumina sequencing, we obtained a total of 166 million reads from triplicate samples of the total root translatome (*UBQ10*-associated) and the suberizing phellem translatome (*GPAT5*-associated).

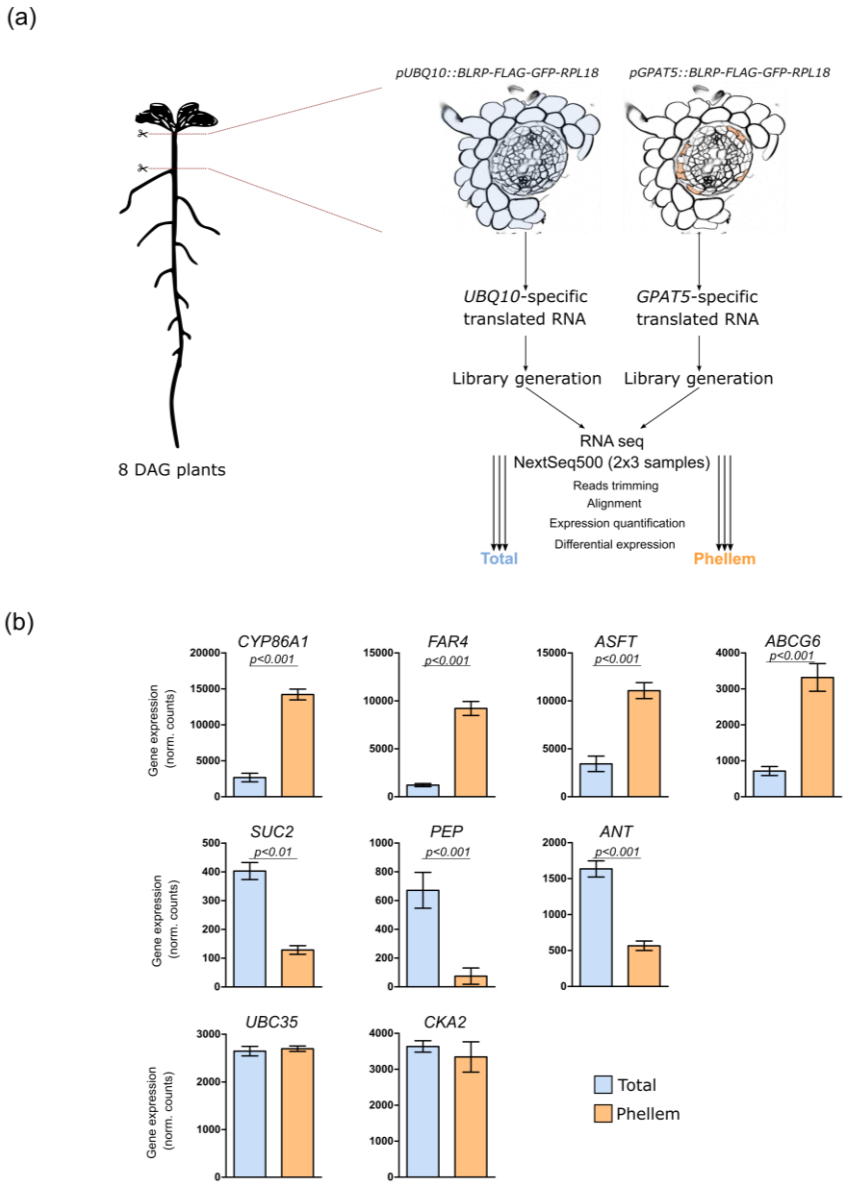

Fig. 2 *Isolation of specific Arabidopsis thaliana phellem transcripts. (a) Arabidopsis roots were collected from phellem development zone, from hypocotyl-root junction to the first emerged lateral root. The GPAT5 and UBQ10*

*promoters were used to drive expression of BLRP-FLAG-GFP-RPL18 cassette in phellem cells and in the total root cells, respectively. Immunocapture of ribosomes containing the fusion tag allowed cell-specific purification of mRNAs attached to these ribosomes followed by RNA sequencing. Biological triplicates were run for each condition. Reads from sequencing data were treated and differential expression of genes between whole root and phellem cells was calculated. (b) Transcript abundance of marker genes from collected phellem cells (GPAT5-*associated*) and total-root (UBQ10-*associated*): CYP86A1, FAR4, ASFT and ABCG6 are markers for cell-wall suberization; SUC2, PEP and ANT are markers for phloem, cortex and vascular cambium cells; UBC35 and CKA2 are housekeeping genes. Data represent mean normalized counts ± standard deviation (n=3). Statistical significance between samples (GPAT5-associated vs.UBQ10-associated gene expression) was assessed using the unpaired t- test.*

A total of 5,385 genes were differentially expressed (adjusted p-value ≤ 0.01, |FC| ≥ 2) between *GPAT5*-associated and *UBQ10*-associated translatomes. From the detected differentially expressed genes (DEGs), 2,750 (51%) were more abundant in suberizing phellem (Table **S2**). To assess the purity of the pull-down, we confirmed the expression profile of genes with known cell-specific localization in the *Arabidopsis* root (Fig. **2b**). Accordingly, genes involved in suberin monomer biosynthesis, *CYP86A1* (Höfer *et al.*, 2008), *FAR4* (Domergue *et al.*, 2010), esterification, *ASFT* (Gou *et al.*, 2009), and transport *ABCG6* (Yadav *et al.*, 2014) were significantly enriched in the *GPAT5*-associated translatome. Moreover, genes specifically expressed in phloem (*SUC2)* (Truernit and Sauer, 1995), root cortex (*PEP*) (Mustroph *et al.*, 2009) and vascular cambium (*ANT*) (Randall *et al.*, 2015) were enriched in *UBQ10*-associated samples, and the expression of genes associated with housekeeping functions *UBC35* and *CKA2* remained unchanged in both translatomes. Also, the expression pattern of these selected genes assessed by RT-qPCR agreed with the RNA-seq data (Fig. **S2**), with both Log2FC showing a linear correlation coefficient of $R^2 = 0.96$ (Fig. **S2**). To further validate the specific enrichment in phellem cells we studied the expression pattern of a GUS-reporter line for Nuclear Factor YC12 (*NF-YC12* - AT5G38140), which was detected to be enriched in the *GPAT5*-associated translatome (Table **S2**). In this line GUS

expression was detected in secondary developed root zone 7 DAG, specifically in cells matching the localization of newly developed phellem (Fig. **S3**).

Overall, these results support the potential of the generated dataset in discriminating the suberizing phellem translatome from the global root translatome, at the onset of phellem development.

Functional categorization of the phellem translatome

Functional enrichment analysis of the DEGs identified contrasting molecular signatures for *GPAT5*-associated and *UBQ10*-associated translatomes (Fig. **3**, **S4**; Tables **S3**). Regarding the phellem-associated translatome, we found a significant enrichment (FDR ≤ 0.05) of 277 GO terms, distributed among Cellular Component (13), Biological Process (117) and Molecular Function (147) categories (Fig. **3**; Table **S3A**). *Membrane* (GO:0016020) was highly overrepresented with 433 DEGs, followed by *Endomembrane system* (GO:0012505) and *Extracellular region part* (GO:0044421) with a lower number of associated DEGs. In the Biological Process category, *Response to stimulus* (GO:050896) was significantly enriched, with 404 DEGs. These were distributed among related terms, including *Response to abiotic stimulus* (GO:0009628), *Response to biotic stimulus* (GO:0009607), and *Response to hormone stimulus* (GO:0009725). More particularly, response to hormones included *Response to abscisic acid* (GO:0009737), *salicylic acid* (GO:0009751) and *jasmonic acid* (GO:009753) stimulus (Fig. **3**, Table **S3A**). *Developmental process* (GO:0032502), *Transport* (GO:0006810) and *Establishment of localization* (GO:0051234) terms are also represented, with each term holding approximately 10% of the DEGs annotated to Biological process terms. GO terms that relate to secondary metabolism were also enriched, namely *Phenylpropanoid metabolic process* (GO:0009698), *Suberin biosynthetic process* (GO:0010345) and *Cutin biosynthetic*

process (GO:0010143). In the Molecular Function category, *Hydrolase* (GO:0016787), *Transferase* (GO:0016740) and *Oxidoreductase activity* (GO:0016491) terms were enriched, individually representing more than 10% of annotated DEGs. Lipid-related Molecular Function terms were also detected, including *Fatty acid synthase activity* (GO:0004312), *Long-chain fatty acid-CoA ligase activity* (GO:0004467) and *Very long-chain fatty acid-CoA ligase activity* (GO:031957).

The *UBQ10-associated* translatome displayed a significant enrichment of 221 terms mostly distinct from the *GPAT5*-associated translatome. We found 8 functional categories were shared with the *GPAT5*-associated translatome, including (Fig. **S4**; Table **S3B**): Cytoplasm (GO: 005737), *Membrane* (GO:0016020), *Response to abiotic stimulus* (GO:0009628), *Response to water* (GO:0009415) and *Response to water deprivation* (GO:009414). Among other terms, the *UBQ10*-associated translatome showed a functional enrichment of: *Intracellular* (GO:0005622), *Organelle* (GO:0043226) and Protein complex (GO:0043234) from Cellular Component category; *Response to auxin stimulus* (GO:0009733), *Regulation of cell cycle* (GO:0051726) and *Regulation of meristem structural organization* (GO:0009934) from Biological Process; and *DNA binding* (GO:0003677) and *Structural molecule activity* (GO:0005198) for Molecular function category.

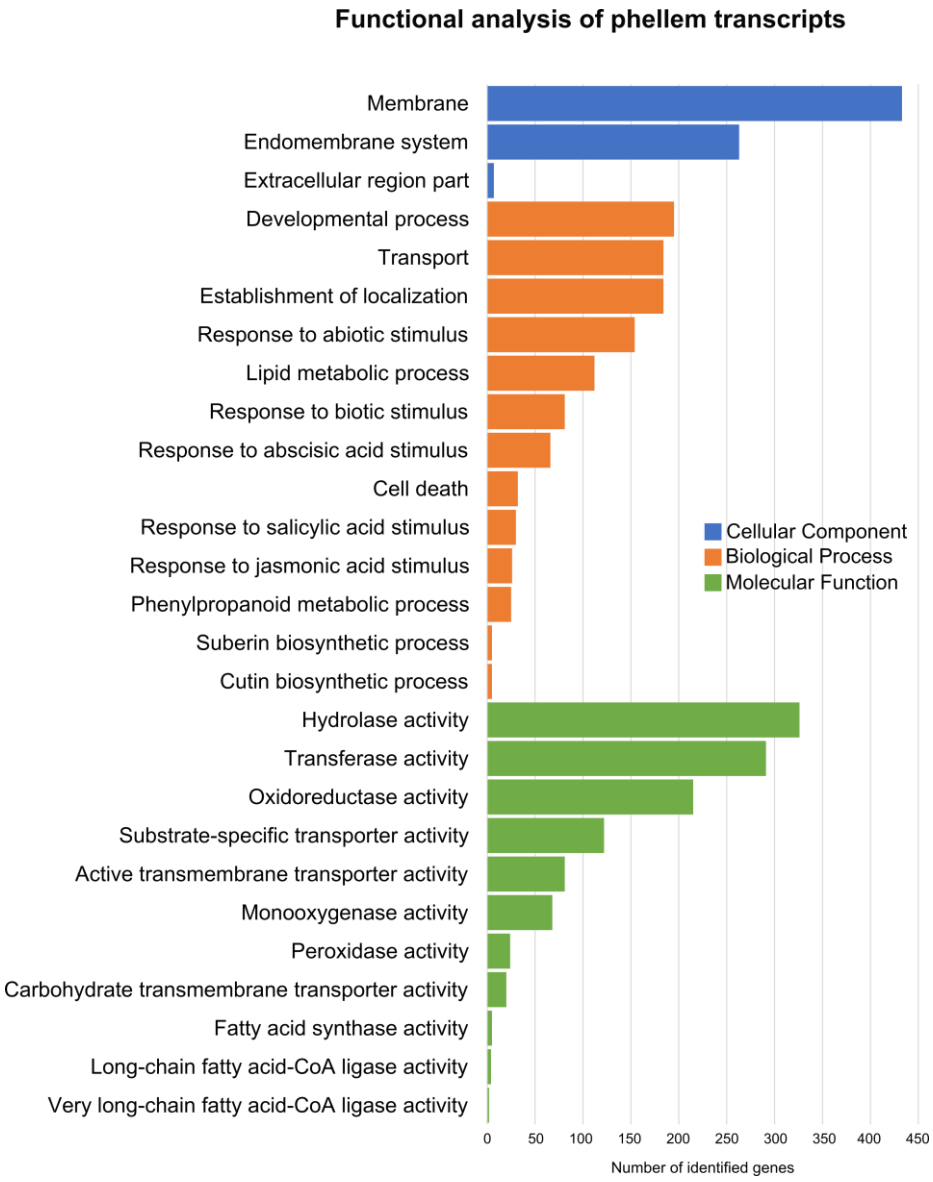

Fig. 3 *Representative GO terms significantly enriched within genes differentially expressed in phellem samples. Colored bars represent the number of genes in the selected GO terms in Cellular component, Biological process and Molecular function.*

Active metabolic pathways in phellem differentiation

Phellem-associated translatome revealed to be significantly distinct from the total root translatome, with a high number of DEGs enriched in this tissue. This is in line with previous analyses which revealed that phellem is the most transcriptional diverse tissue among a variety of other tissues, with the suberization processes being the most distinct characteristic of differentiating phellem (Lopes *et al.*, 2019; Alonso-Serra *et al.*, 2019). Considering this, we selected a short list of genes highly enriched and with putative relevance for phellem differentiation in *Arabidopsis*. The selected genes are associated with regulation, cell wall organization, lipid storage, suberization, and other fatty acid metabolic processes (Table **1**).

Aiming to highlight the most represented molecular pathways involved in phellem development, we selected the DEGs with a FC > 4. With this threshold, we obtained 977 DEGs in phellem cells (Table **S2**), which were organized in a network, according to predicted protein-protein interactions available on STRING database (Szklarczyk *et al.*, 2019).

The generated network retrieved 2,764 interactions across 326 DEGs, and clearly organized in three interconnected clusters (Fig. **4**; Table **S4A**). Genes showing the highest enrichment in phellem cells were mostly found in cluster 2, whereas clusters 1 and 3 comprised genes with lower FC (Fig. **4**). Cluster 1 included genes related to cell wall modifications (Fig. **S5a,** Table **S4B**), namely biosynthesis of diverse cell wall component precursors (*CCoAOMT7*, *PAL4*, *4CL5*), as well as genes described as specifically involved in suberization pathway (*FAR4/5*, *CYP86A1*, *FACT*, *GPAT5*, *ABCG2/6*) (Table **1**).

Other non-characterized genes involved in lipid metabolism were also identified in this cluster, including HXXXD-type acyl-transferase family genes (*AT4G15390* and *AT1G24430*) and Cytochrome P450s

(*AT5G08250, CYP702A5, and CYP71A16*). Genes associated with lipid transport (*RD20*, *ABCA8, AT2G18370* and AT3G58550) and diverse genes related to extracellular polymerization were also represented within cluster 1, including α/β-fold protein hydrolases (*AT2G18360 and AT4G17483*), peroxidases (*AT5G14130*, *AT5G66390*, *AT3G32980*, *AT2G18980*, *AT2G38390* and *AT2G35380*) and a GDSL esterase (*AT5G37690*) (Table **1**).

Table 1: List of selected genes highly represented in phellem cells, with predicted role in suberization and/or secondary cell-wall development

Gene ID	Symbol	Annotation	p-adj	FC
Transcriptional regulation				
AT1G52890	NAC019	NAC domain containing protein 19	1.76E-08	279.98
AT3G24650	ABI3	AP2/B3-like transcriptional factor family protein	1.44E-18	105.79
AT2G24430	NAC038	NAC domain containing protein 38	5.03E-99	7.58
AT3G12720	MYB67	MYB domain protein 67	1.28E-49	5.07
AT3G18400	NAC058	NAC domain containing protein 58	3.33E-76	4.46
AT2G36270	ABI5	Basic-leucine zipper (bZIP) transcription factor family protein	1.50E-03	2.32
Lipid storage and lipid localization				
AT1G05510	AT1G05510	naphthalene 1,2-dioxygenase subunit alpha (DUF1264)	9.27E-10	165.89
AT4G25140	OLEO1	oleosin 1	1.41E-11	102.84
AT5G55410	AT5G55410	Bifunctional inhibitor/lipid-transfer protein/seed storage 2S albumin superfamily protein	2.85E-08	30.31
AT5G40420	OLEO2	oleosin 2	4.37E-08	26.89
AT2G33380	RD20	Caleosin-related family protein	2.10E-06	15.31
AT2G25890	AT2G25890	Oleosin family protein	5.19E-05	14.63
AT1G62510	AT1G62510	Bifunctional inhibitor/lipid-transfer protein/seed storage 2S albumin superfamily protein	4.68E-21	11.85
AT2G18370	AT2G18370	Bifunctional inhibitor/lipid-transfer protein/seed storage 2S albumin superfamily protein	5.56E-147	11.42
AT3G47790	ABCA8	ABC2 homolog 7	2.51E-40	10.16
AT3G58550	AT3G58550	Bifunctional inhibitor/lipid-transfer protein/seed storage 2S albumin superfamily protein	5.18E-116	5.63
Cell wall organization or biogenesis				
AT5G19890	AT5G19890	Peroxidase superfamily protein	2.11E-05	132.76
AT1G65680	EXPB2	Expansin B2	0.00E+00	88.88

AT1G48130	PER1	1-cysteine peroxiredoxin 1	1.627E-16	44.97
AT5G05340	PRX52	Peroxidase superfamily protein	1.622E-75	14.17
AT2G45220	AT2G45220	Plant invertase/pectin Methylesterase inhibitor superfamily	8.13E-140	12.87
AT2G18360	AT2G18360	alpha/beta-Hydrolases superfamily protein	1.95E-145	12.51
AT5G51500	AT5G51500	Plant invertase/pectin methylesterase inhibitor superfamily	6.97E-03	4.58
AT2G18980	AT2G18980	Peroxidase superfamily protein	1.45E-53	4.47
AT4G17483	AT4G17483	alpha/beta-Hydrolases superfamily protein	2.40E-11	4.35
AT5G37690	AT5G37690	SGNH hydrolase-type esterase superfamily protein	3.27E-65	4.30
Related to suberin biosynthesis				
AT2G37360	ABCG2	ABC-2 type transporter family protein	1.61E-18	8.77
AT3G44550	FAR5	fatty acid reductase 5	1.75E-136	8.10
AT5G63560	FACT	HXXXD-type acyl-transferase family protein	1.32E-170	7.91
AT3G44540	FAR4	fatty acid reductase 4	1.01E-129	7.57
AT5G58860	CYP86A1	cytochrome P450, family 86, subfamily A, polypeptide 1	8.36E-68	5.32
AT5G13580	ABCG6	ABC-2 type transporter family protein	5.78E-51	4.64
AT3G11430	GPAT5	glycerol-3-phosphate acyltransferase 5	7.17E-41	4.32
AT1G53270	ABCG10	ABC-2 type transporter family protein	2.66E-23	4.13
Fatty acid metabolic process				
AT1G24430	AT1G24430	HXXXD-type acyl-transferase family protein	1.40E-200	13.72
AT4G00400	GPAT8	glycerol-3-phosphate acyltransferase 8	6.36E-96	8.09
AT5G08250	AT5G08250	Cytochrome P450 superfamily protein	6.13E-08	7.00
AT4G15393	CYP702A5	cytochrome P450, family 702, subfamily A, polypeptide 5	1.07E-23	6.66
AT2G38110	GPAT6	glycerol-3-phosphate acyltransferase 6	2.63E-51	6.08
AT5G42590	CYP71A16	cytochrome P450, family 71, subfamily A, polypeptide 16	2.42E-04	5.55
AT4G15390	AT4G15390	HXXXD-type acyl-transferase family protein	2.81E-55	5.23
AT1G49430	LACS2	long-chain acyl-CoA synthetase 2	1.63E-55	4.30
AT4G15400	BIA1	HXXXD-type acyl-transferase family protein	1.08E-05	4.17
AT2G45970	CYP86A8	cytochrome P450, family 86, subfamily A, polypeptide 8	2.79E-34	4.14
AT1G78990	AT1G78990	HXXXD-type acyl-transferase family protein	5.78E-29	4.05

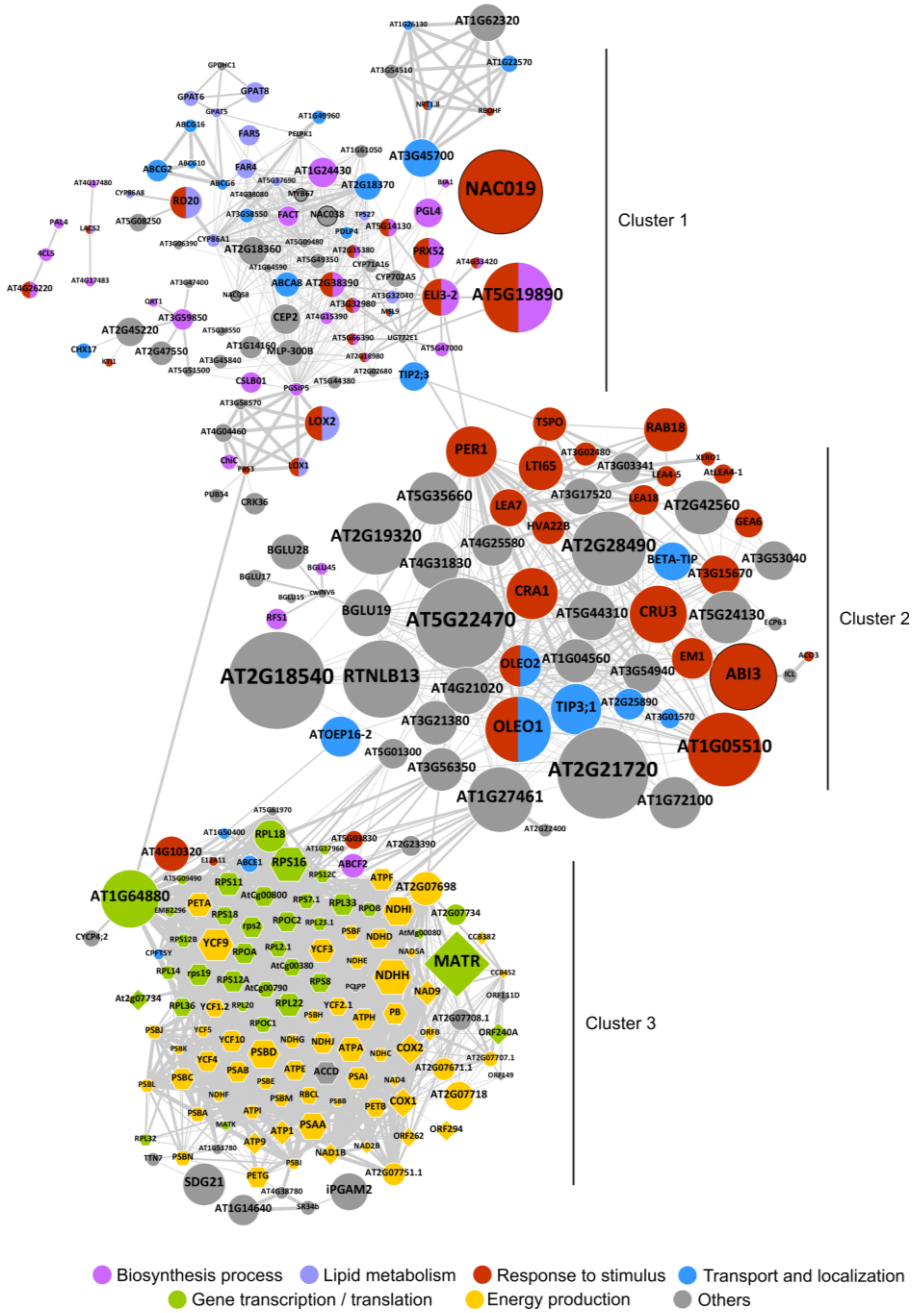

Fig. 4 *Network representation of predicted protein-protein interactions for DEGs enriched in phellem with FC>4. The network was build based on STRING database with each node representing the protein product associated with each DEG, and each connecting edge representing a predicted association (based on co-expression and inferred or validated protein-protein interactions). Node*

size corresponds to the Log2FC of each gene and edge thickness represents the confidence value for each association. Circular nodes represent genes from the nuclear genome, while hexagon and diamond shapes represent gene from plastid and mitochondrion genomes, respectively. Fill colors represent general functions or processes annotated to each gene product. Nodes with black border represent TFs.

In cluster 2, most genes were associated with responses to stimulus, including endogenous and external stimuli, and stress (Fig. **S5b,** Table **S4C**). More specifically, DEGs encoding LEA-family proteins were the most abundant group related to response to abiotic stress stimuli with 13 genes identified. In addition, 11 abscisic acid (ABA)-responsive DEGs in phellem were present in this cluster. Interestingly, DEGs coding for proteins related to transport and localization are also grouped in cluster 2. These included water transport (*TIP3;1*, *BETA-TIP*) and transmembrane transport (*OLEO1*, *OLEO2*, *ATOEP16-2*, *AT3G01570*, *AT2G25890*) (Table **1**).

Finally, in cluster 3 we identified genes mostly related to energy production and transcription or translation activity (Fig. **S5c,** Table **S4D**). Remarkably, this cluster is mainly composed of gene products transcribed from mitochondria and plastid genomes. The grouped DEGs related to energy processes included several elements involved in ATP production, such as ATPases and ATP synthase subunits, NAD(P)H oxidoreductases, electron carriers (cytochrome, ubiquinone and plastoquinone components), and photosystem-related proteins. Besides energy metabolism, a great component of this cluster included DEGs encoding ribosomal subunits (RPL and RPS-related) or related to tRNA activity. DEGs associated with transcription included several plastid-specific RNA polymerases (RPOA, RPOB, RPOC1,-2) and intron maturases (MATK and MATR). In addition, some proteins related to transmembrane transport were also found, such as ABC and TIC

transporter proteins and a signal recognition receptor protein (*AT5G61970*).

Transcription Factors translated in phellem

Among the DEGs enriched in phellem (FC > 2), 158 were annotated as TFs, including several families (Table **1**, **S5**). Interestingly, 58 of these TFs are described as responsive to stimulus, of which 23 are involved in ABA signalling or response, including members of diverse TF families as well as central ABA regulators, such as *ABI3* and *ABI5* (Kim, 2014).

Specific TF families are already reported for their involvement in regulatory pathways related to cell wall modifications, in particular WOX, MYB, and NAC families. To explore intrafamily gene diversity and its functional association with phellem development, we performed a phylogenetic analysis of all DEGs from these families identified in our analysis (Fig. **5**). *WOX* TFs are of particular interest, not only because of their predicted role as meristematic regulators, but also because they are specifically expressed during secondary development in both vascular cambium and phellogen (Lehmann and Hardtke, 2016; Jouannet *et al.*, 2015; Furuta *et al.*, 2014; Motte *et al.*, 2019; Smetana *et al.*, 2019). Four *WOX* family members were detected in our analysis, with contrasting expression patterns. While *WOX12* and *WOX2* were enriched in phellem, the closely related *WOX4* and *WOX13* were represented in the *UBQ10*-associated translatome (Fig. **5a**). Phylogenetic analysis of *NAC* and *MYB* TFs detected in *GPAT5*-associated and *UBQ10*-associated translatome showed association between specific clades and expression pattern. This is the case for two NAC-family clades including the highly enriched *NAC019*, as well as *NAC058* and *NAC38*, which were also previously clustered in STRING analysis together with cell wall modification-related genes (Fig. **5b, S5a**). Interestingly, *NTM1*, *NAC001*, *NAC003* and *NAC048*, which have not been associated with other phellem tissues in previous studies,

clustered together in the same clade. Similar associations between clades from MYB-family members and expression pattern were also found (Fig.**5c**). One example is the clade including *MYB9*, *MYB39*, *MYB92, MYB93* and *MYB107*, which were previously validated for their role in suberization (Gou *et al.*, 2017; Lashbrooke *et al.*, 2016; Cohen *et al.*, 2020; To *et al.*, 2020).

(a)

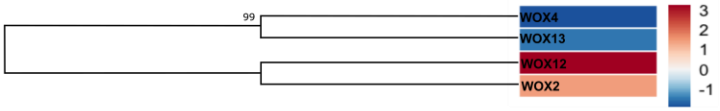
99
WOX4
WOX13
WOX12
WOX2
3
2
1
0
-1

(b)

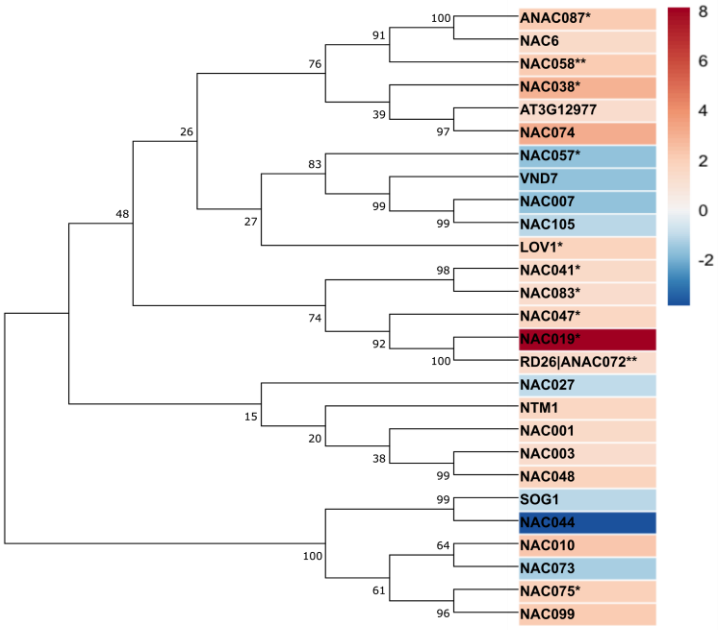
100
91
76
39
97
26
83
99
99
48
27
98
74
92
100
15
20
38
99
99
64
100
61
96
ANAC087*
NAC6
NAC058**
NAC038*
AT3G12977
NAC074
NAC057*
VND7
NAC007
NAC105
LOV1*
NAC041*
NAC083*
NAC047*
NAC019*
RD26|ANAC072**
NAC027
NTM1
NAC001
NAC003
NAC048
SOG1
NAC044
NAC010
NAC073
NAC075*
NAC099
8
6
4
2
0
-2

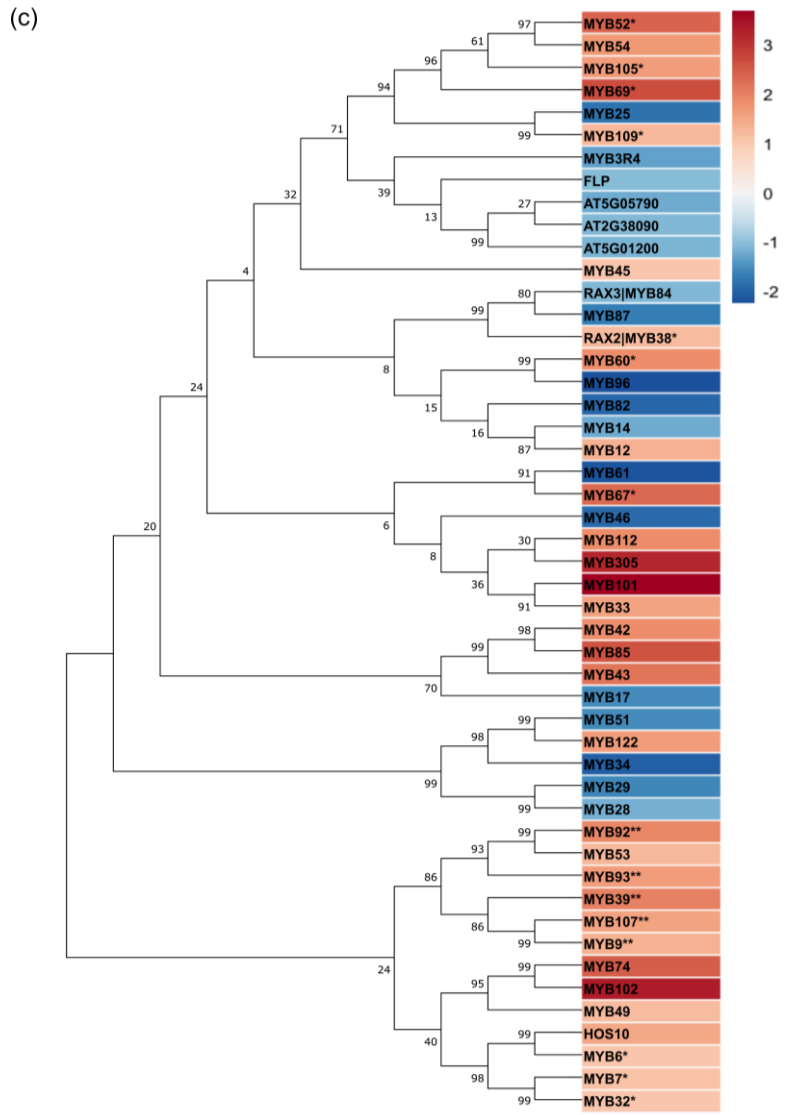

Fig. 5 *Maximum likelihood phylogenetic trees inferred for WOX (a), NAC (b) and MYB (c) transcription factors identified in this study. Bootstrap values for 500 replications are shown next to the branches. Analyses were conducted in MEGA X. Heatmaps represent the LOG2FC obtained for each gene from the comparison between GPAT5-*associated *and UBB10-specific translatomes. * phellem enriched TFs also previously identified in other transcriptomic studies* (Teixeira *et al.*, 2018; Soler *et al.*, 2007; Ginzberg *et al.*, 2009; Rains *et al.*, 2018; Boher *et al.*, 2018; Teixeira *et al.*, 2014; Vulavala *et al.*, 2017; Alonso-Serra *et al.*, 2019; Vulavala *et al.*, 2019; Lopes *et al.*, 2019; Soler *et al.*, 2011)*; ** TFs with demonstrated function in suberization* (Soler *et al.*, 2020; Verdaguer *et al.*, 2016; Gou *et al.*, 2017; Lashbrooke *et al.*, 2016; Cohen *et al.*, 2020)

5. Discussion

Suberization is an early process in phellem development

We studied the initial steps of phellem differentiation in *Arabidopsis* roots, performing a detailed tracing of the suberization process in newly formed cells during periderm development. Previous transcriptomic studies on cork oak and potato using micro-dissected periderm samples (including phellogen and early-developed phellem) detected suberization-related genes, suggesting that suberization occurs at an early stage of periderm development. In *Arabidopsis*, the combined monitoring of suberin marker genes activation and anatomical analysis, confirmed that suberization is active right after initiation of periderm development. Activation of suberin biosynthesis is initiated before the rupture and peel-off of epidermis and cortex, at 7 DAG (Fig. **1**). Gene expression is specifically detected after division of the pericycle-daughter cells that dedifferentiate to generate the phellogen. Later on, suberin is detected in these new cells that are gradually becoming the external layer of the root. Altogether, these observations confirm that suberization is initiated early after phellogen establishment and division in the development of *Arabidopsis* root periderm. This corresponds to stages 2 to 3 of root periderm development, as previously defined by Wunderling *et al*. (2018) for the *Arabidopsis* hypocotyl.

Cell wall modifications characterize the phellem differentiation process

Given its early activation during periderm development, *GPAT5* is here identified as an appropriate marker to track down newly formed phellem cells, and its use for TRAP-SEQ enabled the selection of transcripts enriched in phellem tissue (Fig. **2**). The network analysis of the phellem translatome suggested its organization in at least three main and interconnected regulatory modules. In these modules we found several metabolic processes with a relevant role in phellem development,

including synthesis and transport of cell wall components, namely suberin, response to stress and energy production and translation taking place in the plastids.

The most distinctive feature of periderm layers present in different organs and plant-species is suberin deposition in cell walls. In the *Arabidopsis* root phellem we confirmed the expression of multiple genes previously characterized as specific for synthesis of suberin components (e.g. *CYP86A1*, *CYP86B1*, *FAR1/4/5, GPAT5/7*, *FACT*, *ASFT*), as well as several genes with predicted functions for a potential role in suberin biosynthesis. These genes include several non-described members of Cytochrome P450 and HXXXD-motif/BAHD acyltransferase families (Table **1**). Moreover, network analysis predicting protein-protein interactions clustered these genes together with suberin biosynthetic genes (Fig. **S5a**) supporting the hypothesis of their involvement in phellem development. In addition, several genes required for the production of suberin precursors were detected as well, which included genes from the phenylpropanoid pathway (*4CL5*, *PAL4* and *AT4G26220*), acyl elongation complexes (*KSC1/2/8, KCR1* and *HCD1*) and various long chain acyl-CoA synthases (*LACS1/2/9/6*), indicating the capacity of phellem cells in producing precursors needed for suberization (Andersen *et al.*, 2020). In fact, functional enrichment of phellem DEGs highlighted not only suberin biosynthesis but also specific terms related to lipid, fatty acid and phenylpropanoid metabolic processes (Fig. **3**; Table **S3A**).

DEGs related to transport were also particularly enriched in the phellem translatome, including not only the previously characterized suberin ABC transporter members (*ABCG2/6/10/20*) (Yadav *et al.*, 2014), but surprisingly also other strongly represented genes associated with lipid storage and trafficking. Lipid transfer proteins (LTPs), oleophilic bodies and vesicle mediated transport have been proposed to take a part in

transport of suberin moieties to the apoplast (Philippe *et al.*, 2020; Hoffmann-Benning, 1994), however, these mechanisms have not been experimentally demonstrated. Our targeted analysis detected for the first-time genes associated with these processes in suberizing tissues, namely several LTPs, oleosins and a caleosin, are enriched in phellem cells (Table **1**). This evidence agrees with the hypothesis that suberin monomers are transported in coated oil bodies and LTPs.

Several genes associated with cell wall organization and biogenesis were overrepresented in *Arabidopsis* phellem cells, supporting the described cell wall alterations occurring during phellem differentiation. We detected that specific peroxidases were highly enriched in *Arabidopsis* phellem, and some grouped together in the cell wall modification cluster defined from network analysis (Fig. **S5a**). Peroxidases are described in lignin polymerization (Francoz *et al.*, 2015; Rojas-murcia *et al.*, 2020) and it was hypothesized that such proteins could be also involved in the esterification of suberin phenolic monomers (Bernards *et al.*, 1999; Bernards *et al.*, 2004). In fact several peroxidases are commonly found in the phellem of other plant species (Alonso-Serra *et al.*, 2019; Lopes *et al.*, 2019; Vulavala *et al.*, 2019; Rains *et al.*, 2018; Boher *et al.*, 2018). In addition, GDSL esterase/lipases were identified in phellem, which were recently reported to be involved specifically in suberin biosynthesis and induced by ABA (*AT2G23540*, *AT5G37690*, *AT1G74460*) (Ursache *et al.*, 2020), as well as other members which have not been associated with phellem or suberization *(AT1G73610, GLIP6, AT1G7125*). In parallel, α,β-fold hydrolase are also likely associated with suberin polymerization, and diverse members of this family are identified in our analysis (Table **1**, **S2**), of which *AT1G11090* is for the first-time associated with phellem tissues.

It is likely that the targeted phellem cells were at a stage when major alterations in cell walls were occurring, since genes related to the synthesis of suberin components were found less represented (with lower FC), as compared to genes associated with transport or monomer polymerization and cell wall organization. Synthesis and modification of suberin monomers mostly occur in plastids, corroborating the numerous identified genes associated with protein synthesis in plastids. Moreover, the production of the diverse suberin components requires energy consumption and oxidation power (Bernards, 2002) validating the importance of plastids and mitochondria in the fast process of phellem differentiation.

Molecular Regulators of Phellem Development

Gene ontology analysis revealed that hormonal control of phellem development mostly involves ABA. This hormone has been described to participate in suberization processes of diverse tissues, by controlling the transcription of diverse suberin biosynthesis enzymes, in control or stress conditions (Boher *et al.*, 2013; Bjelica *et al.*, 2016; Lee *et al.*, 2009; Yadav *et al.*, 2014; Barberon *et al.*, 2016). A possible relation of ABA and phellem formation was previously discriminated in phellem of potato and cork oak, where it was mostly associated with stress-responsive genes (Soler *et al.*, 2007; Vulavala *et al.*, 2019). In fact, the ABA-responsive genes enriched in *Arabidopsis* phellem cells are mostly described in responses to biotic or abiotic stimuli (Fig. **S5b**), which can be a result of the increasing exposure of newly formed phellem to the environment. The detection of *ABI3* and *ABI5* TFs, that are described to function as core regulators in ABA signalling in diverse biological processes (Mary *et al.*, 2003; Skubacz *et al.*, 2016), supports a triggering role of ABA in phellem differentiation. Although with low fold-change, compared with *UBQ10*-associated translatome, several salicylic acid (SA)-responsive genes were found in our analysis (Table

S2, **S3A**), mostly associated with stress responses. Although the direct involvement in phellem differentiation is not yet established, these genes could be necessary to minimize the effects of oxidative stress, likely to occur during suberin synthesis (Bernards *et al.*, 2004). On the other hand, jasmonic acid (JA) is likely to participate in some aspects of phellem differentiation. Actually, JA-related transcripts have been associated with phellem in different species, and particularly in potato, JA was described to play a central role in healing through periderm development, although with no impact on suberization (Boher *et al.*, 2013; Lulai and Suttle, 2004; Lulai and Suttle, 2009; Lulai *et al.*, 2011). In our analysis, we identify several transcripts associated to JA synthesis and signalling, including *LOX*, *CYP94B3* and *JAZ* (Table **S2**, **S3A**), corroborating an effective activation of JA signalling. The cross-talk of JA with other hormones has been considered crucial in plant responses to stimuli and in developmental processes (Huang *et al.*, 2017; Yang *et al.*, 2019), and it might be that JA acts as a core signal during phellem development, controlling processes from initial differentiation to final cell death.

Several lines of evidence have indicated that although the structure of the diverse plant meristems differs, there are commonalities in the molecular mechanisms underlying their function. Comparisons between lateral meristems and/or apical meristems allowed to identify not only many common regulatory components, such as TFs, cyclins, and receptor-like-kinases, but also specific characteristics for each of the meristems (Schrader *et al.*, 2004; Du *et al.*, 2010; Baucher *et al.*, 2007; Fischer *et al.*, 2019). TFs are important regulatory components in developmental processes, and some TF families have been more associated with cell fate specification. The WOX family was characterized as important in diverse processes of tissue differentiation (Gaillochet and Lohmann, 2015). Some WOX members were indicated

as potentially involved in periderm development, namely WOX9 (Lopes *et al.*, 2019; Rains *et al.*, 2018), WOX1 (Rains *et al.*, 2018) and WOX4 (Campilho *et al.*, 2020; Boher *et al.*, 2018; Alonso-Serra *et al.*, 2019), as they were previously found in periderm tissues. In our analysis *WOX12* and *WOX2* were identified as enriched in the phellem, being for the first time, associated to this tissue. *WOX12* induction was previously reported in young roots, specifically in pericycle xylem pole cells, after external auxin application (Liu *et al.*, 2014). *WOX2* was proposed to modulate auxin and cytokinin pathways during stem cell initiation in shoot apical meristem (Zhang *et al.*, 2017; Breuninger *et al.*, 2008). The described activation of these *WOX* genes in differentiation events, in particular the expression in root pericycle cells is of particular interest. Although three auxin responsive genes were also upregulated in *Arabidopsis* phellem (Table **S2**), genes related to auxin were not significantly represented. Regardless of the signalling pathway mediating *WOX* expression, these TFs are potentially operating as regulators of phellem cell fate. Contrasting with previous reports, we identified *WOX4* specifically enriched in *UBQ10*-associated translatome. Although being detected in periderm tissues in multiple studies (Alonso-Serra *et al.*, 2019; Boher *et al.*, 2018), WOX4 is also described to be active during vascular development (Alonso-Serra *et al.*, 2019; Smetana *et al.*, 2019), which likely explains the enrichment in the total root translatome.

Several suberization-related TFs were also represented in *Arabidopsis* phellem cells, including MYB and NAC families, among other families. From the previously characterized MYBs, we detected enrichment of *MYB9*, *MYB39*, *MYB93, MYB92* and *MYB107* in *Arabidopsis* phellem cells. Interestingly these genes are phylogenetically related to *MYB53* that was reported for the first time in phellem. *MYB53* expression is induced by ABA in roots (Gibbs *et al.*, 2014), making it a candidate for

ABA-dependent regulation of suberization during phellem development. The phylogenetic analysis performed using all MYB TFs identified in this study agreed with the genome-wide analysis of *Arabidopsis* MYBs performed by Dubos *et al.* (2010), suggesting some degree of functional divergence between the MYBs identified here in two distinct translatomes.

The suberin related *NAC058* (*StNAC103* orthologue) and *NAC072/RD26* (*StNAC101* orthologue) previouslly described in potato (Verdaguer *et al.*, 2016; Soler *et al.*, 2020) were also identified here to be enriched in the *Arabidopsis* phellem cells. Although these orthologs were never associated with the suberization in *Arabidopsis*, they associate with ABA responses (Coego *et al.*, 2014). Particularly *NAC072/RD26* has a central role in ABA-mediated abiotic stress responses, being also a regulator of senescence processes (Tran *et al.*, 2004; Fujita *et al.*, 2004; Kamranfar *et al.*, 2018). The strongly expressed *NAC019* was previously detected in birch suberized phellem cells (Alonso-Serra *et al.*, 2019), and in *Arabidopsis* it is described to have the same expression pattern as *NAC072/RD26* under dehydration, ABA application and high-salinity (Tran *et al.*, 2004). Our network analysis associated this TF with genes related to cell wall modifications, making it a strong candidate to be involved in the regulation of cell wall differentiation throughout phellem development.

Altogether, our targeted transcriptomic analysis of *Arabidopsis* phellem cells revealed the molecular processes of phellem development, unveiling a variety of regulatory and metabolic processes mostly associated to suberization, lipid transport as well as response to a variety of stimuli. In this work we not only highlighted the conservation of the regulatory and metabolic pathways taking place in phellem from different species, but also revealed new candidates for phellem differentiation. Further functional characterization of these candidates

will be promising and necessary for a comprehensive understanding of the molecular mechanisms driving phellem cell fate.

6. Acknowledgments

Ana Rita Leal, Pedro Barros, Boris Parizot, Tom Beeckman and M. Margarida Oliveira designed the research. The Arabidopsis lines used were kindly offered by Dr. Owen Rowland (*pFAR4::GUS*) Dr. Niko Geldner (*pGPAT5::mCITRINE-SYP122*) and Dr. Tonni Andersen (*pUBQ10::BLRP-FLAG-GFP-RPL18* and *pGPAT5::BLRP-FLAG-GFP-RPL18*). Ana Rita Leal performed the experiments with the help of Nick Vangheluwe, Boris Parizot and Helena Sapeta. Ana Rita Leal, Pedro Barros, Boris Parizot, Tom Beeckman and M. Margarida Oliveira analysed and discussed the data.

7. Bibliography

Afgan, E., Baker, D., Batut, B., et al. (2018) The Galaxy platform for accessible, reproducible and collaborative biomedical analyses: 2018 update. *Nucleic Acids Res.*, **46**, W537–W544. Available at: https://academic.oup.com/nar/article/46/W1/W537/5001157.

Alonso-Serra, J., Safronov, O., Lim, K., et al. (2019) Tissue-specific study across the stem reveals the chemistry and transcriptome dynamics of birch bark. *New Phytol.*, **222**, 1816–1831. Available at: https://onlinelibrary.wiley.com/doi/abs/10.1111/nph.15725.

Andersen, T.G., Molina, D., Kilian, J., Franke, R. and Ragni, L. (2020) Tissue-autonomous phenylpropanoid production is essential for establishment of root barriers. *bioRxiv. doi:10.1101/2020.06.18.159475*.

Barberon, M., Vermeer, J.E.M., Bellis, D. De, et al. (2016) Adaptation of Root Function by Nutrient-Induced Plasticity of Endodermal Differentiation. *Cell*, **164**, 447–459. Available at: http://dx.doi.org/10.1016/j.cell.2015.12.021.

Baucher, M., Jaziri, M. El and Vandeputte, O. (2007) From primary to secondary growth : origin and development of the vascular system. , **58**, 3485–3501.

Beeckman, T. and Engler, G. (1994) An easy technique for the clearing of histochemically stained plant tissue. *Plant Mol. Biol. Report.*, **12**, 37–42. Available at: http://link.springer.com/10.1007/BF02668662.

Beeckman, T. and Viane, R. (2000) Embedding Thin Plant Specimens for Oriented Sectioning. *Biotech. Histochem.*, **75**, 23–26. Available at: http://www.tandfonline.com/doi/full/10.3109/10520290009047981.

Beisson, F., Li, Y., Bonaventure, G., Pollard, M. and Ohlrogge, J.B. (2007) The acyltransferase GPAT5 is required for the synthesis of suberin in seed coat and root of

Arabidopsis. *Plant Cell*, **19**, 351–368.
Bernards, M.A. (2002) Demystifying suberin. *Can. J. Bot.*, **80**, 227–240.
Bernards, M.A., Fleming, W.D., Llewellyn, D.B., Priefer, R., Yang, X., Sabatino, A. and Plourde, G.L. (1999) Biochemical characterization of the suberization-associated anionic peroxidase of potato. *Plant Physiol.*, **121**, 135–145.
Bernards, M.A., Summerhurst, D.K. and Razem, F.A. (2004) Oxidases, peroxidases and hydrogen peroxide: The suberin connection. *Phytochem. Rev.*, **3**, 113–126.
Bjelica, A., Haggitt, M.L., Woolfson, K.N., Lee, D.P.N., Makhzoum, A.B. and Bernards, M.A. (2016) Fatty acid ω-hydroxylases from Solanum tuberosum. *Plant Cell Rep.*, **35**, 2435–2448. Available at: http://link.springer.com/10.1007/s00299-016-2045-4.
Boher, P., Serra, O., Soler, M., Molinas, M. and Figueras, M. (2013) The potato suberin feruloyl transferase FHT which accumulates in the phellogen is induced by wounding and regulated by abscisic and salicylic acids. *J. Exp. Bot.*, **64**, 3225–3236. Available at: https://academic.oup.com/jxb/article-lookup/doi/10.1093/jxb/ert163.
Boher, P., Soler, M., Sánchez, A., Hoede, C., Noirot, C., Paiva, J.A.P., Serra, O. and Figueras, M. (2018) A comparative transcriptomic approach to understanding the formation of cork. *Plant Mol. Biol.*, **96**, 103–118. Available at: http://dx.doi.org/10.1007/s11103-017-0682-9.
Breuninger, H., Rikirsch, E., Hermann, M., Ueda, M. and Laux, T. (2008) Differential Expression of WOX Genes Mediates Apical-Basal Axis Formation in the Arabidopsis Embryo. *Dev. Cell*, **14**, 867–876.
Brundrett, M.C., Kendrick, B. and Peterson, C.A. (1991) Efficient Lipid Staining in Plant Material with Sudan Red 7B or Fluoral Yellow 088 in Polyethylene Glycol-Glycerol. *Biotech. Histochem.*, **66**, 111–116. Available at: http://www.tandfonline.com/doi/full/10.3109/10520299109110562.
Campilho, A., Nieminen, K. and Ragni, L. (2020) The development of the periderm: the final frontier between a plant and its environment. *Curr. Opin. Plant Biol.*, **53**, 10–14. Available at: https://doi.org/10.1016/j.pbi.2019.08.008.
Coego, A., Brizuela, E., Castillejo, P., et al. (2014) The TRANSPLANTA collection of Arabidopsis lines: A resource for functional analysis of transcription factors based on their conditional overexpression. *Plant J.*, **77**, 944–953.
Cohen, H., Fedyuk, V., Wang, C., Wu, S. and Aharoni, A. (2020) SUBERMAN regulates developmental suberization of the Arabidopsis root endodermis. *Plant J.*, **102**, 431–447. Available at: https://onlinelibrary.wiley.com/doi/abs/10.1111/tpj.14711.
Crang, R., Lyons-Sobaski, S. and Wise, R. (2018) *Plant Anatomy*, Cham: Springer International Publishing. Available at: http://link.springer.com/10.1007/978-3-319-77315-5_3.
Domergue, F., Vishwanath, S.J., Joubès, J., et al. (2010) Three Arabidopsis fatty acyl-coenzyme A reductases, FAR1, FAR4, and FAR5, generate primary fatty alcohols associated with suberin deposition. *Plant Physiol.*, **153**, 1539–54. Available at: http://www.ncbi.nlm.nih.gov/pubmed/20571114%5Cnhttp://www.pubmedcentral.nih.gov/articlerender.fcgi?artid=PMC2923872.
Du, J., Groover, A. and Groover, A. (2010) Transcriptional Regulation of Secondary Growth and Wood Formation. , **52**, 17–27.
Dubos, C., Stracke, R., Grotewold, E., Weisshaar, B., Martin, C. and Lepiniec, L. (2010) MYB transcription factors in Arabidopsis. *Trends Plant Sci.*, **15**, 573–581. Available at: https://linkinghub.elsevier.com/retrieve/pii/S1360138510001536.
Evert, R.F. (2006) *Esau's Plant Anatomy*, Hoboken, NJ, USA: John Wiley & Sons, Inc. Available at: http://doi.wiley.com/10.1002/0470047380.
Fischer, U., Kucukoglu, M., Helariutta, Y. and Bhalerao, R.P. (2019) The Dynamics of Cambial Stem Cell Activity. *Annu. Rev. Plant Biol.*, **70**, annurev-arplant-050718-100402. Available at: https://www.annualreviews.org/doi/10.1146/annurev-arplant-050718-100402.
Francoz, E., Ranocha, P., Nguyen-Kim, H., Jamet, E., Burlat, V. and Dunand, C. (2015) Roles of cell wall peroxidases in plant development. *Phytochemistry*, **112**, 15–21. Available at: http://dx.doi.org/10.1016/j.phytochem.2014.07.020.

Fujita, M., Fujita, Y., Maruyama, K., Seki, M., Hiratsu, K. and Ohme-takagi, M. (2004) A dehydration-induced NAC protein , RD26 , is involved in a novel ABA-dependent stress-signaling pathway. , 863–876.

Furuta, K.M., Hellmann, E. and Helariutta, Y. (2014) Molecular Control of Cell Specification and Cell Differentiation During Procambial Development. *Annu. Rev. Plant Biol.*, **65**, 607–638.

Gaillochet, C. and Lohmann, J.U. (2015) The never-ending story: From pluripotency to plant developmental plasticity. *Dev.*, **142**, 2237–2249.

Gibbs, D.J., Voß, U., Harding, S.A., et al. (2014) At MYB93 is a novel negative regulator of lateral root development in Arabidopsis. *New Phytol.*, **203**, 1194–1207. Available at: http://doi.wiley.com/10.1111/nph.12879.

Ginzberg, I., Barel, G., Ophir, R., Tzin, E., Tanami, Z., Muddarangappa, T., Jong, W. De and Fogelman, E. (2009) Transcriptomic profiling of heat-stress response in potato periderm. *J. Exp. Bot.*, **60**, 4411–4421.

Gou, J.Y., Yu, X.H. and Liu, C.J. (2009) A hydroxycinnamoyltransferase responsible for synthesizing suberin aromatics in Arabidopsis. *Proc. Natl. Acad. Sci. U. S. A.*, **106**, 18855–18860. Available at: http://www.ncbi.nlm.nih.gov/pubmed/19846769%5Cnhttp://www.pnas.org/content/106/44/18855.full.pdf.

Gou, M., Hou, G., Yang, H., Zhang, X., Cai, Y., Kai, G. and Liu, C.-J. (2017) The MYB107 Transcription Factor Positively Regulates Suberin Biosynthesis. *Plant Physiol.*, **173**, 1045–1058. Available at: http://www.plantphysiol.org/lookup/doi/10.1104/pp.16.01614.

Graça, J. (2015) Suberin: The biopolyester at the frontier of plants. *Front. Chem.*, **3**, 1–11.

Höfer, R., Briesen, I., Beck, M., Pinot, F., Schreiber, L. and Franke, R. (2008) The Arabidopsis cytochrome P450 CYP86A1 encodes a fatty acid ω-hydroxylase involved in suberin monomer biosynthesis. *J. Exp. Bot.*, **59**, 2347–2360. Available at: https://academic.oup.com/jxb/article-lookup/doi/10.1093/jxb/ern101.

Hoffmann-Benning, S. (1994) Characterization of Growth-related Osmiophilic Particles in Corn Coleoptiles and Deepwater Rice Internodes. *Ann. Bot.*, **74**, 563–572. Available at: https://academic.oup.com/aob/article-lookup/doi/10.1006/anbo.1994.1156.

Huang, H., Liu, B., Liu, L. and Song, S. (2017) Jasmonate action in plant growth and development. , **68**, 1349–1359.

Jouannet, V., Brackmann, K. and Greb, T. (2015) (Pro)cambium formation and proliferation: Two sides of the same coin? *Curr. Opin. Plant Biol.*, **23**, 54–60. Available at: http://dx.doi.org/10.1016/j.pbi.2014.10.010.

Kamranfar, I., Xue, G., Tohge, T., Sedaghatmehr, M., Fernie, A.R., Balazadeh, S. and Mueller-roeber, B. (2018) Transcription factor RD26 is a key regulator of metabolic reprogramming during dark-induced senescence. , 1543–1557.

Karimi, M., Bleys, A., Vanderhaeghen, R. and Hilson, P. (2007) Building blocks for plant gene assembly. *Plant Physiol.*, **145**, 1183–1191.

Kim, S.Y. (2014) *Abscisic Acid: Metabolism, Transport and Signaling* D.-P. Zhang, ed., Dordrecht: Springer Netherlands. Available at: http://link.springer.com/10.1007/978-94-017-9424-4.

Kumar, S., Stecher, G., Li, M., Knyaz, C. and Tamura, K. (2018) MEGA X: Molecular Evolutionary Genetics Analysis across Computing Platforms F. U. Battistuzzi, ed. *Mol. Biol. Evol.*, **35**, 1547–1549. Available at: https://academic.oup.com/mbe/article/35/6/1547/4990887.

Kurihara, D., Mizuta, Y., Sato, Y. and Higashiyama, T. (2015) ClearSee: a rapid optical clearing reagent for whole-plant fluorescence imaging. *Development*, 4168–4179. Available at: http://dev.biologists.org/cgi/doi/10.1242/dev.127613.

Laloum, T., Mita, S. De, Gamas, P., Baudin, M. and Niebel, A. (2013) CCAAT-box binding transcription factors in plants: Y so many? *Trends Plant Sci.*, **18**, 157–166.

Lashbrooke, J., Cohen, H., Levy-Samocha, D., et al. (2016) MYB107 and MYB9 Homologs Regulate Suberin Deposition in Angiosperms. *Plant Cell*, **28**, 2097–2116. Available at: http://www.plantcell.org/lookup/doi/10.1105/tpc.16.00490.

Lee, S.B., Jung, S.J., Go, Y.S., Kim, H.U., Kim, J.K., Cho, H.J., Park, O.K. and Suh,

M.C. (2009) Two Arabidopsis 3-ketoacyl CoA synthase genes, KCS20 and KCS2/DAISY, are functionally redundant in cuticular wax and root suberin biosynthesis, but differentially controlled by osmotic stress. *Plant J.*, **60**, 462–475.

Lehmann, F. and Hardtke, C.S. (2016) Secondary growth of the Arabidopsis hypocotyl-vascular development in dimensions. *Curr. Opin. Plant Biol.*, **29**, 9–15. Available at: http://www.ncbi.nlm.nih.gov/pubmed/26667498.

Liu, J., Sheng, L., Xu, Y., Li, J., Yang, Z., Huang, H. and Xu, L. (2014) WOX11 and 12 are involved in the first-step cell fate transition during de novo root organogenesis in Arabidopsis. *Plant Cell*, **26**, 1081–1093.

Lopes, S.T., Sobral, D., Costa, B., Perdiguero, P., Chaves, I., Costa, A. and Miguel, C.M. (2019) Phellem versus xylem: genome-wide transcriptomic analysis reveals novel regulators of cork formation in cork oak. *Tree Physiol.*, 1–39. Available at: https://academic.oup.com/treephys/advance-article/doi/10.1093/treephys/tpz118/5681307.

Love, M.I., Huber, W. and Anders, S. (2014) Moderated estimation of fold change and dispersion for RNA-seq data with DESeq2. *Genome Biol.*, **15**, 550. Available at: http://genomebiology.biomedcentral.com/articles/10.1186/s13059-014-0550-8.

Lulai, E., Huckle, L., Neubauer, J. and Suttle, J. (2011) Coordinate expression of AOS genes and JA accumulation: JA is not required for initiation of closing layer in wound healing tubers. *J. Plant Physiol.*, **168**, 976–982.

Lulai, E.C. and Suttle, J.C. (2009) Signals involved in tuber wound-healing. *Plant Signal. Behav.*, **4**, 620–622.

Lulai, E.C. and Suttle, J.C. (2004) The involvement of ethylene in wound-induced suberization of potato tuber (Solanum tuberosum L.): A critical assessment. *Postharvest Biol. Technol.*, **34**, 105–112.

Maere, S., Heymans, K. and Kuiper, M. (2005) BiNGO: a Cytoscape plugin to assess overrepresentation of Gene Ontology categories in Biological Networks. *Bioinformatics*, **21**, 3448–3449. Available at: https://academic.oup.com/bioinformatics/article-lookup/doi/10.1093/bioinformatics/bti551.

Mary, S., Sarkar, S.F., Bonetta, D., Ã, P.M. and Mary, S. (2003) The ABSCISIC ACID INSENSITIVE 3 (ABI3) gene is modulated by farnesylation and is involved in auxin signaling and lateral root development in Arabidopsis. , **3**, 67–75.

Motte, H., Vanneste, S. and Beeckman, T. (2019) Molecular and Environmental Regulation of Root Development. *Annu. Rev. Plant Biol.*, **70**, 465–488.

Mustroph, A., Zanetti, M.E., Jang, C.J.H., Holtan, H.E., Repetti, P.P., Galbraith, D.W., Girke, T. and Bailey-Serres, J. (2009) Profiling translatomes of discrete cell populations resolves altered cellular priorities during hypoxia in Arabidopsis. *Proc. Natl. Acad. Sci.*, **106**, 18843–18848. Available at: http://www.pnas.org/cgi/doi/10.1073/pnas.0906131106.

Patro, R., Duggal, G., Love, M.I., Irizarry, R.A. and Kingsford, C. (2017) Salmon provides fast and bias-aware quantification of transcript expression. *Nat. Methods*, **14**, 417–419. Available at: http://www.nature.com/articles/nmeth.4197.

Pereira, H. (2007) *Cork: Biology, Production and Uses*, Elsevier. Available at: https://linkinghub.elsevier.com/retrieve/pii/B9780444529671X50006.

Pfaffl, M.W. (2001) A new mathematical model for relative quantification in real-time RT-PCR. *Nucleic Acids Res.*, **29**, 16–21.

Philippe, G., Sørensen, I., Jiao, C., Sun, X., Fei, Z., Domozych, D.S. and Rose, J.K. (2020) Cutin and suberin: assembly and origins of specialized lipidic cell wall scaffolds. *Curr. Opin. Plant Biol.*, **55**, 11–20. Available at: https://linkinghub.elsevier.com/retrieve/pii/S1369526620300194.

R Foundation for Statistical Computing. (2018) *R: a Language and Environment for Statistical Computing.*,.

Ragni, L. and Greb, T. (2018) Secondary growth as a determinant of plant shape and form. *Semin. Cell Dev. Biol.*, **79**, 58–67. Available at: http://dx.doi.org/10.1016/j.semcdb.2017.08.050.

Rains, M.K., Silva, N.D.G. De and Molina, I. (2018) Reconstructing the suberin pathway

in poplar by chemical and transcriptomic analysis of bark tissues. *Tree Physiol.*, **38**, 340–361.

Randall, R.S., Miyashima, S., Blomster, T., et al. (2015) AINTEGUMENTA and the D-type cyclin CYCD3;1 regulate root secondary growth and respond to cytokinins. *Biol. Open*, 1–8. Available at: http://www.ncbi.nlm.nih.gov/pubmed/26340943.

Rojas-murcia, N., Hématy, K., Lee, Y., Emonet, A. and Ursache, R. (2020) High-order mutants reveal an essential requirement for peroxidases but not laccases in Casparian strip lignification. , **117**.

Schrader, J., Nilsson, J., Mellerowicz, E., Berglund, A., Nilsson, P. and Hertzberg, M. (2004) A High-Resolution Transcript Profile across the Wood-Forming Meristem of Poplar Identifies Potential Regulators of Cambial Stem Cell Identity. , **16**, 2278–2292.

Siefers, N., Dang, K.K., Kumimoto, R.W., Bynum IV, W.E., Tayrose, G. and Holt, B.F. (2009) Tissue-specific expression patterns of Arabidopsis NF-Y transcription factors suggest potential for extensive combinatorial complexity. *Plant Physiol.*, **149**, 625–641.

Skubacz, A., Daszkowska-Golec, A. and Szarejko, I. (2016) The role and regulation of ABI5 (ABA-insensitive 5) in plant development, abiotic stress responses and phytohormone crosstalk. *Front. Plant Sci.*, **7**, 1–17.

Smetana, O., Mäkilä, R., Lyu, M., et al. (2019) High levels of auxin signalling define the stem-cell organizer of the vascular cambium. *Nature*, **565**, 485–489. Available at: http://www.nature.com/articles/s41586-018-0837-0.

Soler, M., Serra, O., Fluch, S., Molinas, M. and Figueras, M. (2011) A potato skin SSH library yields new candidate genes for suberin biosynthesis and periderm formation. *Planta*, **233**, 933–945.

Soler, M., Serra, O., Molinas, M., Huguet, G., Fluch, S. and Figueras, M. (2007) A Genomic Approach to Suberin Biosynthesis and Cork Differentiation. *Plant Physiol.*, **144**, 419–431.

Soler, M., Verdaguer, R., Fernández-Piñán, S., et al. (2020) Silencing against the conserved NAC domain of the potato StNAC103 reveals new NAC candidates to repress the suberin associated waxes in phellem. *Plant Sci.*, **291**, 110360. Available at: https://linkinghub.elsevier.com/retrieve/pii/S016894521931533X.

Szklarczyk, D., Gable, A.L., Lyon, D., et al. (2019) STRING v11: Protein-protein association networks with increased coverage, supporting functional discovery in genome-wide experimental datasets. *Nucleic Acids Res.*, **47**, D607–D613.

Teixeira, R.T., Fortes, A.M., Bai, H., Pinheiro, C. and Pereira, H. (2018) Transcriptional profiling of cork oak phellogenic cells isolated by laser microdissection. *Planta*, **247**, 317–338.

Teixeira, R.T., Fortes, A.M., Pinheiro, C. and Pereira, H. (2014) Comparison of good- and bad-quality cork: Application of high-throughput sequencing of phellogenic tissue. *J. Exp. Bot.*, **65**, 4887–4905.

To, A., Joubès, J., Thueux, J., Kazaz, S., Lepiniec, L. and Baud, S. (2020) AtMYB92 enhances fatty acid synthesis and suberin deposition in leaves of Nicotiana benthamiana. *Plant J.*, **33**, 0–2. Available at: http://doi.wiley.com/10.1111/tpj.14759.

Tran, L.P., Nakashima, K., Sakuma, Y., et al. (2004) Isolation and Functional Analysis of Arabidopsis Stress-Inducible NAC Transcription Factors That Bind to a Drought-Responsive cis -Element in the early responsive to dehydration stress 1 Promoter. , **16**, 2481–2498.

Truernit, E. and Sauer, N. (1995) The promoter of the Arabidopsis thaliana SUC2 sucrose-H+ symporter gene directs expression of β-glucuronidase to the phloem: Evidence for phloem loading and unloading by SUC2. *Planta*, **196**. Available at: http://link.springer.com/10.1007/BF00203657.

Ursache, R., Andersen, T.G., Marhavý, P. and Geldner, N. (2018) A protocol for combining fluorescent proteins with histological stains for diverse cell wall components. *Plant J.*, **93**, 399–412. Available at: https://onlinelibrary.wiley.com/doi/abs/10.1111/tpj.13784.

Ursache, R., Vieira-teixeira, C.D.J., Tendon, V.D., et al. (2020) GDSL-domain containing proteins mediate suberin biosynthesis and degradation , enabling developmental

plasticity of the endodermis during lateral root emergence. *bioRxiv. doi:10.1101/2020.06.25.171389*.

Verdaguer, R., Soler, M., Serra, O., Garrote, A., Fernández, S., Company-Arumí, D., Anticó, E., Molinas, M. and Figueras, M. (2016) Silencing of the potato StNAC103 gene enhances the accumulation of suberin polyester and associated wax in tuber skin. *J. Exp. Bot.*, **67**, 5415–5427. Available at: https://academic.oup.com/jxb/article-lookup/doi/10.1093/jxb/erw305.

Vishwanath, S.J., Delude, C., Domergue, F. and Rowland, O. (2015) Suberin: biosynthesis, regulation, and polymer assembly of a protective extracellular barrier. *Plant Cell Rep.*, **34**, 573–586. Available at: http://link.springer.com/10.1007/s00299-014-1727-z.

Vulavala, V.K.R., Fogelman, E., Faigenboim, A., Shoseyov, O. and Ginzberg, I. (2019) The transcriptome of potato tuber phellogen reveals cellular functions of cork cambium and genes involved in periderm formation and maturation. *Sci. Rep.*, **9**, 10216. Available at: http://www.nature.com/articles/s41598-019-46681-z.

Vulavala, V.K.R., Fogelman, E., Rozental, L., Faigenboim, A., Tanami, Z., Shoseyov, O. and Ginzberg, I. (2017) Identification of genes related to skin development in potato. *Plant Mol. Biol.*, **94**, 481–494. Available at: http://link.springer.com/10.1007/s11103-017-0619-3.

Wunderling, A., Ripper, D., Barra-Jimenez, A., Mahn, S., Sajak, K., Targem, M. Ben and Ragni, L. (2018) A molecular framework to study periderm formation in Arabidopsis. *New Phytol.*, **219**, 216–229. Available at: http://doi.wiley.com/10.1111/nph.15128.

Yadav, V., Molina, I., Ranathunge, K., Castillo, I.Q., Rothstein, S.J. and Reed, J.W. (2014) ABCG Transporters Are Required for Suberin and Pollen Wall Extracellular Barriers in Arabidopsis. *Plant Cell*, **26**, 3569–3588. Available at: http://www.plantcell.org/cgi/doi/10.1105/tpc.114.129049.

Yang, J., Duan, G., Li, C., Liu, L., Han, G., Zhang, Y. and Wang, C. (2019) The Crosstalks Between Jasmonic Acid and Other Plant Hormone Signaling Highlight the Involvement of Jasmonic Acid as a Core Component in Plant Response to Biotic and Abiotic Stresses. , **10**, 1–12.

Zhang, Z., Tucker, E., Hermann, M. and Laux, T. (2017) A Molecular Framework for the Embryonic Initiation of Shoot Meristem Stem Cells. *Dev. Cell*, **40**, 264-277.e4.

Zhao, H., Wu, D., Kong, F., Lin, K., Zhang, H. and Li, G. (2017) The Arabidopsis thaliana nuclear factor Y transcription factors. *Front. Plant Sci.*, **7**, 1–11.

8. Supplementary information

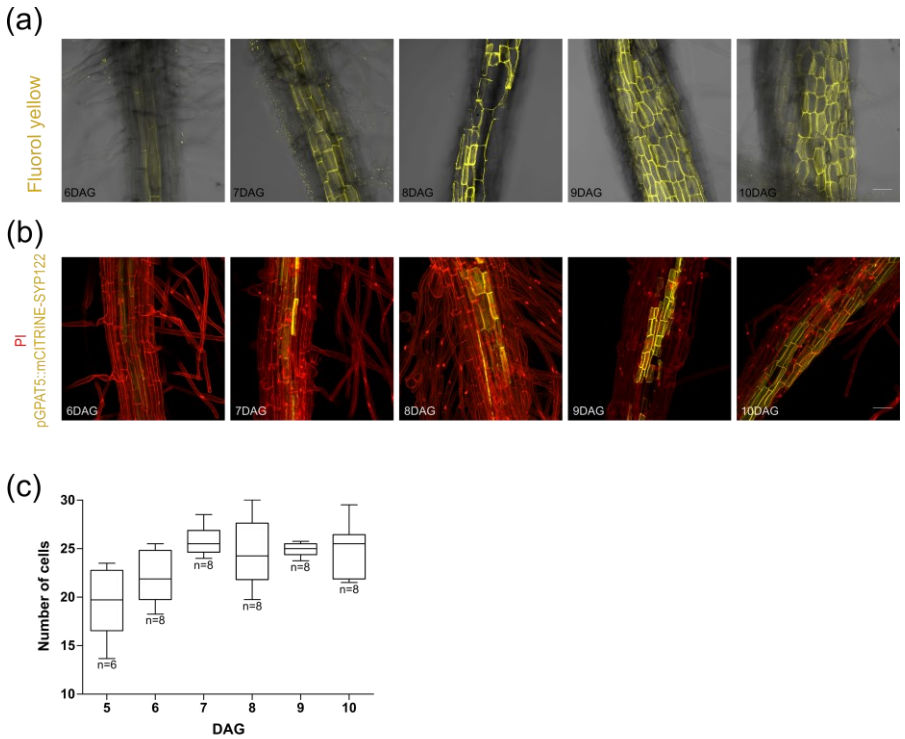

Fig. S1 *Development and suberization of periderm tissue in Arabidopsis thaliana roots. (a) Fluorol yellow staining of suberin (yellow) in primary roots. (b) GPAT5::mCITRINE-SYP122 expression (yellow) and propidium iodide staining (red) of primary roots. Images were taken in the periderm development region, below root-hypocotyl junction, between 6 and 10 DAG. The 3D maximum projection figures were obtained by confocal laser scanning with Z-stack images. Scale bar: 50 µm. Images are representative of all analysed samples. (c) Number of circumference cells in the stele (from pericycle to phellem) from 5 to 10 DAG. Cell number was counted in plastic-embedded pFAR4::GUS sections (representatives in Fig. 1a). Middle line of the boxplot is median for n ≥ 6 plants.*

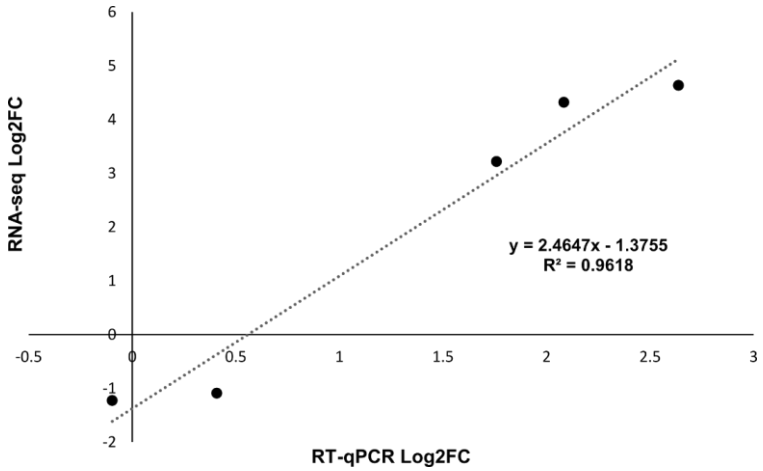

Fig. S2 *Validation of differential expression levels in phellem (pGPAT5-specific / pUBQ10-specific RNA) for 5 selected genes. Linear regression with the correlation coefficient (R^2). RNA used in RT-qPCR and in RNA-seq was obtained by TRAP.*

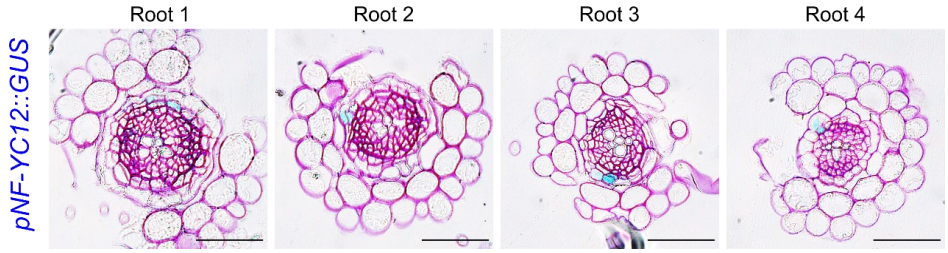

Fig. S3 *Activation of NF-YC12 gene during periderm development of Arabidopsis thaliana roots. Plastic embedded cross-sections of pNF-YC12::GUS, taken below the hypocotyl-root junction between 7 and 8 DAG. Four independent representative roots are shown. Scale bar: 50 µm. NF-YC12 was previously detected to be expressed in primary developed root tips and in leaf cells* (Siefers *et al.*, 2009)*. In this work, when observations are targeted to the secondary developed root, we detected punctual expression of NF-YC12 in new phellem cells. NF-Y transcription factors (also known as CCAAT box binding factors -CBFs) are discussed to be important regulators of numerous plant developmental and stress-induced responses. NF-YCs are sequence-specific transcription factors with histone-like subunits and are described to form heterotrimeric complexes composed of single subunits from each of three protein families: NF-YA, NF-YB, and NF-YC* (Laloum *et al.*, 2013; Zhao *et al.*, 2017)*.*

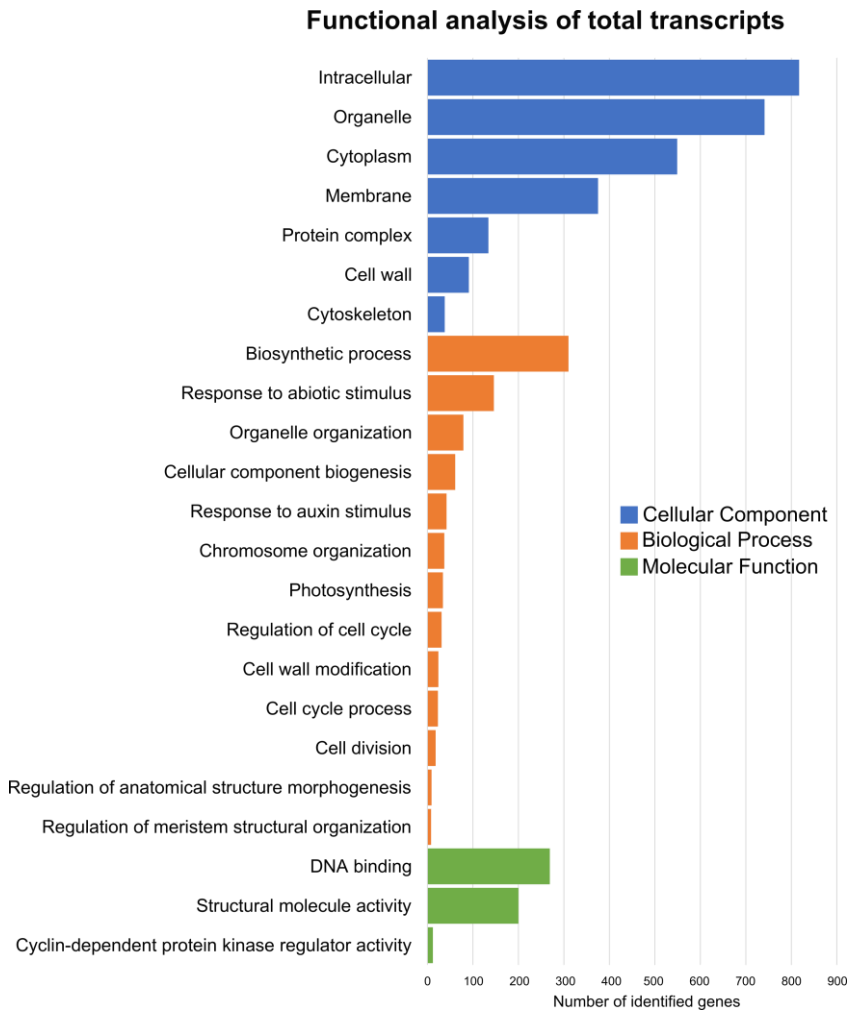

Fig. S4 *Representative GO terms significantly enriched within genes differentially expressed in total root samples. Colored bars represent the number of genes in the selected GO terms in Cellular component, Biological process and Molecular function.*

(a)

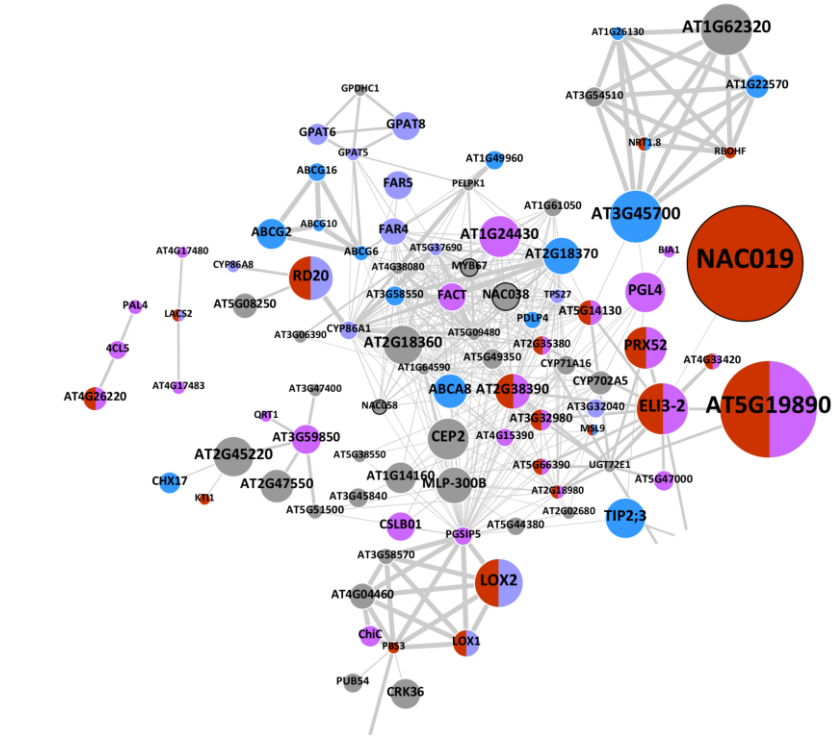
AT1G62320
AT1G26130
AT1G22570
AT3G54510
GPDHC1
GPAT8
GPAT6
GPAT5
NPT1.8
RBOHF
AT1G49960
ABCG16
FAR5
PELPK1
AT1G61050
AT3G45700
ABCG2
ABCG10
FAR4
AT1G24430
NAC019
AT4G17480
ABCG6
AT5G37690
AT2G18370
BIA1
CYP86A8
AT4G38080
MYB67
RD20
AT3G58550
FACT
NAC038
TPS27
PGL4
PAL4
LACS2
AT5G08250
AT5G14130
PDLP4
CYP86A1
AT3G06390
AT5G09480
AT2G18360
AT2G35380
PRX52
4CL5
AT5G49350
AT4G33420
AT1G64590
CYP71A16
AT4G26220
AT4G17483
AT3G47400
ABCA8
AT2G38390
CYP702A5
AT5G19890
ELI3-2
AT3G32040
ORT1
NAC058
AT3G32980
MYB19
AT3G59850
CEP2
AT4G15390
AT2G45220
AT5G38550
AT5G66390
UGT72E1
CHX17
AT2G47550
AT1G14160
MLP-300B
AT5G47000
AT3G45840
AT2G18980
KIT1
AT5G51500
AT2G02680
TIP2;3
CSLB01
AT5G44380
PGSIP5
AT3G58570
LOX2
AT4G04460
ChiC
PBS3
LOX1
PUB54
CRK36

(b)

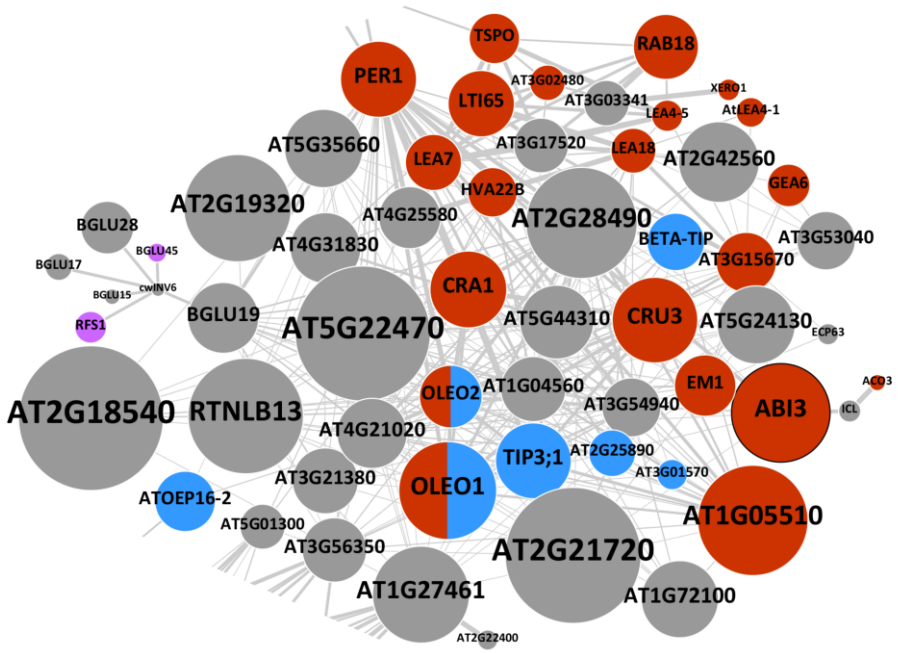
TSPO
RAB18
PER1
AT3G02480
LTI65
AT3G03341
XERO1
AtLEA4-1
LEA4-5
AT5G35660
AT3G17520
LEA18
AT2G42560
LEA7
GEA6
HVA22B
AT2G19320
AT4G25580
AT2G28490
BETA-TIP
AT3G53040
BGLU28
AT4G31830
AT3G15670
BGLU45
BGLU17
CRA1
cwINV6
BGLU15
AT5G44310
CRU3
AT5G24130
ECP63
BGLU19
AT5G22470
RFS1
EM1
ACO3
OLEO2
AT1G04560
ABI3
AT2G18540
RTNLB13
AT3G54940
ICL
AT4G21020
TIP3;1
AT2G25890
AT3G21380
OLEO1
AT3G01570
ATOEP16-2
AT1G05510
AT5G01300
AT3G56350
AT2G21720
AT1G27461
AT1G72100
AT2G22400

(c)

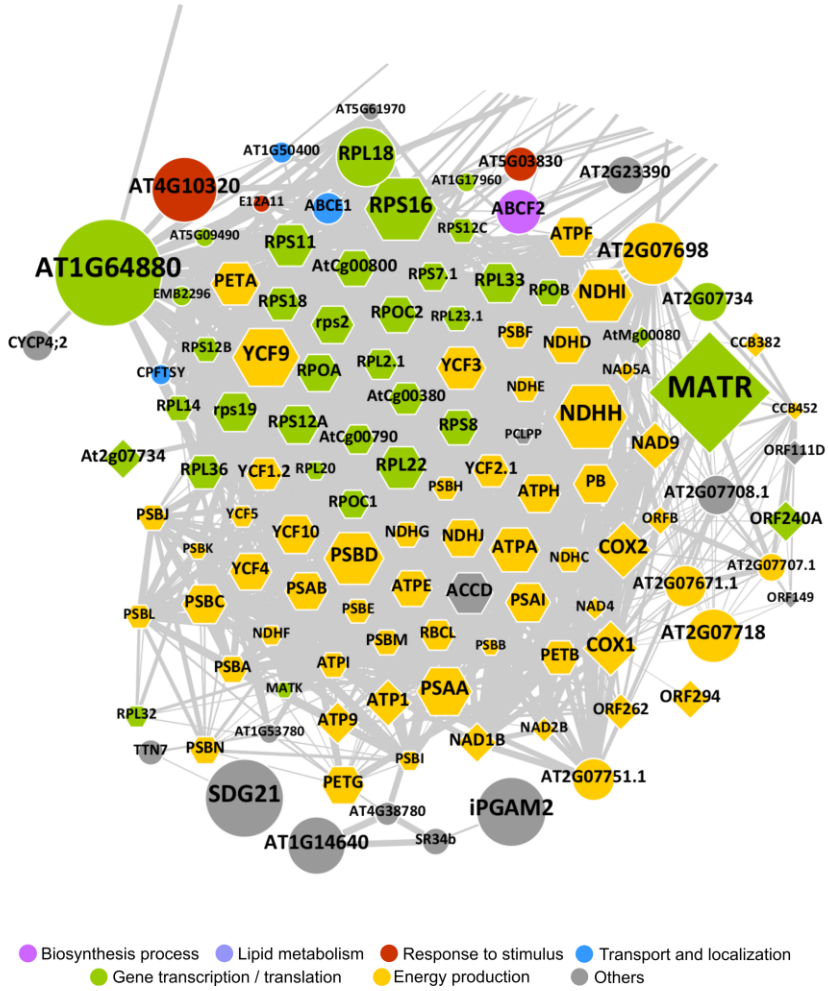

Fig. S5 *Detailed representation of the different clusters identified from network for predicted associations of phellem-enriched DEGs. Protein identifiers are attributed to each network node to cluster 1 (a), cluster 2 (b) and cluster 3 (c). Node size corresponds to the Log2FC of each gene and thickening of connecting edges represent the confidence value for the association. Circle nodes represent genes present in the nuclear genome, while hexagon and diamond shapes represent genes present in plastid and mitochondrion genomes, respectively. Fill colors represent functions or processes attributed to each gene product. Nodes with black border represent TFs.*

Table S1 List of primers used in overlapping PCR and in RT-qPCR.

Primer name	Sequence (5'-3')	Description
B1-BLRP-FLAG-GFP_F	AAAAAGCAGGCTTAATGGGACTTAACGATATC TTCGAAGCTCAGAAGATTGAATGGCATGGAGG TGATTATAAGGATGATGATGATAAGGGAGGTG TGAGCAAGGGCGAGG	Primers used for overlapping PCR. BLRP - Biotin Ligase Recognition Peptide; FLAG - DYKDDDDK-tag; GFP-Green Fluorescence Protein; RPL18 – Ribosomal Protein L18.
GFP-RPL18_R	GATCAATACCGGACATCTTGTACAGCTCGTCC	
GFP-RPL18_F	GGACGAGCTGTACAAGATGTCCGGTATTGATC	
B2-RPL18_R	AGAAAGCTGGGTTTAAACCTTGAATCCACGAC TCTTCC	
AtGPAT5_qPCR1_F	GGGTTTGAGTGCACCAACTT	Primers used for RT-qPCR. The corresponding gene identifiers are: *GPAT5* - AT3G11430; *ASFT*- AT5G41040; *ABCG6* - AT5G13580; *UBCE2* - AT5G25760; *CKA,1* - AT3G48750; *CKA2* - AT3G50000.
AtGPAT5_qPCR1_R	GGAGACAAGGCTCGAAAGTG	
AtASFT_qPCR1_F	GGTCAAACCTGAATCCGAGA	
AtASFT_qPCR1_R	CTTGGACTGCTTCCTCGTTC	
AtABCG6_qPCR1_F	ATGAACCAACTTCGGGTCTG	
AtABCG6_qPCR1_R	CGGGACAAGAAGAGAAGACG	
AtUBCE2_qPCR1_F	CTTGGACGCTTCAGTCTGTG	
AtUBCE2_qPCR1_R	GGCGAGGCGTGTATACATTT	
CDKA;,1_qPCR1_F	ATTGCGTATTGCCACTCTCATAGG	
CDKA,;1_qPCR1_R	TCCTGACAGGGATACCGAATGC	
CKA2_qPCR1_F	ACCACCATTAACGTGCGTCAAC	
CKA2_qPCR1_R	GATCTTGGCGAGAGAATCGGTATC	

Table S2 to **Table S5** are available by request to the corresponding authors or at:

https://drive.google.com/drive/folders/1ABrAUi7o5UmoANWPgWRaDLyciSfpympU?usp=sharing

Chapter III

The combined effect of heat and osmotic stress on suberization of *Arabidopsis* roots

Ana Rita Leal[1, 2, 3], Joana Belo[1], Pedro Barros[1*], Tom Beeckman[2, 3] and M. Margarida Oliveira[1*]

[1] Instituto de Tecnologia Química e Biológica António Xavier, Universidade Nova de Lisboa (ITQB NOVA), GPlantS, Av. da República, 2780-157 Oeiras, Portugal;

[2] Ghent University, Department of Plant Biotechnology and Bioinformatics, Technologiepark 71, 9052 Ghent, Belgium

[3] VIB Center for Plant Systems Biology, Technologiepark 71, 9052 Ghent, Belgium

* co-corresponding authors

Table of contents

1. Summary

Climate abnormalities associated with climate change, and especially the simultaneous occurrence of heat and drought stresses, are becoming more regular and described to cause extensive agricultural losses. Generally, heat and drought have shown some opposite morphologic and physiologic effects when applied alone. However, its combination still induces similar effects, also affecting flowering time, seed development (causing abortion) and reducing final yield. Interestingly root suberization was found to be affected similarly upon individual application of heat and drought stress, with increased suberization observed in several tissues and species. In this work we chose *Arabidopsis* as model plant to study how the suberization process is affected by the combination of heat and drought stress. At the onset of secondary development, the *Arabidopsis* primary root shows a gradient of development along its length, from primary to secondary development, and with suberization of the endodermis and the phellem, respectively. We found that the application of combined heat and osmotic stress at this root developmental stage differently affects the suberization process depending on the root zone. When the combined stress is applied, the younger root zone (with primary development) is not affected, while the developing lateral roots (LRs) show ectopic suberization after the application of the combined stress. In addition, we found that the chemical composition of the cell walls in the older zone (with secondary development and including the LRs) and younger zone of primary roots is differentially affected by the combined stress, by changing the relative concentration of its components. Our results show that, under combined drought and heat stress, Arabidopsis undergoes cell wall remodelling, with modifications in the biosynthesis and / or assembly of major cell wall components.

2. Introduction

Climate abnormalities associated with climate change, and especially the simultaneous occurrence of different abiotic stresses, are becoming more regular and severely affecting crop growth and yield (European Environment Agency, 2019). In fact, the combination of heat and drought stress is described to cause extensive agricultural losses (Vogel *et al.*, 2019). However, despite the frequent occurrence of the combined stress episodes under field conditions, most studies involving both model and crop plants have mostly focused on independent heat or drought stress responses. Generally, heat and drought have shown some opposite effects when applied alone (under controlled conditions). In response to heat, plants open the stomata to increase transpiration and cool the leaf surface, while the opposite is observed during drought treatments, with stomata closing to prevent water loss (Rizhsky *et al.*, 2004; Prasch & Sonnewald, 2013). Concerning general plant morphology, heat stress alone leads to the development of thinner and elongated leaves with increased leaf area and reduced root growth. However, regarding drought, it is described to lead to decreased leaf area and increased root growth, to minimize water loss and optimize water uptake (Vile *et al.*, 2012). The studies of drought and heat independently imposed treatments have provided important insights into plant stress responses, yet they do not allow predicting plant responses in field conditions. The experimental setup for combined stresses is more challenging than for single stresses, and different designs may strongly influence the results. Some of the variables to take into consideration include the developmental stage of the plant, the timing of stress application (consecutive or simultaneous) and the severity of each stress. Despite these challenges, several transcriptomic studies of combined stresses have been performed. These studies revealed that there is only a small number of the genes expressed in single stresses that also show up in combined heat and drought , emphasizing the

unique nature of the combined stress situation (Rizhsky *et al.*, 2004; Rasmussen *et al.*, 2013; Jia *et al.*, 2017; Lawas *et al.*, 2018). Despite these obvious differences, heat and drought alone or in combination, induce similar results, affecting flowering time, seed development and final yield (Mittler, 2006; Zhang & Sonnewald, 2017; Lawas *et al.*, 2018).

One trait that has shown to respond similarly in individual drought and heat stress is root suberization. Several studies have shown that changes in root suberin deposition can affect the way plants cope with the applied stresses. Generally, abiotic stresses cause increased suberization in several plant species and tissues. In barley, osmotic stress leads to significantly enhanced endodermis suberization in modern cultivars, whereas this response is much weaker in the wild accessions. Under drought, barley wild accessions can keep their water transport constant, but the enhanced suberization in modern cultivars significantly reduce radial water transport, compromising osmotic stress adaptation (Ranathunge *et al.*, 2017; Kreszies *et al.*, 2019). Increased suberin deposition in root, often with upregulation of suberin biosynthesis genes, was found in response to drought in grapevine (Zhang *et al.*, 2020), rice (Henry *et al.*, 2012) and *Arabidopsis* (Lee *et al.*, 2009; Rasheed *et al.*, 2016). Adaptative endodermis suberization may act to reduce water leakage from xylem and/or minimize excessive salt penetration into the stele and accumulation at toxic concentrations.

Regarding response to heat treatments, only the impact on potato skin suberization and development is well characterized. Heat-stressed potato tubers develop multiple suberized and denser skin layers, with higher suberization and increased expression of suberin biosynthesis genes (Ginzberg *et al.*, 2009; Soler *et al.*, 2011). The increased suberization improves potato thermal-insulation, reducing water loss from the tuber flesh.

Interestingly, the phytohormone abscisic acid (ABA), the main signalling hormone detected in heat and drought response (Tuteja, 2007; Vile *et al.*, 2012), is also described as the main transcriptional activator of suberin biosynthesis (Barberon *et al.*, 2016; Leal *et al.*, 2020). Mimicking the abiotic stress situation (Tuteja, 2007), ABA application induces suberin biosynthesis genes, as well as suberin deposition, in root cells that normally do not suberize (Kosma *et al.*, 2014; Barberon *et al.*, 2016).

In general, plants produce more suberin to cope with the applied stresses, with induction of suberin biosynthesis and correspondent suberization being detected after stress imposition. However, the suberin efficiency in stress adaptation is also influenced by its total monomeric composition, microstructure, and localization of the suberin barrier in each plant system. In this chapter, we used *Arabidopsis* as model to study the suberization process during combined heat and drought stress, at the onset of secondary development of the root. At this stage, *Arabidopsis* roots display a gradient of development, from primary (closer to root tip) to secondary growth (below the hypocotyl) (Wunderling *et al.*, 2018). At the onset of secondary development, the same root exhibits two distinct suberized tissues: the endodermis, in the region of primary development, and the phellem, in the region of secondary development. Suberized endodermis surrounds the central vasculature in primary developed roots, which can be found in younger region of primary root and in full emerged and developed lateral roots (LRs). In turn, phellem cells are only found in the secondary developed region of the tap root, at the outermost layer. We found that the application of combined heat and osmotic stress at this developmental stage influence the suberization depending on the root zone. While the young tap root zone was not affected by the applied combined stress, the young LRs developed ectopic suberization.

This work shows the importance of precisely defining the experimental setup, selecting the appropriate plant developmental stage and identifying the timing of stress application, as these may strongly influence root suberization in stress response.

3. Materials and Methods

Plant lines used:

Arabidopsis thaliana ecotype Columbia (Col-0) was used for gene expression and chemical analysis. The transgenic line *pGPAT5::mCITRINE-SYP122*, previously reported by Barberon *et al.* (2016) was used for fluorescence microscopy.

Plant growth conditions and combined stress treatment

For *in vitro* growth assays, seeds were surface sterilized with 70% (v/v) ethanol for 5 minutes, 20% (v/v) bleach for 5 minutes and rinsed 5 times with sterile water. Surface sterilized seeds were sown on square plates containing sterile half-strength Murashige and Skoog (1/2 MS) medium [0.5 x MS salts, 1% sucrose, 0.5 g/L 2-(*N*-morpholino) ethanesulfonic acid MES, 0.1g/L Myo-Inositol, and 1% w/v agar, pH 5.7] and stratified at 4 °C for 3 days in the dark. Seeds were germinated in the vertical position in a growth chamber at 21 °C under continuous light (100 µmol m^{-2} s^{-1}).

Polyethylene glycol (PEG)-infused medium was prepared on plates by overlaying an equal volume of 40% PEG 6000 solution (dissolved in 1/2 MS and re-adjusting the pH to 5.7) on a same volume of solid 1/2 MS medium. The agar medium and PEG solution were then allowed to equilibrate for at least 12 h and the excess liquid solution was further removed, resulting in 1/2 MS plates supplemented ~20% PEG 6000 (Van Der Weele *et al.*, 2000; Verslues & Bray, 2004).

For the combined heat and osmotic stress treatment, young plants were transferred to PEG-infused plates 8 days after germination (DAG), and

grown at 32˚C for 24h (continuous light, 100 µmol m^{-2} s^{-1}). For mock treatments, 8 DAG plants were transferred to new 1/2 MS plates and grown at control conditions. For abscisic acid (ABA) treatment, 8DAG plants were transferred to 1/2 MS plates supplemented with 1µM ABA and grown at the above-described control conditions.

Microscopy:

Confocal laser scanning microscopy imaging was performed either with a Leica SP5 or a Zeiss LSM 710. Excitation and detection windows were set as follows: Propidium iodide: Ex:514nm and Em: 650-700; mCITRINE: Ex: 488nm and Em:500-550nm; Fluorol Yellow: Ex:488nm and Em: 500-550nm. For Fluorol Yellow staining (Brundrett *et al.*, 1991) plants were incubated in a freshly prepared solution of 0.01% (w/v) Fluorol Yellow (FY, Santa Cruz Biotechnologies) in lactic acid (80%) at 70 °C for 30 min. The samples were washed (3x 5min) in water and counter-stained with aniline blue (0.5% w/v, in water) at room temperature in darkness for 30 min. Afterwards, plants were again washed (3x 10 min) in water and mounted on 50% glycerol. For propidium iodide (PI) staining, fresh plants were incubated in a fresh solution of 15mM PI for 5min, rinsed twice in water and mounted in 50% glycerol. For epi-fluorescence imaging, a Leica DM6 B Upright Microscope equipped with a L5 filter cube was used.

Gene expression analysis

Root material was collected before treatment (0h) and 1h, 2h, 3h, 4h, 6h and 24h after each treatment. Roots were segmented for sampling two different zones: secondary development zone, containing the region undergoing secondary development together with any formed lateral roots (1.5 cm from hypocotyl); and primary developmental zone, from root tip until the first visible lateral root (Fig. **S1**). The harvested root segments were immediately frozen in liquid nitrogen, with each collection point corresponding to a pool of 90-100 plants. Total RNA

from *Arabidopsis* roots was extracted using the Direct-zol RNA kit (Zymo research). In column DNAse I treatment was performed according to the manufacturers' instructions. For quantitative PCR analysis, first strand cDNA synthesis was performed using 1 µg total RNA with an oligo-dT primer using Transcriptor High Fidelity cDNA Synthesis Kit (Roche), according to the manufacturer's instructions. The cDNA was diluted and used as template for amplification by qPCR using gene-specific primers (listed on Table S1). Ubiquitin-conjugating enzyme E2 was used as housekeeping gene (At5g25760) and internal control. Real Time qPCR was done in a Lightcycler 480 (Roche), using Lightcycler 480 Master I Mix (Roche). Amplification reactions were performed in triplicate for each cDNA sample. Target transcript abundance was calculated according to Pfaffl (2001).

Attenuated total reflection Fourier transform infrared spectroscopy (ATR-FTIR)

For ATR-FTIR analysis, roots were collected from primary and secondary developmental zones (as described above for RNA extraction) at 24h after mock or combined heat and osmotic stress. After sample collection, plant material was immediately washed with ice cold water for 5x, to remove growth media traces. Plant material was then flash frozen in liquid nitrogen, lyophilized and powdered prior to the analysis. A solid PEG6000 sample was used to identify possible contamination of root samples. ATR-FTIR spectra were collected on a Bruker IFS66/S FTIR spectrometer (Bruker Daltonics, MA, USA) using a single reflection ATR cell (DuraDisk, equipped with a diamond crystal). Data were recorded using OPUS v5.0 software, at room temperature, in the range of 4000–600 cm^{-1}, by accumulating x scans with a resolution of 2 cm^{-1}. Five replicate spectra were collected for each sample to evaluate reproducibility.

4. Results

Suberization pattern of Arabidopsis roots changes during combined heat and osmotic stress

Combination of heat and osmotic stress was imposed to *Arabidopsis* plants 8 DAG, at the onset of root secondary development (Leal *et al.*, 2020). In order to evaluate the effect of combined stress on root suberization, we performed a morphological and spacio-temporal characterization of root suberization, targeting the expression of the suberin biosynthesis maker Glycerol-3-phosphate acyltransferase 5 - *GPAT5 (pGPAT5:mCITRINE-SYP122*(Barberon *et al.*, 2016), as well as cell-wall suberization, using FY staining (Brundrett *et al.*, 1991). At 8 DAG, *Arabidopsis* root exhibits two distinct suberized tissues: the endodermis and the phellem. Suberized endodermis surrounds the central vasculature in primary developed roots, which can be found in the young region of the primary root and in LRs. In turn, phellem cells are only found in the root region undergoing secondary development and at the outermost root layer.

After 6h of combined heat and osmotic treatment, *GPAT5* marker expression was detected in endodermis and phellem cells of main root, with similar marker expression intensity as mock plants (Fig. **1a, c**; Fig. **S1a, c**). Also, the suberization detected in endodermis and phellem cells by FY staining had similar fluorescence intensities detected between mock and treated plants. (Fig. **1d, f**; Fig. **S2d, f**). In turn, *GPAT5* marker was detected not only in endodermis of LRs (as in mock plants), but also in cortex cells of plants exposed to the combined stress (Fig. **1b**). This ectopic *GPAT5* marker expression pattern was detected in 66% of total emerged LRs in the combined heat and osmotic stress, compared with only 5% of ectopic marker expression detected in LRs of mock treated plants (Fig. **S3**). However, at this time point, ectopic suberin was not detected by FY staining in LRs (Fig. **2e**).

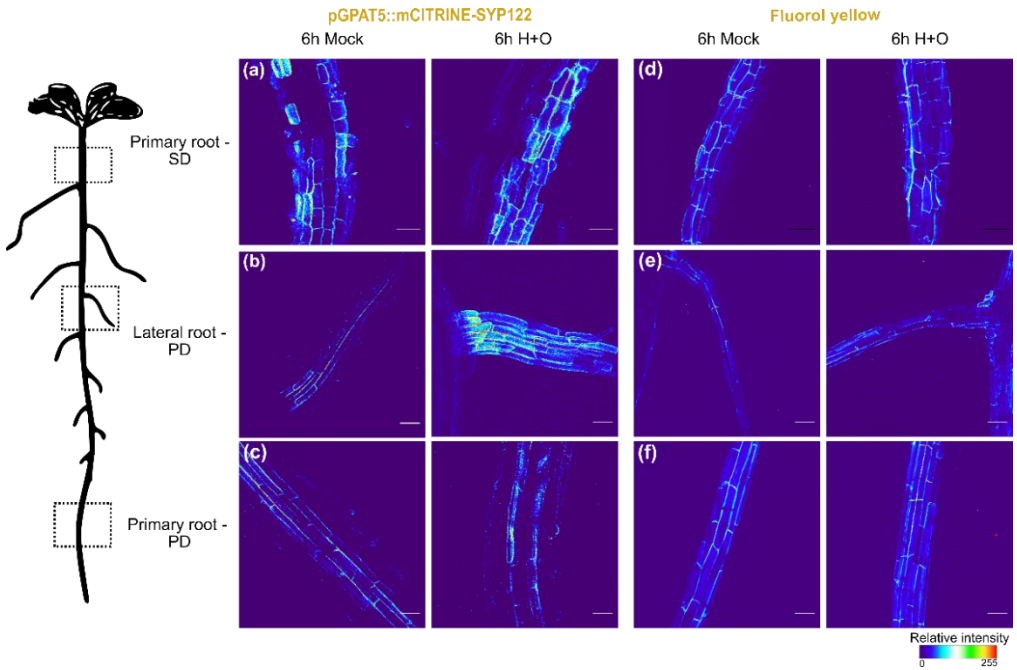

Fig. 1 Effect of combined heat and osmotic stress on the suberization pattern of secondary (a, d) and primary development (b, c, e, f) in lateral (LR) and primary root (PR) of Arabidopsis. Expression of suberin biosynthesis specific gene GPAT5 in the promoter line pGPAT5::mCITRINE-SYP122 (Thermal color) was detected after 6h of mock and combined heat and osmotic stress treatments in different zones of root: (a) secondary developmental region, (b) lateral roots (LR) and in (c) young primary root. Fluorol yellow staining (Thermal color) was used in col-0 Arabidopsis to detect suberin after 6h of mock and combined heat and osmotic stress treatments in the different zones of the root (d, e, f). The 3D maximum projection figures were obtained by confocal laser scanning with Z-stack images.Pixel values were converted in a thermal look- up-table Scale bar: 50 µm.

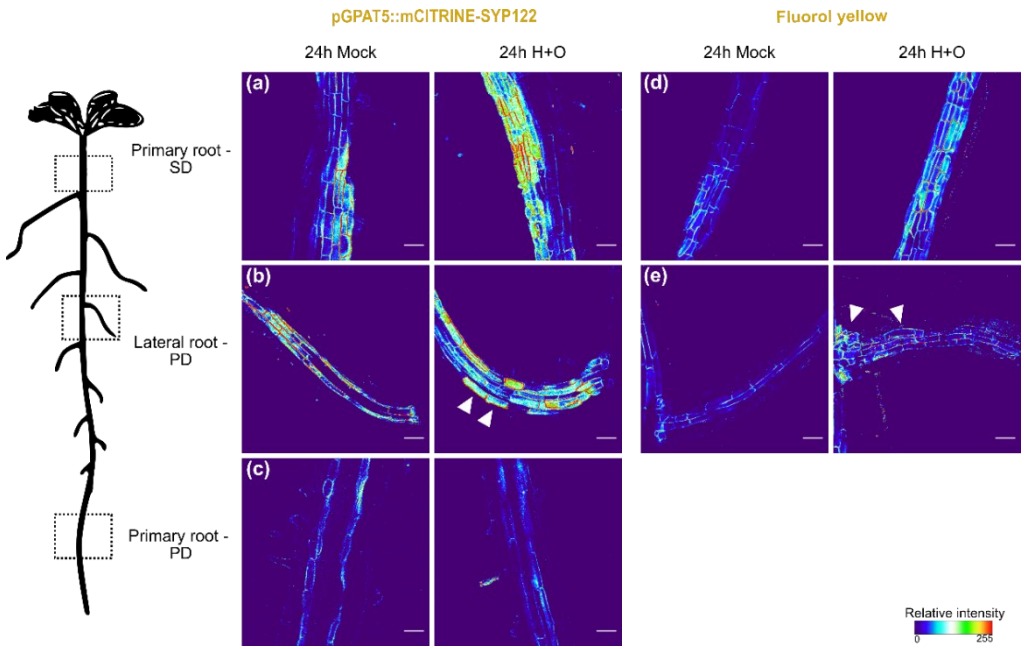

Fig. 2 Effect of combined heat and osmotic stress on the suberization pattern of secondary (a, d) and primary development (b, c, e) in lateral (LR) and primary root (PR) of Arabidopsis. Expression of suberin biosynthesis specific gene GPAT5 in the promoter line pGPAT5::mCITRINE-SYP122 (Thermal color) was detected after 24h of mock and combined heat and osmotic stress treatments in different zones of root: (a) secondary developmental region, (b) lateral roots (LR) and in (*c*) young primary root. Fluorol yellow staining (Thermal color) was used in col-0 Arabidopsis to detect suberin after 24h of mock and combined heat and osmotic stress treatments in the different zones of the root *(d, e)*. Arrowheads indicate GPAT5 expression and fluorol yellow staining in cortex cells of LRs The 3D maximum projection figures were obtained by confocal laser scanning with Z-stack images. Pixel values were converted in a thermal look- up-table. Scale bar: 50 µm

After 24h of combined heat and osmotic stress, *GPAT5* promoter activity was detected to be stronger in phellem cells of stress treated plants (Fig. **2a**). In parallel, FY staining fluorescence was found stronger in these phellem cells, as compared with mock treated plants (Fig. **2d**). In LRs, *GPAT5* ectopic marker expression is still detected after 24h of combined heat and osmotic treatment (Fig. **2b,** Fig. **S3**). In addition, suberin was detected by FY staining in LR cortex cells (Fig**. 2e** arrowheads). In young main root, as in the previous timepoint, no differences were detected with *GPAT5* marker expression (Fig. **2c**), as well as for FY staining, which were only detected in endodermis, similarly to mock treatment.

These results show that the root suberization process, including biosynthesis and deposition of suberin in cell walls is induced within 24h after the imposition of the combined heat and osmotic stress treatment, particularly in the phellem and ectopically in young lateral roots.

Aiming to elucidate the signalling pathway mediating suberization on *Arabidopsis* roots under the combination of heat and osmotic treatment we tested the external application of ABA. ABA is long known as key regulator of systemic responses during abiotic stress response, including combined drought and heat stresses (Vile *et al.*, 2012). In addition, ABA is described as inducer of suberin-associated genes and as a mediator in several suberization processes in control and stress conditions (Lulai *et al.*, 2008; Leide *et al.*, 2012; Barberon *et al.*, 2016). Using 1µM ABA, we found that *GPAT5* expression is induced in a very similar pattern as for the combination of heat and osmotic stress (Fig. **3**). After 20h of ABA treatment, *GPAT5* marker expression was detected in cortical and epidermis cells of LR (Fig. **3b**), and mostly no differences in *GPAT5* expression pattern were detected in main root, in primary or secondary growth zones, when compared with mock treatments (Fig. **3a, c**). Although this is a preliminary result, due the low number of replicates, this result may indicate ABA as candidate regulator of ectopic

GPAT5 expression in LRs in response to combined heat and osmotic stress.

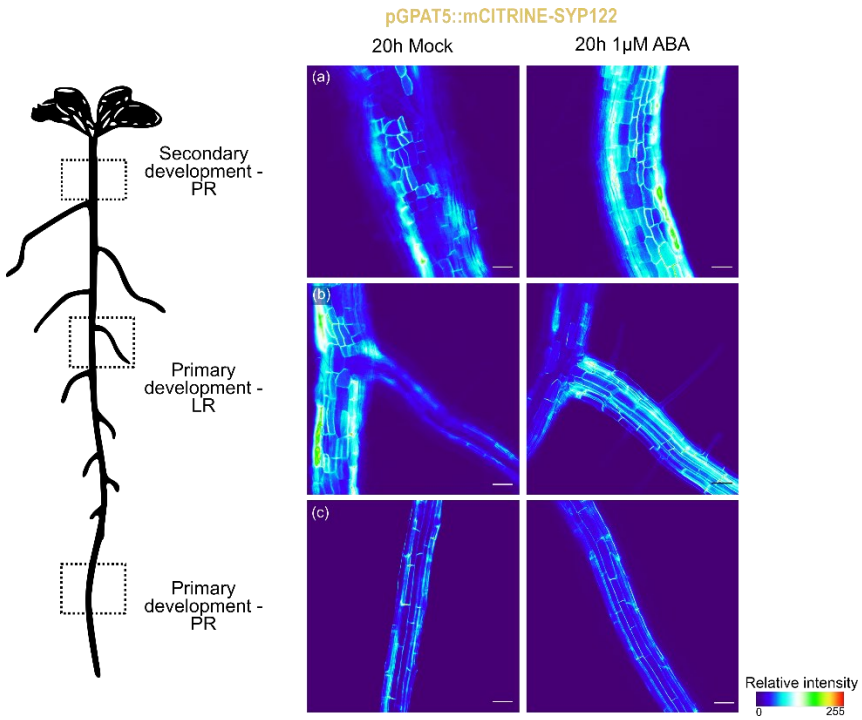

Fig. 3 *GPAT5::mCITRINE-SYP122 expression 20 hours after ABA and mock treatments in different zones of root: secondary (a) and primary development in lateral (LR)(b) and primary root (PR) (c). Pixel values were converted in a thermal look- up-table. Scale bar: 50 µm*

Differential gene expression in suberization induced under combined heat and osmotic stress

To get a wider view over the molecular pathways mediating suberin deposition in roots in response to combined heat and osmotic stress, we further evaluated the expression of several genes with demonstrated involvement in suberization. Considering the distinct responses detected between root zones, we sampled the root in two distinct segments (Fig. **S1**). Zone A, which includes secondary developed root zone and LRs, and Zone B, which is collected from main root tip to the first emerged LR. The targeted genes included *GPAT5* (Beisson *et al.*,

2007), Aliphatic Suberin Feruloyl Transferase - *ASFT* (Molina *et al.*, 2009) and ATP-Binding Cassette G6 - ABCG6 (Yadav *et al.*, 2014), which are involved in different steps of suberin biosynthesis and deposition, and the *MYB41* transcription factor, reported as a regulator of suberization process in response to osmotic, ABA and salt stress (Kosma *et al.*, 2014). In addition, a FK506-binding protein - *ROF2* and Responsive to dehydration 22 - *RD22* were selected as marker genes for heat and osmotic stresses, respectively. Casparian strip membrane protein 1 - *CASP1* expression was also assessed to determine if Casparian strip was affected by the imposed stress.

In the zone A (**Fig. 4a**), genes involved directly in the suberization process - *GPAT5*, *ABCG6* and *ASFT* - showed a similar expression pattern, being upregulated shortly after 1h of stress imposition, and reaching a peak of expression at 3h (3 to 5-fold upregulation, compared to mock). After this time-point, gene expression decreased in combined stress, reaching the levels detected for mock treatment, at 24h. In turn, *MYB41* expression peaks shortly at 1h after combined stress application (> 3-fold upregulation, compared to mock), and only reach mock expression levels after 3h. Interestingly, *ROF2* expression was also highly upregulated 1h after stress initiation, decreasing afterwards and reaching basal levels at 24h in stress. The osmotic stress-specific *RD22* gene showed a stepwise increase in expression in the first hours after stress, reaching a peak only after 4h, and decreasing in the following time-points analysed. Contrastingly, *CASP1* expression showed to be downregulated in response to combined heat and osmotic stress, showing reduced levels of expression along the 24h treatment.

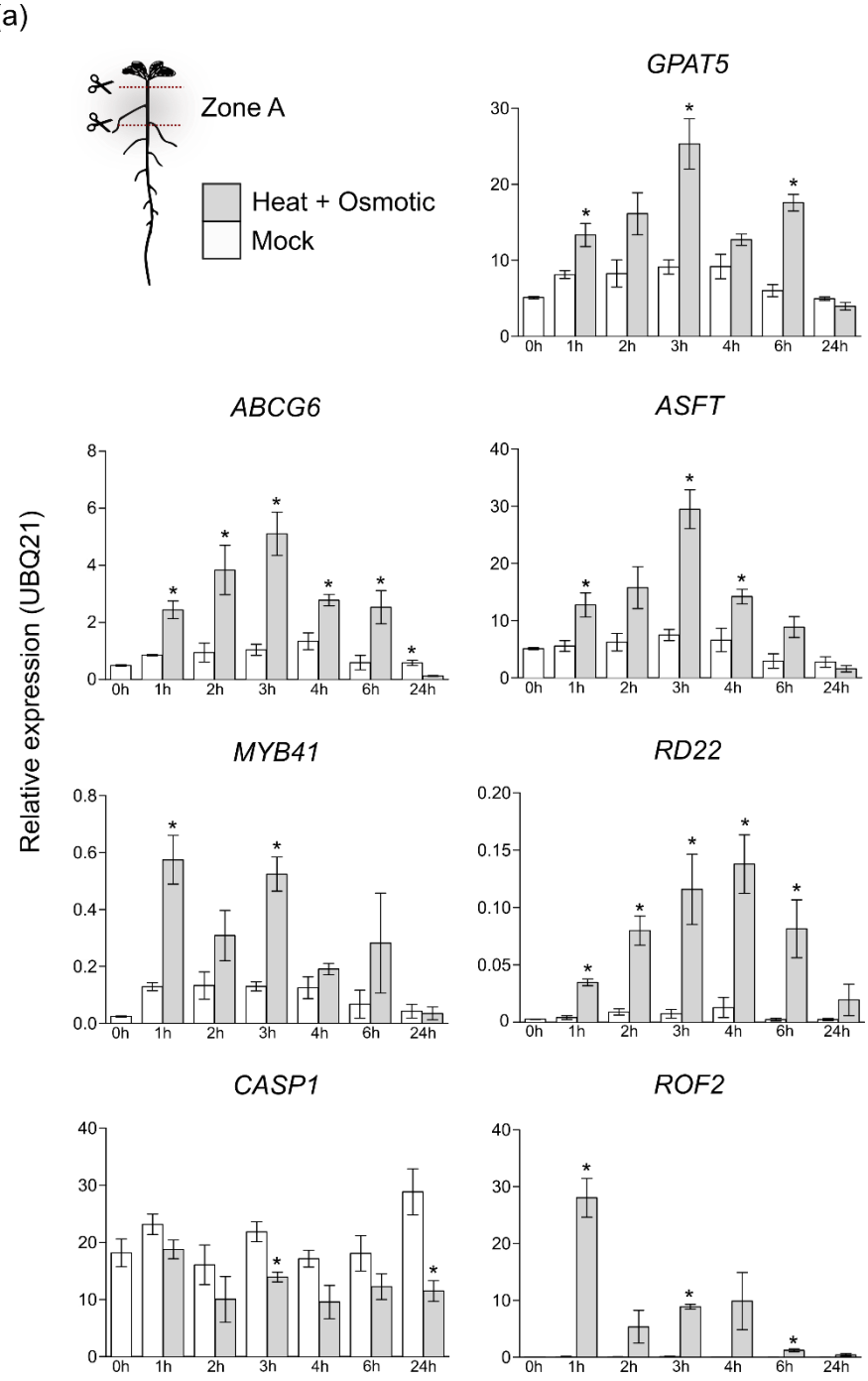
(a)
Zone A
Heat + Osmotic
Mock
Relative expression (UBQ21)
GPAT5
ABCG6
ASFT
MYB41
RD22
CASP1
ROF2
0h
1h
2h
3h
4h
6h
24h

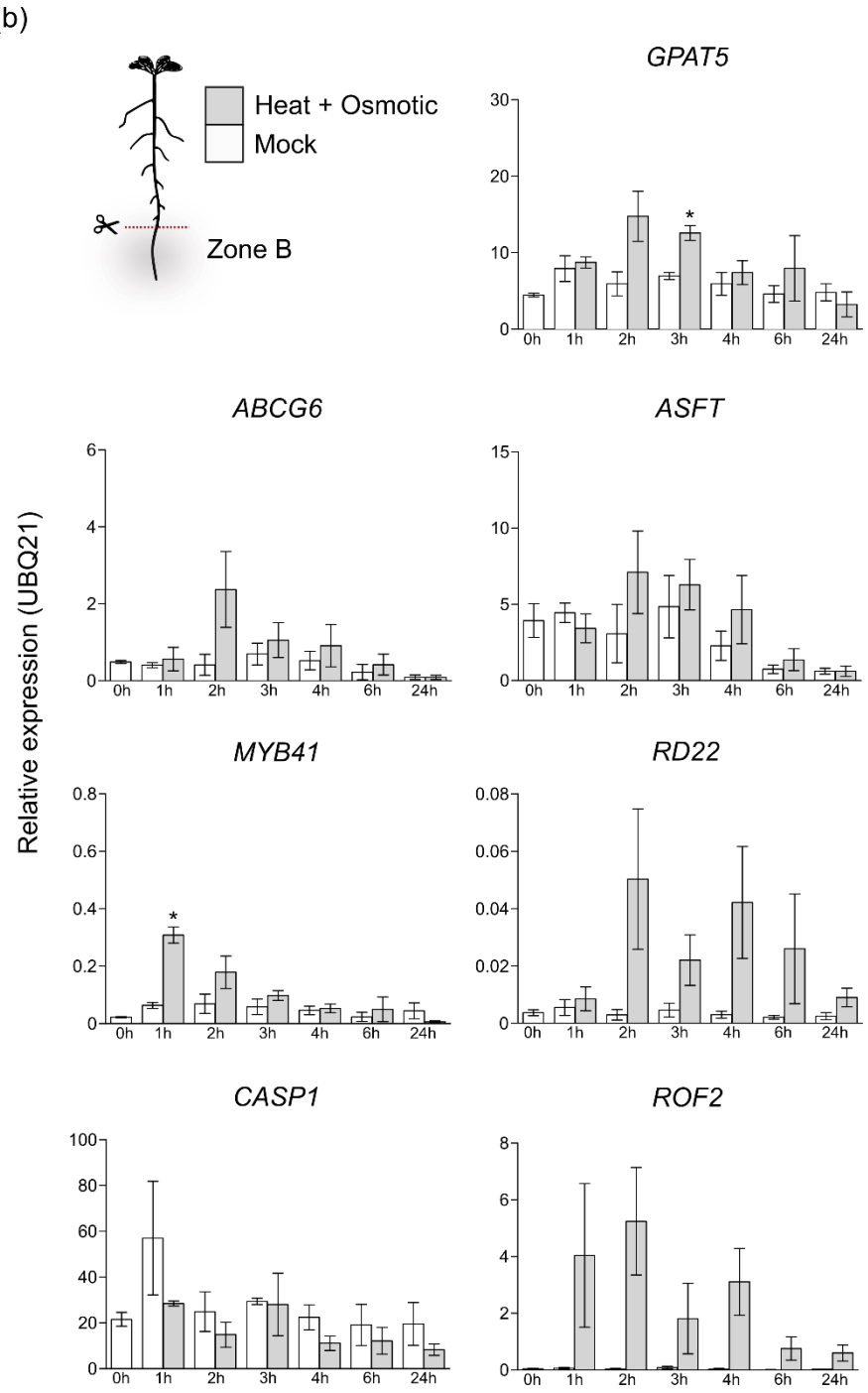
(b)
Heat + Osmotic
Mock
Zone B
Relative expression (UBQ21)
GPAT5
ABCG6
ASFT
MYB41
RD22
CASP1
ROF2
0h
1h
2h
3h
4h
6h
24h

Fig. 4 *(previous pages) Relative expression of selected genes involved in suberization and response to stress, in Arabidopsis roots subjected to combined heat and osmotic stress and mock treatments. Zone A (a) and zone B (b) of roots were evaluated individually for time points before stress imposition (0) and at multiple time points until 24h after stress initiation. Gene expression was analyzed by RT-qPCR and normalized with the housekeeping gene UBC21. Mean expression ± standard deviation from 3 independent experiments is represented for each timepoint. (*) represents significative difference (p<0.05 – unpaired t-test) when comparing mock with combined heat and osmotic stress in each timepoint.*

In zone B, the impact of combined stress in the expression of suberin-related genes is lower than what was observed for zone A (Fig. **4b**). We found some tendency to increase expression in *GPAT5*, *ASFT* and *ABCG6* during combined stress, however the differences to mock expression were mostly not statistically significant. Nevertheless, an expression peak was detected for these genes at 2h after combined stress imposition. An upregulation of *MYB41* expression was also detected in this root zone 1h after treatment, reaching mock expression levels after 4h. Equally, *ROF2* and *RD22* were also induced, but this response was again less pronounced than what was observed for the root zone A. In turn, *CASP1* does not suffer significant alterations in expression in this region of the root after combined heat and osmotic imposition.

Generally, the combination of heat and osmotic stress influenced root suberization depending on the overall development, with stronger induction of suberization observed in the older root zone, where LRs and phellem have already developed.

Combined heat and osmotic stress changes root cell wall composition

The impact of combined heat and osmotic stress in global cell wall composition in the different zones of the root after combined heat and osmotic treatments was further assessed by ATR-FTIR. This is a fast

procedure that provides information of cell wall polymers and functional groups, without the need to prepare extracts or make solubilizations. The fundamental vibration modes of molecular functional groups produce characteristic spectral absorption features that can serve to 'fingerprint' many cell wall compounds (Largo-Gosens *et al.*, 2014). For strongly suberized cells, their ATR-FTIR spectra is recognised to peak at several wavenumbers, generating a fingerprint representing typical suberin monomer groups including long aliphatic chains (2921, 2852 cm^{-1}), carboxyl and ester groups (1737, 1242, and 1158 cm^{-1}), phenolic compounds (1430 cm^{-1}), and wax or suberin-like aliphatic components (1318 and 1372cm^{-1}) (Zeier & Schreiber, 1999; Ferreira *et al.*, 2012; Garcia *et al.*, 2014) (Table S2). ATR-FTIR spectra were obtained for the root zones A and B (Fig. **S1**) of plants subjected to 24h of combined heat and osmotic and for mock treatment. Under mock conditions, the ATR-FTIR spectra obtained for the two different developmental zones (Zone A and Zone B) were similar, and several peaks assigned to suberin could be identified, including the aliphatic chains and carboxyl and ester groups (Fig. **S4**, dashed lines 1-2 and 3,7-8). The main difference between spectra obtained for zones A and B was found between 1030 and 1053 cm^{-1} (Fig. **S4**, arrowheads). Strong bands between 1032 cm^{-1} and 1055 cm^{-1} are assigned to the C–O stretching of primary and secondary alcohols (Maréchal & Chanzy, 2000; Fahey *et al.*, 2017) (Table S2), associated with diverse polysaccharides, such as cellulose, hemicellulose and pectin molecules (Ribeiro da Luz, 2006). In primary development sample, Zone B, a plateau is detected in this region of the spectra, and a peak at 1035cm^{-1} for zone A sample (LR and secondary development). These results suggest that in control conditions, B root zone has an equivalent composition in primary and secondary alcohols from diverse polysaccharides, whereas in root zone A the primary alcohols are prevalent.

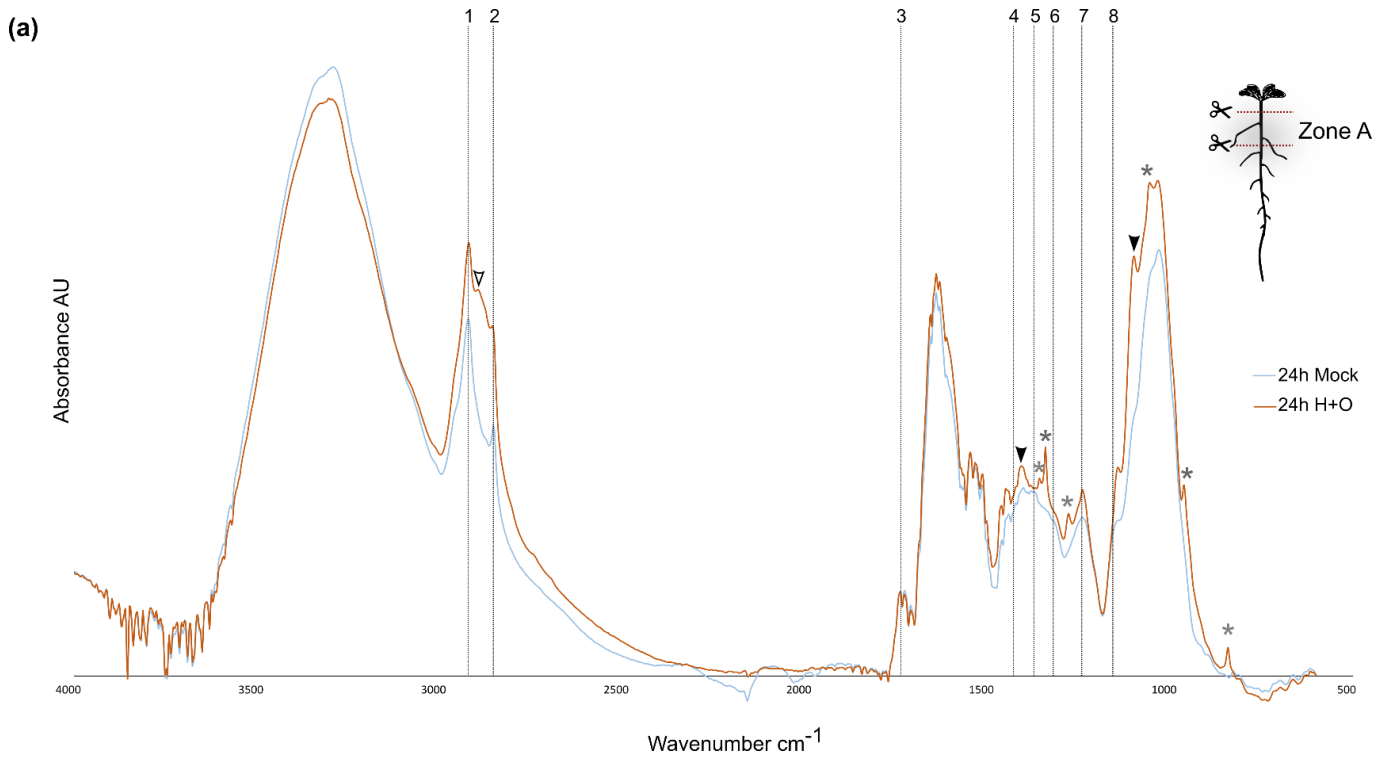
(a)
1
2
3
4
5
6
7
8
Zone A
Absorbance AU
24h Mock
24h H+O
4000
3500
3000
2500
2000
1500
1000
500
Wavenumber cm-1

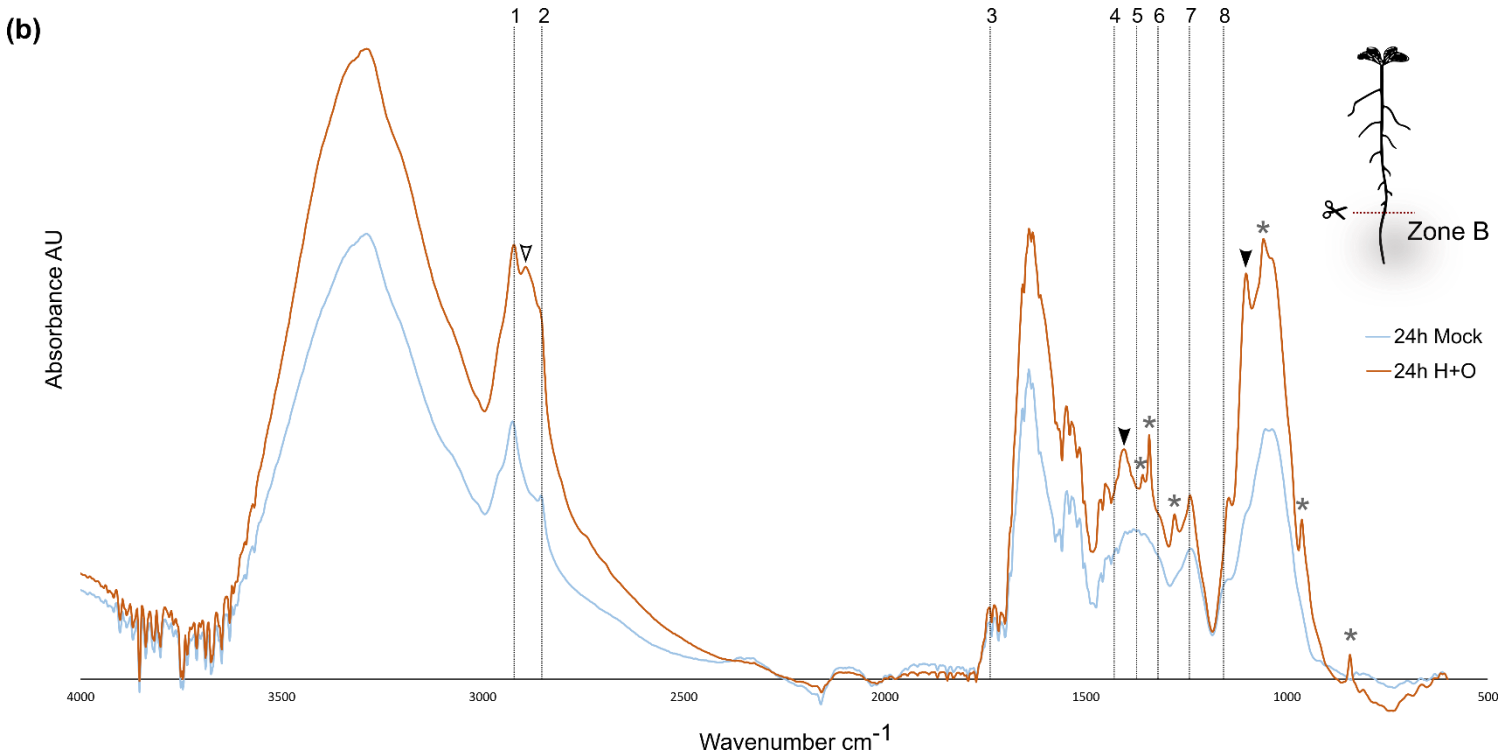

Fig. 5 *ATR-FTIR spectra of the Arabidopsis root zone A (a) and zone B (b), collected 24h after application of mock or combined heat and osmotic stress (H+O). Vertical dashed lines highlight major peaks assigned for suberin groups: 1 and 2- long aliphatic chains of suberin (2921, 2852 cm^{-1}); 3, 7 and 8 – carboxyl and ester groups (1737, 1242, and 1158 cm^{-1}); 4 - phenolic compounds (1430 cm^{-1}); 5 and 6 - wax or suberin-like aliphatic components (1318 and 1372cm^{-1}). Arrowheads indicate novel peaks detected in response to combined stress. Asterisks indicate strong peaks detected in PEG6000 sample.*

The ATR-FTIR profile obtained for root samples after 24h of combined stress was similar to mock, in what concerns absorbance peaks attributed to suberin monomer groups, for both root zones analysed (**Fig. 5**, dashed lines). Nevertheless, specific changes were observed in samples exposed to combined stress, which were also found in both root zones. More specifically, three new absorbance peaks at 2889 (Fig. **5**, white filled arrowheads), 1407 and 1097 cm^{-1} (Fig. **5**, black filled arrowheads) were found in the ATR-FTIR spectra in these samples. Absorbance at 2889 cm^{-1} in ATR-FTIR spectra is assigned to cellulose molecules (C-H stretching vibrations) (Tran *et al.*, 2016) (Fig. **5**, white filled arrowheads), while 1407 and 1097 cm^{-1} are both assigned to pectin (Alonso-Simón *et al.*, 2011; Szymanska-Chargot & Zdunek, 2013) (Fig. **5**, black filled arrowheads) (Table S2). In addition, other new absorbance peaks were also identified (**Fig. 5**, asterisks), however, these could be attributed to possible contaminations with PEG6000, used in media for osmotic treatment.

The assignment of peaks of non-extracted samples makes possible the occurrence of overlapping bands/peaks that correspond to different cell wall components or even contaminants. Nevertheless, the global changes detected by the ATR-FTIR spectra suggests that the combined heat and osmotic stress induces changes in the cell wall load of cellulose and pectin.

5. Discussion

Suberization is being regarded as an interesting trait to improve plant response to abiotic stress. Several studies have shown that changes in root suberin deposition can affect the way plants cope with the applied stresses. Heat and drought showed some different effects on plants when applied alone (Rizhsky *et al.*, 2004; Prasch & Sonnewald, 2013), and concerning root growth, opposite effects were described (Vile *et al.*,

2012). In contrast, heat and drought alone have shown similar effects concerning suberization, with increasing suberization detected in several plant species and organs when individual stresses are applied (Lee *et al.*, 2009; Henry *et al.*, 2012; Rasheed *et al.*, 2016; Zhang *et al.*, 2020). Induced suberization in roots after stress application also proved different depending on the root developmental stage (Kreszies *et al.*, 2019). Thus, it is of great importance to study the effect of abiotic stress in suberization, taking into account the root anatomy and developmental stage, to better understand the influence of suberized barriers in adaptation to stress.

In this work we used 8 DAG *Arabidopsis* to study the influence of a combination of heat and osmotic treatment on suberization in roots. At 8 DAG, *Arabidopsis* root system is already complex, with secondary development is present in a small portion of the upper part of the main root, with suberized phellem as the outermost layer (Leal *et al.*, 2020), and bellow this region, in primary development, the main root has a layer of suberized endodermis around the stele. In addition, LRs are already present, showing equivalent morphology of younger root, both undergoing primary development.

Using plants undergoing secondary growth, we could detect a distinct response to the combined heat and osmotic stress in the different developmental zones of the root system. In the endodermal cells of the main root, no significant differences were observed, regarding expression levels of suberin biosynthesis genes or in terms of suberin deposition (as assessed by fluorol yellow staining). Contrastingly, in the older part of the root, phellem cells showed increased *GPAT5* expression, as well as a stronger FY staining, after the combined heat and osmotic treatment (Figs. **1 and 2**). On the other hand, the suberization pattern of LRs was drastically altered upon combined stress treatment, with the activation of *GPAT5* expression and suberin

deposition being detected, not only in the endodermis cells, but also in cortex and epidermal cells, which do not undergo suberization in mock conditions (Figs. **1 and 2**). In our study, the expression of suberin-related genes and the overall suberization pattern was almost undisturbed by the combined Heat and Osmotic stress in the young zone of the root (zone B), as compared with the secondary development zone (the older part, A) (**Fig. 4**). The increased transcription levels of the target genes observed in zone A could be biased by the presence of LRs, as observed by microscopy, compared to phellem. Therefore, an independent evaluation of gene expression in phellem and LRs would be important to further understand the effective contribution of each organ for estimation of gene expression. Also, to better prove the impact on the suberization in the different root zones, the quantification of fluorescence intensity would be important, although a higher number of pictures from different plant replicates would be necessary.

Interestingly, ABA treatment induced a similar response to combined heat and osmotic stress, with activation of suberin marker ectopically in cortex and epidermis cells of LRs, whereas no obvious alteration was detected in the main root. Previous studies have demonstrated that ABA not only induces expression of suberin biosynthesis genes in tissues that are commonly suberized, but is also able to induce ectopic suberization in other tissues (Lee *et al.*, 2009; Boher *et al.*, 2013; Kosma *et al.*, 2014; Yadav *et al.*, 2014; Barberon *et al.*, 2016). In fact, ABA treatment of 4 DAG *Arabidopsis*, not only leads to an early onset of endodermis suberization, but also to ectopic suberization in cortex and epidermal cells of main roots (Barberon *et al.*, 2016). ABA treatment also induced ectopic expression of the suberin synthesis regulator TF MYB41 (Kosma *et al.*, 2014) namely in the root cortex and epidermis of 5 days-old *Arabidopsis* plants. Ectopic suberization or activation of suberin-related genes induced by ABA was only experimentally tested

in young *Arabidopsis* roots, with no ongoing secondary development (Kosma *et al.*, 2014; Barberon *et al.*, 2016). However, the ABA-induced ectopic suberization phenotype previously described for young *Arabidopsis* roots appears identical to the suberization phenotype we observed in LRs after combined stress imposition, likely pointing for a role of ABA in this process. The use of ABA biosynthesis or response mutants, under the control of a phellem promoter, would provide a deeper understand of the involvement of this hormone, in the stress response. On other way, the repression of the ABA signal, using an inducible promoter, at the same time as the stress treatment, would make clear if the different root suberization pattern under stress (in lateral roots) is due the ABA signalling alone.

Using ATR-FTIR it was possible to obtain a preliminary understanding of other compositional changes in root cell walls in response do combined stress. ATR-FTIR has been extensively used to analyse and monitor cell wall changes occurring as a result of various processes, such as growth and development (Zeier & Schreiber, 1999; Dokken *et al.*, 2005), genetic modifications (Mouille *et al.*, 2003) and responses to abiotic or biotic stresses (Cai *et al.*, 2011). In our samples, typical absorbance peaks attributed to suberin were equally identified in the spectra of both developmental zones analysed. Despite the increased suberization found in response to combined stress (as assessed by microscopy and gene expression analyses), the suberin monomeric relative composition is apparently unaltered. Nevertheless, changes in the ATR-FTIR spectra indicate other possible alterations in root cell walls induced by the combined stress treatment. For both root developmental zones analysed, ATR-FTIR spectra show new peaks that indicate a possible relative increase in cellulose and pectin levels (new bands at 2889 and 1407 and 1097 cm^{-1}, respectively) after the stress treatment. The plant cell wall is long believed to be composed of

two separate networks: a pectin network and a hemicellulose/cellulose network (Cosgrove, 2005). Although this model of the plant cell wall is still generally accepted, increasing evidence shows interactions between these two networks and a more dominant role of pectin as part of the load-bearing cell wall structures (Peaucelle *et al.*, 2012). Pectins are often described as modified in plants exposed to stress. In drought stress, increased amount of pectins and more ramified pectin backbones were proposed to form hydrogel capsules that would limit the cell damage (Leucci *et al.*, 2008; Tenhaken, 2015). Also, heat was described to modulate the degree of methylesterification/ramification of the pectins, by the induction of pectin methylesterase (Yang *et al.*, 2006; Huang *et al.*, 2017; Wu *et al.*, 2018). Nevertheless, modulation of pectin in response to abiotic stress still remains largely unknown. The identification of bands attributed to pectin in root samples exposed to combined stress may indicate not only a relative increase in pectin levels but probably also in its side chains / ramifications. Investigation on pectin methylesterase gene expression would be necessary to test this hypothesis.

Regarding cellulose levels, a contrasting effect of different abiotic stresses has described (Wang *et al.*, 2016). Mild osmotic or ionic stress caused a decrease in cellulose synthesis by rapid internalization of cellulose synthase enzymes (CesAs) from the plasma membrane into small subcellular compartments (Crowell *et al.*, 2009; Gutierrez *et al.*, 2009). In turn, high temperatures alone were reported to cause an increase of CesA movement in the plasma membrane and a decrease in crystalline cellulose (Fujita *et al.*, 2011) suggesting an opposite relationship between the rate of cellulose synthesis and its crystallinity (Fujita *et al.*, 2012). Additionally, several evidences point for an increase in cellulose content when plants are exposed to heat (Yang *et al.*, 2006; Lima *et al.*, 2013; Guerriero *et al.*, 2014). Evaluation of CesAs

expression may elucidate about the putative increase in cellulose loading in *Arabidopsis* roots after combined stress treatment. ATR-FTIR analysis on non-extracted cell walls are preliminary and do not allow effective quantification of components, only relative quantifications. To better monitor the cell wall alterations and elucidate specific changes in cell wall components, it would be necessary to extract cell wall components from the differently affected root zones (phellem, young root and LRs) and perform detailed analysis by mass spectrometry (Bauer, 2012). This would further allow to identify and quantify suberin components in the different regions of the root, validating the suberization microscopy differences detected in stress treatments (Lopes *et al.*, 2000). Transmission electron microscopy, could also help investigating cell wall modifications across different root developmental zones and stress imposed treatment, specifically regarding cell wall thickening or modified suberin lamella features in different cell types (Franke *et al.*, 2005; Zhou *et al.*, 2015).

The plant cell wall is critical to maintain cellular structural integrity, simultaneously providing resistance to internal hydrostatic pressures and flexibility to support cell division and expansion in tissue differentiation, besides acting as environmental barrier protecting the cells in stress response. Alterations in cell wall pectin and cellulose components and structure upon combined stresses must also strongly influence the cell wall performance in its structural functions. Moreover, the observed expansion of suberization into the cortex and epidermis of LRs should profoundly impact the water and nutrient transport capacity of roots. More than detected increases in suberin, pectin and cellulose, our results support the idea that upon combined abiotic stress, the plant undergoes cell wall reorganization, with modified biosynthesis and / or assembly of major cell wall components, as also defended by (Ezquer *et al.*, 2020).

6. Acknowledgments

Ana Rita Leal performed this experimental work with the collaboration of Joana Belo. The Arabidopsis line of *pGPAT5::mCITRINE-SYP122* was kindly provided by Dr. Nico Geldner. Pedro Barros, M. Margarida Oliveira and Tom Beckman helped to design the research experiment and discuss the results.

7. Bibliography

Alonso-Simón A, García-Angulo P, Mélida H, Encina A, Álvarez JM, Acebes JL. **2011**. The use of FTIR spectroscopy to monitor modifications in plant cell wall architecture caused by cellulose biosynthesis inhibitors. *Plant Signaling and Behavior* **6**: 1104–1110.

Barberon M, Vermeer JEM, De Bellis D, Wang P, Naseer S, Andersen TG, Humbel BM, Nawrath C, Takano J, Salt DE, *et al.* 2016. Adaptation of Root Function by Nutrient-Induced Plasticity of Endodermal Differentiation. *Cell* **164**: 447–459.

Bauer S. **2012**. Mass spectrometry for characterizing plant cell wall polysaccharides. *Frontiers in Plant Science* **3**: 1–6.

Beisson F, Li Y, Bonaventure G, Pollard M, Ohlrogge JB. **2007**. The acyltransferase GPAT5 is required for the synthesis of suberin in seed coat and root of Arabidopsis. *The Plant cell* **19**: 351–368.

Boher P, Serra O, Soler M, Molinas M, Figueras M. **2013**. The potato suberin feruloyl transferase FHT which accumulates in the phellogen is induced by wounding and regulated by abscisic and salicylic acids. *Journal of Experimental Botany* **64**: 3225–3236.

Brundrett MC, Kendrick B, Peterson CA. **1991**. Efficient Lipid Staining in Plant Material with Sudan Red 7B or Fluoral Yellow 088 in Polyethylene Glycol-Glycerol. *Biotechnic & Histochemistry* **66**: 111–116.

Cai X, Chen T, Zhou Q, Xu L, Qu L, Hua X, Lin J. **2011**. Development of Casparian strip in rice cultivars. *Plant Signaling & Behavior* **6**: 59–65.

Cosgrove DJ. **2005**. Growth of the plant cell wall. *Nature Reviews Molecular Cell Biology* **6**: 850–861.

Crowell EF, Bischoff V, Desprez T, Vernhettes S. **2009**. Pausing of Golgi Bodies on Microtubules Regulates Secretion of Cellulose Synthase Complexes in Arabidopsis. **21**: 1141–1154.

Dokken KM, Davis LC, Marinkovic NS. **2005**. Use of Infrared Microspectroscopy in Plant Growth and Development. *Applied Spectroscopy Reviews* **40**: 301–326.

European Environment Agency. **2019**. Climate change adaptation in the agriculture sector in Europe. *EEA Report*: 112.

Ezquer I, Salameh I, Colombo L, Kalaitzis P. **2020**. Plant Cell Walls Tackling Climate Change: Biotechnological Strategies to Improve Crop Adaptations and Photosynthesis in Response to Global Warming. *Plants* **9**: 212.

Fahey LM, Nieuwoudt MK, Harris PJ. **2017**. Predicting the cell-wall compositions of Pinus radiata (radiata pine) wood using ATR and transmission FTIR spectroscopies. *Cellulose* **24**: 5275–5293.

Ferreira R, Garcia H, Sousa AF, Petkovic M, Lamosa P, Freire CSRR, Silvestre AJDD, Rebelo LPN, Pereira CS. **2012**. Suberin isolation from cork using ionic liquids: Characterisation of ensuing products. *New Journal of Chemistry* **36**: 2014–2024.

Franke R, Briesen I, Wojciechowski T, Faust A, Yephremov A, Nawrath C, Schreiber L. **2005**. Apoplastic polyesters in Arabidopsis surface tissues - A typical suberin and a particular cutin. *Phytochemistry* **66**: 2643–2658.

Fujita M, Himmelspach R, Hocart CH, Williamson RE, Mansfield SD, Wasteneys GO. **2011**. Cortical microtubules optimize cell-wall crystallinity to drive unidirectional growth in Arabidopsis. : 915–928.

Fujita M, Lechner B, Barton DA, Overall RL, Wasteneys GO. **2012**. The missing link: Do cortical microtubules define plasma membrane nanodomains that modulate cellulose biosynthesis? *Protoplasma* **249**: 59–67.

Garcia H, Ferreira R, Martins C, Sousa AF, Freire CSR, Silvestre AJD, Kunz W, Rebelo LPN, Silva Pereira C. **2014**. Ex situ reconstitution of the plant biopolyester suberin as a film. *Biomacromolecules* **15**: 1806–1813.

Ginzberg I, Barel G, Ophir R, Tzin E, Tanami Z, Muddarangappa T, De Jong W, Fogelman E. **2009**. Transcriptomic profiling of heat-stress response in potato periderm. *Journal of Experimental Botany* **60**: 4411–4421.

Guerriero G, Legay S, Hausman J. **2014**. Alfalfa Cellulose Synthase Gene Expression under Abiotic Stress : A Hitchhiker ' s Guide to RT-qPCR Normalization. **9**.

Gutierrez R, Lindeboom JJ, Paredez AR, Emons AMC, Ehrhardt DW. **2009**. Arabidopsis cortical microtubules position cellulose synthase delivery to the plasma membrane and interact with cellulose synthase trafficking compartments. *Nature Publishing Group* **11**.

Henry A, Cal AJ, Batoto TC, Torres RO, Serraj R. **2012**. Root attributes affecting water uptake of rice (Oryza sativa) under drought. *Journal of Experimental Botany* **63**: 4751–4763.

Huang YC, Wu HC, Wang Y Da, Liu CH, Lin CC, Luo DL, Jinn TL. **2017**. PECTIN METHYLESTERASE34 contributes to heat tolerance through its role in promoting stomatal movement. *Plant Physiology* **174**: 748–763.

Jia J, Zhou J, Shi W, Cao X, Luo J, Polle A, Luo Z Bin. **2017**. Comparative transcriptomic analysis reveals the roles of overlapping heat-/drought-responsive genes in poplars exposed to high temperature and drought. *Scientific Reports* **7**: 1–17.

Kosma DK, Murmu J, Razeq FM, Santos P, Bourgault R, Molina I, Rowland O. **2014**. AtMYB41 activates ectopic suberin synthesis and assembly in multiple plant species and cell types. *Plant Journal* **80**: 216–229.

Kreszies T, Shellakkutti N, Osthoff A, Yu P, Baldauf JA, Zeisler-Diehl V V., Ranathunge K, Hochholdinger F, Schreiber L. **2019**. Osmotic stress enhances suberization of apoplastic barriers in barley seminal roots: analysis of chemical, transcriptomic and physiological responses. *New Phytologist* **221**: 180–194.

Largo-Gosens A, Hernáindez-Altamirano M, García Calvo L, Alonso-Simón A, Álvarez J, Acebes JL. **2014**. Fourier transform mid infrared spectroscopy applications for monitoring the structural plasticity of plant cell walls. *Frontiers in Plant Science* **5**: 1–15.

Lawas LMF, Zuther E, Jagadish SK, Hincha DK. **2018**. Molecular mechanisms of combined heat and drought stress resilience in cereals. *Current Opinion in Plant Biology* **45**: 212–217.

Leal AR, Barros PM, Parizot B, Sapeta H, Nick V, Tonni Grube A, Tom B, Oliveira MM. **2020**. Phellem translational landscape throughout secondary development in Arabidopsis roots. *Chapter 2*: 3–29.

Lee SB, Jung SJ, Go YS, Kim HU, Kim JK, Cho HJ, Park OK, Suh MC. **2009**. Two Arabidopsis 3-ketoacyl CoA synthase genes, KCS20 and KCS2/DAISY, are functionally redundant in cuticular wax and root suberin biosynthesis, but differentially controlled by osmotic stress. *Plant Journal* **60**: 462–475.

Leide J, Hildebrandt U, Hartung W, Riederer M, Vogg G. **2012**. Abscisic acid mediates the formation of a suberized stem scar tissue in tomato fruits. *New Phytologist* **194**: 402–415.

Leucci MR, Lenucci MS, Piro G, Dalessandro G. **2008**. Water stress and cell wall polysaccharides in the apical root zone of wheat cultivars varying in drought tolerance. *Journal of Plant Physiology* **165**: 1168–1180.

Lima RB, dos Santos TB, Vieira LGE, Ferrarese MDLL, Ferrarese-Filho O, Donatti L, Boeger MRT, Petkowicz CLDO. **2013**. Heat stress causes alterations in the cell-wall polymers and anatomy of coffee leaves (Coffea arabica L.). *Carbohydrate Polymers* **93**: 135–143.

Lopes MH, Gil AM, Silvestre AJD, Neto CP. **2000**. Composition of Suberin Extracted upon Gradual Alkaline Methanolysis of Quercus suber L. Cork. *Journal of Agricultural and Food Chemistry* **48**: 383–391.

Lulai EC, Suttle JC, Pederson SM. **2008**. Regulatory involvement of abscisic acid in potato tuber wound-healing. *Journal of Experimental Botany* **59**: 1175–1186.

Maréchal Y, Chanzy H. **2000**. The hydrogen bond network in I(β) cellulose as observed by infrared spectrometry. *Journal of Molecular Structure* **523**: 183–196.

Mittler R. **2006**. Abiotic stress, the field environment and stress combination. *Trends in Plant Science* **11**: 15–19.

Molina I, Li-Beisson Y, Beisson F, Ohlrogge JB, Pollard M. **2009**. Identification of an Arabidopsis feruloyl-coenzyme A transferase required for suberin synthesis. *Plant physiology* **151**: 1317–28.

Mouille G, Robin S, Lecomte M, Pagant S, Höfte H. **2003**. Classification and identification of Arabidopsis cell wall mutants using Fourier-Transform InfraRed (FT-IR) microspectroscopy. *Plant Journal* **35**: 393–404.

Peaucelle A, Braybrook S, Höfte H. **2012**. Cell wall mechanics and growth control in plants: The role of pectins revisited. *Frontiers in Plant Science* **3**: 1–6.

Pfaffl MW. **2001**. A new mathematical model for relative quantification in real-time RT-PCR. *Nucleic acids research* **29**: 16–21.

Prasch CM, Sonnewald U. **2013**. Simultaneous application of heat, drought, and virus to Arabidopsis plants reveals significant shifts in signaling networks. *Plant physiology* **162**: 1849–66.

Ranathunge K, Kim YX, Wassmann F, Kreszies T, Zeisler V, Schreiber L. **2017**. The composite water and solute transport of barley (Hordeum vulgare) roots: effect of suberized barriers. *Annals of botany* **119**: 629–643.

Rasheed S, Bashir K, Matsui A, Tanaka M, Seki M. **2016**. Transcriptomic analysis of soil-grown arabidopsis thaliana roots and shoots in response to a drought stress. *Frontiers in Plant Science* **7**.

Rasmussen S, Barah P, Suarez-Rodriguez MC, Bressendorff S, Friis P, Costantino P, Bones AM, Nielsen HB, Mundy J. **2013**. Transcriptome responses to combinations of stresses in Arabidopsis. *Plant Physiology* **161**: 1783–1794.

Ribeiro da Luz B. **2006**. Attenuated total reflectance spectroscopy of plant leaves: A tool for ecological and botanical studies. *New Phytologist* **172**: 305–318.

Rizhsky L, Liang H, Shuman J, Shulaev V, Davletova S, Mittler R. **2004**. When defense pathways collide: the response of Arabidopsis to a combination of drought and heat stress. **134**: 1683–1696.

Soler M, Serra O, Fluch S, Molinas M, Figueras M. **2011**. A potato skin SSH library yields new candidate genes for suberin biosynthesis and periderm formation. *Planta* **233**: 933–945.

Szymanska-Chargot M, Zdunek A. **2013**. Use of FT-IR Spectra and PCA to the Bulk Characterization of Cell Wall Residues of Fruits and Vegetables Along a Fraction Process. *Food Biophysics* **8**: 29–42.

Tenhaken R. **2015**. Cell wall remodeling under abiotic stress. *Frontiers in Plant Science* **5**: 1–9.

Tran TN, Paul U, Heredia-Guerrero JA, Liakos I, Marras S, Scarpellini A, Ayadi F, Athanassiou A, Bayer IS. **2016**. Transparent and flexible amorphous cellulose-acrylic hybrids. *Chemical Engineering Journal* **287**: 196–204.

Tuteja N. **2007**. Abscisic acid and abiotic stress signaling. *Plant Signaling and Behavior* **2**: 135–138.

Verslues PE, Bray EA. **2004**. LWR1 and LWR2 are required for osmoregulation and osmotic adjustment in Arabidopsis. *Plant physiology* **136**: 2831–2842.

Vile D, Pervent M, Belluau M, Vasseur F, Bresson J, Muller B, Granier C, Simonneau T. **2012**. Arabidopsis growth under prolonged high temperature and water deficit: Independent or interactive effects? *Plant, Cell and Environment* **35**: 702–718.

Vogel E, Donat MG, Alexander L V, Meinshausen M, Ray DK, Karoly D, Meinshausen N, Frieler K. **2019**. The effects of climate extremes on global agricultural yields.

Wang T, McFarlane HE, Persson S. **2016**. The impact of abiotic factors on cellulose synthesis. *Journal of Experimental Botany* **67**: 543–552.

Van Der Weele CM, Spollen WG, Sharp RE, Baskin TI. **2000**. Growth of Arabidopsis thaliana seedlings under water deficit studied by control of water potential in nutrient-agar media. *Journal of Experimental Botany* **51**: 1555–1562.

Wu HC, Bulgakov VP, Jinn TL. **2018**. Pectin methylesterases: Cell wall remodeling proteins are required for plant response to heat stress. *Frontiers in Plant Science* **871**: 1–21.

Wunderling A, Ripper D, Barra-Jimenez A, Mahn S, Sajak K, Targem M Ben, Ragni L. **2018**. A molecular framework to study periderm formation in Arabidopsis. *New Phytologist* **219**: 216–229.

Yadav V, Molina I, Ranathunge K, Castillo IQ, Rothstein SJ, Reed JW. **2014**. ABCG Transporters Are Required for Suberin and Pollen Wall Extracellular Barriers in Arabidopsis. *The Plant Cell* **26**: 3569–3588.

Yang KA, Lim CJ, Hong JK, Park CY, Cheong YH, Chung WS, Lee KO, Lee SY, Cho MJ, Lim CO. **2006**. Identification of cell wall genes modified by a permissive high temperature in Chinese cabbage. *Plant Science* **171**: 175–182.

Zeier J, Schreiber L. **1999**. Fourier transform infrared-spectroscopic characterisation of isolated endodermal cell walls from plant roots: Chemical nature in relation to anatomical development. *Planta* **209**: 537–542.

Zhang L, Merlin I, Pascal S, Bert PF, Domergue F, Gambetta GA. **2020**. Drought activates MYB41 orthologs and induces suberization of grapevine fine roots. *Plant Direct* **4**: 1–17.

Zhang H, Sonnewald U. **2017**. Differences and commonalities of plant responses to single and combined stresses. *Plant Journal* **90**: 839–855.

Zhou X, Ding D, Ma J, Ji Z, Zhang X, Xu F. **2015**. Ultrastructure and Topochemistry of Plant Cell Wall by Transmission Electron Microscopy. In: The Transmission Electron Microscope - Theory and Applications. InTech.

8. Supplementary information

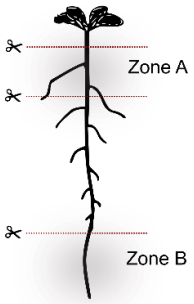

Fig. S1 *Schematic representation of the sampling performed in Arabidopsis roots. Roots were segmented for sampling in two different zones: secondary developmental zone – Zone A, containing the main root in secondary development and emerged lateral roots (±1.5 cm from hypocotyl); and primary development zone – Zone B, from root tip until the first visible lateral root*.

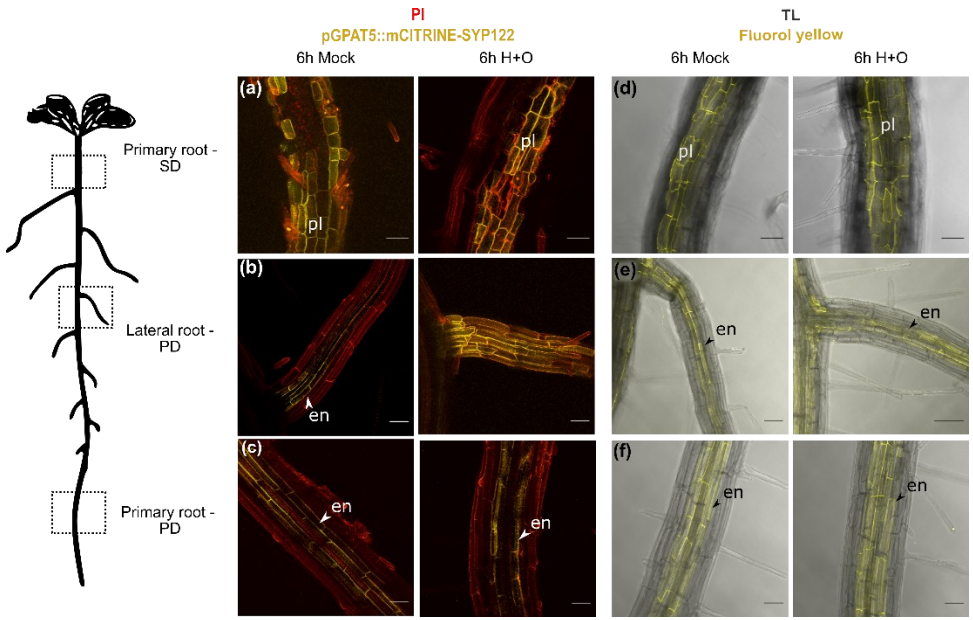

Fig. S2 Effect of combined heat and osmotic stress on the suberization pattern of secondary (a, d) and primary development (b, c d, e) in lateral (LR) and primary root (PR) of Arabidopsis. Expression of suberin biosynthesis specific gene GPAT5 in the promoter line pGPAT5::mCITRINE-SYP122 (yellow) was detected after 6h of mock and combined heat and osmotic stress treatments in different zones of root: (a) secondary developmental region, (b) lateral roots (LR) and in (a) young primary root. Propidium iodide (PI) was used to stain cell walls (red). Fluorol yellow staining (yellow) was used in col-0 Arabidopsis to detect suberin after 6h of mock and combined heat and osmotic stress treatments in the different zones of the root (d-f). The 3D maximum projection figures were obtained by confocal laser scanning with Z-stack images. Scale bar: 50 µm

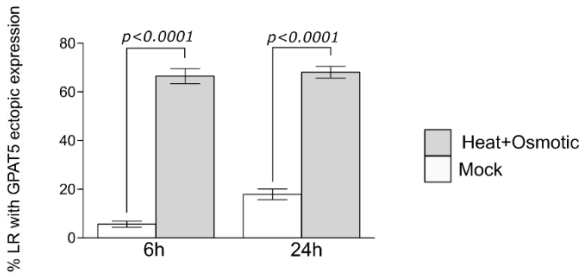

Fig. S3 *Percentage of lateral roots (LR) with ectopic pGPAT5::mCITRINE-SYP122 (GPAT5) expression after 6h and 24h of combined heat and osmotic stress. A total of 20 plants were analysed for each situation. Percentage relative to total number of emerged LR. Statistical significance between treatments for each timepoint was assessed using the unpaired t-test.*

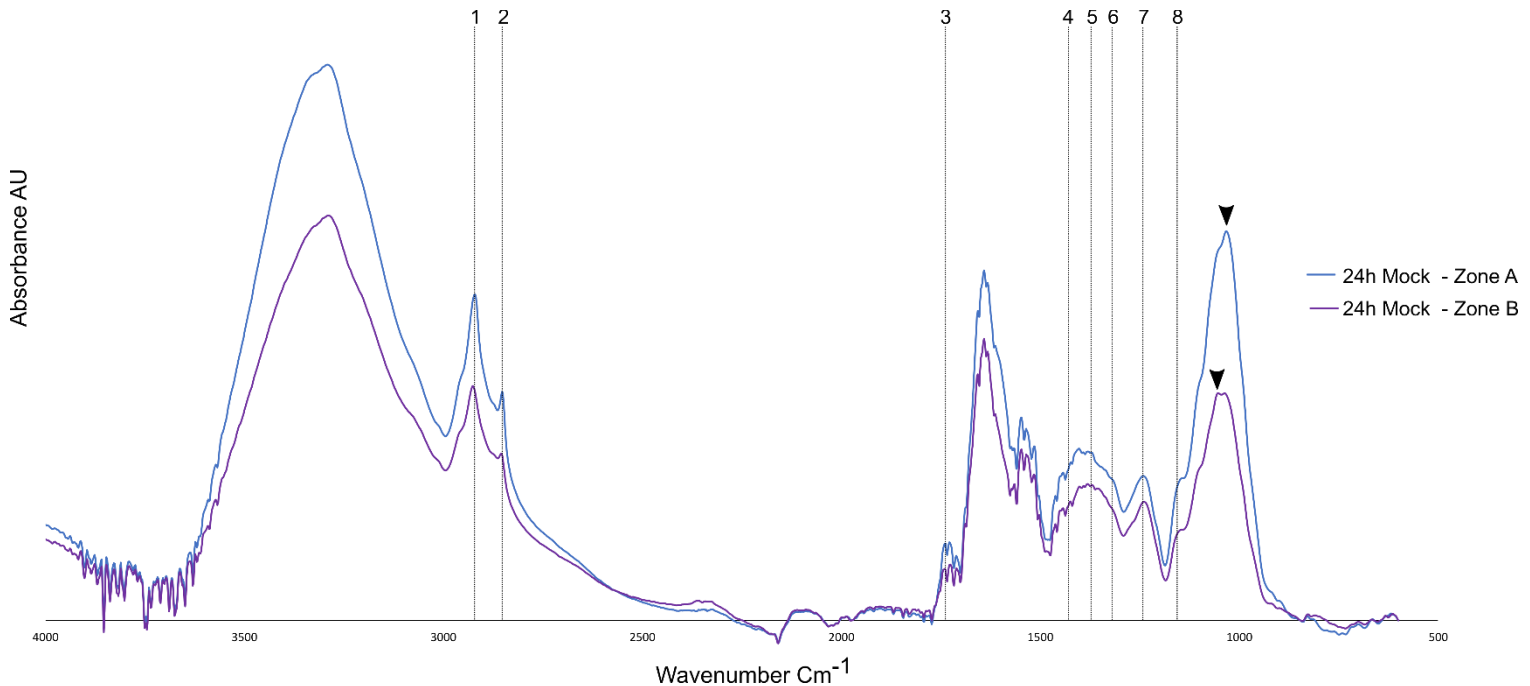

Fig. S4: ATR-FTIR spectra of the Arabidopsis secondary and primary developmental zone of root, collected 24h after mock treatment. *Vertical dashed lines highlight major peaks assigned for suberin monomer groups: 1 and 2- long aliphatic chains of suberin (2921, 2852 cm^{-1}); 3, 7 and 8 – carboxyl and ester groups (1737, 1242, and 1158 cm^{-1}); 4 - phenolic compounds (1430 cm^{-1}); 5 and 6 - wax or suberin-like aliphatic components (1318 and 1372cm^{-1}). Arrowheads indicate different peaks detected between both samples.*

Table S1: Primers used in this work.

Gene ID	Primer name	Sequence
AT2G36100 (CASP1)	AtCASP1_qPCR1_Fw	CGAAGAAGAAGGGCTTTGTG
	AtCASP1_qPCR1_Rv	GCTTGGAACTGGAGGAACTG
AT5G25760 (UBC21)	AtUBC10_qPCR1_Fw	CTTGGACGCTTCAGTCTGTG
	AtUBC10_qPCR1_Rv	GGCGAGGCGTGTATACATTT
AT5G13580 (ABCG6)	AtABCG6_qPCR1_Fw	ATGAACCAACTTCGGGTCTG
	AtABCG6_qPCR1_Rv	CGGGACAAGAAGAGAAGACG
AT3G11430 (GPAT5)	AtGPAT5_qPCR1_Fw	GGGTTTGAGTGCACCAACTT
	AtGPAT5_qPCR1_Rv	GGAGACAAGGCTCGAAAGTG
AT5G41040 (ASFT)	AtASFT_qPCR1_Fw	GGTCAAACCTGAATCCGAGA
	AtASFT_qPCR1_Rv	CTTGGACTGCTTCCTCGTTC
AT5G48570 (ROF2)	AtROF2_qPCR_Fw	TCGACACGCAGAACCAGTTT
	AtROF2_qPCR_Rv	GATCTCCATTTCCTCGCCGA
AT5G25610 (RD26)	AtRD22_qPCR_Fw	GTAGGAGTCGGTAAAGGCGG
	AtRD22_qPCR_Rv	TAGGATCGTCGTGGAGCTGA
AT4G28110 (MYB41)	AtMYB41_qPCR_Fw	CAATAGCCGCTCGTCTACCA
	AtMYB41_qPCR_Rv	TCAAGGCGTGGAGAATGAGT

Table S2: Summary of main peaks obtained by ATR-FTIR that are assignment to cell wall components.

Wavelength (cm^{-1})	Assigned functional groups	Assigned functional group chemical structure	Assigned cell wall component	Reference
2921and 2852	Long aliphatic chains		Suberin long chain aliphatic components	(Zeier and Schreiber, 1999; Ferreira *et al.*, 2012; Garcia *et al.*, 2014)
1737, 1242 and 1158	Carboxyl and ester groups	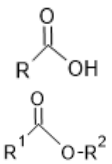	Carboxyl groups of the suberin fatty acids, ester groups of the suberin ester links	
1430	Phenolic compounds	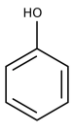	Suberin aromatic components	
1318 and 1372	Aliphatic components		wax or suberin-like aliphatic components	
1032	Primary alcohols	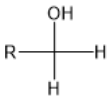	Polysaccharides	(Maréchal and Chanzy, 2000; Fahey *et al.*, 2017)
1055	Secondary alcohols	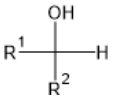	Polysaccharides	(Maréchal and Chanzy, 2000; Fahey *et al.*, 2017)
1407 and 1097	Galacturonic acid	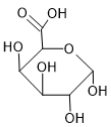	Pectin	(Alonso-Simón *et al.*, 2011; Szymanska-Chargot and Zdunek, 2013)
2889	Glucose	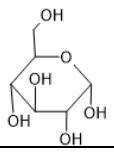	Cellulose	(Tran *et al.*, 2016)

Chapter IV

Cork oak root as a model for secondary growth – the phellem case study

Ana Rita Leal[1,2,3], Pedro M. Barros[1]*, Helena Sapeta[1], Joana Belo[1], Tom Beeckman[2], M. Margarida Oliveira[1]*

[1] Instituto de Tecnologia Química e Biológica António Xavier, Universidade Nova de Lisboa (ITQB NOVA), GPlantS, Av. da República, 2780-157 Oeiras, Portugal;

[2] Ghent University, Department of Plant Biotechnology and Bioinformatics, Technologiepark 71, 9052 Ghent, Belgium

[3] VIB Center for Plant Systems Biology, Technologiepark 71, 9052 Ghent, Belgium

* co-corresponding authors

Table of contents

1. Summary

The longevity and high activity of the cork cambium (or phellogen) from *Quercus suber* (cork oak) are the cornerstones for the sustainable exploitation of a unique raw material. Cork (or phellem) is mainly composed of dead cells with a high deposition of suberin in the cell walls, providing the first defense against abiotic/biotic stresses in organs undergoing secondary growth. In this study we used young cork oak tap roots to follow the development and suberization of cork tissues (phellem). In parallel we selected root segments undergoing secondary (SD) and primary development (SD), grown under different conditions, to perform a comparative transcriptomic analysis. We showed that phellem suberization is initiated early in root development, at 8 days after sowing, and accumulation of suberized phellem cells are detected thereafter. The SD transcriptional landscape showed enrichment in the expression of genes related to cell-wall modifications, mainly lignification and suberization, independently of the growth condition applied. In addition, several regulatory elements, particularly transcription factors and hormone related transcripts, show homology with previously identified genes involved in phellem differentiation in other species, indicating that the secondary development in cork oak root is relatively conserved. Our work provides an integrated view on the pathways regulating secondary growth in cork oak, which further support the design of science-based strategies capable of promoting cork oak growth acceleration while ensuring cork quality.

2. Introduction

Cork oak (*Quercus suber* L.) forests, known as Montado, are unique and emblematic resources in the Mediterranean region, especially in Portugal, where they cover 23% of total country forested area (‘APCOR - Associação Portuguesa de Cortiça’). Cork oak outer bark (or cork) is a raw material highly rich in suberin that acts as a major carbon sink and

develops along the tree life cycle, unlike other tree species (Aguado *et al.*, 2017; Leite & Pereira, 2017). The ability to fully regenerate new layers of outer bark after each harvest (done with 9 years intervals) allows regular extraction, being a sustainable system over many production cycles. Cork oak stands significantly contribute to ecosystem conservation in addition to the economic and social sustainability of the rural areas where the species is found. Also, industry investments in R&D have been of high importance, leading to new products and processes, as well as in improved quality of the cork products, resulting in 816 M € of international trade ('APCOR - Associação Portuguesa de Cortiça'). The cork added value for many applications (from production of wine stoppers to construction materials) is due to the physical and morphological characteristics of its cells, providing insulation, lightness and flexibility.

Cork cells (phellem) are formed from the phellogen (the cork cambium), after secondary growth initiation, in stems, branches and roots (Evert, 2006; Crang *et al.*, 2018). In cork oak stems, phellogen dedifferentiates from subepidermal cells during the first year of growth, extending as a continuous layer around the branch (Graça & Pereira, 2004). Preliminary studies detected the establishment of phellogen activity in 1.2 - 2 mm diameter stems (Cardoso, 2011), which are developed usually 2-months after germination. After phellogen division, phellem cells undergo several differentiation steps, which include massive cell wall suberization, cell expansion and programmed cell death (Evert, 2006; Crang et al., 2018). Histological studies showed that, during the first growth year, cork oak stems only develop 6–8 suberized phellem cell layers (Graça & Pereira, 2004).

The molecular pathways active during phellem development were investigated in cork oak using diverse comparative transcriptomic approaches (Soler *et al.*, 2007; Teixeira *et al.*, 2014, 2018; Boher *et al.*,

2018; Lopes *et al.*, 2019). Through the comparison of contrasting secondary developing tissues, namely phellem and xylem, multiple genes related to phellem differentiation could be highlighted, in particular those involved in the suberization process (Soler *et al.*, 2007; Lopes *et al.*, 2019). The expression of cork oak orthologs of genes involved in the synthesis of specific aliphatic (*Long-Chain acyl-CoA Synthetase 2* - LACS2, *Fatty acyl-coenzyme A reductas*e 1/4/5 - *FAR1/4/5*, *Cytochrome P450 86A1 - CYP86A1* and *CYP86B1*) and aromatic components (*phenylalanine ammonia lyase - PAL, Cinnamate-4-hydroxylase - C4H* and *Ferulate 5-hydroxylase - F5H*) and its assembly (*Glycerol-3-phosphate Acyl- Transferase 5/7 - GPAT5/7* , *Aliphatic suberin feruloyl transferase - ASFT* and *Fatty alchol:caffeoyl-CoA transferase- FACT*) and transport (*ATP-binding cassette G2/6/20 - ABCG2/6/20*) are more abundant in phellem, as compared to xylem (Soler *et al.*, 2007; Lopes *et al.*, 2019). Also, multiple transcription factors (TFs), including members of the MYB, NAC and WOX families, were detected in cork oak phellem transcriptomes (Soler *et al.*, 2007; Lopes *et al.*, 2019). These results suggest that the core pathways required for cell-wall suberization, as determined in model tree and herbaceous species, are conserved in cork oak. In another approach, where the transcriptome of good *versus* bad quality cork tissues was compared, the expression of genes encoding heat-shock, as well as lignin and suberin biosynthetic proteins was found enriched in the good quality cork (Teixeira *et al.*, 2014, 2018), highlighting the quality association with secondary cell wall modifications, including suberin deposition. These studies additionally revealed that cork oak phellem (cork) and xylem (wood) share several regulatory mechanisms, probably reflecting a similar ontogeny (Boher *et al.*, 2018; Lopes *et al.*, 2019).

Cork oak is a symbolic model for studies related to phellem and suberin chemistry, not only due its economic relevance, but mostly because of

the high production capacity of phellem cells. Despite the efforts made in recent years, the molecular regulation of cork oak secondary development, particularly phellem differentiation, is still poorly understood. The time required to establish the first phellem layer in stems complicates the use of cork oak in studies targeting the regulation of phellogen activity. As mentioned above, cork oak roots are also known to undergo secondary development, with phellem cells differentiating in old lateral/secondary roots (Machado *et al.*, 2013). In the model *Arabidopsis thaliana*, the root phellogen layer is described to dedifferentiate from the pericycle cells located beneath the root endodermis (Wunderling *et al.*, 2018; Chapter II) contrasting with the process of phellem development described in stems (of either cork oak or other species) (Graça & Pereira, 2004; Evert, 2006; Crang *et al.*, 2018). The development of phellem inside the root leads to the detachment of the external cortex and epidermal layers, making the suberized phellem the outermost tissue and protection layer. While this morphodynamic pattern of development is somewhat similar in both Arabidopsis (Wunderling *et al.*, 2018) and cork oak (Machado *et al.*, 2013), so far there is no data on the ontogeny of root phellogen and phellem in the latter, more particularly in primary roots. Remarkably, the secondary development of *Arabidopsis* root was observed early in plant development, even before secondary development could be detected in the stem (Wunderling *et al.*, 2018; Chapter II). Also, homologues of previously identified markers of cork oak phellem differentiation, were found in *Arabidopsis* newly formed root phellem cells, indicating a regulation process that is conserved not only across species but also in different organs (Wunderling *et al.*, 2018; Chapter II).

In this chapter, we aimed to test the use of cork oak tap roots as a proxy for functional studies targeting phellem development. We followed the development of cork tap roots until the establishment of secondary

development, with detailed morphological characterization and molecular profiling of phellem development. We found that phellogen activity starts early after radicle emergence from the seed, along with the activation of transcriptional networks regulating phellem development. We further discuss the advantages and constraints of this model system for experimental studies in cork oak.

3. Material and Methods

Plant material and seed storage

Half-sibling *Quercus suber* acorns were collected from a field-grown tree located in Alcochete (Portugal, Lat. 38.747491; Long. -8.931877) in November 2017, 2018 and 2019. Acorns were submerged in tap water to remove floating or damaged acorns and any residual debris. After, acorns were transferred and kept in a 45ºC water bath for 2 hours (h). Finally, acorns were surface dried, and the excess moisture was removed in a 30ºC chamber for 24h. Acorns were kept in plastic bags and stored at 4ºC until further use.

Growth conditions and sampling

Seeds were sown on a mixture of sand and vermiculite (1:1) at 100% field capacity in 700ml pots (1/pot) and maintained under 12h/12h day/night photoperiod (light intensity 400 µmol m^{-2} s^{-1}) at 25ºC/20ºC. Pots were covered with saran wrap (with poked holes), to avoid excess water evaporation, and seeds were kept in these conditions for 7 days without re-watering. After this period, seedlings were shifted to contrasting growth conditions or re-watered to 80% field capacity (mock) Heat, osmotic, and combined heat and osmotic (H+O) treatments were performed, always maintaining a 12h photoperiod. For osmotic treatment, a 20% (w/v) PEG6000 water solution was applied to each pot in the volume needed to restore 80% field capacity. Excess PEG6000 solution extruding the pot was removed from the supporting tray and

pots were kept at 25ºC/20ºC day/night. For heat treatment, plants were re-watered to 80% field capacity and transferred to 38ºC/30ºC day/night in the growth chamber. For combined heat and osmotic treatment, cork oak seedlings were watered with a 20% PEG6000 water solution (up to 80% field capacity) and transferred to 38ºC/30ºC day/night. Pots were again covered with saran wrap with poked holes and kept in these conditions for 1 week.

To follow tap (main) root morphological development, seedlings maintained at mock conditions were collected at 4, 6, 8 and 15 days after sowing (DAS). At each timepoint small tap root segments (< 0.5 cm) were collected from older/mature zone of roots (1cm below root collar). To map the development along the root axis, small segments were also taken at 3 cm intervals along 15 DAS roots. Collected segments were immersed in a fixative solution with 4% formaldehyde and 1% glutaraldehyde (in 0.1M phosphate buffer, pH 7.2).

For RNA extraction from cork oak seedlings grown in different conditions, 1.5 cm root segments were collected from 2 contrasting development zones (Fig. S5): secondary development zone (SD), 1 cm bellow root collar, and primary root development zone (PD) including 1 cm from the root tip. Roots were sampled 24h (8 DAS) and 1 wk (15 DAS) after each treatment and frozen in liquid N_2. Each sample corresponded to a pool of segments collected from 4-5 root seedlings, and 3-4 pools were collected per treatment (biological replicates).

Photographs of cork oak seedlings were taken at the end of each treatment and before sampling for RNA and microscopy. Individual root length measurements were taken from each photograph using FIJI (Schindelin *et al.*, 2012). Kruskal-Wallis test was used to compare root length measurements.

Microscopy

Root samples previously fixed in 1% formaldehyde and 4% glutaraldehyde solution (in 0.1M phosphate buffer, pH 7.2) were subjected to sequential dehydration with increasing EtOH concentrations [30%, 50%, 70%, 85% and 96% (twice) (v/v)] and further embedded in Technovit 7100 resin (Heraeus Kulzer, Wehrheim, Germany). Semi-thin sequential sections (5-10 µm thick) were obtained with a microtome (Leica RM2235), transferred to water droplets on glass slides and dried (37ºC - 40ºC, 5-10 min) for complete adhesion to the glass.

For Toluidine Blue O (TBO) staining, sections were first cleared for 30 min in 5% sodium hypochlorite (w/v) and 1 min in 1% Acetic acid (v/v) and washed in water. Sections were then incubated for 5 min in TBO (0,05%) and washed with water. Stained sections were then mounted in DPX (Sigma – Aldrich), observed using a Leica DM6 B upright light microscope and photographed.

Fluorol Yellow (FY) staining was performed according to Brundrett *et al.* (1991) with minor modifications. Briefly, glass slides with cross sections were incubated in a freshly prepared solution of 0.01% (w/v) FY (Santa Cruz Biotechnologies) in 80% lactic acid (v/v) at 60 °C for 30 min. The slides were then counter-stained with 0.5% Aniline Blue (w/v) for 30 min in darkness, washed 3x 5min in water at room temperature and mounted on 50% glycerol. Observations were performed using a Zeiss 880 confocal microscope.

RNA extraction

For RNA extraction, frozen root samples were ground with mortar and pestle. Pre-warmed (65ºC) extraction buffer [2% w/v CTAB, 1.4 M NaCl, 20 mM EDTA (pH 8), 100 mM Tris-HCl (pH 8), 1% w/v PVP40, and 2% v/v β-mercaptoethanol] was added to the powdered tissue (1 mL/100

mg of tissue) and shaken vigorously. Samples were incubated at 65°C for 10 min, shaking every couple of minutes. Mixture was extracted twice with equal volumes chloroform : isoamyl alcohol (24:1) then centrifuged at 3,500 × g for 15 min at 4°C. The aqueous layer was transferred to a new tube and centrifuged at 30,000 × g for 20 min at 4°C to remove any remaining insoluble material. The final supernatant was collected and mixed with 0.1 vol. 3 M NaOAc (pH 5.2) and 0.6 vol isopropanol and stored at -80°C for 30 min to precipitate the nucleic acids. Samples were further centrifuged at 3,500 × g for 30 min at 4°C, and resulting pellets were dissolved in 1 ml TE (10mM Tris, 1mM EDTA, pH 7.5). To selectively precipitate the RNA, 0.3 vol of 8 M LiCl was added and the sample was stored overnight at 4°C. RNA was pelleted by centrifugation at 20,000 × g for 30 min at 4°C, washed with ice cold 70% EtOH, air dried, and dissolved in 50 µL nuclease-free milli-Q water. Possible DNA contaminations were removed using TURBO™ DNase (ThermoFisher Scientific). RNA quality was evaluated by electrophoresis in agarose gels and quantified by NanoDrop ND-1000 spectrophotometer.

Gene expression analysis

For quantitative PCR analysis, first strand cDNA synthesis was performed using 1 µg total RNA with an oligo-dT primer using Transcriptor High Fidelity cDNA Synthesis Kit (Roche), according to the manufacturer's instructions. The cDNA was diluted and used as template for amplification by qPCR using gene-specific primers (listed on Table **S1**). Elongation factor (LOC112038967) was used as internal control. Real Time qPCR was done in a Lightcycler 480 (Roche), using Lightcycler 480 Master I Mix (Roche). Amplification reactions were performed in triplicate for each cDNA sample. Target transcript abundance was calculated according to Pfaffl, 2001.

Transcriptome sequencing

RNA-seq was performed using total RNA collected from control and stress conditions, 24h after treatment, in young and mature root segments (with 3-4 biological replicates). RNA was quantified using Qubit™ RNA BR Assay Kit (ThermoFisher Scientific, MA, USA) and RNA integrity was assessed with Fragment Analyzer (Agilent, CA, USA). cDNA synthesis was performed using 10ng total RNA and using an optimized SMARTSeq2 protocol. cDNA-libraries from each sample were equimolarly pooled and sequenced on Illumina NextSeq 500 instrument (v2.5, High Output, 75 bp, Single Reads). cDNA libraries preparation and sequencing was performed at the IGC Genomics Unit (Oeiras, Portugal). The sequencing data and corresponding metadata were deposited on National Center for Biotechnology Information (NCBI) Short Read Archive and BioSample databases, under the BioProject PRJNA690098.

Bioinformatics analysis

Raw FASTQ files analysed before and after quality trimming using FastQC v0.11.8 (Andrews S, 2010). Trimming of adapters and low quality bases was performed using Trimmomatic v0.39 (Bolger *et al.*, 2014) with single-end mode and additional parameters: LEADING:3, TRAILING:3, SLIDINGWINDOW:4:15, MINLEN:36. High-quality reads were mapped on the *Q. suber* reference genome CorkOak1.0 (GCF_002906115.1, (Ramos *et al.*, 2018)) using STAR v2.7.0f_0328 (Dobin *et al.*, 2013), with modified parameters (twopassMode=Basic, alignIntronMax=100,000) and read counts per gene were further obtained using featureCounts v1.6.4 (Liao *et al.*, 2014). Differential expression analysis was conducted using the DESeq2 package (Love *et al.*, 2014) in R v.3.6.2 (R Foundation for Statistical Computing., 2018). Principal component analysis (PCA) was conducted using normalized counts of the 1000 genes showing the highest variance. Statistical

analysis was conducted using a multifactorial design (~ root_zone + root_zone:treatment) and '*apeglm'* log fold change shrinkage estimator (Zhu *et al.*, 2019). Differentially expressed genes (DEGs) between roots zones and control vs. stress conditions (in each root zone) were filtered based on fold-change (FC) > |2| (log2FC > |1|) and adjusted p-value (padj) < 0.1. Candidate *A. thaliana* orthologs were determined using Blastp searches of cork oak predicted amino acid sequences on TAIR10 (Araport11) predicted proteins.

Gene Ontology (GO) functional enrichment was performed with BiNGO plugin for Cytoscape version 3.7.1 (Maere *et al.*, 2005) using unique Arabidopsis homologues attributed to cork oak DEGs. Significant GO terms related to cellular component, biological processes and molecular function categories were retrieved by applying hypergeometric distribution and an adjusted p-value < 0.05.

Functional associations between Arabidopsis homologues of the cork oak DEGs enriched in SD zone (FC > -4) were predicted using STRING v.11.0 database (Szklarczyk *et al.*, 2019). Confidence score for interactions was set for medium score (above 0.4), taking into account co-expression data and protein-protein interaction evidences. The gene network obtained from STRING v.11 was imported into Cytoscape version 3.7.1 for further analysis and display.

4. Results

Cork oak seed storage and seedling root growth

Annual cork oak acorns develop mainly in late summer and autumn and complete their maturation in November. Given its high abundance, we aimed to test the use of cork oak acorns to study periderm development. After collection, acorns were treated and screened to obtain mature, intact and healthy (without visible signs of biotic infection) acorns, and remove excess moisture, being further preserved at 4ºC. Despite

previous treatment before storage, some acorns tended to germinate during storage, and at the time of experiments most acorns had already visible radicles (Suppl. Fig. **S1**). Given this fact, each germination trial was performed using pre-selected acorns (based on radicle emergence or length), in order to guarantee that most of them were at similar and early developmental stages. In order to follow acorn germination and root development, acorns were sown on individual pots with easy to remove mixture of sand and vermiculite. For a morpho-histological assessment of tap root development, seedlings were removed from the substrate at 4, 6, 8 and 15 days after sowing (DAS) (Fig. **1**).

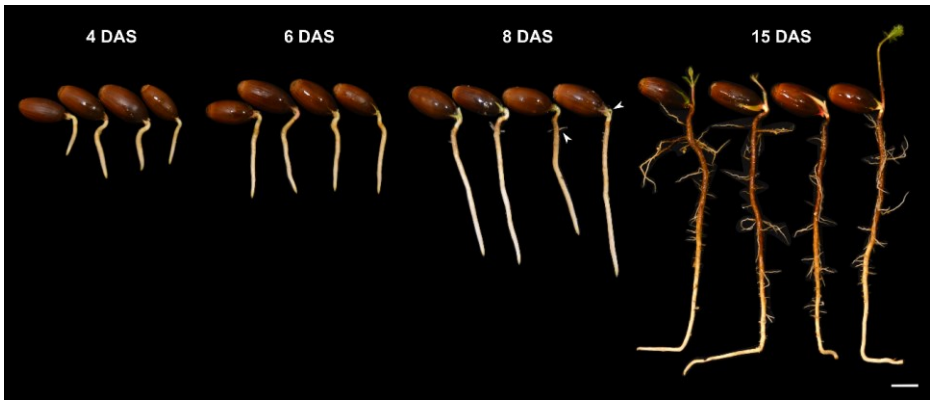

Fig. 1 *Quercus suber seedling development and tap root growth in different days after sowing (DAS) at 25ºC. Representative cork oak seedlings were collected and targeted for different studies at 4, 6, 8 and 15 DAS. The arrowheads indicate the emerged lateral root and shoot development. Scale bar 2cm*

At 4 days after sowing, acorns were already germinated, showing a small tap root around 3.18 ± 0.63 cm (Suppl. Fig. **S2**). Under the selected growth conditions, tap roots reached 5.72 ± 1.03 cm at 6 DAS, with no visible lateral roots nor shoot development (Fig.**1**; Suppl. Fig**. S2**) and at 8 DAS (13.17± 2.03 cm) a colour gradient was visible along

the root, ranging from white/beige in the root tips to brown bellow the collar region (Fig. **1**, Suppl. Fig. **S2**). At this stage, development of lateral roots and shoots started to occur in some seedlings (Fig. **1**, arrowheads). After 15 days, tap root length reached 20.95 ± 3.07 cm (Suppl. Fig. **S2**), displaying an increase in a dark brown area in the upper (mature) region. At this stage the majority of cork oak seedlings already showed shoot development and a root system composed of developed lateral roots covering most of the root length.

Timeline of periderm development and suberization in cork oak roots.

Plant roots display a gradient of cellular development, with primary development detected near the root tip and secondary development at fully matured regions, being detected first near the root collar of primary root (Dolan *et al.*, 1993; Machado *et al.*, 2013; Wunderling *et al.*, 2018; Campilho *et al.*, 2020). Secondary development is characterized by the establishment of lateral meristems, the of vascular cambium, which produces secondary phloem and xylem, and cork cambium (phellogen), which produces phelloderm and phellem (Crang *et al.*, 2018).

In order to determine the onset of secondary growth and particularly phellem initiation, we analysed cross sections taken at the mature root zone (below root collar, Suppl. Fig. **3**) at 4, 6, 8 and 15 DAS. TBO staining was used for general morphology observation (Pradhan Mitra & Loqué, 2014; Verhertbruggen *et al.*, 2017) and FY staining allowed the detection of suberized cells (Brundrett et al., 1991). At 4 DAS, the rhizodermis was the outermost tissue of the root, followed by several layers of cortex and a central stele delimited by primary vascular tissues (xylem and phloem) (Fig. **2a**). Stele is displayed in a round-edged rectangular shape where some cell clusters are visible, namely xylem (blue stained cell walls) and phloem (smaller and purple stained cell walls) (Fig. **2a**, **b**). At this stage, FY staining did not detect any suberized

cell walls (Fig. **2c**), suggesting that endodermis is not differentiated at this stage. At 6 DAS the central stele was showing evidence of secondary development (Fig. **2d**). Periclinal cell divisions were found between xylem and phloem tissues (Fig. **2e**, red arrowheads), indicating the establishment of the vascular cambium, with more phloem and xylem cells produced (as compared to 4 DAS). At this stage, cell-wall suberization was also not found (Fig. **2f**), yet, periclinal cell divisions were found outside the stele region (Fig. **2e**, yellow arrowheads) in parenchyma cells, which is often display mitotic activity (Crang *et al.*, 2018). At 8 DAS periclinal cell divisions were still identified in the vascular cambium, with more new cells detected with thin cell walls and flatten shape (Fig. **2g**, **h**, red arrows). Although fragmentation of cortex cells occurred in the sections, the rhizodermis was still detected as the outermost layer of the root. Suberin was detected at this stage, in a row of cells surrounding the central vascular cylinder (Fig. **2i**), highlighting the establishment of a mature endodermis. The flattened cells appearing below the endodermis suggest the occurrence of periclinal divisions, likely resulting from resumed phellogen activity (Fig. **2 e**, **h**, yellow arrows). Finally, at 15 DAS, root sections showed a similar global morphology as the previous stage, with the presence of rhizodermis, cortex and the central vascular cylinder showing secondary development (Fig. **2j**, **k**). At this time point, suberin is detected in 1-2 rows of cells (Fig. **2l**) indicating that besides the endodermis, phellem cells are already differentiated, supporting phellogen initiation earlier, after 8 DAS. In fact, sections taken from 22 DAG samples, in the same region, showed a fully suberized, continuous and multi-layered phellem. At this stage, the more external suberized layer shows a less intense staining by fluorol yellow and higher disorganization (not parallel to underlying FY-stained cell rows) (Supp. Fig. **S4**, arrow), suggesting some suberin degradation in these cells.

As an additional note, at all time points analysed we found two parallel and independent vascular bundles inserted in the cortex, composed of xylem and phloem tissues (Fig. **2a**, **d**, **g**, **j**). These lateral vascular bundles have been previously described as meridian cotyledonary traces by (Verdaguer & Molinas, 1997). Yet, the exact origin and function of such bundles remains unknown.

With this histological analysis we suggest that in *Q. suber* roots, phellogen de-differentiation starts at approximately 8 DAS. Although putative meristem activity in similar location was found at earlier stages (6 DAS), phellogen ontogeny appears to occur immediately after endodermis suberization.

Morphological development map of a cork oak root

To gain more insight into the different stages of cellular development and confirm the early establishment of suberized barriers in cork oak tap roots, cross sections were taken at regular intervals along the root axis in 15 DAS seedlings (Fig. **3a**). At 1 cm from root tip, several cortex layers and a central vascular cylinder were observed, but phloem and xylem are not clearly distinguished indicating early stages of primary growth (Fig. **3b**). Suberized cells were not observed in this segment (Fig. **3c**). A non-continuous layer of suberized cells was first detected 3 cm from the root tip (Fig. **3e**), between cortex and vascular cylinder, where xylem cells are already differentiated (Fig. **3d**). In the next developmental stage (6 cm from root tip), more xylem cells could be observed, surrounded by a complete row of suberized cells, suggesting that the endodermis was fully differentiated (Fig. **3f**, **g**). Evidence of secondary development was visible in sections collected at 9 cm from the root tip, particularly periclinal divisions that maybe related to vascular and cork cambium (Fig. **3h**, **i**, red and yellow arrowheads, respectively). The activity of both meristems was particularly evident in the above segments, by numerous periclinal divisions in both predicted locations. At 16 cm from root tip,

several suberized cells were detected below the endodermis, at some locations (Fig. **3m**, arrowheads). This pattern became more evident in the upstream segments, suggesting the early onset of phellem development (Fig **3o**, **q**, **s**). Interestingly, we found no evidence for a collapse of the endodermis layer, upon the establishment of the root secondary development, as reported in *Arabidopsis* (Wunderling *et al.*, 2018; Chapter II).

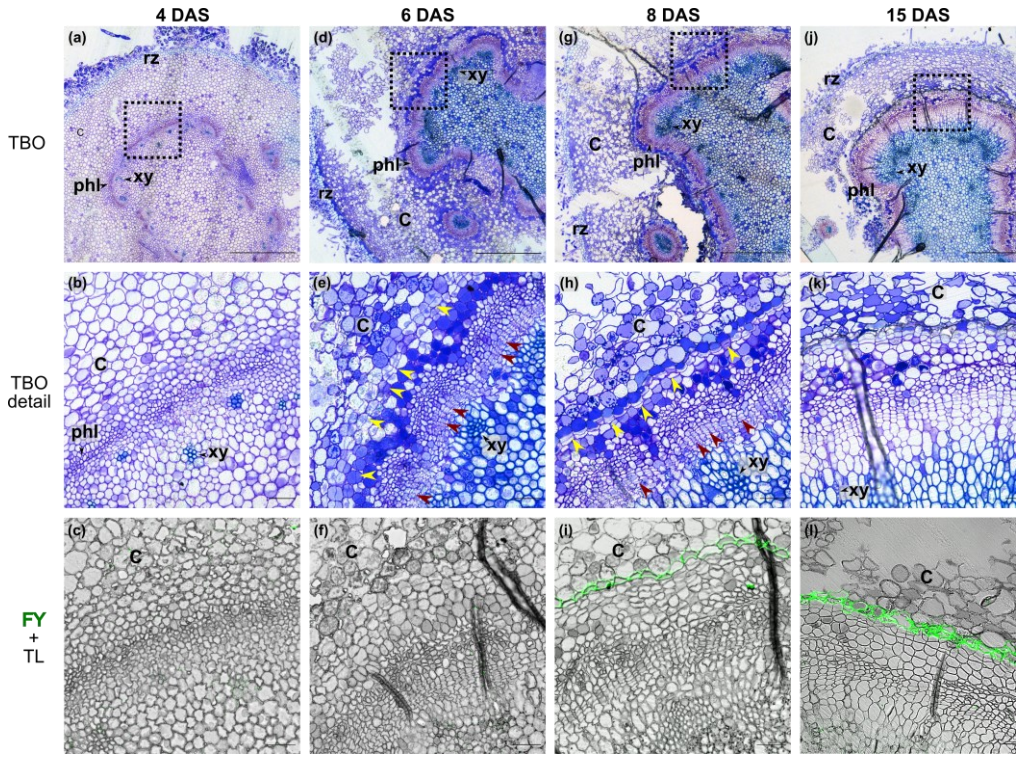

Fig. 2 *Histological development and cell-wall suberization in cork oak tap roots at 4, 6, 8 and 15 DAS. Cross sections were taken in the mature zone of root (1cm bellow root collar) and analysed with TBO and FY staining. At 4DAG (a, b, c) root shows primary growth with no suberization detected. At 6DAS (d, e, f) secondary development is identified by the recent periclinal cell divisions (red and yellow arrows). At 8DAG (g, h, i), secondary development is ongoing (red and yellow arrows) and suberization is detected in one row of cells. At 15 DAS (J, k, l) secondary developed tissues are expanded and two rows of suberized cells can be detected. C: cortex; phl: phloem; rz: rhyzodermis; xy: xylem. TL: transmitted light. Representative images of 2 seedlings analysed. Scale bars: TBO (a, d, g, j):500µm; TBO detail and FY (b, c, e, f, h, I, k, l):50 µm*

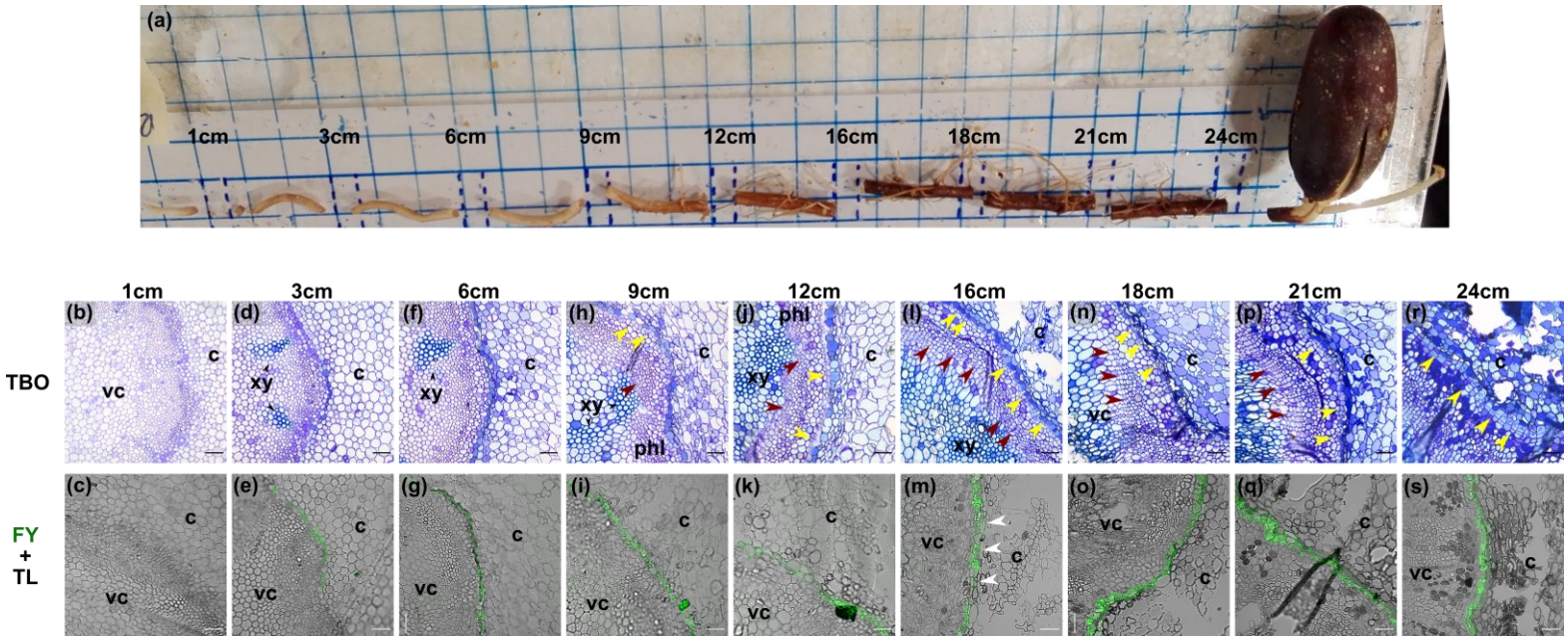

Fig. 3 *Histological development and tissue-specific suberization analysed in a single cork oak root with 15DAS, from root tip to rot collar. Cross sections were made from root segments taken with intervals of 3 cm(a). Cross sections from the collected segments were analysed with TBO and FY staining (b-s). c: cortex; phl: phloem; vc: vascular cylinder; xy: xylem. TL: transmitted light. Representative images of 3 seedlings analysed. Scale bars: 50 µm*

Activation of suberin biosynthesis pathway in root development

Suberin deposition in specific cells surrounding the stele was observed 8 DAS in mature root zones undergoing secondary development. To confirm the activation of the suberin biosynthesis pathway we analysed the expression of genes involved in the suberin biosynthesis in root segments dissected from the mature (SD) and young (PD) root regions, collected at 8 and 15 DAS (Suppl. Fig. **S3**). We selected cork oak homologs for well described genes involved in diverse steps of suberin synthesis and deposition, namely *AtLACS*, *AtPAL*, *AtF5H*, *AtCYP86A1*, At*GPAT5*, *AtASFT*, *StFHT and AtABCG6.* For both timepoints, the expression of most target genes was higher in SD as compared to PD regions (Fig. **4**).

In SD, genes related to activation (*QsLACS*) and conjugation of monomers are more expressed, particularly *QsASFT-2* (*StFHT* homolog), which shows the strongest expression. Other genes directly related to suberin synthesis, as *QsCYP86A1* and *QsF5H*, or suberin monomer transport, *QsABCG6*, have lower expression. This gene expression profile is maintained at 15 DAS (Fig. **4b**) and, in both timepoints, well-recognized markers of suberin pathway, homologues of *GPAT5*, *ASFT* and *ABCG6*, show very low gene expression. On the other hand, in the PD region at 8 DAS, gene expression is only detected for *QsLACS* and *QsPAL* genes (Fig. **4c**) while, at 15 DAS, other genes described as directly involved in the suberization pathway also become active (*QsCYP86A1*, *QsF5H*, *QsASFT-2*, *QsGAPT5*, *QsASFT* and *QsABCG6*) (Fig. **4d**). Altogether these results support a suberization event at 8 DAS in the cork oak mature (SD) root region while in the young (PD) regions, expression of most suberin-related genes is only detected at 15 DAS and with lower levels.

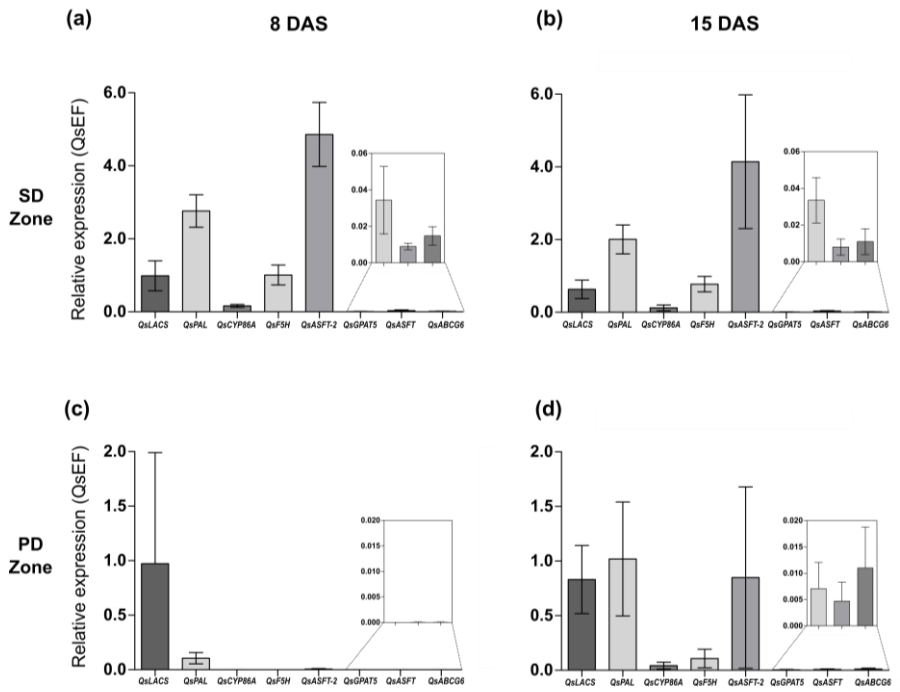

Fig. 4 *Relative expression of genes related to suberization. SD (a, b) and PD (c, d) zone of root was collected and gene expression of QsLACS, QsPAL, QsCYP86A, QsF5H, QsASFT-2, QsASFT, QsGPAT5 and QsABCG6 were analysed by RT-qPCR at 8 (a, c) and 15 (b, d) DAS. Gene expression of interest genes was normalized with the housekeeping gene QsEF. Mean expression ± standard deviation from independent experiments is represented for each timepoint*

Transcriptomic analysis of primary and secondary development zones of cork oak tap roots

In order to obtain a genome-wide view over the transcriptomic changes occurring in cork oak roots between primary and secondary development, specific RNAseq libraries were prepared by sampling young (PD) and mature (SD) root regions at 8 DAS. Sequencing of the different libraries yielded a total of ~713 M high quality reads (average 27,430,387.46 single-end reads per library), with a mean read length of 73.46 bp. The percentage of uniquely mapped reads successfully assigned to annotated genes ranged between 56.52% and 74.29%

(average 67.93%). The overall effect of the experimental variables on gene expression was further explored by PCA (Suppl. Fig. **S6**). In this analysis we observed that libraries representing biological replicates clustered together and the overall organization of the libraries was strongly influenced by the different root zones collected, which were separated along PC1, representing 79% of variance. In this analysis, growth conditions (treatment) had a smaller, but still clear effect on sample clustering. These results showed that gene expression profiles are, to a great extent, affected by the root developmental zones.

Differential expression was performed using a multifactorial design, allowing the determination of DEGs between SD and PD regions independently of the growth condition (the response to contrasting growth conditions is described in Chapter 5). For a log2FC > |1| and padj < 0.1, a total of 10,106 DEGs was obtained between the two developmental zones, with 6,766 of these (66.95%) being enriched in SD (Suppl. Table S2). From these, 1,641 correspond to pseudogenes (without or with incomplete annotation) and 5,024 could be assigned as orthologs for 3,347 genes from *Arabidopsis*. In turn, 3,338 (33.03%) DEGs are enriched in the PD root zone, from which 506 are pseudogenes and 2,777 are orthologs of 2,257 Arabidopsis genes (Suppl. Table **S2**).

Functional profile of DEGs enriched in root regions undergoing primary and secondary development

A functional enrichment of the DEGs identified for the SD and PD root zones was further performed using the corresponding *Arabidopsis* homologs. The DEGs highly expressed in the SD zone showed a specific enrichment of 326 terms (Fig. **5a**; Suppl. Table **S3A**). In the most enriched terms in the *Cellular Component* category, we found the C*hloroplast part* (GO:0044434), *Thylakoid* (GO:0009579) and *Plastid envelope* (GO:0009526). Regarding *Biological Process*, multiple terms

associated with regulation were represented, including *Regulation of biosynthetic process* (GO:0009889), *Transcription* (GO:0045449), *Developmental process* (GO:0050793) and *Cell death* (GO:0010941). Multiple terms related to hormone metabolism were also represented, namely *Response to abscisic acid (ABA)* (GO:0009737), *salicylic acid* (SA) (GO:0009751), *jasmonic acid (JA)* (GO:0009753), *gibberellin (GA)* (GO:0009739) and *ethylene* (GO:0009723). GO terms related to secondary metabolic processes including *P*henylpropanoid (GO:0009698), *Cutin* (GO:0010143) and *Suberin* (GO:0010345) *biosynthesis* were also significantly enriched. Other enriched *Biological process* terms exclusive to SD zone were related to *Meristem development* (*GO:0048507*) and *maintenance* (GO:0010073). In the *Molecular function* category, *DNA binding* (GO:0003677), *Transcription factor* (GO:0003700), *Kinase* (GO:0016301) and *Electron carrier* (GO:0009055) *activity* were among the most enriched terms.

From the functional annotation of DEGs found in the PD zone, 247 GO terms were significantly enriched (Fig. **5b**, Suppl. Table **S3B**). From the *Cellular Component* category, *Intracellular organelle part* (GO:0064446), *Nucleus* (GO:0005634), *Mitochondrion* (GO:0005739) and *Ribonucleoprotein complex* (GO:0030529) are some of the most enriched terms. In the *Biological process* category, genes related to primary metabolism-related were the most represented, including *Protein* (GO:0019538), *Lipid* (GO:0006629) and Cellular amino acid (GO:0006520) *metabolic processes*. Also, specific terms related to developmental processes were enriched in PD transcriptome, including C*ellular developmental process* (GO:0048869), *Regulation of cell size* (GO:0008361), *Developmental growth* (GO:0048589), *Root development* (GO:0048364), *Cell division* (GO:0051301) and *Root hair elongation* (GO:0048767).

(a)

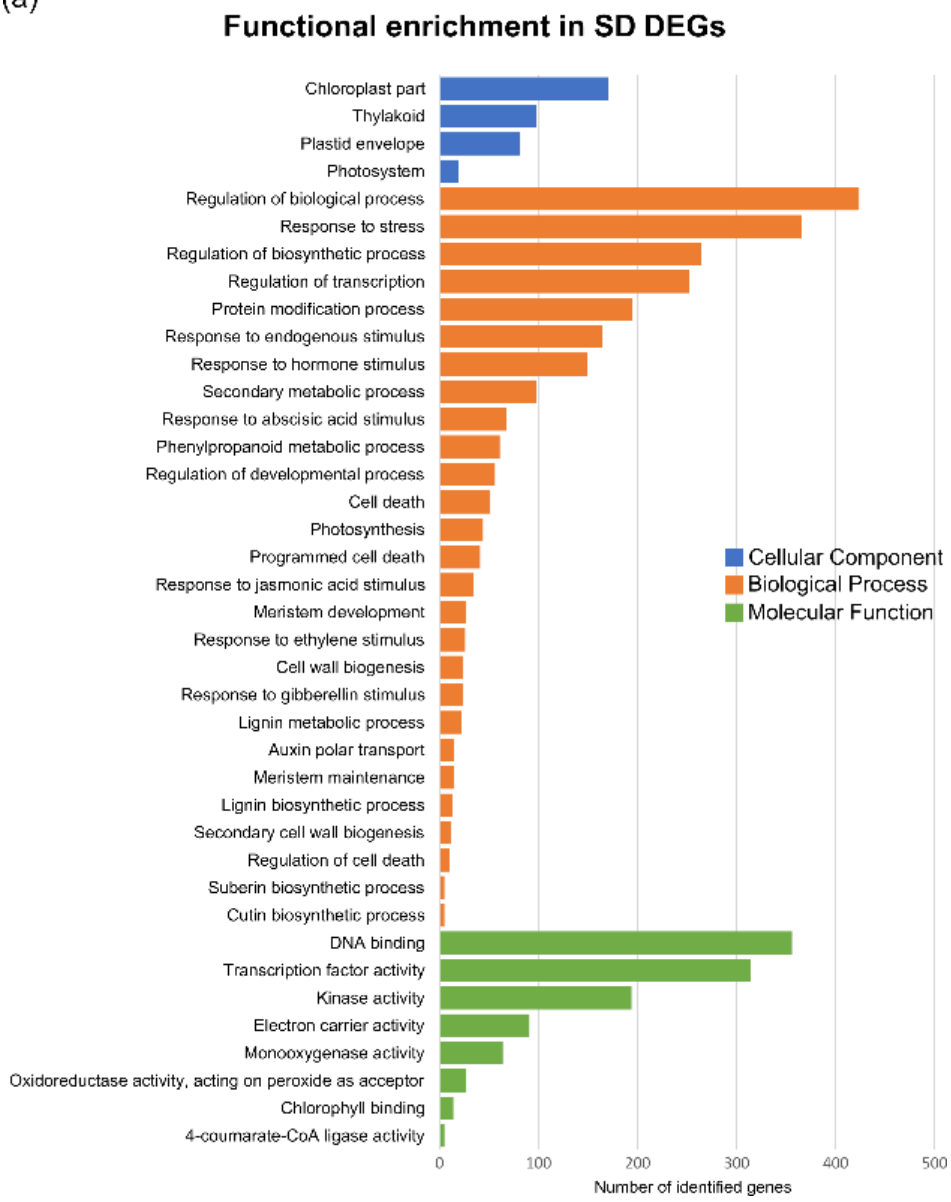
Functional enrichment in SD DEGs
Chloroplast part
Thylakoid
Plastid envelope
Photosystem
Regulation of biological process
Response to stress
Regulation of biosynthetic process
Regulation of transcription
Protein modification process
Response to endogenous stimulus
Response to hormone stimulus
Secondary metabolic process
Response to abscisic acid stimulus
Phenylpropanoid metabolic process
Regulation of developmental process
Cell death
Photosynthesis
Programmed cell death
Response to jasmonic acid stimulus
Meristem development
Response to ethylene stimulus
Cell wall biogenesis
Response to gibberellin stimulus
Lignin metabolic process
Auxin polar transport
Meristem maintenance
Lignin biosynthetic process
Secondary cell wall biogenesis
Regulation of cell death
Suberin biosynthetic process
Cutin biosynthetic process
DNA binding
Transcription factor activity
Kinase activity
Electron carrier activity
Monooxygenase activity
Oxidoreductase activity, acting on peroxide as acceptor
Chlorophyll binding
4-coumarate-CoA ligase activity
Cellular Component
Biological Process
Molecular Function
0
100
200
300
400
500
Number of identified genes

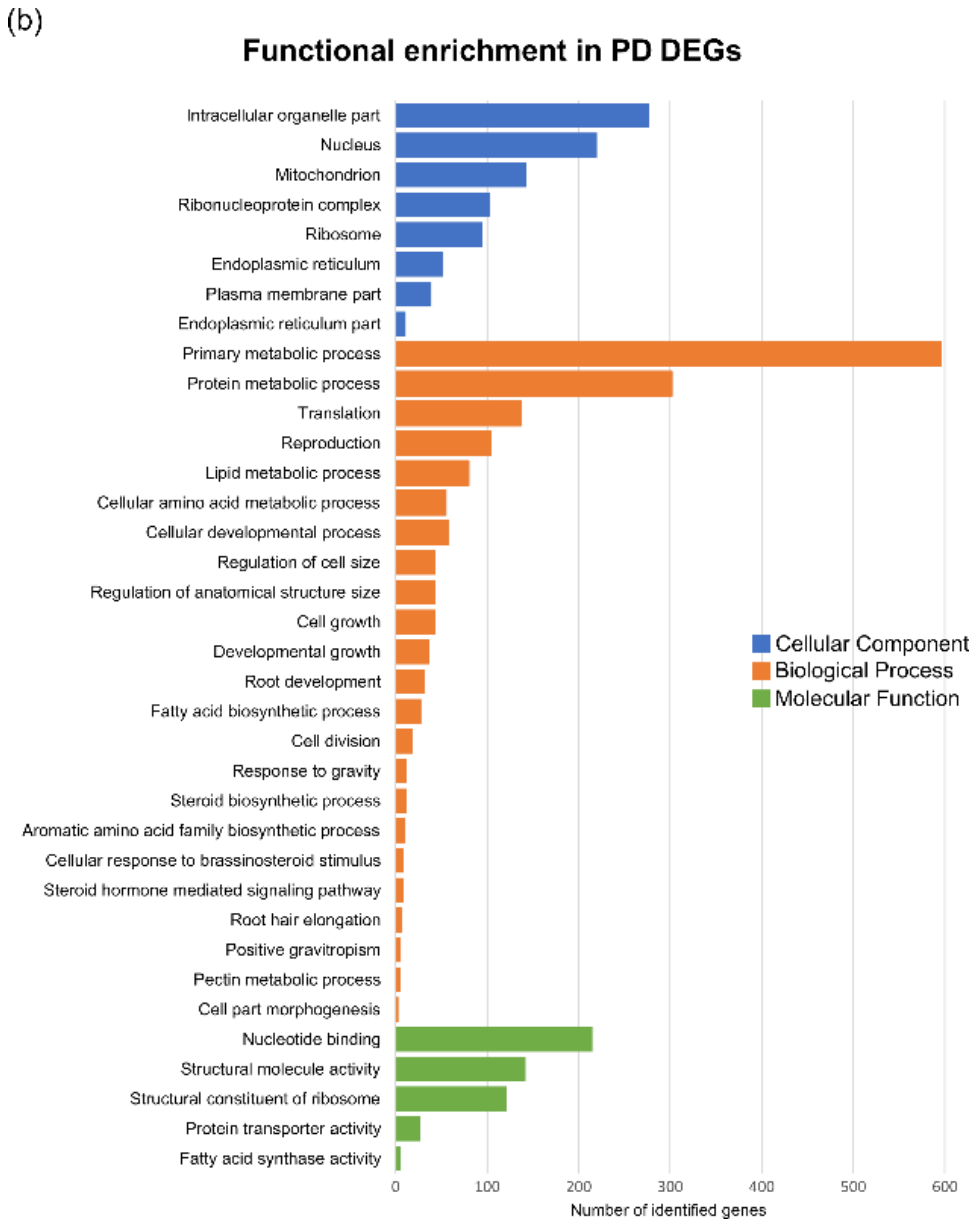

Fig. 5 *Representative GO terms significantly enriched in DEGs for SD (a) and PD (b) zones of cork oak root. Coloured bars represent the number of genes in the selected GO terms in Cellular component (blue), Biological process (orange) and Molecular function (green).*

Regarding hormone metabolism, several terms related to steroids were enriched, including *Steroid biosynthetic process* (GO:0006694), *Cellular response to brassinosteroid stimulus* (GO:0071367) and S*teroid hormone mediated signalling pathway* (GO:0043401). Concerning *Molecular function*, *Nucleotide binding* (GO:0000166), *Structural molecule activity* (GO:0005198) and *Structural constituent of ribosome* (GO:0003735) are the most enriched and exclusive identified terms in primary developmental zone.

A total of 73 GO terms were commonly enriched in DEGs abundant in SD or PD (Table **S3A**, **S3B**; Suppl. Fig, **S7**). Among these we found: *Intracellular membrane-bounded organelle* (GO:0043231)*, Membrane* (GO:0016020), *Plastid* (GO:0009536), *Chloroplast* (GO:0009507) and *Cell wall* (GO:0005618)*,* from the Cellular Component category; *Response to stimulus* (GO:0050896)*, Developmental process* (GO:0032502)*, Localization* (GO:0051179) *and Aromatic compound biosynthetic process* (GO:0019438) from *Biological Process;* and *Transferase* (GO:0016740)*, Oxidoreductase* (GO:0016491), and *Transmembrane transporter activity* (GO:0022857), from *Molecular Function.*

Reference marker genes for primary and secondary development are conserved in cork oak roots

Characteristic gene markers for molecular processes known to occur during secondary and primary development of roots were analysed in more detail in PD and SD DEG (Fig. **6**). Particularly, homologues factors previously associated to secondary vascular development (xylem and phloem) are found to be differentially expressed in the SD zone of roots. These included *QsANT* (LOC112030198, LOC111985236), *QsWOX4* (LOC111988759), *QsCYCD3;1* (LOC112038380), *QsHB8* (LOC112029705), *QsPXY* (LOC112019802), *QsSTM*

(LOC112032307), *QsKNAT1* (LOC112015571) (Ragni & Greb, 2018), *QsPTL* (LOC111994212, LOC111983073) and *QsLBD4* (LOC112038775, LOC111997151) (Zhang *et al.*, 2019). Transcription of general regulators of secondary wall biosynthesis [VASCULAR-RELATED NAC DOMAINS (*Qs*VND1/3/4 - LOC111996673/LOC111994497/LOC112007201, LOC111988979) and Xylem NAC domain 1 - LOC112009005] and direct regulators of lignin biosynthesis (*QsMYB4* - LOC112023509, LOC112037069, LOC112035436, LOC111990470, LOC111991808; *QsMYB83* - LOC112038777; and *QsMYB46* - LOC111996538) (Taylor-Teeples *et al.*, 2015; Zhang *et al.*, 2018) was also more abundant in SD root zones. In the PD zone, we found several cork oak homologs for gene markers for root apical meristems, including *QsPLT2* (LOC112019105), *QsAIL6* (LOC112018242), *QsBBM* (LOC111984882), *QsGRF* (LOC111985233, LOC112028562) and *QsIAA17* (LOC112027116). These are TFs involved in maintenance of root quiescent centres and cell specification in *Arabidopsis* (Aida *et al.*, 2004; Tian *et al.*, 2014; Moreno-Risueno *et al.*, 2015; Du & Scheres, 2017; Motte *et al.*, 2019). Moreover, homologues of *QsMGP* (LOC112011855, LOC112027530), *QsRVN* (LOC112030349) and *QsSCZ* (LOC112012980), associated with control of root tissue patterning (Moreno-Risueno *et al.*, 2015), also homologues of *QsSMB (LOC112006384)*, *QsBRN2* (LOC111997697) and *QsFEZ* (LOC112031616), regulating root cap, and *QsAHP6* (LOC112034194), involved in protoxylem specification, were also highly expressed in PD as compared to SD (Perilli *et al.*, 2012; Petricka *et al.*, 2012; Drisch & Stahl, 2015; Slovak *et al.*, 2016; Motte *et al.*, 2019).

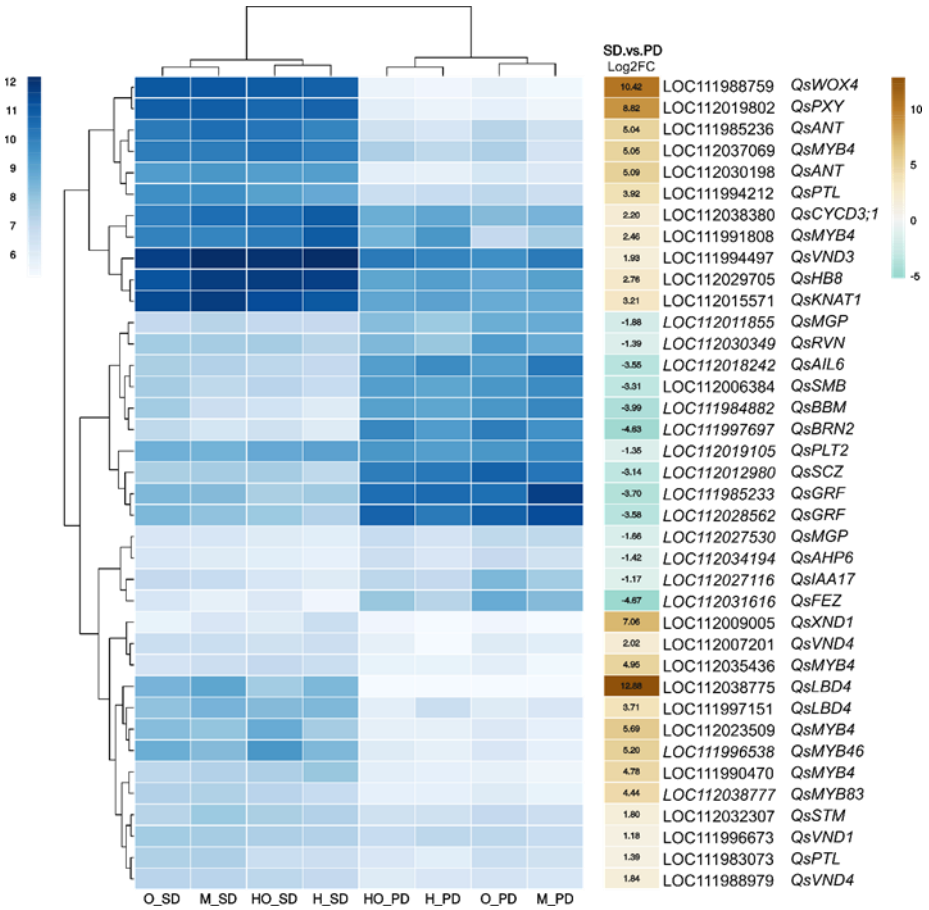

Fig. 6 *Heatmap showing the expression of selected DEG between SD and PD regions. The blue heatmap represents the expression (mean of normalized read counts) obtained for each independent treatment (M-mock, O-osmotic, H-heat and HO – combined heat and osmotic) at each root zone (PD and SD). The corresponding Log2FC between SD and PD regions, independently of the growth condition, is represented on the right heatmap.*

Molecular pathways active during secondary development in cork oak roots

For a better assessment of the most relevant molecular networks active during cork oak root secondary development, we further drew a regulatory network based on co-expression and protein-interactions, profiting from the extensive data available for *Arabidopsis spp*. In this analysis we selected only the DEGs enriched in SD with a high fold

change (log2FC > |4|) resulting in a total of 1,554 DEGs. Of these, 1,508 had a representative ortholog in *Arabidopsis*, with several cork oak genes being assigned to the same *Arabidopsis* gene. Using the STRING database (Szklarczyk *et al.*, 2019), a protein-protein network could be retrieved showing 1547 interactions between 339 unique *Arabidopsis* homologues (Suppl. Table **S4A**), where most of the interactions were organized in 3 interconnected clusters (Fig. **7**).

Cluster 1 included a total of 136 unique *Arabidopsis* protein homologues (nodes) representing 210 unique differentially expressed cork oak transcripts (Suppl. Table **S4B**, Suppl. Fig. **S8a**). The proteins in this cluster have predicted functions related to cell wall synthesis and modification, in particular secondary cell wall formation. These included proteins involved in synthesis and modification of the major cell wall components of cellulose (IRX1, IRX3, IRX6 and CESA4) and pectin (AT2G45220, AT3G53190, AT1G67750). Regarding secondary cell wall formation, we identified the core genes involved in suberin (GPAT5, FAR4, RWP1(ASFT), CYP86A1 and CYP86B1) and lignin biosynthesis (IRX4, CYP84A1 and ATCAD4), as well as several genes know to be involved in the biosynthesis of common phenylpropanoid precursors (PAL, C4H, CCCAMT, CCoAOMT). Other gene families associated with lipid and secondary metabolism which are also related to synthesis of suberin and lignin components were also organized in this cluster. These included several CYP450 (CYP87A2, CYP86A2 and CYP81D8) and HXXXD acyl transferase (AT1G24430 and AT4G31910) members. Proteins with functions associated to transport were also present, namely several ABCG (ABCG1/10/23/37) and Lipid Transfer Protein (EDA4, AT2G18370, AT3G22620, AT2G48130 and AT3G22600) family members. Regarding polymerization of suberin and lignin in the cell wall, the represented families include GDSL lipases (AT5G37690, AT2G23540, AT1G74460), multiple peroxidases (e.g. PRX52, PER64,

PA2), laccases (LAC3/7/12/17 and IRX12), CASP-like (AT3G06390 and CASP5/3) and an α,β-hydrolase (AT2G18360). Also in cluster 1, we found 3 Glutathione S-transferases (GSTU25, GSTU10, GSTF7) as well as several proteins associated with signal transduction, including cell wall associated receptor kinases (WNK4, RLP7, IOS1, CRK25, AT1G24030, AT1G18390).

Cluster 2 (Suppl. Table **S4C**, Suppl. Fig. **S8b**) included 50 *Arabidopsis* protein homologues, which represented 82 different cork oak DEGs in SD. This cluster was mostly represented by proteins associated with transport and response to stimulus. Within the transport functions, the Major facilitator family was represented by 8 *Arabidopsis* homologues members, which are mostly associated with oligopeptide (AT1G22540, AT2G37900, AT2G40460 and AT5G14940) and nitrate transport (AT1G68570, AT3G21670 and AT3G45660). Regarding response to stimulus, many of the interacting proteins are involved in protein structure stabilization and folding, such as heat shock proteins (Hsp70b, HSP70, HSP21, AT2G42750) and chaperones (BAG6, ATHSP22.0, AT1G53540). Also in this cluster we found proteins involved in jasmonic acid (LOX2), abscisic acid (ABA2) and auxin (GH3.1, GH3.9, YUC6) synthesis.

Finally, cluster 3 included 62 Arabidopsis proteins particularly associated with chloroplastidial activity and photosynthesis, which were representative of 66 single cork oak DEGs in SD zone (Suppl. Table **S4D**, Suppl. Fig. **S8c**). Among these, proteins of the photosystem complexes I and II were identified, including reaction centre subunits (PSBY, PSBX, PSBW, PSBR, PSAO, PSAL, PSAK, PSAG, PSAF, PSAE-2, PSAD-2), Oxygen-evolving enhancer proteins (PSBQ-2, PSBP-1, PSBO2) and light harvesting complex proteins (CAB1, LHCB6, LHCB5, LHCB4.3, LHCB4.2, LHCB3, LHCB2.2, LHCB2.1, LHCA4, LHCA3, LHCA2, LHCA1, LHB1B1). In this cluster we also found proteins

involved in lipid metabolism (LPP2, PLDDELTA, PLDEPSILON, PLDALPHA2, LPP3 and AT4G28780), as well as a variety of transporters (WAT, PIP3, PIP1;4, and TIC55-II).

Key regulators of secondary growth in cork oak roots

Functional enrichment analysis of DEGs in the mature zone of the root (SD) highlighted an over-representation of genes associated with regulation, including response to hormone stimulus, regulation of biosynthesis and regulation of developmental processes.

Regulation of secondary development in cork oak roots by specific hormones can be suggested by the candidate DEGs involved in hormone synthesis, transport or signalling (Fig. **7**). These hormones include ABA, JA, GA, SA and Ethylene. Among these, the signal transduction pathway mediated by ABA was the most represented, not only by strongly expressed TFs know to be responsive to ABA (*QsMYB53* - LOC112006609 and LOC112034724, *QsMYB102* - LOC111989495 and LOC112004686, *QsHB12* - LOC111993972, LOC111993269 and LOC111987296, *QsMYB93* - LOC112030452) but also by PYL ABA receptors (LOC111996210 and LOC112010415) and SNF1-related protein kinases 2 (SnRK2s) homologues (LOC112039491, LOC112017767 and LOC112032862).

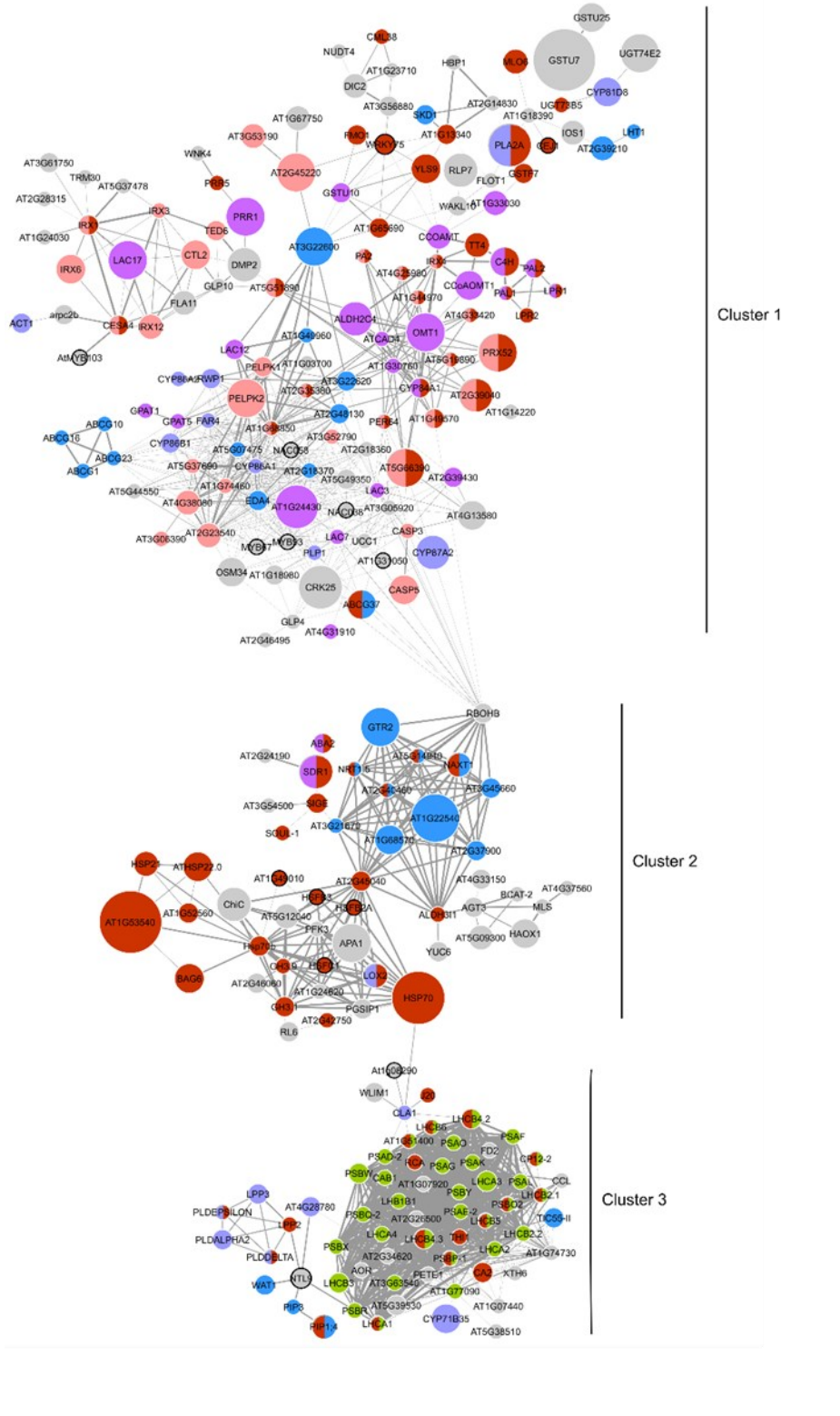
Cluster 1
Cluster 2
Cluster 3
Secondary metabolic process
Lipid metabolism
Response to stimulus
Transport and localization
Photosynthesis
Cell wall biosynthesis
Others

Fig. 7 *(previous page) Network representation of predicted protein-protein interactions for Arabidopsis homologues representing the DEGs in SD zone of cork oak roots (Log2FC > |4|). The network was built based on the STRING database with each node representing the protein product associated with each DEG, and each connecting edge representing a predicted association (based on co-expression and inferred or validated protein-protein interactions). Node size corresponds to the number of cork oak genes associated with the same Arabidopsis homologue and edge thickness represents the confidence value for each association. Fill colour represents general functions or processes annotated to each gene product. Nodes with black borders represent TFs.*

In parallel, also abundant in SD, is the expression of key components of the GA regulation, namely the GA receptor GIBBERELLIN INSENSITIVE DWARF1 (*QsGID1* - LOC112001486), the DELLA growth inhibitors (LOC112035777), as well as the F-box proteins SLEEPY1 (*QsSLY1* - LOC111990570).

Regarding direct regulation of gene expression, we identified 419 cork oak DEGs highly enriched in SD with predicted functions as TFs. Several TF families were strongly represented, including multiple MYB (48 DEGs), NAC (38 DEGs), WRKY (34 DEGs), AP2/ERF (34 DEGs) and bHLH (34 DEGs) and HSF (10 DAG) candidate TFs (Suppl. Table **S5**, Table **1**). In fact, several transcription factors were included in the regulatory network (Fig. **7**) which may highlight candidate downstream regulators. Cluster 1 included TF homologues of NAC058 (LOC112037487), NAC038 (LOC112004385), MYB67 (LOC112010947, LOC112012379), MYB93 (LOC112030452), AtMYB103 (LOC112002235), WRKY75 (LOC112006478, LOC112033440, LOC111983199) and CEJ1(LOC111988769, LOC111995794), which are mostly connected to cell wall component biosynthesis protein homologues. In cluster 2, candidate Heat Shock Factor family relatives *QsHSFB3* (LOC112013936), *QsHSFC1* (LOC112040819) and *QsHSFB2A* (LOC111990149, LOC111997737) are interacting with genes related to response to stress. Interestingly on cluster 3, we find the strongly expressed *QsWIP3* (LOC111992789)

(Table **1**), as well as *QsNTL9* (LOC112036697, LOC112036693), a calmodulin-regulated transcriptional repressor.

Looking more particularly to phellem development and suberization, we looked to TF homologues that were formerly identified in phellem targeted transcriptomic studies in diverse species. Interestingly, several DEGs homologues highly represented in SD were identified to be common in other phellem tissues, with the majority overlapping MYB and NAC families (Table **1**). From these, several were previously described to be involved in suberization in other tissues, including NAC058, MYB93 and MYB9 (Lashbrooke *et al.*, 2016; Soler *et al.*, 2020; To *et al.*, 2020). Additionally, other close homologues identified in other suberized tissues were also expressed mostly in the SD zone, including MYB52, MYB102, MYB53 and RD26 (Table **1**). Also common in other phellem tissues are other TF homolog families that are of special interest regarding secondary development and meristem maintenance processes, as the case of ARF, GRAS and LBD TF families (Table **1**). In the case of GRAS family, all members identified in cork oak SD zone as DEGs were also previously identified as enriched in phellem (Soler *et al.*, 2011; Rains *et al.*, 2018; Alonso-Serra *et al.*, 2019; Lopes *et al.*, 2019). Despite having a lower fold-change, homologues of ARF18 and ARF6 were not previously associated with secondary development, as well as LOB and LBD25. Other strongly expressed TF homologues and not previously associated with secondary development of roots include AT5G66940 (Dof domain-containing), AT1G01250 (ERF), AT2G31730 (bHLH), MUTE and BLH8 (Table **1**).

Table 1: Candidate regulators of secondary development in cork oak roots that are differentially expressed between SD and PD regions.

Gene ID (cork oak)	log2FC (SD vs PD)	Gene ID Arabidopsis *	Gene name	References **
LOC111992789	13.09	AT1G08290	WIP3	(Rains *et al.*, 2018)
LOC112038775	12.88	AT1G31320	LBD4	(Vulavala *et al.*, 2019; Alonso-Serra *et al.*, 2019; Lopes *et al.*, 2019)
LOC111993972	12.52	AT2G46680	HB-7	(Boher *et al.*, 2018; Vulavala *et al.*, 2019; Alonso-Serra *et al.*, 2019)
LOC112025693	12.22	AT5G41410	BEL1	(Rains *et al.*, 2018; Alonso-Serra *et al.*, 2019; Lopes *et al.*, 2019)
LOC111984334	11.54	AT1G17950	MYB52	(Rains *et al.*, 2018; Alonso-Serra *et al.*, 2019; Lopes *et al.*, 2019; Chapter II)
LOC111989495	11.41	AT4G21440	MYB102	(Rains *et al.*, 2018; Vulavala *et al.*, 2019; Alonso-Serra *et al.*, 2019; Lopes *et al.*, 2019; Chapter II)
LOC112032779	10.26	AT5G66940	-	-
LOC112005026	10.23	AT1G01250	-	-
LOC111999436	9.79	AT1G07900	LBD1	(Rains *et al.*, 2018; Alonso-Serra *et al.*, 2019; Lopes *et al.*, 2019)
LOC111990126	9.36	AT4G18170	WRKY28	(Rains *et al.*, 2018; Alonso-Serra *et al.*, 2019; Lopes *et al.*, 2019)
LOC111990209	8.90	AT2G46130	WRKY43	(Soler *et al.*, 2007; Rains *et al.*, 2018; Boher *et al.*, 2018; Alonso-Serra *et al.*, 2019; Lopes *et al.*, 2019; Chapter II)
LOC112037487	8.88	AT3G18400	NAC058	(Soler *et al.*, 2007; Vulavala *et al.*, 2017; Rains *et al.*, 2018; Alonso-Serra *et al.*, 2019; Lopes *et al.*, 2019; Chapter II)
LOC112006609	8.84	AT5G16770	MYB9	(Rains *et al.*, 2018; Alonso-Serra *et al.*, 2019; Lopes *et al.*, 2019; Chapter II)
LOC112030452	7.97	AT1G34670	MYB93	(Rains *et al.*, 2018; Teixeira *et al.*, 2018; Vulavala *et al.*, 2019; Alonso-Serra *et al.*, 2019; Lopes *et al.*, 2019; Chapter II)
LOC111999143	7.68	AT5G61430	NAC100	(Vulavala *et al.*, 2017, 2019; Boher *et al.*, 2018; Alonso-Serra *et al.*, 2019; Lopes *et al.*, 2019)
LOC112022199	7.68	AT4G27410	RD26	(Alonso-Serra *et al.*, 2019; Lopes *et al.*, 2019; Chapter II)

LOC111995720	7.59	AT2G31730	-	-
LOC112035674	7.23	AT5G63090	LOB	-
LOC112040135	6.23	AT4G37850	-	(Rains *et al.*, 2018; Vulavala *et al.*, 2019; Alonso-Serra *et al.*, 2019)
LOC112012012	6.05	AT3G06120	MUTE	-
LOC112035238	5.36	AT2G27990	BLH8	-
LOC112035777	4.20	AT1G66350	RGL1	(Rains *et al.*, 2018; Lopes *et al.*, 2019)
LOC111990207	2.64	AT5G62000	ARF2	(Boher *et al.*, 2018; Vulavala *et al.*, 2019)
LOC111988750	2.51	AT5G62000	ARF2	(Boher *et al.*, 2018; Vulavala *et al.*, 2019)
LOC112033252	1.54	AT1G50420	SCL3	(Rains *et al.*, 2018; Alonso-Serra *et al.*, 2019; Lopes *et al.*, 2019)
LOC112011902	1.04	AT5G52510	SCL8	(Soler *et al.*, 2011; Vulavala *et al.*, 2019; Alonso-Serra *et al.*, 2019)

* Best Blastp hit

** References of comparative transcriptomic studies targeting phellem tissues from cork oak, potato and birch. The highlighted genes (or homologs) were overrepresented in phellem tissues.

5. Discussion

In this chapter we followed cork oak root development, highlighting the process of secondary development and particularly phellem differentiation. Secondary development in roots is described to appear early in plant development, and particularly the process of phellem differentiation, in which suberization can be detected at early stages (Teixeira *et al.*, 2018; Wunderling *et al.*, 2018; Vulavala *et al.*, 2019; Chapter II). In cork oak tap root we observed a gradient of cellular development and differentiation along its axis, with primary growth starting in root tip and advanced secondary growth below root collar, at 15 DAS (Fig. **2**, **3**). At this matured region, suberized barriers of endodermis and phellem can be identified. These results suggest an

early differentiation of the phellogen, most likely without disappearance of the endodermis layer, opposite to what was reported in *Arabidopsis* (Wunderling *et al.*, 2018; Chapter II). This result agrees with the time course experiment, with the onset of secondary growth detected in tap roots at least 6 DAS (Fig. **2**). Interestingly, the first detection of secondary meristem activity in cork oak roots closely overlapped for both vascular and cork cambia (between 6 and 8 DAS). This contrasts with other plant models, where vascular cambium is recognised to be initiated earlier than phellogen/cork cambium (Crang *et al.*, 2018; Wunderling *et al.*, 2018; Smetana *et al.*, 2019; Chapter II). Periclinal divisions just above the central vascular bundle, observed at 6 DAS, before suberization is detected, may reveal the onset of phellogen activity. Suberized cells were detected from 8 DAS (Fig. **2d-i**), in line with the detection of gene expression of core suberin biosynthesis genes (Fig. **4a**, **b**). Given its position surrounding the vascular cylinder we considered the first layer of suberized cells as endoderm. In plant root development, suberin is described to first appear during primary growth, in mature endodermis cells, just after complete elongation process and casparian strip formation (Verdaguer & Molinas, 1997; Naseer *et al.*, 2012; Machado *et al.*, 2013; Andersen *et al.*, 2015). The partial suberization pattern observed in lower portions of 15 DAS roots (Fig. **3e**) relates to the patchy phenotype described for intermediate stages of endodermis suberization in *Arabidopsis* and barley (Geldner, 2013; Kreszies *et al.*, 2018). Yet, the fact that, in cork oak roots, the endodermis suberization occurs after secondary development initiation is intriguing and will require further studies. The detection of a Casparian strip would help to accurately identify the endodermis cells. At 15 DAS, mature sections taken below the root collar had 2-3 rows of suberized cells, revealing its phellem nature. Nonetheless, we may still consider the simultaneous presence of suberized endodermis cells.

Aiming to highlight the molecular pathways involved in secondary development in cork oak roots, a transcriptomic experiment was performed targeting tap roots from 8 DAS seedlings, when a developmental gradient is evident between PD and SD targeted zones. Comparing RNAseq libraries obtained from SD (with active secondary meristems) *versus* PD, we found specific regulators of each developmental region, including suberization and phellem development (exclusively found in SD at that stage). The inclusion of samples exposed to different developmental conditions increased sequencing depth and confidence on the DEGs found exclusively between SD and PD, independently of the condition. Specific gene markers for primary and secondary development were differentially expressed, demonstrating the efficiency of this strategy to distinguish molecular pathways between developmental zones. Among these, we found ANT, WOX4 and PLT homologues in the SD zone and SMB, BRN2 and FEZ in the PD zone. Interestingly the SD region showed a higher number of enriched genes, as compared to the young one. This increased transcriptional activity can be due to the higher diversity of tissues and the active growth and differentiation that result from vascular and cork cambium activities.

Phellem was previously characterized as the most transcriptional distinct tissue among various isolated plant tissues during secondary development (Alonso-Serra *et al.*, 2019; Lopes *et al.*, 2019). After cellulose metabolism, the regulatory pathways for lignin and suberin metabolism are the most evident active processes denoted in the mature zone of cork oak root, probably related to the cell divisions ongoing and differentiation of phloem, xylem and phellem, respectively. Based on our gene expression, regulation of lignin and suberin synthesis was represented in SD zones by genes involved in the phenylpropanoid pathway, which produces precursors for both cell wall

polymers (Bernards, 2002; Li-Beisson *et al.*, 2013). Considering genes associated exclusively with lignin biosynthesis process, we found cork oak homologs for *IRX4* (*LOC112009904*) and *ATCAD4* (*LOC112035939*), *CAD1 (LOC112030208)* and *SAM2* (LOC111997747) overexpressed in SD zones (Fig. **7**, Cluster **1**). Multiple genes with demonstrated roles in different steps of suberization were also enriched in SD zone. Among these we found cork oak homologs of genes related to the biosynthesis of aliphatic components (*QsKCS2*, *QsCYP86A1*, *QsCYP86B1*, *QsFAR4*), as well as conjugation (*QsGPAT5/1*, *QsRWP1*) and transport (*QsABCG1/16/10/23*) of suberin monomers. These results were supported by our targeted transcriptional analysis using qPCR. In addition, several lipid transfer proteins were enriched in SD (LOC111987449, LOC112015107, LOC112011078, LOC111994753, LOC112022577, LOC111994752), which despite not being functionally validated, could be putatively involved in suberin monomer transport (Rains *et al.*, 2018; Boher *et al.*, 2018; Vulavala *et al.*, 2019; Alonso-Serra *et al.*, 2019; Lopes *et al.*, 2019; Chapter II).

Regarding the polymerization of cell wall components, several protein families of interest were also enriched in SD zone, including peroxidases, laccases, CASPs, GDSL lipases and α,β- hydrolases. While suberin polymerization is still poorly described, several GDSL lipases were experimentally proven to be involved in this process (Ursache et al., 2020) and cork oak homologs of *GELP38* (LOC111998717), *GELP51* (LOC112038093, LOC112009101, LOC112038078) and GELP96 (LOC111989476) were overexpressed in SD zone. These proteins were interacting with other suberin biosynthesis-related proteins in the predicted interaction network (Fig. **7**). On the other hand, lignin polymerization is achieved by peroxidases, laccases and CASPs (Tobimatsu & Schuetz, 2019), which have also been proposed as candidates for suberization. In our data, we found

multiple cork oak homologs from the laccase and peroxidase families enriched in SD zone, that were previously identified in other transcriptomic studies targeting isolated phellem cells: such as *QsLAC7* (LOC111988990), *QsLAC3* (LOC112000435), *QsPRX52* (LOC111996725), and *QsPER64* (LOC111989638). Therefore, we believe these genes are very likely to be involved in both suberin and lignin polymerization. CASPs (Casparian strip membrane proteins) are required for targeted deposition of lignin in the Casparian band, and their active expression in SD zone of cork oak root, supports the presence of a functional endodermis at 8 DAS. However, CASP and CASP-like proteins are also suggested as coordinators of polymerization of other polymers and may also be involved in polymerization of suberin phenolic components, since members of this family were found in suberized tissues lacking Casparian bands (Roppolo *et al.*, 2014; Lashbrooke *et al.*, 2016; Legay *et al.*, 2016; Vulavala *et al.*, 2017).

In the predicted regulatory network, several stress-response proteins were interacting with other proteins associated with the cell wall modifications (Fig. **7**, Cluster 1). This was the case of glutathione S-transferases (GSTs) proteins, involved in detoxification and attenuation of oxidative stress (Gullner *et al.*, 2018), likely to occur during suberization (Bernards *et al.*, 2004) and lignification (Dixon *et al.*, 2010). Other genes related to stress response, encoding HSPs, chaperons and LEA proteins, were also induced in SD zones (compared to PD) independently of the tested growth conditions. Interestingly, this class of stress responsive proteins was reported to play a role in cell cycle regulation (Menges *et al.*, 2002) and in meristem dedifferentiation (Chalifa-caspi & Ransbotyn, 2011). These proteins promote the molecular reprogramming required for plant survival in response to stress, a molecular reprograming process that may be similar to what occurs for dedifferentiation of lateral meristem cells. In fact, heat shock

proteins have been reported not only in isolated phellem cells (Lopes *et al.*, 2019; Chapter II), but also in dissected phellogen cells (Teixeira *et al.*, 2018; Vulavala *et al.*, 2019), supporting their relevance in periderm development.

Remarkably, several genes encoding photosystem-related proteins were differentially expressed in the SD zone. Since this region was located near the root collar at lower depth, it could be exposed to limited amounts of light, eventually penetrating between the substrate (Tester *et al.*, 1987; Baluška, 2015). Remarkably, the expression of photosynthesis-related genes was previously reported in shoot periderm, due to the presence of phelloderm, which is photosynthetically active in shoots (Rains *et al.*, 2018; Alonso-Serra *et al.*, 2019). In Arabidopsis roots, the phellem cell-specific transcriptome also showed an enrichment in photosynthesis-related genes, most of which transcribed from the plastid genome (Chapter II), Moreover, potato phellogen showed enrichment in photomorphogenesis transcripts (Vulavala *et al.*, 2019). All together these results suggest that the periderm is putatively enriched in plastids, eventually derived from the phelloderm (Evert, 2006), although precursors for suberin and tannins, two major components of phellem, are produced in plastids (Bernards, 2002; Li-Beisson *et al.*, 2013; Brillouet *et al.*, 2013, 2014; Solymosi *et al.*, 2018). The fact that the SD root zone may be exposed to light may induce plastid conversion and production of photosystem proteins at periderm level. Yet, it would be interesting to further confirm the transcriptional activity of such genes in deeper zones of the root and later developmental stages.

Specific hormones are known to have a spatial and/or gradient distribution over secondary developed tissues, resulting in a distinct developmental response in the respective tissues. Control of secondary development in plants is specially well characterized in vascular tissues

(phloem and xylem), and the respective vascular cambium. An increase in auxin is described in the actively dividing vascular cambium, while a cytokinin peak occurs in the developing phloem, and gibberellin increases in the developing xylem cells (Immanen *et al.*, 2016; Ragni & Greb, 2018). Despite the morphological evidences of an active vascular cambium in the SD zone of cork oak roots, in the PD zone no enrichment in auxin signalling-related genes was detected. This may be due the fact that regulation by auxin pathways are shared in the root apical meristem (Ragni & Greb, 2018; Motte *et al.*, 2019). This is also the case for cytokinin, particularly since mutual interaction between cytokinin and auxin signalling cascades are reported during primary vascular development (Motte *et al.*, 2019; Wybouw & De Rybel, 2019). In contrast, we found GA as a potential regulator in the cork oak mature root zone, and identified several genes associated with GA response and its signalling pathway, in particular, key components likely to be involved in xylem differentiation through KNAT1 and GA-dependent mechanism. In the presence of GA, the formation of GA-GID1-DELLA complexes is stimulated, leading to further proteasome-dependent degradation of DELLA proteins (Davière & Achard, 2013). We may assume that in SD root, upon DELLA degradation, *QsKNAT1* (LOC112015571) is free to activate genes involved in secondary cell wall modifications and phenylpropanoid biosynthesis (Felipo-Benavent *et al.*, 2018).

In our SD transcriptome analysis, we also found a significant enrichment in genes involved in ABA-response. An expression enrichment in ABA-related genes has been reported for periderm tissues of *Arabidopsis*, cork and potato (Soler *et al.*, 2007, 2011; Chapter II), being mostly associated with stress response. However, this hormone was also described to be crucial for suberization processes in diverse tissues, through the activation of numerous genes from the suberin pathway

(Lee *et al.*, 2009; Boher *et al.*, 2013; Yadav *et al.*, 2014; Barberon *et al.*, 2016; Bjelica *et al.*, 2016), which are also enriched in the SD zone in our study. In addition, ABA can be involved in xylem development, as recently reported for fibre differentiation (Ramachandran *et al.*, 2018; Campbell *et al.*, 2018) and in the secondary cell wall thickening and lignification (Liu *et al.*, 2021). We may speculate that the hormonal control of secondary development in cork oak roots may happen in a similar way as experimentally determined for other species, through a gradient of different hormones in each tissue (hormonal domains), controlling meristem size, cell divisions and tissue differentiation. Determination of hormonal content in each tissue might help to clarify this hypothesis. Nevertheless, we may consider that the outcome of hormonal signalling is highly dependent on the specific context, with the possibility of the same hormone having a versatile role during different developmental processes.

Determination of cell fate is known to be in part regulated by different TFs. Particularly *WOX4* homolog (LOC111988759), which is described to be involved in vascular (Smetana *et al.*, 2019; Alonso-Serra *et al.*, 2019) and periderm differentiation (Boher *et al.*, 2018; Alonso-Serra *et al.*, 2019), is overrepresented in the SD zone. Interestingly, in cork oak trunk, WOX4 was strongly expressed in phellem, as compared with xylem (Boher *et al.*, 2018). Since *WOX4* has been shown to trigger cambial proliferation (Ji *et al.*, 2010), it was hypothesised that the stronger expression of *WOX4* in cork oak phellem (and/or phellogen) could lead to stronger and longer activity of the cambium, which ultimately results in the characteristic thicker outer bark tissue (Boher *et al.*, 2018).

LOB-Domain (LBD) proteins are also predicted to contribute for lateral meristem development (Xu *et al.*, 2016), and lately regarded with special interest considering periderm development. In poplar, some members

of this family were shown to participate in vascular patterning along secondary growth. Namely expression of *LBD4* together with *LBD1* poplar homologues was upregulated in secondary phloem, while *LBD15* and *LBD18* were enriched in xylem (Yordanov *et al.*, 2010). Interestingly, expression of *QsLBD1*(LOC111999436), *QsLBD4* (LOC11203877) and *QsLBD15* (LOC111987448), were enriched in SD root zones in our study, as well as in isolated phellem cells of *Arabidopsis*, cork oak and birch (Alonso-Serra *et al.*, 2019; Lopes *et al.*, 2019; Chapter II). Therefore, it is likely that these LBD TFs play a role, not only in vascular tissue patterning, but also in periderm development. Moreover, the strongly expressed *QsLOB/ASL4* (LOC112035674) (Table 1), that limits growth in organ boundaries (Bell *et al.*, 2012), may also have similar functions in cork oak root secondary development.

In the present study we also identified multiple TFs highly overexpressed in SD root zones with a predicted role in secondary metabolism. These includes a *WIP3* homolog, previously identified in poplar phellem (Rains *et al.*, 2018), which showed the highest fold-change in SD root zone (compared to PD). Members of WIP proteins are described as regulators of proanthocyanidin biosynthesis, also known as condensed tannins. These are polyphenolic secondary metabolites synthesized as oligomers or polymers via the flavonoid pathway (Sagasser *et al.*, 2002; Appelhagen *et al.*, 2010, 2011). We can hypothesize that the strongly expressed WIP3 is specially involved in the control of flavonoid and tannin accumulation, that are very likely to be accumulating in the new cork oak phellem cells (Silva *et al.*, 2005; Pinheiro *et al.*, 2019), or other new secondary tissues(Crang *et al.*, 2018). Also in mature cork oak roots we detected the expression of TFs described as the first layer of regulation for secondary cell walls, such as the *QsVND1/3/4* (LOC111996673 / LOC111994497 / LOC112007201, LOC111988979) and *QsXND1* (LOC112009005)

homologs (Zhang *et al.*, 2018). In grasses, these TFs were described to activate a second layer of regulation, mediated by *QsMYB46* (LOC111996538) and *QsMYB83*(LOC112038777), as well as structural genes involved in biosynthesis of secondary cell wall (Rao & Dixon, 2018). The enriched expression of these TFs in the SD root zone suggests a conserved regulation mechanism in cork oak. Looking in particular for regulators of cell wall suberization of phellem, some differentially expressed TFs could be of special interest, including *QsMYB93*, *QsMYB9*, *QsNAC58* and *QsRD26* (Table **1**). These specific TFs were not only previously identified in dissected phellem tissues (Soler *et al.*, 2007; Vulavala *et al.*, 2017, 2019; Rains *et al.*, 2018; Teixeira *et al.*, 2018; Boher *et al.*, 2018; Alonso-Serra *et al.*, 2019; Lopes *et al.*, 2019; Chapter II) but also have demonstrated functions as direct regulators of the suberin biosynthesis genes (Verdaguer *et al.*; Lashbrooke *et al.*, 2016; Legay *et al.*, 2016; Soler *et al.*, 2020). In addition, these TFs are reported to be involved in ABA mediated regulation (Tran *et al.*, 2004; Coego *et al.*, 2014; Gibbs *et al.*, 2014), reinforcing the possibility of their involvement in phellem differentiation and necessary for cell wall remodelling and suberization.

In this work we looked for the first time to cork oak tap root development as a model to study phellem regulation. Our results show that the onset of secondary growth, and more particularly phellem development occur very early in cork oak tap roots. The gathered data suggests that phellogen is developed in close overlap with endodermis suberization, although further studies are still required. Despite the extended complexity of cork oak tap roots, displaying high secondary growth activity, in both vascular and cork cambium, our transcriptomic data indicate that the secondary development in these organs is relatively conserved with other species, with the identification of a similar fingerprint in the main regulatory networks. Moreover, some genes

detected in our study were also reported during stem secondary development in diverse species, reinforcing the use of tap roots as a proxy for cork development in cork oak. Although there are still limitations in the use of acorns (such as the genetic variability due to open pollination and inefficient long-term storage) our study demonstrated that tap roots are a simpler, easier and faster model to study phellem development in cork oak, when compared to trunks or shoots.

6. Acknowledgments

Ana Rita Leal performed this experimental work with the collaborations of Pedro Barros, Helena Sapeta and Joana Belo. Pedro Barros, M. Margarida Oliveira and Tom Beckman help to design and discuss the research experiments and results.

7. Bibliography:

Aguado PL, Curt MD, Pereira H, Fernández J. **2017**. The influence of season on carbon allocation to suberin and other stem components of cork oak saplings. *Tree physiology* **37**: 165–172.

Aida M, Beis D, Heidstra R, Willemsen V, Blilou I, Galinha C, Nussaume L, Noh Y-S, Amasino R, Scheres B. **2004**. The PLETHORA Genes Mediate Patterning of the Arabidopsis Root Stem Cell Niche. *Cell* **119**: 109–120.

Alonso-Serra J, Safronov O, Lim K, Fraser-Miller SJ, Blokhina OB, Campilho A, Chong S, Fagerstedt K, Haavikko R, Helariutta Y, *et al.* 2019. Tissue-specific study across the stem reveals the chemistry and transcriptome dynamics of birch bark. *New Phytologist* **222**: 1816–1831.

Andersen TG, Barberon M, Geldner N. **2015**. Suberization-the second life of an endodermal cell. *Current Opinion in Plant Biology* **28**: 9–15.

Andrews S. **2010**. FastQC: A quality control tool for high throughput sequence data.

APCOR - Associação Portuguesa de Cortiça.

Appelhagen I, Huep G, Lu G, Strompen G, Weisshaar B, Sagasser M. **2010**. Weird fingers : Functional analysis of WIP domain proteins. *FEBS Letters* **584**: 3116–3122.

Appelhagen I, Lu G, Huep G, Schmelzer E, Weisshaar B, Sagasser M. **2011**. TRANSPARENT TESTA1 interacts with R2R3-MYB factors and affects early and late steps of flavonoid biosynthesis in the endothelium of Arabidopsis thaliana seeds. *The Plant Journal* **67**: 406–419.

Baluška F. **2015**. How and why do root apices sense light under the soil surface ? **6**: 1–8.

Barberon M, Vermeer JEM, De Bellis D, Wang P, Naseer S, Andersen TG, Humbel BM, Nawrath C, Takano J, Salt DE, *et al.* 2016. Adaptation of Root Function by Nutrient-Induced Plasticity of Endodermal Differentiation. *Cell* **164**: 447–459.

Bell EM, Lin W, Husbands AY, Yu L, Jaganatha V. **2012**. Arabidopsis LATERAL ORGAN

BOUNDARIES negatively regulates brassinosteroid accumulation to limit growth in organ boundaries. **109**.

Bernards MA. **2002**. Demystifying suberin. *Canadian Journal of Botany* **80**: 227–240.

Bernards MA, Summerhurst DK, Razem FA. **2004**. Oxidases, peroxidases and hydrogen peroxide: The suberin connection. *Phytochemistry Reviews* **3**: 113–126.

Bjelica A, Haggitt ML, Woolfson KN, Lee DPN, Makhzoum AB, Bernards MA. **2016**. Fatty acid ω-hydroxylases from Solanum tuberosum. *Plant Cell Reports* **35**: 2435–2448.

Boher P, Serra O, Soler M, Molinas M, Figueras M. **2013**. The potato suberin feruloyl transferase FHT which accumulates in the phellogen is induced by wounding and regulated by abscisic and salicylic acids. *Journal of Experimental Botany* **64**: 3225–3236.

Boher P, Soler M, Sánchez A, Hoede C, Noirot C, Paiva JAP, Serra O, Figueras M. **2018**. A comparative transcriptomic approach to understanding the formation of cork. *Plant Molecular Biology* **96**: 103–118.

Bolger AM, Lohse M, Usadel B. **2014**. Trimmomatic: a flexible trimmer for Illumina sequence data. *Bioinformatics* **30**: 2114–2120.

Brillouet J, Romieu C, Lartaud M, Jublanc E, Torregrosa L, Cazevieille C. **2014**. Formation of vacuolar tannin deposits in the chlorophyllous organs of Tracheophyta: from shuttles to accretions. *Protoplasma* **251**: 1387–1393.

Brillouet J, Romieu C, Schoefs B, Solymosi K, Cheynier V, Fulcrand H, Verdeil J-L, Conéjéro G. **2013**. The tannosome is an organelle forming condensed tannins in the chlorophyllous organs of Tracheophyta. *Annals of Botany* **112**: 1003–1014.

Brundrett MC, Kendrick B, Peterson CA. **1991**. Efficient Lipid Staining in Plant Material with Sudan Red 7B or Fluoral Yellow 088 in Polyethylene Glycol-Glycerol. *Biotechnic & Histochemistry* **66**: 111–116.

Campbell L, Etchells JP, Cooper M, Kumar M, Turner SR. **2018**. An essential role for abscisic acid in the regulation of xylem fibre differentiation. *Development* **145**: dev161992.

Campilho A, Nieminen K, Ragni L. **2020**. The development of the periderm: the final frontier between a plant and its environment. *Current Opinion in Plant Biology* **53**: 10–14.

Cardoso MSQ. **2011**. Caracterização histológica e histoquímica das células suberosas em diferenciação das peridermes do sobreiro e da batata.

Chalifa-caspi GGV, Ransbotyn V. **2011**. Plant response to stress meets dedifferentiation. : 433–438.

Coego A, Brizuela E, Castillejo P, Ruíz S, Koncz C, Del Pozo JC, Piñeiro M, Jarillo JA, León J, Paz-Ares J, *et al.* 2014. The TRANSPLANTA collection of Arabidopsis lines: A resource for functional analysis of transcription factors based on their conditional overexpression. *Plant Journal* **77**: 944–953.

Crang R, Lyons-Sobaski S, Wise R. **2018**. *Plant Anatomy*. Cham: Springer International Publishing.

Davière JM, Achard P. **2013**. Gibberellin signaling in plants. *Development (Cambridge)* **140**: 1147–1151.

Dixon DP, Skipsey M, Edwards R. **2010**. Phytochemistry Roles for glutathione transferases in plant secondary metabolism. *Phytochemistry* **71**: 338–350.

Dobin A, Davis CA, Schlesinger F, Drenkow J, Zaleski C, Jha S, Batut P, Chaisson M, Gingeras TR. **2013**. STAR: ultrafast universal RNA-seq aligner. *Bioinformatics* **29**: 15–21.

Dolan L, Janmaat K, Willemsen V, Linstead P, Poethig S, Roberts K, Scheres B. **1993**. Cellular organisation of the Arabidopsis thaliana root. *Development* **119**: 71–84.

Drisch RC, Stahl Y. **2015**. Function and regulation of transcription factors involved in root apical meristem and stem cell maintenance. *Frontiers in Plant Science* **6**: 1–8.

Du Y, Scheres B. **2017**. PLETHORA transcription factors orchestrate de novo organ patterning during Arabidopsis lateral root outgrowth. *Proceedings of the National Academy of Sciences* **114**: 11709–11714.

Evert RF. **2006**. *Esau's Plant Anatomy*. Hoboken, NJ, USA: John Wiley & Sons, Inc.

Felipo-Benavent A, Úrbez C, Blanco-Touriñán N, Serrano-Mislata A, Baumberger N, Achard P, Agustí J, Blázquez MA, Alabadí D. **2018**. Regulation of xylem fiber differentiation by gibberellins through DELLA-KNAT1 interaction. *Development* **145**: dev164962.

Geldner N. **2013**. The endodermis. *Annu Rev Plant Biol* **64**: 531–558.

Gibbs DJ, Voß U, Harding SA, Fannon J, Moody LA, Yamada E, Swarup K, Nibau C, Bassel GW, Choudhary A, *et al.* 2014. At MYB93 is a novel negative regulator of lateral root development in Arabidopsis. *New Phytologist* **203**: 1194–1207.

Graça J, Pereira H. **2004**. The periderm development in Quercus suber. *IAWA Journal* **25**: 325–335.

Gullner G, Komives T, Király L, Schröder P. **2018**. Glutathione S-transferase enzymes in plant-pathogen interactions. *Frontiers in Plant Science* **871**: 1–19.

Immanen J, Nieminen K, Smolander O-P, Kojima M, Alonso Serra J, Koskinen P, Zhang J, Elo A, Mähönen AP, Street N, *et al.* 2016. Cytokinin and Auxin Display Distinct but Interconnected Distribution and Signaling Profiles to Stimulate Cambial Activity. *Current Biology* **26**: 1990–1997.

Ji J, Strable J, Shimizu R, Koenig D, Sinha N, Scanlon MJ. **2010**. WOX4 Promotes Procambial Development. *Plant Physiology* **152**: 1346–1356.

Kreszies T, Schreiber L, Ranathunge K. **2018**. Suberized transport barriers in Arabidopsis, barley and rice roots: From the model plant to crop species. *Journal of Plant Physiology* **227**: 75–83.

Lashbrooke J, Cohen H, Levy-Samocha D, Tzfadia O, Panizel I, Zeisler V, Massalha H, Stern A, Trainotti L, Schreiber L, *et al.* 2016. MYB107 and MYB9 Homologs Regulate Suberin Deposition in Angiosperms. *The Plant Cell* **28**: 2097–2116.

Leal AR, Barros PM, Parizot B, Sapeta H, Nick V, Tonni Grube A, Tom B, Oliveira MM. **2020**. Phellem translational landscape throughout secondary development in Arabidopsis roots. *Chapter 2*: 3–29.

Lee SB, Jung SJ, Go YS, Kim HU, Kim JK, Cho HJ, Park OK, Suh MC. **2009**. Two Arabidopsis 3-ketoacyl CoA synthase genes, KCS20 and KCS2/DAISY, are functionally redundant in cuticular wax and root suberin biosynthesis, but differentially controlled by osmotic stress. *Plant Journal* **60**: 462–475.

Legay S, Guerriero G, André C, Guignard C, Cocco E, Charton S, Boutry M, Rowland O, Hausman J-F. **2016**. MdMyb93 is a regulator of suberin deposition in russeted apple fruit skins. *New Phytologist* **212**: 977–991.

Leite C, Pereira H. **2017**. Cork-Containing Barks—A Review. *Frontiers in Materials* **3**: 1–19.

Li-Beisson Y, Shorrosh B, Beisson F, Andersson MX, Arondel V, Bates PD, Baud S, Bird D, DeBono A, Durrett TP, *et al.* 2013. Acyl-Lipid Metabolism. *The Arabidopsis Book* **11**: e0161.

Liao Y, Smyth GK, Shi W. **2014**. featureCounts: an efficient general purpose program for assigning sequence reads to genomic features. *Bioinformatics* **30**: 923–930.

Liu C, Yu H, Rao X, Li L, Dixon RA. **2021**. Abscisic acid regulates secondary cell-wall formation and lignin deposition in Arabidopsis thaliana through phosphorylation of NST1. *Proceedings of the National Academy of Sciences* **118**: e2010911118.

Lopes ST, Sobral D, Costa B, Perdiguero P, Chaves I, Costa A, Miguel CM. **2019**.

Phellem versus xylem: genome-wide transcriptomic analysis reveals novel regulators of cork formation in cork oak. *Tree Physiology*: 1–39.

Love MI, Huber W, Anders S. **2014**. Moderated estimation of fold change and dispersion for RNA-seq data with DESeq2. *Genome Biology* **15**: 550.

Machado A, Pereira H, Teixeira RT. **2013**. Anatomy and Development of the Endodermis and Phellem of Quercus suber L . Roots. *Microscopy and Microanalysis*: 1–10.

Maere S, Heymans K, Kuiper M. **2005**. BiNGO: a Cytoscape plugin to assess overrepresentation of Gene Ontology categories in Biological Networks. *Bioinformatics* **21**: 3448–3449.

Menges M, Hennig L, Murray JAH, Menges M, Hennig L, Gruissem W, Murray JAH. **2002**. Cell Cycle-regulated Gene Expression in Arabidopsis.

Moreno-Risueno MA, Sozzani R, Yard mc GG, Petricka JJ, Vernoux T, Blilou I, Alonso J, Winter CM, Ohler U, Scheres B, *et al.* 2015. Transcriptional control of tissue formation throughout root development. *Science* **350**: 426–430.

Motte H, Vanneste S, Beeckman T. **2019**. Molecular and Environmental Regulation of Root Development. *Annual Review of Plant Biology* **70**: 465–488.

Naseer S, Lee Y, Lapierre C, Franke R, Nawrath C, Geldner N. **2012**. Casparian strip diffusion barrier in Arabidopsis is made of a lignin polymer without suberin. *Proceedings of the National Academy of Sciences of the United States of America* **109**: 10101–10106.

Perilli S, Di Mambro R, Sabatini S. **2012**. Growth and development of the root apical meristem. *Current Opinion in Plant Biology* **15**: 17–23.

Petricka JJ, Winter CM, Benfey PN. **2012**. Control of Arabidopsis Root Development . *Annual Review of Plant Biology* **63**: 563–590.

Pfaffl MW. **2001**. A new mathematical model for relative quantification in real-time RT-PCR. *Nucleic acids research* **29**: 16–21.

Pinheiro C, Wienkoop S, de Almeida JF, Brunetti C, Zarrouk O, Planchon S, Gori A, Tattini M, Ricardo CP, Renaut J, *et al.* 2019. Phellem Cell-Wall Components Are Discriminants of Cork Quality in Quercus suber. *Frontiers in Plant Science* **10**: 1–15.

Pradhan Mitra P, Loqué D. **2014**. Histochemical Staining of Arabidopsis thaliana Secondary Cell Wall Elements. *Journal of Visualized Experiments*.

R Foundation for Statistical Computing. 2018. *R: a Language and Environment for Statistical Computing.*

Ragni L, Greb T. **2018**. Secondary growth as a determinant of plant shape and form. *Seminars in Cell and Developmental Biology* **79**: 58–67.

Rains MK, De Silva NDG, Molina I. **2018**. Reconstructing the suberin pathway in poplar by chemical and transcriptomic analysis of bark tissues. *Tree Physiology* **38**: 340–361.

Ramachandran P, Wang G, Augstein F, de Vries J, Carlsbecker A. **2018**. Continuous root xylem formation and vascular acclimation to water deficit involves endodermal ABA signalling via miR165. *Development* **145**: dev159202.

Ramos AM, Usié A, Barbosa P, Barros PM, Capote T, Chaves I, Simões F, Abreu I, Carrasquinho I, Faro C, *et al.* 2018. The draft genome sequence of cork oak. *Scientific Data* **5**: 1–12.

Rao X, Dixon RA. **2018**. Current models for transcriptional regulation of secondary cell wall biosynthesis in grasses. *Frontiers in Plant Science* **9**: 1–11.

Roppolo D, Boeckmann B, Pfister A, Boutet E, Rubio MC, Dénervaud-Tendon V, Vermeer JEM, Gheyselinck J, Xenarios I, Geldner N. **2014**. Functional and evolutionary analysis of the CASPARIAN STRIP MEMBRANE DOMAIN PROTEIN family. *Plant Physiology* **165**: 1709–1722.

Sagasser M, Lu G, Hahlbrock K, Weisshaar B. **2002**. is involved in seed coat

development and defines the WIP subfamily of plant zinc finger proteins. : 138–149.

Schindelin J, Arganda-Carreras I, Frise E, Kaynig V, Longair M, Pietzsch T, Preibisch S, Rueden C, Saalfeld S, Schmid B, *et al.* 2012. Fiji: an open-source platform for biological-image analysis. *Nature Methods* **9**: 676–682.

Silva SP, Sabino MA, Fernandes EM, Correlo VM, Boesel LF, Reis RL. 2005. Cork: properties, capabilities and applications. *International Materials Reviews* **50**: 345–365.

Slovak R, Ogura T, Satbhai SB, Ristova D, Busch W. 2016. Genetic control of root growth: From genes to networks. *Annals of Botany* **117**: 9–24.

Smetana O, Mäkilä R, Lyu M, Amiryousefi A, Sánchez Rodríguez F, Wu M-FF, Solé-Gil A, Leal Gavarrón M, Siligato R, Miyashima S, *et al.* 2019. High levels of auxin signalling define the stem-cell organizer of the vascular cambium. *Nature* **565**: 485–489.

Soler M, Serra O, Fluch S, Molinas M, Figueras M. 2011. A potato skin SSH library yields new candidate genes for suberin biosynthesis and periderm formation. *Planta* **233**: 933–945.

Soler M, Serra O, Molinas M, Huguet G, Fluch S, Figueras M. 2007. A Genomic Approach to Suberin Biosynthesis and Cork Differentiation. *Plant Physiology* **144**: 419–431.

Soler M, Verdaguer R, Fernández-Piñán S, Company-Arumí D, Boher P, Góngora-Castillo E, Valls M, Anticó E, Molinas M, Serra O, *et al.* 2020. Silencing against the conserved NAC domain of the potato StNAC103 reveals new NAC candidates to repress the suberin associated waxes in phellem. *Plant Science* **291**: 110360.

Solymosi K, Lethin J, Aronsson H. 2018. Diversity and plasticity of plastids in land plants. *Methods in Molecular Biology* **1829**: 55–72.

Szklarczyk D, Gable AL, Lyon D, Junge A, Wyder S, Huerta-Cepas J, Simonovic M, Doncheva NT, Morris JH, Bork P, *et al.* 2019. STRING v11: Protein-protein association networks with increased coverage, supporting functional discovery in genome-wide experimental datasets. *Nucleic Acids Research* **47**: D607–D613.

Taylor-Teeples M, Lin L, de Lucas M, Turco G, Toal TW, Gaudinier A, Young NF, Trabucco GM, Veling MT, Lamothe R, *et al.* 2015. An Arabidopsis gene regulatory network for secondary cell wall synthesis. *Nature* **517**: 571–575.

Teixeira RT, Fortes AM, Bai H, Pinheiro C, Pereira H. 2018. Transcriptional profiling of cork oak phellogenic cells isolated by laser microdissection. *Planta* **247**: 317–338.

Teixeira RT, Fortes AM, Pinheiro C, Pereira H. 2014. Comparison of good- and bad-quality cork: Application of high-throughput sequencing of phellogenic tissue. *Journal of Experimental Botany* **65**: 4887–4905.

Tester M, Morris C, Sehool B, Street D. 1987. The penetration of light through soil. : 281–286.

Tian H, Wabnik K, Niu T, Li H, Yu Q, Pollmann S, Vanneste S, Govaerts W, Rolčík J, Geisler M, *et al.* 2014. WOX5–IAA17 Feedback Circuit-Mediated Cellular Auxin Response Is Crucial for the Patterning of Root Stem Cell Niches in Arabidopsis. *Molecular Plant* **7**: 277–289.

To A, Joubès J, Thueux J, Kazaz S, Lepiniec L, Baud S. 2020. AtMYB92 enhances fatty acid synthesis and suberin deposition in leaves of Nicotiana benthamiana. *The Plant Journal* **33**: 0–2.

Tobimatsu Y, Schuetz M. 2019. Lignin polymerization: how do plants manage the chemistry so well? *Current Opinion in Biotechnology* **56**: 75–81.

Tran LP, Nakashima K, Sakuma Y, Simpson SD, Fujita Y, Maruyama K, Fujita M, Seki M, Shinozaki K, Yamaguchi-shinozaki K. 2004. Isolation and Functional Analysis of Arabidopsis Stress-Inducible NAC Transcription Factors That Bind to a Drought-Responsive cis -Element in the early responsive to dehydration stress 1 Promoter. **16**: 2481–2498.

Verdaguer D, Molinas M. **1997**. Development and ultrastructure of the endodermis in the primary root of cork oak (Quercus suber). *Canadian Journal of Botany* **75**: 769–780.

Verdaguer R, Soler M, Serra O, Garrote A, Fernández S. Silencing of the potato tuber skin-induced StNAC103 gene enhances accumulation of suberin and suberin-associated wax.

Verhertbruggen Y, Walker JL, Guillon F, Scheller H V. 2017. A comparative study of sample preparation for staining and immunodetection of plant cell walls by light microscopy. *Frontiers in Plant Science* **8**: 1–17.

Vulavala VKR, Fogelman E, Faigenboim A, Shoseyov O, Ginzberg I. **2019**. The transcriptome of potato tuber phellogen reveals cellular functions of cork cambium and genes involved in periderm formation and maturation. *Scientific Reports* **9**: 10216.

Vulavala VKR, Fogelman E, Rozental L, Faigenboim A, Tanami Z, Shoseyov O, Ginzberg I. **2017**. Identification of genes related to skin development in potato. *Plant Molecular Biology* **94**: 481–494.

Wunderling A, Ripper D, Barra-Jimenez A, Mahn S, Sajak K, Targem M Ben, Ragni L. **2018**. A molecular framework to study periderm formation in Arabidopsis. *New Phytologist* **219**: 216–229.

Wybouw B, De Rybel B. **2019**. Cytokinin – A Developing Story. *Trends in Plant Science* **24**: 177–185.

Xu C, Luo F, Hochholdinger F. **2016**. LOB Domain Proteins: Beyond Lateral Organ Boundaries. *Trends in Plant Science* **21**: 159–167.

Yadav V, Molina I, Ranathunge K, Castillo IQ, Rothstein SJ, Reed JW. **2014**. ABCG Transporters Are Required for Suberin and Pollen Wall Extracellular Barriers in Arabidopsis. *The Plant Cell* **26**: 3569–3588.

Yordanov YS, Regan S, Busov V. **2010**. Members of the LATERAL ORGAN BOUNDARIES DOMAIN transcription factor family are involved in the regulation of secondary growth in populus. *Plant Cell* **22**: 3662–3677.

Zhang J, Eswaran G, Alonso-Serra J, Kucukoglu M, Xiang J, Yang W, Elo A, Nieminen K, Damén T, Joung JG, *et al.* 2019. Transcriptional regulatory framework for vascular cambium development in Arabidopsis roots. *Nature Plants* **5**: 1033–1042.

Zhang J, Xie M, Tuskan GA, Muchero W, Chen JG. **2018**. Recent advances in the transcriptional regulation of secondary cell wall biosynthesis in the woody plants. *Frontiers in Plant Science* **871**: 1–14.

Zhu A, Ibrahim JG, Love MI. **2019**. Heavy-tailed prior distributions for sequence count data: removing the noise and preserving large differences (O Stegle, Ed.). *Bioinformatics* **35**: 2084–2092.

8. Supplementary information

Fig. S 1 *Cork oak acorns after 1 to 2 months storage at 4ºC. Scale bar: 2cm*

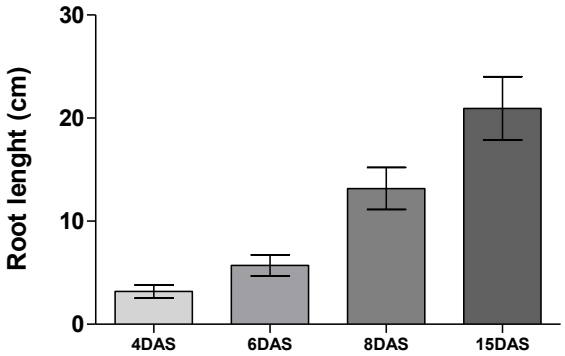

Fig. S2 *Cork oak tap root length measured at 4, 6, 8 and 15 days after sowing (DAS). Plot represents mean tap root length ± standard deviation (4DAS: n=8; 6DAS: n=16; 8DAS: n=20 ;15 DAS: n=19).*

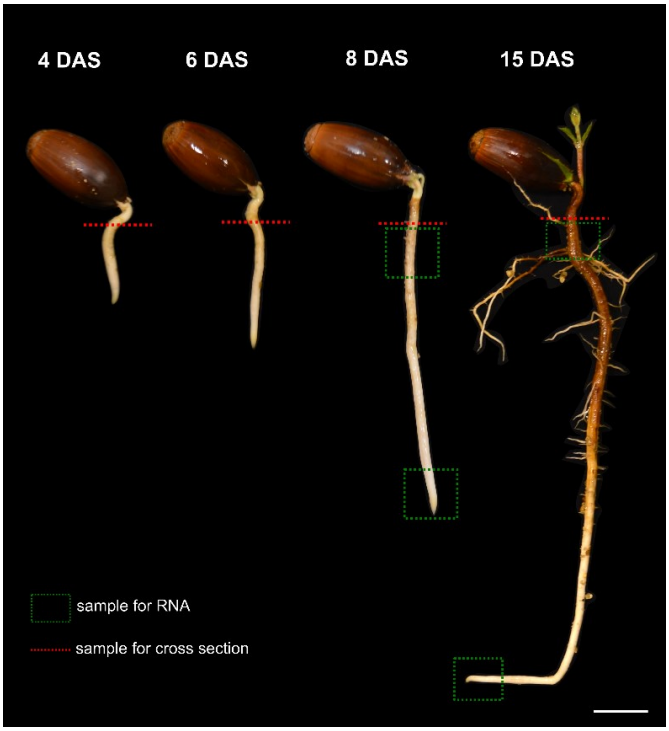

Fig. S3 *Representative cork oak seedlings at 4, 6, 8 and 15 DAS. For histological studies, ±0.5 cm segments of mature zone (SD) of root were collected (red dash lines). For RNA extraction, roots were segmented in two different zones (green dashed-squares) - 1cm bellow root collar (SD) and 1cm from root tip (PD) - and snap frozen in liquid N_2. Scale bar: 2 cm.*

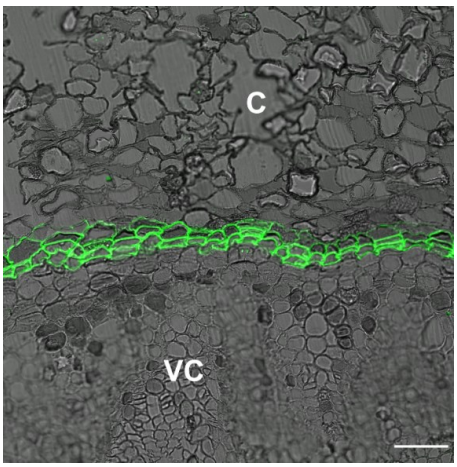

Fig. S4 *Cell-wall suberization in mature zone (SD) of cork oak tap roots at 3 weeks of growing. c: cortex; vc: vascular cylinder. Scale bar: 50 µm.*

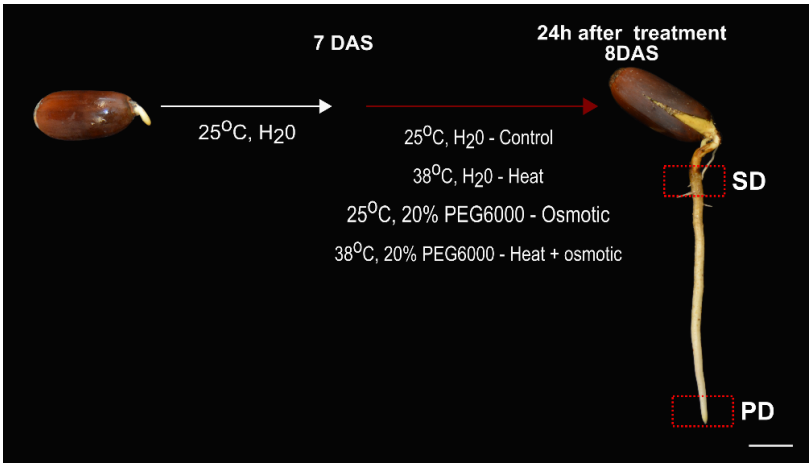

Fig. S5 *Representation of the different growth conditions and root developmental zones targeted in the present study. Acorns were sown and grown for 7 days at 25ºC and further exposed to different growth conditions - heat, osmotic, heat + osmotic and mock (control). Roots segments were collected from two different zones (red dashed-squares) – 1 cm below root collar (SD) and 1cm from root tip (PD). Scale bar: 2 cm*

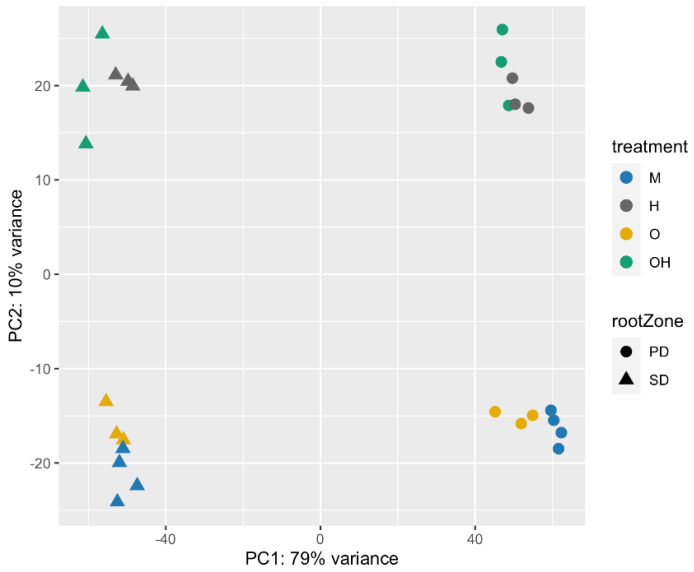

Fig. S6 *Principal component analysis (PCA) of the multiple RNA-seq libraries obtained for cork oak roots from two regions of the tap root (SD and PD) and exposed to different growth conditions (M-mock, H-heat, O-osmotic, OH – combined osmotic and heat) for 24h.*

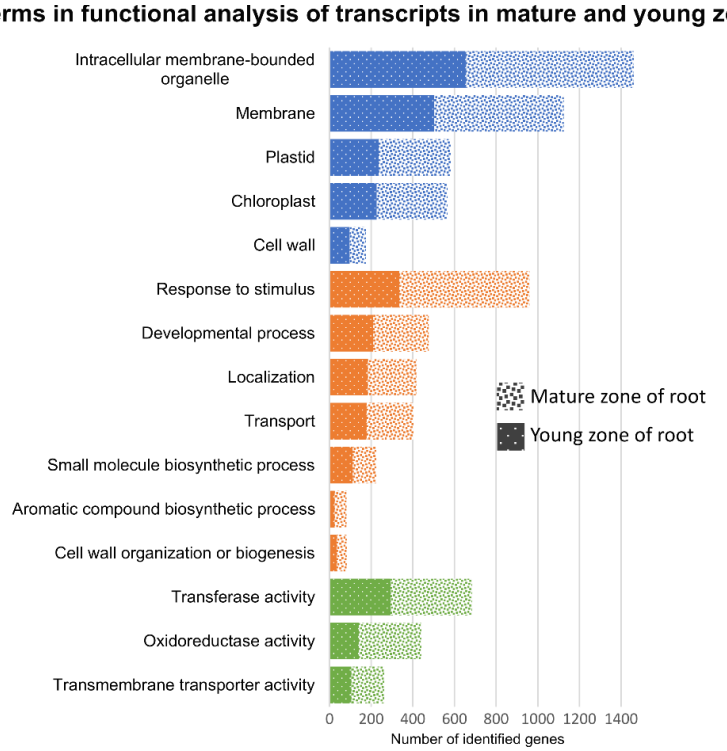

Fig. S7 *Representative GO terms significantly enriched from DEGs of both SD and PD zones of cork oak roots. Coloured bars represent the total number of genes in annotated for each represented GO term for Cellular Component (blue), Biological Process (orange) and Molecular Function (green) in mature and young cork oak root zone.*

(a)

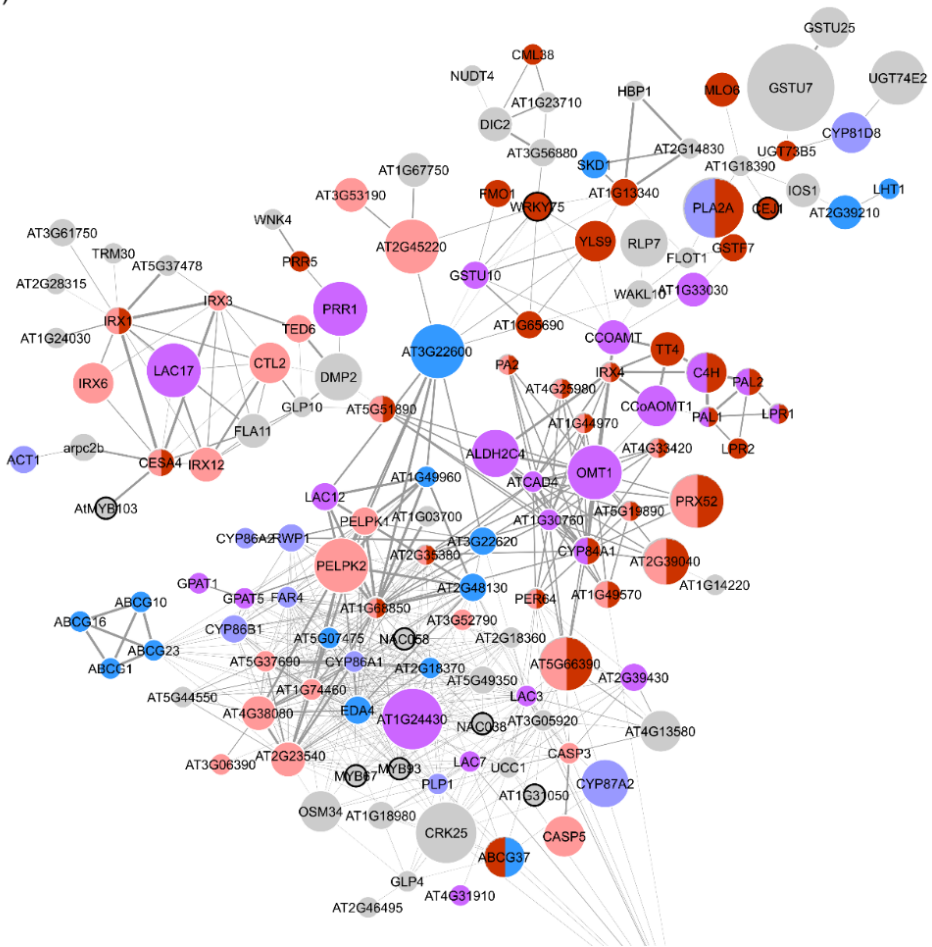
GSTU25
CML38
NUDT4
AT1G23710
HBP1
MLO6
GSTU7
UGT74E2
DIC2
CYP81D8
AT3G56880
AT2G14830
UGT73B5
SKD1
AT1G18390
AT1G67750
AT3G53190
RMO1
AT1G13340
PLA2A
IOS1
LHT1
WRKY75
CEJ1
AT2G39210
WNK4
AT3G61750
AT2G45220
YLS9
RLP7
GSTF7
TRM30
PRR5
FLOT1
AT5G37478
GSTU10
AT2G28315
WAKL10
AT1G33030
IRX3
PRR1
IRX1
AT1G65690
CCOAMT
AT1G24030
TED6
AT3G22600
TT4
LAC17
CTL2
PA2
IRX4
C4H
PAL2
IRX6
DMP2
AT4G25980
CCoAOMT1
GLP10
AT5G51890
PAL1
LPR1
AT1G44970
FLA11
ALDH2C4
AT4G33420
LPR2
arpc2b
ACT1
CESA4
IRX12
OMT1
AT1G49960
ATCAD4
LAC12
PRX52
AtMYB103
PELPK1
AT1G03700
AT5G19890
AT1G30760
CYP86A2
RWP1
AT3G22620
AT2G35380
CYP84A1
AT2G39040
PELPK2
AT1G14220
GPAT1
AT2G48130
ABCG10
GPAT5
FAR4
PER64
AT1G49570
AT1G68850
ABCG16
AT3G52790
CYP86B1
AT5G07475
NAC058
AT2G18360
ABCG23
AT5G37690
CYP86A1
AT2G18370
AT5G66390
AT2G39430
ABCG1
AT5G49350
AT5G44550
AT1G74460
LAC3
AT4G38080
EDA4
AT1G24430
NAC038
AT3G05920
AT4G13580
AT3G06390
AT2G23540
CASP3
MYB87
MYB93
LAC7
UCC1
PLP1
CYP87A2
AT1G31050
OSM34
AT1G18980
CRK25
CASP5
ABCG37
GLP4
AT4G31910
AT2G46495

(b)

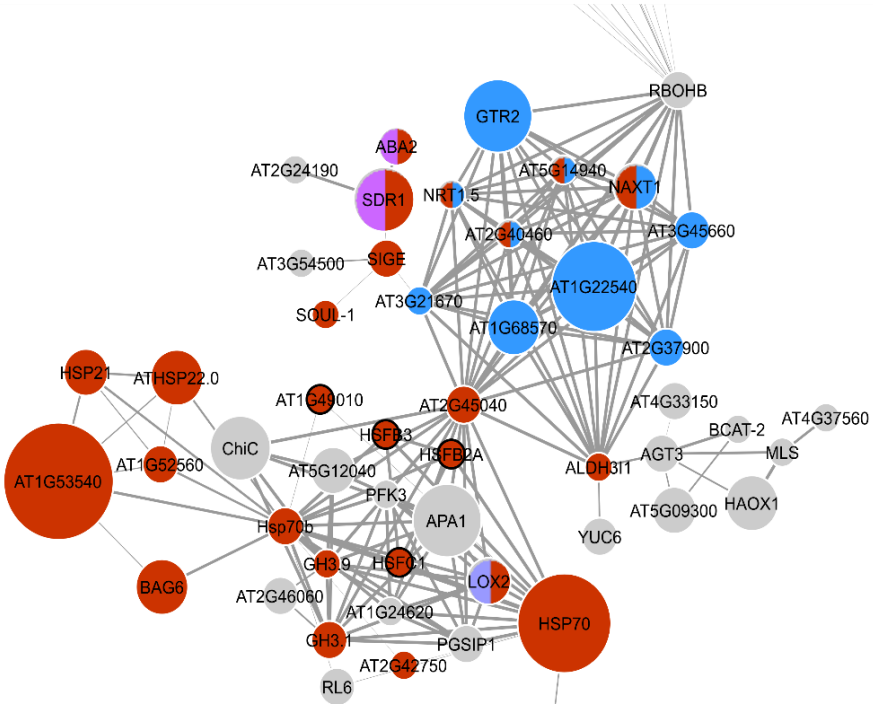
RBOHB
GTR2
ABA2
AT2G24190
SDR1
AT5G14940
NAXT1
NRT1.5
AT2G40460
AT3G45660
AT3G54500
SIGE
AT1G22540
AT3G21670
SOUL-1
AT1G68570
AT2G37900
HSP21
ATHSP22.0
AT1G49010
AT2G45040
AT4G33150
AT4G37560
BCAT-2
HSFB3
ChiC
AGT3
MLS
AT1G53540
AT1G52560
HSFB2A
AT5G12040
ALDH3I1
PFK3
AT5G09300
HAOX1
APA1
Hsp70b
YUC6
GH3.9
HSFC1
BAG6
LOX2
AT2G46060
HSP70
AT1G24620
GH3.1
PGSIP1
AT2G42750
RL6

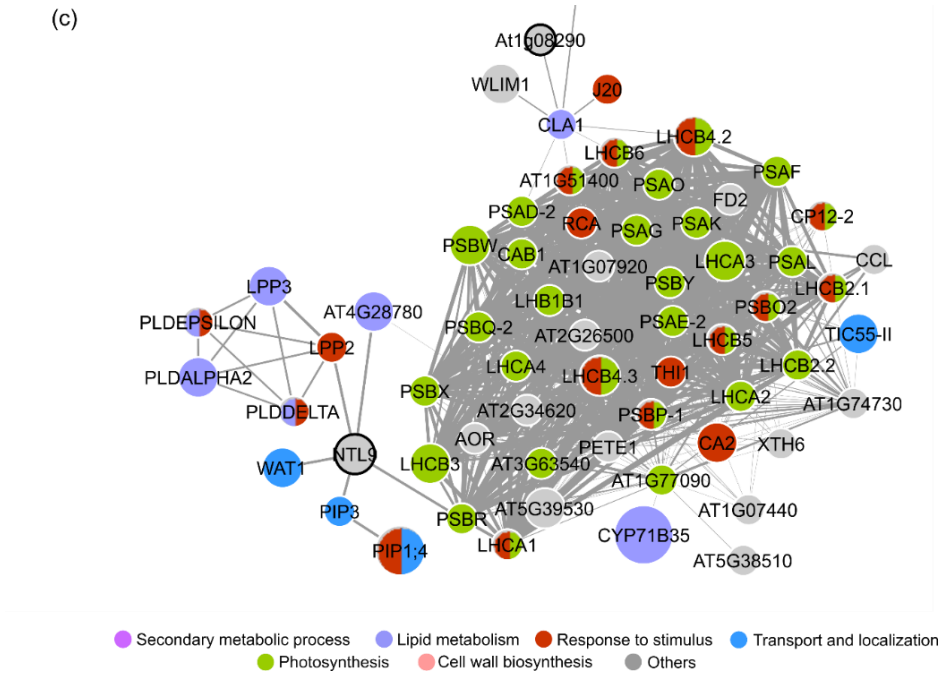

Fig. S 8 *Detailed representation of the network represented in Figure 6, highlighting the 3 main clusters from the network representation of predicted protein-protein interactions for Arabidopsis homologues representing the DEGs in mature zone of cork oak root (FC>-4). Protein identifiers are attributed to each network node to cluster 1 (a), cluster 2 (b) and cluster 3 (c). Node size corresponds to the number of cork oak genes associated to the same Arabidopsis homologue and edge thickness represents the confidence value for each association. Fill colour represent general functions or processes annotated to each gene product. Nodes with black border represent TFs.*

Supplemental tables are available by request to the corresponding authors or at:

https://drive.google.com/drive/folders/1ABrAUi7o5UmoANWPgWRaDLyciSfpympU?usp=sharing

Chapter V

Heat and Osmotic stresses have contrasting effects on cell-wall suberization and secondary development in cork oak roots

Ana Rita Leal[1,2,3], Pedro M. Barros[1]*, Helena Sapeta[1], Joana Belo[1], Diogo Lucas[1], Tom Beeckman[2], M. Margarida Oliveira[1]*

[1] Instituto de Tecnologia Química e Biológica António Xavier, Universidade Nova de Lisboa (ITQB NOVA), GPlantS, Av. da República, 2780-157 Oeiras, Portugal;

[2] Ghent University, Department of Plant Biotechnology and Bioinformatics, Technologiepark 71, 9052 Ghent, Belgium

[3] VIB Center for Plant Systems Biology, Technologiepark 71, 9052 Ghent, Belgium

* co-corresponding authors

Table of Contents

1. Summary

Cork outer bark is an important forest-based material, with valuable physical properties and lately seen as an eco-friendly material. Most cork properties rely on phellem (cork cells) tissue organization in compact cell layers and the intense cell wall suberization. For breeding high-quality cork material, particularly in the context of climate changes, it is important to understand how the fluctuating environment affects the development of cork. With this in mind, we used young cork oak roots to study the development and suberization of phellem cells under contrasting environmental conditions. Root development, suberized-cell pattern, and suberin-related gene expression were monitored in a targeted root zone undergoing secondary development (SD), throughout independent and combined osmotic and heat stress treatments. Early at 24h after treatment initiation, a positive effect of osmotic stress (over mock, heat, and combined stress) was detected by the upregulation of suberin biosynthesis genes, which was later supported by the detection of a higher number of suberized cells in the SD zone. On the opposite, a negative effect of heat and combined heat and osmotic stress was detected on phellem growth and suberization. To further understand the detected morphologic effects, a targeted transcriptomic analysis on the tissues undergoing SD was performed in the early time point, having a special focus on putative pathways regulating cell wall components. Our work provides an integrated view on the molecular pathways regulated under contrasting conditions, which may further support the design of science-based strategies to promote cork growth.

2. Introduction

Forest-based materials, including non-wood products such as cork, are key raw materials with high added-value properties (‘APCOR - Associação Portuguesa de Cortiça’). Cork oak forests are emblematic resources in the

Mediterranean region, having high economical, ecological and social significance, due to the sustainable exploitation of its outer bark. Cork cells (phellem) derived from the phellogen (or cork cambium), and accumulate along secondary growth, in stems, branches and roots. After phellogen division, phellem cells undergo several differentiation steps, which include massive cell wall suberization, cell expansion and programmed cell death (Evert, 2006; Crang *et al.*, 2018). The structure and chemical composition of cork oak phellem cell walls determines its physical properties, and consequently its suitability for multiple industrial applications (Pereira, 2007, 2013, 2016; Lauw *et al.*, 2018).

In cork oak, phellogen displays a uniquely long lifespan, being fully regenerated after cork removal. Phellogen activity is seasonally regulated and multiple evidence highlights a direct impact of environmental factors. In fact, cork outer bark rings have engraved signals of the direct effect of precipitation and temperature, correlating high phellogen activity with previous year winter or spring precipitation (Caritat *et al.*, 2000; Costa *et al.*, 2002; Oliveira *et al.*, 2016). High temperature showed a negative effect particularly in late summer (Caritat *et al.*, 2000). The cork cellular structure is also prone to environmental regulation, as cork developed after drought events shows not only thinner cork rings, but also smaller cells (Pereira *et al.*, 1992).

Cork cell walls are highly enriched in suberin (Silva *et al.*, 2005), a complex biopolymer composed of different aliphatic and aromatic domains (Graça, 2015), also found in other cellular layers including root endodermis (Andersen *et al.*, 2015; Doblas *et al.*, 2017; Barberon, 2017) and bundle sheath cells (Mertz & Brutnell, 2014; Fakult, 2020). In the endodermis, the suberization process is induced by numerous external factors, such as drought (Franke *et al.*, 2009; Lee *et al.*, 2009; Yadav *et al.*, 2014; Kreszies *et al.*, 2019), salt (Kosma *et al.*, 2014; Yadav *et al.*, 2014), or ABA treatments (Kosma *et al.*, 2014; Barberon *et al.*, 2016). In these situations,

higher accumulation of suberin is described as a physical barrier, protecting the plant from water loss as well as excluding the transport of toxic ions across root cell layers (Doblas *et al.*, 2017; Barberon, 2017). Evidence of positive transcriptional regulation of suberin biosynthesis via ABA were detected in a variety of species and tissues, including *Arabidopsis* roots (Efetova *et al.*, 2007), potato tubers (Boher *et al.*, 2013), tomato fruit (Leide *et al.*, 2012), and kiwifruit (Han *et al.*, 2019). The external application of ABA was able to induce not only genes directly involved in suberin synthesis, as *GPAT5* (Barberon *et al.*, 2016), *FHT* (Boher *et al.*, 2013) or *ABCG6* (Yadav *et al.*, 2014), but also the suberin-associated transcription factor *MYB41* (Kosma *et al.*, 2014). In addition, the blocking of ABA biosynthesis (by fluridone, an inhibitor of de novo ABA biosynthesis), significantly reduced the accumulation of suberin detected in wound-healing in potato tubers (Lulai *et al.*, 2008) and tomato fruit (Leide *et al.*, 2012). Interestingly wound phellem suberization was also characterized in kiwifruit, where ABA induces *AchnMYB41*, *AchnMYB107*, and *AchnMYC2*, which further activate suberin biosynthesis genes of *AchnFAR*, *AchnFHT* and *AchnCYP86A* (Wei *et al.*, 2019, 2020). Although the molecular mechanisms of ABA-mediated suberization are not yet determined, some evidence points for the possible involvement of Snf1-RELATED KINASES2 (SnRK2s). Upon ABA signal, activated SnRK2s phosphorylate and activate target proteins, including ABF transcription factors (TFs) (Fujita *et al.*, 2009). Interestingly, in *Arabidopsis,* the expression induction of *MYB41* and *ASFT* after an ABA treatment was impaired in the *abf1/2/3/4* quadruple mutant (Yoshida *et al.*, 2015), suggesting the involvement of SnRK2s and ABFs in the suberization response. In addition, suberization in *Arabidopsis* roots was shown to be a highly flexible process, being also detected to be reduced through ethylene-mediated regulation (Barberon *et al.*, 2016; Barberon, 2017). Whether this regulation can be extended to phellem is still not known.

Considering that the Mediterranean region is a predicted hotspot for climate change, with intensification of extreme temperatures and decreased precipitation during the warm season, it is of extreme importance to identify genetic modulators of cork oak development in those conditions, in order to predict the impact on cork production. So far, only a limited number of studies have focused on the molecular regulation of the response to drought or heat stress in cork oak. Transcriptomic analysis of lateral roots from plants exposed to long-term drought conditions highlighted a conserved regulation of known components of the ABA-dependent signalling network involving ABF TFs (Magalhães *et al.*, 2016). In young stems, the expression of a MYB TF with a suggested role in lignification and suberization (Capote *et al.*, 2018) was also found upregulated under drought but downregulated upon temperature increase (Almeida *et al.*, 2013). To further describe the effect of drought and heat stress in cork oak, we performed a morphophysiological and transcriptomic analysis in taproots, with a particular focus on secondary development and phellem differentiation. Taproots of germinated acorns were selected as a model system given their fast growth and easy manipulation. Our studies also detected phellogen activity one week after sowing, allowing expeditious characterization in different growth conditions (Chapter IV). The comparative analysis of the transcriptomes of contrasting developmental regions of the root under osmotic, heat and combined stresses unveiled multiple molecular pathways and genes contributing for the observed morphologic alterations. The data presented here may contribute to understand better the molecular regulation of suberization and cork development, particularly under environmental stresses conditions.

3. Material and Methods

Plant material and seed storage

Half-sibling *Quercus suber* acorns were collected from a field-grown tree located in Alcochete (Portugal, Lat. 38.747491; Long. -8.931877) in November 2017, 2018 and 2019. Acorns were submerged in tap water to identify and remove floating or damaged acorns, and any residual debris. thereafter, acorns were transferred to a 45ºC water bath for 2 hours (h). Finally, acorns were surface dried, and the excess moisture was removed in a 30ºC chamber for 24h. Acorns were kept in plastic bags and stored at 4ºC until further use.

Growth conditions, root sampling and measurements

Seeds were sown on a mixture of sand and vermiculite (1:1) at 100% field capacity in 700ml pots (1/pot) and maintained in 12h/12h day/night photoperiod (light intensity 400 µmol m^{-2} s^{-1}) at 25ºC/20ºC. Pots were covered with saran wrap with poked holes to limit water evaporation and seeds were kept in these conditions for 7 days without re-watering. After this period, seedlings were exposed to contrasting growth conditions, as described in Chapter IV.

Osmotic and combined Heat and Osmotic (H+O) treatments were conducted in 2017 and 2018, while Heat treatments were conducted in 2018 and 2019. Mock treatments were conducted every year. This was performed in order to increase biological representation.

Sampling was performed 24h (8 DAS) and 1 week after stress imposition, in taproot segments collected from 2 contrasting development zones, namely: the secondary development zone (SD), taken 1 cm below root collar; and primary development zone (PD), including the root tip (Fig. **S1**). For RNA extraction, 1 cm root segments were collected and frozen in liquid N_2. Each sample corresponded to a pool of segments collected from 4-5 root seedlings, and 3-4 pools were collected per treatment (biological

replicates). For microscopy observations, segments of 0.5 cm were collected immediately above the regions collected for RNA extraction.

Photographs of cork oak seedlings were always taken before harvesting samples for transcriptomic and microscopic analysis. Root length measurements were taken from each photograph using FIJI (Schindelin *et al.*, 2012). Differences in total root length between treatments were assessed using the Kruskal-Wallis test, followed by Dunn's multiple comparison test.

Microscopy

Root samples were fixed in 1% formaldehyde and 4% glutaraldehyde solution (in 0.1M phosphate buffer, pH 7.2) and subjected to sequential dehydration with increasing EtOH concentrations [30%, 50%, 70%, 85% and 96% (twice) (v/v)] and further embedded in Technovit 7100 resin (Heraeus Kulzer, Wehrheim, Germany). Semi-thin sequential sections (5-10 µm thick) were obtained with a microtome (Leica RM2235), transferred to water droplets on glass slides and dried (37ºC - 40ºC, 5-10 min) for complete adhesion to the glass.

Fluorol Yellow (FY) staining was performed according to Brundrett *et al.*, 1991 with minor modifications. Briefly, glass slides with cross sections were incubated in a freshly prepared solution of 0.01% (w/v) FY (Santa Cruz Biotechnologies) in 80% lactic acid (v/v) at 60 °C for 30 min. The sections were then counter-stained with 0.5% Aniline Blue (w/v) for 30 min in darkness, washed 3x 5min in water at room temperature and mounted on 50% glycerol. Observations were performed using a Zeiss 880 confocal microscope. The number of FY-stained cells was counted in the 3D maximum projection figures obtained with Z-stack images. To calculate the FY-stained cell ratio, the number of FY-stained cells was divided by the length of the captured FY-stained layer, measured in the same picture.

RNA extraction

Frozen root samples were ground with a mortar and pestle and RNA extraction was performed according to Reid *et al.*, 2006 with minor modifications: extraction buffer included 2% w/v CTAB, 1.4 M NaCl, 20 mM EDTA (pH 8), 100 mM Tris-HCl (pH 8), 1% w/v PVP40, and 2% v/v β-mercaptoethanol; after selective precipitation of the RNA with 0.3 vol of 8 M LiCl, pellets were washed with ice cold 70% EtOH and dissolved in 50 µL nuclease-free mili-Q water, followed by DNAse treatment using TURBO™ DNase (ThermoFisher Scientific). RNA quality was evaluated by electrophoresis in agarose gels and quantified by NanoDrop ND-1000 spectrophotometer.

Gene expression analysis

For quantitative PCR analysis, first strand cDNA synthesis was performed using 1 µg total RNA with an oligo-dT primer using Transcriptor High Fidelity cDNA Synthesis Kit (Roche), according to the manufacturer's instructions. The cDNA was diluted and used as template for amplification by qPCR using gene-specific primers (listed on Table **S1**). The Elongation factor (LOC112038967) was used as internal control. Real Time qPCR was performed in a Lightcycler 480 (Roche), using Lightcycler 480 Master I Mix (Roche). Amplification reactions were performed in triplicate for each cDNA sample. Target transcript abundance was calculated according to Pfaffl, 2001.

Transcriptome sequencing

RNA-seq was performed using total RNA collected from control and stress conditions, 24h after treatment, PD and SD root segments (with 3-4 biological replicates). RNA was quantified using Qubit™ RNA BR Assay Kit (ThermoFisher Scientific, MA, USA) and RNA integrity was assessed with Fragment Analyzer (Agilent, CA, USA). cDNA synthesis was performed using 10ng total RNA and using an optimized SMARTSeq2 protocol. cDNA-libraries from each sample were equimolarly pooled and sequenced

on Illumina NextSeq 500 instrument (v2.5, High Output, 75 bp, Single Reads). cDNA libraries preparation and sequencing were performed at the IGC Genomics Unit (Oeiras, Portugal). The sequencing data and corresponding metadata were deposited on the National Center for Biotechnology Information (NCBI) Short Read Archive and BioSample databases, under the BioProject PRJNA690098.

Bioinformatics analysis

FASTQ files were analysed before and after quality trimming using FastQC v0.11.8 (https://www.bioinformatics.babraham.ac.uk/projects/fastqc/). Trimming of adapters and low quality bases was performed using Trimmomatic v0.39 (Bolger *et al.*, 2014) with single-end mode and additional parameters: LEADING:3, TRAILING:3, SLIDINGWINDOW:4:15, MINLEN:36. High-quality reads were mapped on the *Q. suber* reference genome CorkOak1.0 (GCF_002906115.1) (Ramos *et al.*, 2018) using STAR v2.7.0f_0328 (Dobin *et al.*, 2013), with modified parameters (twopassMode=Basic, alignIntronMax=100000) and read counts per gene were further obtained using featureCounts v1.6.4 (Liao *et al.*, 2014). Differential expression analysis was conducted using the DESeq2 package (Love *et al.*, 2014) in R v.3.6.2 (R Foundation for Statistical Computing., 2018). Principal component analysis (PCA) was conducted using normalized counts of the 1000 genes showing the highest variance. Statistical analysis was conducted using a multifactorial design (~ root_zone + root_zone:treatment) and the '*apeglm'* algorithm (Zhu *et al.*, 2019). Differentially expressed genes (DEGs) between control and stress conditions (in PD and SD) were filtered based on fold-change |FC| > 2 (|log2FC| > 1) and adjusted p-value (padj) < 0.1. Candidate *A. thaliana* orthologs were determined using Blastp searches of cork oak predicted amino acid sequences on TAIR10 (Araport11) predicted proteins.

Gene Ontology (GO) functional enrichment was performed with ClueGo plugin for Cytoscape version 3.7.1 (Bindea *et al.*, 2009) using unique Arabidopsis homologues attributed to cork oak DEGs.

4. Results

Stress treatments affect the cork oak root growth and development

One-week old cork oak seedlings were subjected to distinct growth conditions, including Mock, Heat, Osmotic and H+O regimes. Aiming to follow root development under these conditions, cork oak seedlings were collected and analysed 24h and one week after treatment initiation. Cork oak seedlings collected 24h after stress initiation showed no visible morphological effects from the treatments (Fig. **S1a**), although some differences were detected in root length between the combined H+O treatment and the isolated stresses (Fig. **S1b**). At this time point, cork oak root seedlings showed an evident colour gradient, ranging from white/beige in the root tips to brown below the collar region. Also, development of lateral roots (LRs) and shoots was visible in some seedlings, independently of the growth conditions (Fig. **S1a**). At 1 week after treatment initiation, seedlings grown under Heat and H+O treatments showed notable morphologic differences when compared with Mock-treated seedlings (Fig. **1a**).

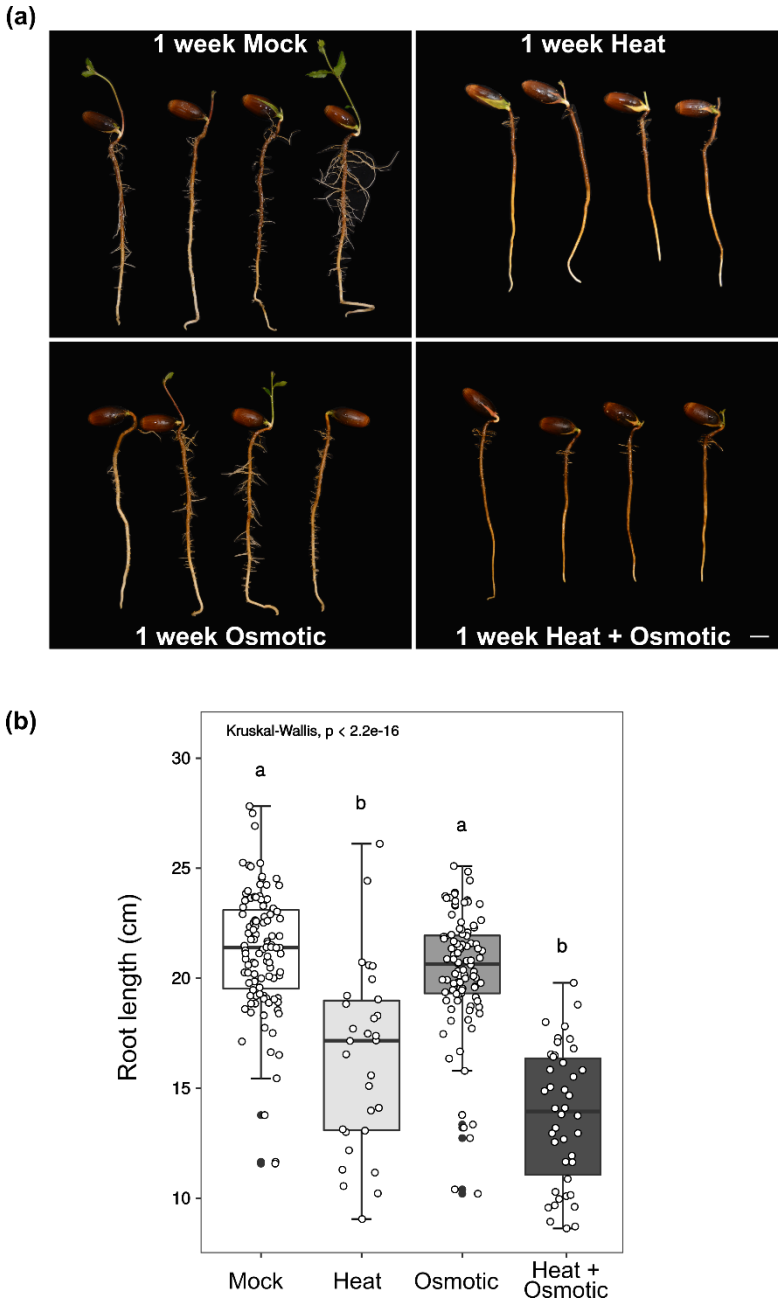

Fig. 1 *(a) Representative cork oak seedlings one week after application of Mock , Heat, Osmotic and combined Heat and Osmotic treatments. Scale bar: 2 cm. (b) Cork oak taproot length measured one week after application of different treatments. Box plots represent length distribution for n > 20 roots (Mock: n=107; Heat: n=30; Osmotic: n=100; Heat and Osmotic: n=42). Different lower-case letters represent statistical significance (p < 0.05) determined using Kruskal-Wallis test followed by Dunn's Multiple Comparison test.*

Heat and H+O treatments lead to a significant decrease in mean taproot length (Fig. **1b**), with a stronger negative effect in H+O, when compared with Mock. In these conditions, tap roots were also darker near root tips, particularly in H+O, and showed an overall impairment of LRs development (Fig. **1a**). In turn, Osmotic- and Mock-treated seedlings showed similar phenotypes, with a dark brown area towards root collar, and development of LRs along the tap root (Fig. **1a**). Also, some seedlings from Mock and Osmotic groups showed advanced development of shoots and leaves and bent root tips (caused by growth constraints imposed by pot size) (Fig. **1a**). Together, these results showed an evident effect of Heat stress on general root morphology and development. The effect of Osmotic stress was only suggested by the differences found between Heat in H+O groups.

Stress treatments affect the cell-wall suberization in SD root

During root primary development, the endodermis is established as a single suberized cell layer that delimits the stele. After the onset of secondary development, the root phellogen layer is established immediately below endodermis (Crang *et al.*, 2018). While in *Arabidopsis*, the new developed phellem layer replaces endodermis (Wunderling *et al.*, 2018; Chapter II), our studies in cork oak root revealed the co-occurrence of phellem and endodermis (Chapter IV). To evaluate the impact of each stress treatment on these suberized barriers, we conducted histological observations in root zones undergoing secondary (SD) and primary development (PD) at 1 week after treatments. In the SD zone, Mock treated plants showed mostly one, and occasionally 2, layers of suberized cells (Fig. **2a**; **S2**), indicating the presence of endodermis and phellem cells. The endodermis layer is represented as the round-shaped cells, with a fainter FY signal and in direct contact with the cortex cells.

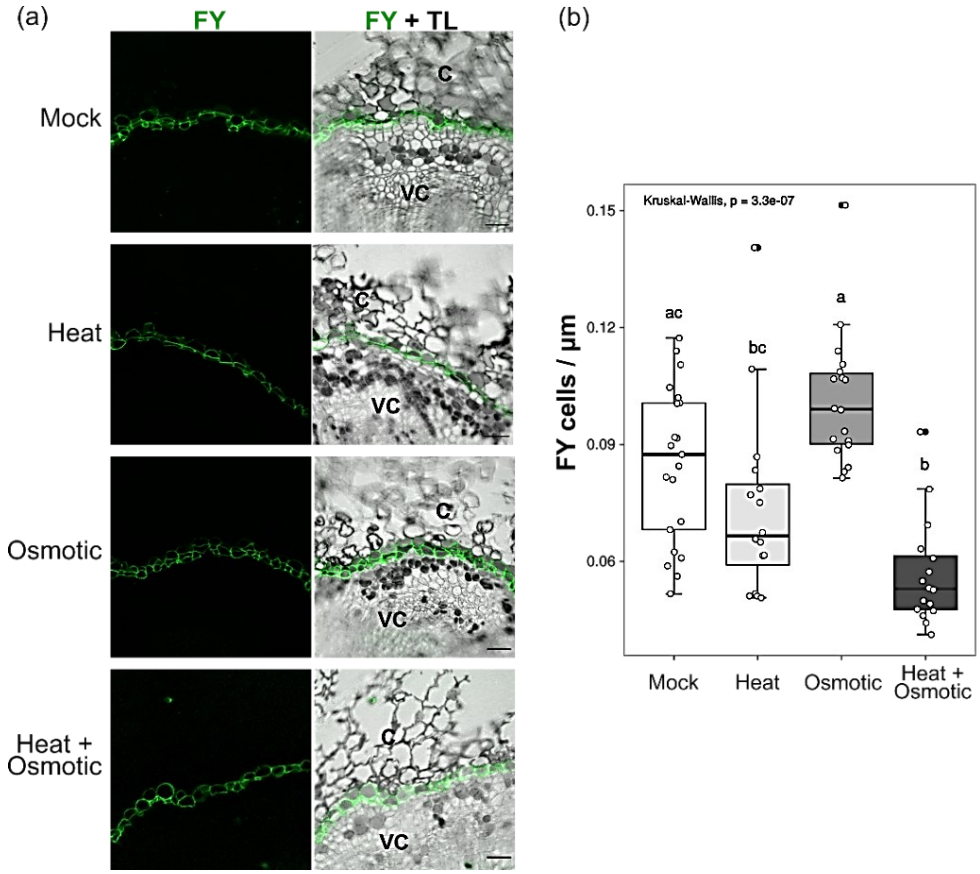

Fig. 2 *(a) Cell-wall suberization in the SD zone of cork oak tap roots (1 cm below root collar), analysed one week after Mock, Heat, Osmotic, and combined Heat and Osmotic treatments. Cross sections were stained with FY. Images are representative of 4 independent experiments. C: cortex; VC: vascular cylinder; TL: transmitted light. Scale bar: 50 µm. (b) Number of suberized cells (FY-stained) per length (µm) of suberized layer measured one week after the different treatments: Mock; Osmotic, Heat; Combined Heat and Osmotic. Number of suberized cells was counted in FY stained images and divided by the total length of the suberized layer on the correspondent picture. At least 5 seedlings from two independent experiments were analysed and 2-3 pictures were captured for each seedling in different regions of the root circumference (Mock: n=21. Heat: n=16. Osmotic: n=18. Heat and Osmotic: n=16). Different lower-case letters represent statistical significance ($p < 0.05$) determined using Kruskal-Wallis test followed by Dunn's Multiple Comparison test*

In turn, FY-stained cells located in the side of the vascular cylinder, with a flatten rectangular shape, are identified as phellem cells, in the initial stages of differentiation. The cell pattern of the suberized layer of SD zone in Mock was similar to the Heat and H+O-treated plants, with most of the analysed

roots displaying one row of suberized cells, interposed with occasional 2 suberized layers (Fig. **2a, S2**). Contrastingly, the SD zone from roots exposed to Osmotic treatment had additional suberized (FY-stained) cells, with flat rectangular shape (Fig. **2a, S2**). For a better estimation of the number of suberized cells developed under different treatments, we calculated the number suberized cells per length (μm) of the suberized layer (observed in the microphotographs) in multiple seedlings (Fig. **2b**). Interestingly, Osmotic treatment provided higher ratios of FY-stained cells/μm than the remaining groups, however this observation was not statistically significant, when compared to Mock (possibly due the high variability found in this condition). Contrastingly, a reduction in this parameter was observed for Heat and H+O-treated seedlings, confirming that less suberized cells are formed during these treatments (Fig. **2b**).

Given that stress treatments lead to changes in cell-wall suberization in the SD zone, we hypothesised that this effect could also be observed in the PD zone, particularly in developing endodermis. Therefore, root sections taken 1 cm above root tip were also targeted for FY staining. Although we were able to detect FY-stained cells in some sections, cell-wall suberization patterns were inconsistent between biological replicates of each treatment (Fig. **S3**). In some of the analysed roots we were able to detect suberization in one layer of cells between the vascular cylinder and the cortex, suggesting an early maturation of the endodermis (Fig. **S3a**, **i**, **I**). Yet, a pattern for early endoderm cell-wall suberization depending on the growth condition could not be confirmed.

Suberin biosynthesis genes are differentially regulated by heat and osmotic stress

To get a deeper view over the suberin biosynthesis pathway in response to the different growth conditions, we further evaluated the expression of several cork oak homologs of genes with demonstrated role in suberization. These included candidate genes involved in synthesis or transport of

suberin monomers - *QsCYP86A1*, *QsGPAT5*, *QsF5H*, *QsASFT*, *QsASFT-2* and *QsABCG6* - and two genes involved in the synthesis of suberin monomer precursors - *QsLACS* and *QsPAL*. This analysis was conducted for the distinct development zones of the root (PD and SD), at 24h and 1 week after treatment initiation.

In the SD zone, moderate changes in gene expression were observed 24h after stress application, particularly for *QsCYP86A*, *QsABCG6*, *QsASFT* and *QsASFT-2* (Fig. **3**). In comparison to Mock, Osmotic treatment induced the expression of *QsABCG6*, *QsASFT*, while Heat and H+O showed no significant effect. Expression of *QsASFT-2* decreased in H+O, particularly when compared to Osmotic treatment, but this difference was not significant in comparison to Mock. Additionally, significant downregulation of *QsCYP86A1* was detected in H+O relative to other treatments (Fig. **3**). One week after treatment initiation, differences in expression of suberin-related genes were mainly detected for *QsCYP86A1*, *QsF5H*, *QsGPAT5* and *QsASFT-2* (Fig. **3**). These genes showed a downregulation trend in Heat- and H+O-treated roots, yet only *QsGPAT5* expression was significantly reduced in combined H+O treatment, when compared with Mock (Fig. **3**). Interestingly, *QsCYP86A1*, *QsF5H*, and *QsASFT-2* mean expression was significantly different between Heat and Osmotic treatments. Additionally, no differences were detected between treatments for *QsLACS* and *QsPAL* in both time points. These results support the potential negative effect of Heat and H+O treatments in suberin biosynthesis, starting 24h after stress induction, in agreement with the lower number of suberized cells detected after 1 week (Fig. **2**). In parallel, the induction of specific suberin biosynthetic genes in Osmotic treatment agrees with the tendency for increased number of suberized cells (Fig. **2**).

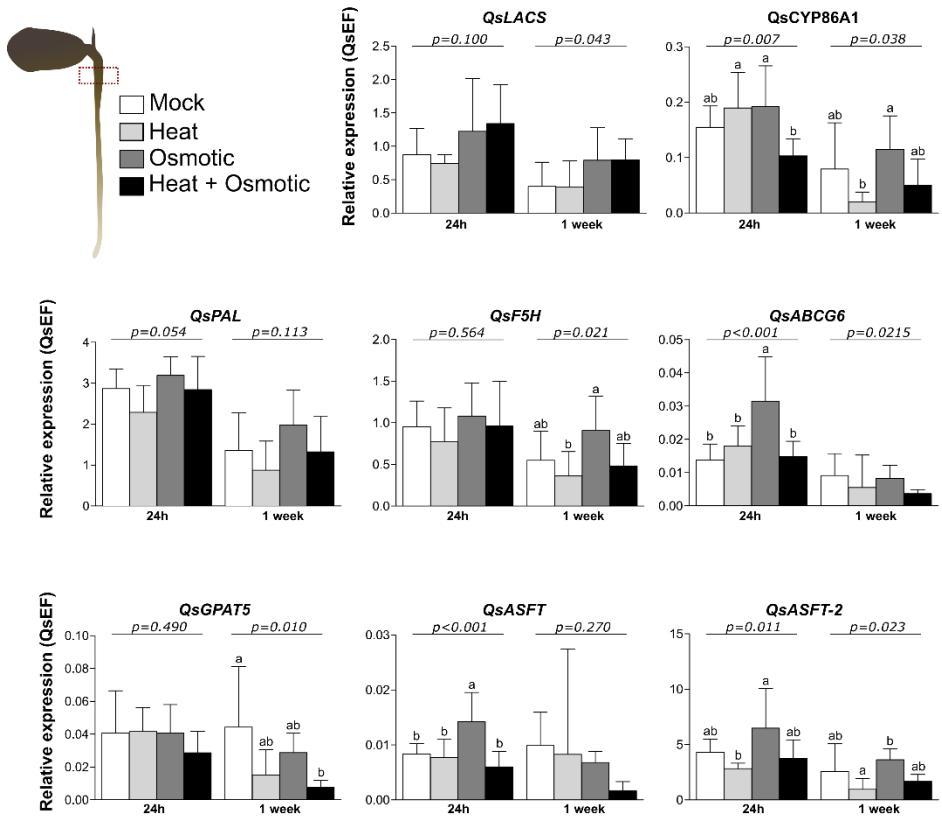

Fig. 3 *Relative expression of genes involved in the suberin biosynthesis and precursor pathways, after application of different treatments in the SD zone (1cm below root collar). Root segments were collected, at 24h and 1 week after treatment initiation, and gene expression of QsLACS, QsPAL, QsCYP86A, QsF5H, QsASFT-2, QsASFT, QsGPAT5 and QsABCG6 was analysed by RT-qPCR. Relative gene expression was determined using the QsEF as housekeeping gene. Mean expression ± standard deviation from two independent experiments is represented for each timepoint (M: n=13. H: n=7. O: n=8. H+O: n=8). Statistical significance between treatments for each timepoint was assessed using the ANOVA test. Different lower-case letters represent significant differences determined by Tukey's HSD test.*

In the PD zone, only genes involved in the synthesis of suberin monomer precursors *QsPAL* and *QsLACs* were transcriptionally active 24h after treatment initiation, although no significant differences were found between the different conditions (Fig. **4**). Expression of genes directly involved in the suberin biosynthesis was only detected in the PD zone 1 week after

treatment initiation (Fig. **4**). Interestingly, in this root zone, Osmotic treatment induced *QsABCG6*, *QsGPAT5* and *QsASFT* expression, when compared with Mock. A similar trend was also observed for *QsGPAT5* in Heat and H+O conditions.

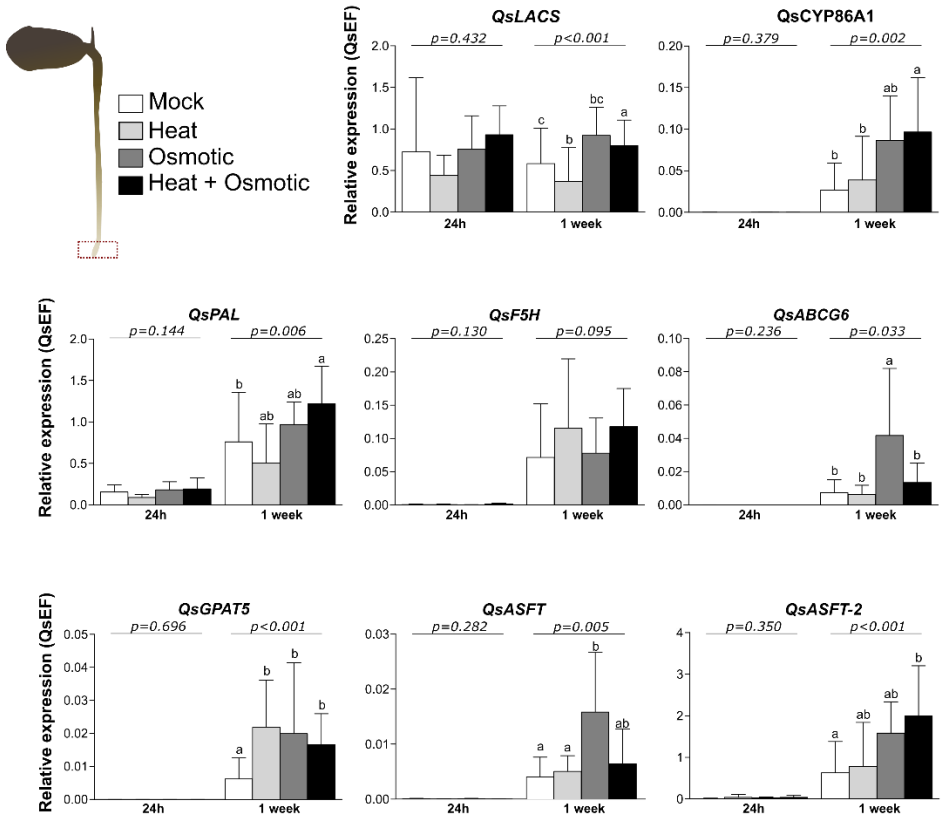

Fig. 4 *Relative expression of genes involved in the suberin biosynthesis and precursor pathways, after application of different treatments in the PD zone (1cm root tip). Root segments were collected, at 24h and 1 week after treatment initiation, and gene expression of QsLACS, QsPAL, QsCYP86A, QsF5H, QsASFT-2, QsASFT, QsGPAT5 and QsABCG6 was analysed by RT-qPCR. Relative gene expression was determined using the QsEF as housekeeping gene. Mean expression ± standard deviation from two independent experiments (. M: n=13. H: n=7. O: n=8. H+O: n=8) is represented for each timepoint. Statistical significance between treatments for each timepoint was assessed using the ANOVA test. Different lower-case letters represent significant differences determined by Tukey's HSD test.*

Moreover, H+O treatment also induced the expression of *QsCYP86A1*, *QsPAL*, and *QsASFT-2*, when compared to Mock conditions This analysis showed that specific genes related to suberin biosynthesis are differentially regulated by the imposed stresses, at different timepoints.

Differential transcriptomic response of SD and PD root zones after stress imposition

Although changes in cell-wall suberization in SD root zones were found 1 week after stress imposition, the changes in expression of key suberization genes (*QsASFT*, *QsABCG6* and *QsCYP86A1*) were already detected at 24h. Therefore, we used this time point for genome-wide transcriptomic profiling in order to identify early signal transduction pathways occurring in cork oak roots upon exposure to the different treatments.

A total of 713 million high quality reads were obtained, including the two root zones, four treatments and biological replicates (with an average of 27,430,387.46 single-end reads per library). The mean read mapping efficiency using the reference cork oak genome sequence and annotation was 67.93% ± 4.73. The effect of experimental variability on gene expression assessed by Principal Component Analysis (Chapter IV: Fig. **S8**), showed a consistent clustering of (biological) replicate libraries, and an overall display of samples strongly associated with root differentiation zones, represented along PC1 (79% of sample variance). Moreover, the different treatments had clear effects on sample clustering, particularly evident along PC2. Comparisons 'stress vs Mock' were further performed to assess the genome-wide transcriptomic changes occurring in response to stress for each root zone (Fig. **5**). Considering a |Log2FC| ≥ 1 and a p-adj ≤ 0.01 a total of 3666, 1500 and 2880 DEGs were detected respectively in Heat, Osmotic, and H+O treated samples, distributed between PD and SD zones (Fig. **5**; Tables **S2**, **S3**). In all the treatments, PD zone displayed the higher number of DEGs: 2201 for Heat stress, 1416 for Osmotic stress, and 2328 for H+O treatment (Fig. **5**; Tables **S3**). Considering the SD zone, Heat treatment imposed higher transcriptomic changes as compared with

Mock, with 2142 DEGs, followed by H+O with 1070 DEGs. Intriguingly, Osmotic treated plants showed the smallest alterations in SD zone, with only 122 DEGs (Fig. **5**; Tables **S2**).

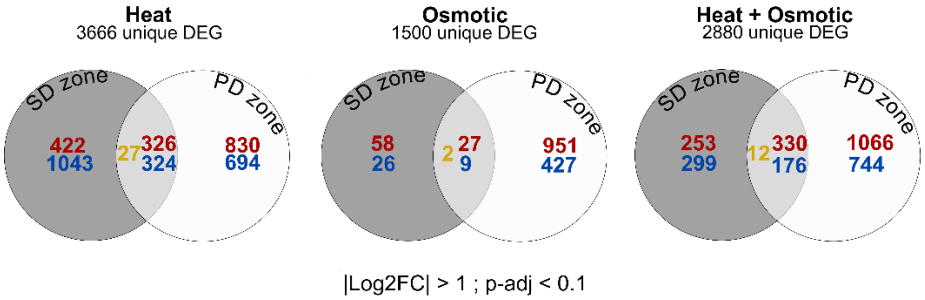

Fig. 5 *Venn diagrams representing common and unique DEGs found between the SD and the PD zones of cork oak tap roots, in response to Heat, Osmotic and combined Heat and Osmotic treatments. Upregulated DEGs are represented in red, downregulated DEGs in blue and common DEGs with opposite expression patterns are represented in yellow.*

In order to clarify the molecular mechanisms regulated by each treatment specifically during secondary development and contributing to the morphologic alterations detected in cell wall suberization and phellem development, we further selected the DEGs only found in the SD zone in the three 'stress vs Mock' comparisons (Fig. **5**; Tables **S2**, **S3**). To sort root zone specific from common DEG for each treatment, we intersected the DEG list of SD zone (Fig. **6**). Globally, Heat stress alone induced higher transcriptomic changes in SD, with the differential expression of 1257 exclusive genes, while Osmotic stress induced minor changes, with only 54 DEGs. In combined H+O treatment, 316 DEGs were exclusively regulated in the SD zone. Interestingly, this condition shared a higher number of DEGs with Heat (226 DEGs) than with Osmotic stress (24 DEGs). Only two genes were equally influenced by all treatments in SD zone, being both downregulated in comparison to mock (Fig. **6**): a

chaperone *QsDJC66* (LOC112037424) and a cysteine proteinase *QsALPHA-VPE* (LOC112015987).

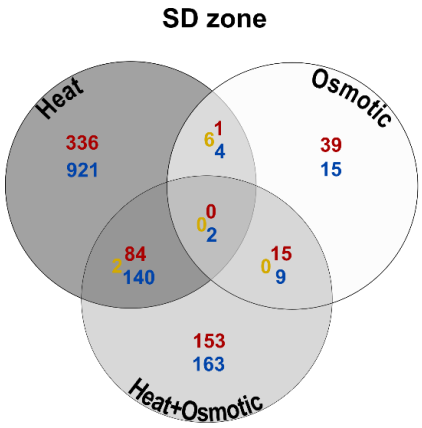

Fig. 6 *Venn diagrams representing common and unique DEGs found in the SD zone of cork oak tap roots in response to Heat, osmotic and combined Heat and Osmotic treatments. Upregulated DEGs are represented in red, downregulated DEGs in blue and overlapping genes with opposite expression patterns are represented in yellow.*

In order to validate the RNAseq analysis we selected 9 DEGs, selected based on their expression profile in the SD zone, and performed RT-qPCR using RNA samples obtained for all treatments, previously targeted for RNA-seq. The validation of the RNAseq data was assessed by determining the relative expression of each gene, and corresponding Log2FC ('stress vs Mock'). The Log2FC values determined by both approaches showed a strong linear correlation ($R^2 = 0.96$), thus validating the RNAseq expression estimates (Fig. **S4**)

Functional categorization of cork oak DEGs in roots after heat and osmotic treatments

For a general overview on the functional categories enriched in the previously determined DEGs we performed a GO term overrepresentation analysis based on the annotation of the corresponding *Arabidopsis*

homologs. DEGs with common expression patterns in both root zones (PD and SD) were analysed separately from root zone-specific DEGs. Considering our interest in cell wall suberization in the different development stages (PD and SD) we highlighted terms that can be correlated to cell wall modification or molecular regulation of development. Among the common DEGs found between SD and PD in response to Heat, we found an enrichment of 122 GO terms (Tables **S4A),** while 90 GO terms were enriched within common DEGs responsive to H+O treatment (Tables **S4C**). These two groups were particularly enriched in terms such as *Response to heat* (GO:0009408), *Cellular response to hypoxia* (GO:0071456) and *Heat shock protein binding* (GO:0031072). Similarly, we also found terms related to cell wall metabolism, including *Phenylpropanoid biosynthetic process* (GO:0009699) in Heat treatment, or *Lignin biosynthesis* (GO:0009809) in combined H+O treatment. Contrastingly, the common DEGs between both root zones found in response to Osmotic treatment only retrieved 2 enriched terms, Response to heat *(GO:0009408)* and *Defence response, incompatible interaction* (GO:0009814) (Tables **S4B**).

The DEGs exclusively found in the SD zone in response to Heat and H+O treatments, showed a significant enrichment of 408 and 78 GO terms, respectively (Fig. **7**; Tables **S5**). In both treatments, most GO terms are annotated to downregulated DEGs. The DEGs determined for Osmotic treated samples had an enrichment in 17 GO terms, mostly associated with genes upregulated by stress (Fig. **7**; Tables **S5B**)**.**

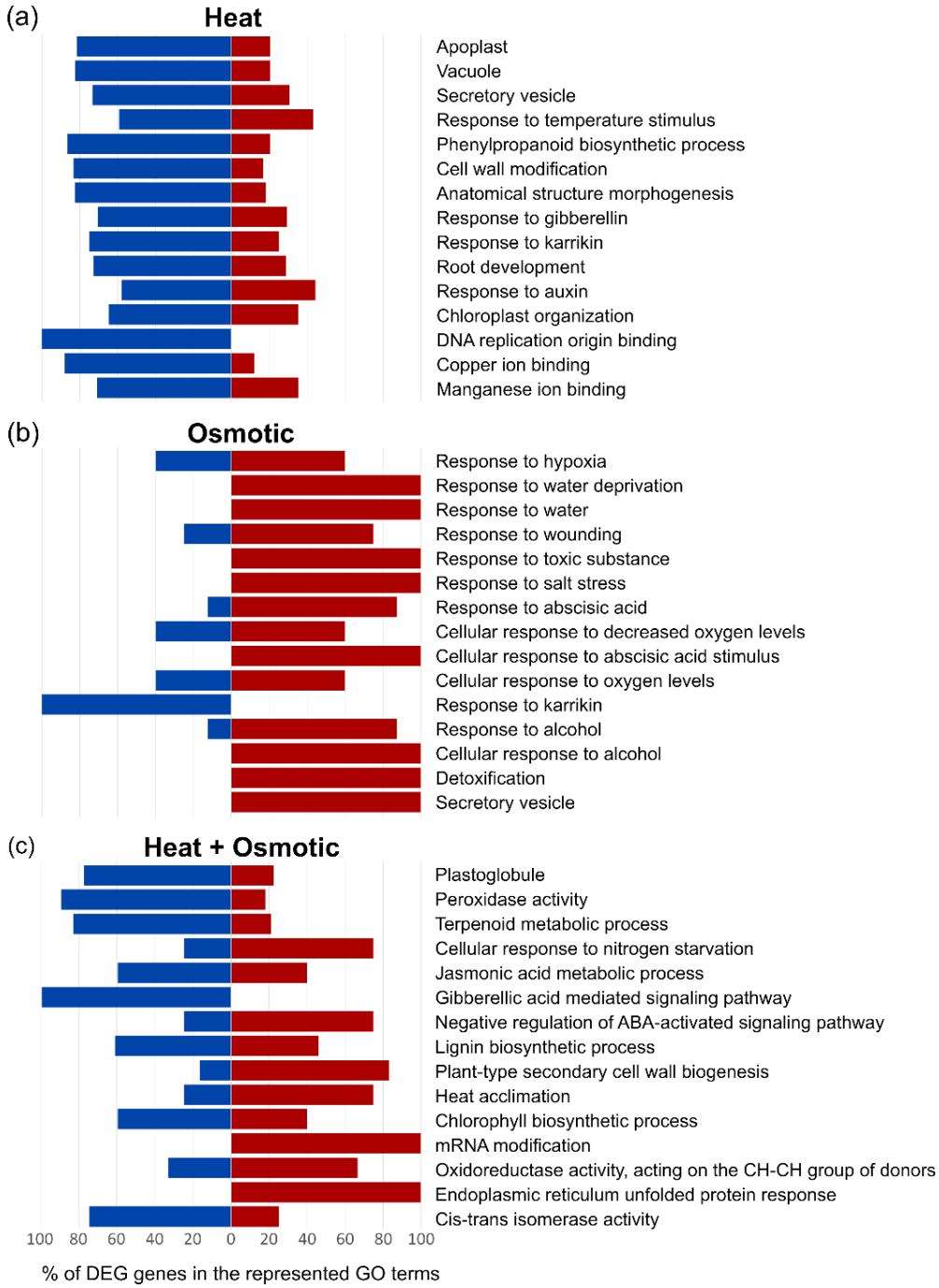

Fig. 7 *Representative GO terms significantly enriched in DEGs for SD zone of cork oak roots after 24h of Heat, Osmotic or combined Heat and Osmotic treatments. Coloured bars represent the percentage of upregulated (red) or downregulated (blue) genes enriched in each GO term.*

Multiple GO terms enriched in DEG groups from Heat and combined Heat and Osmotic treatments were related to cell wall metabolism, namely *Phenylpropanoid biosynthesis process* (*GO:0009699* in Heat) and *Cell wall modification* (*GO:0042545* in Heat) and *Lignin biosynthesis processes* (*GO:0009809* in H+O). Remarkably, no cell wall-related GO term was enriched in the DEGs determined for Osmotic treatment in this root zone. Responses to stimulus were also represented for all the applied stresses. In the Heat treatment we found *Response to temperature* (GO:0009266), *karrikin* (*GO:0080167), Gibberellin (GA) (GO:0009739)* and *Auxin* (*GO:0009733*). In turn, Osmotic treatment mostly regulated genes associated with *Response* to *hypoxia* (*GO:0001666*), *Water* (*GO:0009415*), *Wounding* (*GO:0009611*), *Salt* (*GO:0009651*), *Abscisic acid (ABA)* (GO:0009737) and *Response to karrikin* (GO:0080167). DEGs found that the combined Heat and Osmotic treatment DEG were enriched in terms related to hormone response, such as *Jasmonic acid metabolic process* (GO:0009694), *Gibberellin acid mediated signalling pathway* (GO:0009740) and *Negative regulation of ABA-activated signalling pathway* (GO:0009788).

In PD zone 235, 272 and 329 GO terms were enriched among DEGs determined for Heat, Osmotic and H+O treatments, respectively. For all the treatments, enriched GO terms were to a great extent associated with the higher proportion of upregulated DEGs found in this zone of the root (Fig. **S5**; Tables **S6**). Cell wall-related GO terms were identified in all stress treatments, including *Plant-type cell wall* (*GO:0009505* in Heat), *Cell wall biogenesis* (*GO:0042546* in Osmotic) and *Plant-type cell wall biogenesis* (*GO:0009832* in H+O). Moreover, several terms related to biosynthesis of cell wall polymers were also enriched, namely *Phenylpropanoid* (*GO:0009699* in all treatments) and *Suberin* (*GO:0010345* in Heat stress) *biosynthetic process*, as well as *Regulation of lignin biosynthetic process* (*GO:1901141* in Osmotic and H+O treatments). Also, diverse terms related

to hormone regulation processes are highlighted in the GO enrichment analysis. Among these, *Response to karrikin* is common to all treatments (*GO:0080167*), while *Response to auxin* is common to Heat and Osmotic treatments (*GO:0009733*). Equally, *Response to Ethylene* (*GO:0009723*) and *Gibberellin* (*GO:0009739*) were enriched in DEGs regulated by Osmotic stress, whereas *Response to salicylic acid* (SA) (*GO:0009751*) and ABA (*GO:0009737*) were enriched in H+O regulated DEGs. F

Regulation of genes associated with secondary development and cell-wall components throughout stress treatments in SD zone of roots

DEGs found exclusively in SD were analysed in more detail in the three conditions, aiming to identify molecular mechanisms contributing to the alterations in cell wall suberization and phellem development. Concerning genes directly associated with secondary development and cell wall modifications, an overall tendency for downregulation was evident in the Heat treatment. These included genes involved in secondary metabolic processes and developmental factors related to the secondary vascular development and morphogenesis (xylem and phloem), particularly *QsMYB83* (*LOC112038777*), *QsKNAT1* (*LOC112015571*), *QsANT* (*LOC111985236*), *QsPLT* (*LOC111983073*, *LOC111994212*), *QsSTM* (*LOC111993990*, *LOC112032307*), (Fig **8a**). In addition, genes involved in production of cell wall components for suberin (*QsFAR4, LOC112006016; QsASFT-2, LOC112001733; QsABCG16, LOC112008981*) and particularly lignin (*QsATCAD4*, *LOC112030041; QsCAD1, LOC112030209; QsCAD9, LOC112027513; QsCCoAOMT1, LOC111984638*) were also downregulated (Fig. **8b**).

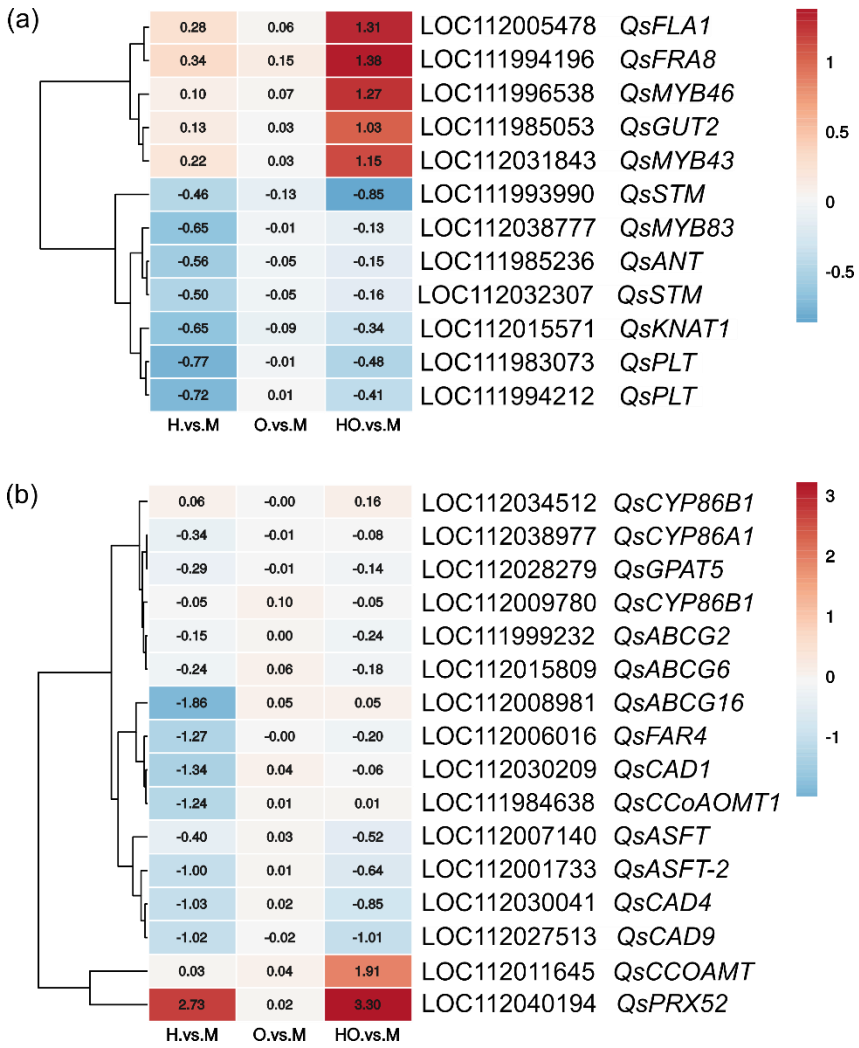

Fig. 8 *Heat map representing the expression profile (Log2FC) of genes involved in (a) secondary development and secondary cell wall formation and (b) suberin biosynthesis pathway, in response to Heat (H. vs M), Osmotic (O. vs M) and combined Heat and Osmotic (HO. vs M) treatments, in SD root zones*

In this treatment, downregulation of cell cycle/division candidate regulatory genes was detected (*LOC111991906, LOC112008724, LOC112028095, LOC112025658, LOC112021070, LOC112003699, LOC111983205, LOC112002890, LOC112025659*) (Fig. **S6b**). In the H+O treatment we detected the upregulation of genes involved in production and alteration of

secondary cell wall components (*QsFLA11,* LOC112005478; *QsFRA8,* LOC111994196; *QsGUT2*/*IRX10,* LOC111985053; *QsCCOAMT*, LOC112011645; *QsPRX52,* LOC112040194) (Fig. **8b**), as well as the TF regulators *QsMYB46* (LOC111996538) and *QsMYB63* (LOC112031843) (Fig. 8**a**). As found for the Heat treatment, the H+O treatment also imposed a negative effect in the expression of suberin biosynthesis genes, yet this pattern was not statistically significant, based on RNA-seq data (Fig. **8b**). Remarkably, genes related to the secondary development and cell wall precursors of lignin or/and suberin were not differentially expressed (following the filtering thresholds set for DEGs) at 24h of Osmotic treatment in the SD zone (Fig. **8**), despite the changes in relative expression pattern determined by qPCR (Fig. **3**, *QsASFT* and *QsABCG6*) and the observed increase in suberized cells observed after 1 week (Fig. **2**). Intriguingly, pectin modulation related transcripts are exclusively regulated in Osmotic sample. These include the Pectin lyase-like superfamily protein (LOC112029400, LOC112033999), Plant invertase/pectin methylesterase inhibitor superfamily (LOC111991575, LOC112003015) and Pectin acetylesterase family protein (LOC112020993) genes.

Gene expression profile of protein stability and stress responsive genes are affected by heat and osmotic stresses in SD root zone

Among the DEGs regulated by Heat treatment in the SD zone we found several upregulated genes related to protein stability, folding and activation (Fig. **S6a**). These included diverse HSP-like chaperones (e.g.: *QsHsp89-1, LOC112028495*; *QsHSP17.8, LOC112017952*; *QsHSP21, LOC112039029*), hsp interactors, (*hsp70-Hsp90 organizing protein 3-like - QsHOP3, LOC111986258; QsHsp70-binding protein 1, LOC112030881*), mitochondrial chaperonin *QsHSP60* (*LOC112017962*) and a heat shock factor *QsHSFB2B* (*LOC112016010*). Other HSPs and interactors were also upregulated in the SD root zone in response to H+O (*LOC112038351*; *QsTPR1, LOC112007582*; *QsBIP2, LOC112034582*; *QsBOB1,*

LOC112017996; QsHSP91, LOC112012050), chaperons (*QsCPN10, LOC112035803; QsCPN60BETA2, LOC112038662*) in addition to Endoplasmic-reticulum-associated protein degradation pathway genes (*LOC112018291; QsRBL15, LOC111994074; QsAtERDJ3B, LOC112034928; QsCNX1, LOC112039564*). In parallel, additional genes related to protein stability, folding and activation were downregulated in both Heat and H+O treatment, namely *QsHSP1* (LOC111990739) *QsHSP70 (*LOC112019500), *Qs*HSC70-1 (LOC112007355), *QsDJC66 (*LOC112037424), and *QsTPR4 (*LOC111996532). In response to Osmotic treatment, we detected a smaller number of DEG related to protein stability. *QsHSP21 (*LOC112008682), two HSP20-like chaperones (*QsHSP26.5,* LOC112036142; *QsHSP17.8,* LOC112025928) and two endomembrane-localized small HSP (LOC112015923 and *ATHSP22.0* - LOC112016302) were upregulated in SD zones, while a chaperone DnaJ-domain (*QsDJC66,* LOC112037424) was downregulated. All these genes followed a similar expression trend in Heat and combined H+O treatments, when compared to Mock.

Signalling and hormonal related pathways are altered in the SD root under stress

Multiple DEGs regulated by the applied treatments in the SD region were associated with known signalling and/or regulatory pathways. Considering phytohormones, regulation by GA stood out among the DEGs found in response to Heat treatment (Fig. **9a**). More particularly, GA-responsive TFs homologues of *SCARECROW-LIKE3* (*LOC112033247*), *QsMYB6* (*LOC111990468*) and *QsMYBH* (*LOC112029884*) were upregulated, while *QsGIS3* (LOC112034935), *QsGRF5* (LOC111985505), *QsMYB3/PC-MYB1* (LOC112011850), *QsTOPP4* (LOC112022537) and *QsTPR4* (LOC111996532) were downregulated. In parallel, the occurrence of auxin signalling is also suggested in response to Heat, through the downregulation of auxin transporters *QsABCB19* (LOC111998006),

QsPIN1 (LOC111993333) and *QsPIN5* (LOC112012573), as well as auxin-responsive genes *QsARF17*(LOC112025063), *QsFEZ (LOC112031616)*, and *QsMYB93* (LOC112030452) (Fig. **9b**). Considering the signalling pathways responsive in the Osmotic treatment, we mostly found upregulation of ABA-related genes. These include not only genes related to water deprivation response, such as *QsLTI65* (*LOC112001611*) and *QsHB-7* (*LOC112022148*, *LOC111987296*, *LOC111993269*), but also genes involved in the core cellular ABA signalling, namely the ABA biosynthesis gene *QsNCED3* (*LOC112006543*), PP2C-like genes *QsAHG1* (*LOC111987714*) and *QsHAI3* (*LOC112022545*), the negative feedback regulator *QsAITR5* (*LOC111992498*) and the *QsATAF1* (*LOC112035692*) TF. Remarkably, DEGs related to ABA response or signalling were also upregulated in combined H+O treatment (Fig. **9a**). In fact, some were also upregulated in the Osmotic treatment, namely *QsLTI65* (LOC112001611), *QsHB-7* (LOC111993269, LOC112022148) and *QsAHG1* (LOC111987714), as well as *QsAITR5* (LOC111992498) and *QsATAF1* (LOC112035692) TF. On the other hand, *QsCYP707A4* (LOC112011065), which is involved in ABA catabolism, is strongly upregulated in H+O (log2FC = 7.34) as well as in the Heat treatment (log2FC = 6.56) (Fig. **9a**).

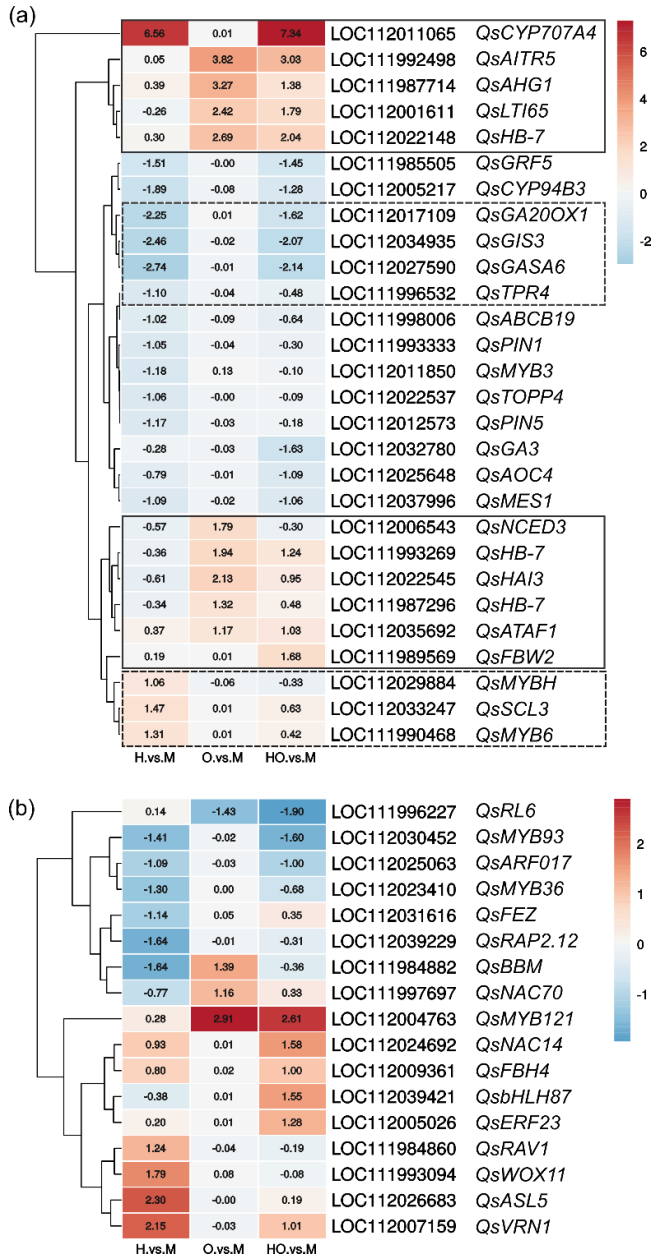

Fig. 9 Heat maps representing the expression profile (Log2FC) of genes involved in (a) hormone signalling and metabolism and (b) other representative TFs (b), in response to Heat (H. vs M), Osmotic (O. vs M) and combined Heat and Osmotic (HO. vs M) treatments, in SD root zones. Gibberellin and Abscisic acid related genes are highlighted in grey boxes, dashed and continuous line, respectively.

Moreover, the regulation of GA signalling is likely in combined H+O, given the downregulation of *QsGIS3* (*LOC112034935*), *QsGASA6* (*LOC112027590*), *QsGA2OX1* (*LOC112017109*) and *QsGA3* (*LOC112032780).* Combined H+O treatment as well as Heat alone also affected JA biosynthesis, with downregulation of the biosynthetic genes *QsAOC4* (*LOC112025648*), *QsCYP94B3* (*LOC112005217*) and *QsMES1* (*LOC112037996*).

5. Discussion

Heat and Osmotic treatments differentially affect cork oak root development and cell wall suberization

Several studies have shown that changes in cell-wall suberin deposition in roots can affect the way plants cope with stress (Schreiber *et al.*, 2005; Ginzberg *et al.*, 2009; Watanabe *et al.*, 2013; Kreszies *et al.*, 2020). For example, Kreszies *et al* reported that suberization response on barley, subjected to osmotic treatment, ranges from no changes to enhanced endodermal suberization of certain root zones and the formation of a suberized exodermis, which was not observed in the modern barley cultivars. In this chapter we aimed to characterize the development of cork oak roots under different abiotic treatments, including heat, osmotic and combined heat and osmotic stress, targeting general developmental changes, particularly in suberized barriers, namely endodermis and phellem. We previously found that cork oak taproots collected 8 DAS show a fully developed endodermis in addition to phellogen activity, immediately below endodermis (Chapter IV). Using cork oak roots at this stage we could further study the response to those stresses in two contrasting developmental zones of the root system (PD and SD). In the SD zone we analysed the effect of stresses on suberization of developing phellem cells. The PD zone was also targeted to assess changes in endodermis suberization and was also used to better discriminate the specific

transcriptomic changes occurring in response to stress between this zone and SD zone.

After the application of the different treatments, visual inspection of developed cork oak roots pointed for a prominent negative effect of Heat and combined H+O conditions in root growth and development (e.g. emergence of lateral roots), particularly 1 week after treatment. Conversely, Osmotic treatment showed no visual effect, displaying an overall morphology like Mock (Fig. **1**). Cell-wall suberization in the PD zone showed only little changes upon stress treatments. In fact, expression of selected candidate genes involved in synthesis of suberin monomers was not detected in this region after 24h of stress (Fig. **4**), being only detected 1 week after, in all conditions, including in Mock treatment. While this response could be related to root differentiation at this stage, this may be also a response to the mechanical stress imposed by the root contact with the bottom of the vessel, causing root bending phenotypes. We also found changes in gene expression in response to the stresses, including *QsGPAT5*, *QsASFT* and *QsABCG6*, which may suggest an increase in cell wall suberization. Yet, the FY staining of several root sections taken immediately above the PD region targeted for RNA extraction was not consistent with the previous assumption. This was mainly due to the variability found among replicates of the same treatment, with only some showing a fully suberized endodermis (Fig. **S3**). Also, the fact that the analysed area is a transition zone, where endodermis is undergoing maturation, justifies those minor differences in collection point will show different stages of endodermis maturation and suberization. Nonetheless, we previously showed in *Arabidopsis* that combined Heat and Osmotic treatment applied after SD initiation, has no significant effect on endodermis suberization in the PD zone (Chapter III). These results suggest that abiotic stress has a minor effect on suberization in PD zone when roots are undergoing SD. Yet, additional studies are required to

validate this hypothesis, particularly in what concerns effects on water movement.

When cell-wall suberization was assessed in the root SD zone, distinct effects were detected between the applied treatments. In the Heat treatment the number of suberized cells decreased when compared to mock, with mostly one layer/row of suberized cells clearly observed and identified as endodermis cells (Fig. **2**). Also, the transcription of specific suberin genes tend to decline immediately after 24h of Heat treatment initiation, being more pronounced after 1 week for *QsCYP68A1* (Fig. **3**). Together, these results indicate that suberization and particularly phellem development are delayed by Heat stress. In turn, Osmotic treatment was found to increase cell-wall suberization in SD zone. We demonstrated that this was not only due to the expression induction of suberin biosynthesis genes at 24h (Fig. **3**), but also by the suggested accumulation of suberized cells 1 week after treatment initiation (Fig. **2**). Osmotic or other drought-simulated conditions (e.g. ABA treatment) have been widely described as inducers of cell-wall suberization, in endodermis or in cells that normally do not suberize (Barberon *et al.*, 2016; Kreszies *et al.*, 2020). An accumulation of suberized cells in Osmotic treatment in cork oak roots may be a result of early suberization process of pre-determined phellem cells, as previously described for endodermis of *Arabidopsis* plants (Barberon *et al.*, 2016). Remarkably in our study we found that in cork oak Heat and Osmotic stress have distinct effects in phellem differentiation, especially regarding suberization. In particular the effect of heat in cork oak roots suberization was not at all expected, since a previous study targeting traumatic phellem formation in potato tubers revealed a higher number of phellem cells in heat treatments (Ginzberg *et al.*, 2009). The contrasting response observed in cork oak Heat treated roots may either reflect a different developmental reprogramming occurring in different organs (tuber *versus* root) or otherwise result from the observed Heat negative impact on taproot

development. Similarly, combined H+O treatment also decreased the number of suberized cells (Fig. **2**), which was also reflected on the downregulation of suberin related genes (Fig. **3**). This may reflect a predominant effect of Heat over the Osmotic stress. The application of combined Heat and Osmotic and its impact on cork oak root suberization actually shows similarities with cork development features described for *Q. suber* trunks. During late summer, when heat and drought are very likely to occur in combination, stem phellogen activity is described to slow down and produce less phellem cells (Costa *et al.*, 2002; Pereira, 2007). However, a direct correlation must be cautious, since roots and shoots are distinct organs, not necessarily sharing the same regulatory mechanisms. To help uncovering the molecular pathways underlying the treatment responses observed in taproot growth and cell-wall suberization, we performed a genome-wide transcriptomic analysis targeting SD and PD root zones (harvested 24h after treatment initiation). To particularly target processes related to SD, we focused on DEGs that were only identified (specific) in SD zone. Remarkably, the number of DEGs detected in SD zone was higher in Heat stress, and a hypothetical additive effect in response to combined Heat and Osmotic treatment was not observed. Still, Heat and combined treatments shared a greater proportion of DEGs (as compared to Osmotic treatment) (Fig. **6**).

Heat and H+O treatments induce GA signalling pathways

In the SD zone, the GA signalling pathway was particularly affected 24h after Heat treatment, with downregulation of genes involved in GA cellular homeostasis, regulation and signal transduction (e.g. *QsGA2OX1, QsGIS3*, *QsGASA6* and *QsTPR4*). Interestingly this molecular response was also detected in the combined Heat and Osmotic treatment (Fig. **9a**). GA is a regulator of secondary cell-wall formation (xylem fibers), in part by promoting the activity of *KNAT1*, a key regulator of multiple genes involved in secondary cell wall modifications and phenylpropanoid biosynthesis

(Felipo-Benavent *et al.*, 2018). Interestingly, a cork oak homolog of *KNAT1* was also downregulated in both Heat and combined Heat and Osmotic conditions, as observed for genes involved in secondary xylem development (phenylpropanoid and lignin biosynthesis genes). The downregulation of genes involved in GA metabolism, phenylpropanoid and lignin biosynthesis genes, agrees with a negative impact on secondary cell wall modifications through a GA-dependent mechanism in response to Heat and combined Heat and Osmotic conditions. Downregulation of suberin-related genes was also observed among the Heat and Heat and Osmotic treatments DEG, agreeing with the reduction of suberized cells in the SD zone (Fig. **2**)**.** Yet this was not evident in the RT-PCR study for suberin biosynthesis genes (Fig. **3**).

Interestingly, the key regulators of meristem and cell fate found highly expressed in SD (*versus* PD) in cork oak roots (Chapter IV), namely *QsPTL*, *QsSTM* and *QsANT*, showed a tendency for downregulation in Heat and combined Heat and Osmotic treatments (Fig. **8a**). Moreover, several cyclins were downregulated in these treatments (Fig. **S6b**), reinforcing the hypothesis of reduced cell divisions. Altogether, the molecular profile obtained for SD zones in response to Heat and combined Heat and osmotic support an overall negative impact of these treatments on secondary growth, highlighting candidate genes and pathways actively involved in cork oak root response.

ABA signalling controls cork oak SD in Osmotic stress

Application of the Osmotic treatment induced an upregulation of ABA related genes in the SD zone (Fig. **9a**), which was not evident in the PD root zone. In addition to homologues of well-known dehydration responsive genes (*QsLTI65*, *QsHB-7*) other core ABA-signalling genes were found positively regulated. The upregulation of PP2C (protein phosphatases) family members (*QsAHG1* and *QsHAI3*) are of particular interest, since these genes are part of a well-described signalling cascade in response to

drought described in *Arabidopsis* (Ali *et al.*, 2020). It has been reported that PYL (Pyrabactin resistance - ABA receptor)-PP2C-SnRK2-mediated ABA signalling cascade is involved in abiotic stress response (Fujita *et al.*, 2009, 2013; Kim, 2014; Vishwakarma *et al.*, 2017), and particularly PP2Cs are described to be upregulated in response to osmotic stress and ABA treatments (Saez *et al.*, 2004; Zhang *et al.*, 2017; He *et al.*, 2019; Lu *et al.*, 2019). A previous *in silico* analysis of cork oak DEGs in drought treatment revealed a the existence of a transcriptional regulatory network of ABA-responsive genes involving the PP2C-SnRK2-ABF in roots (Magalhães *et al.*, 2016), together with a strong activation of *LTI65*, which homologues (*RD29B*) are described to be induced through phosphorylation induced by ABA signalling (Uno *et al.*, 2000; Fujita *et al.*, 2005). Together with these previous studies, our results show the possible activation of this signalling cascade during osmotic stress in the SD zone of cork oak roots.

Notably, ABA is a fundamental hormone for suberization processes in diverse tissues, inducing the activation of numerous genes from the suberin pathway (Lee *et al.*, 2009; Boher *et al.*, 2013; Yadav *et al.*, 2014; Barberon *et al.*, 2016; Bjelica *et al.*, 2016). Although the specific ABA signalling cascade involved in this process is not yet described, *Arabidopsis* mutants of SnRK target genes (*ABF*s) have reduced expression of some suberin biosynthesis genes after ABA treatments, as compared to WT plant (Yoshida *et al.*, 2015). The higher expression of PYL ABA receptors (LOC111996210 and LOC112010415) and SnRKs homologues (LOC112039491, LOC112017767 and LOC112032862) in SD zone (*versus* PD), also suggested an association of ABA with secondary growth (Chapter IV). Thus, in cork ok roots subjected to Osmotic treatment, the observed increased number of suberized phellem cells and the upregulation of ABA mediated signalling cascade genes, suggests that phellem development and suberization maybe regulated through activation of ABA–PYL-PP2C-SnRK2-ABF cascade. In addition, ABA can also be

involved in the cell wall thickening, through the protein kinase SnRK2, which is recently describe to be also able to phosphorylate NST1, a master regulator in secondary cell wall formation and lignin deposition (Liu *et al.*, 2021).

Despite suberin transcripts are not differentially expressed upon osmotic treatment, another evidence points to cell wall modulation that we can speculate to be the cell wall preparation for the suberization. Suberin monomers are hypothesised to be connected to the primary cell wall through ester or ether bonds to its polysaccharide components. Interestingly, only the Osmotic treated cork oak roots, which also have increased levels of suberized cells, showed alterations in the expression pattern of pectin modulation genes. Together with the previous identification of these gene homologues in phellem specific translatome of Arabidopsis roots (chapter II), we suggest that the suberin molecule is connected to the primary cell wall through pectin molecules, and its modulation may be essential for the suberin deposition. Reinforcing this hypothesis is also the differences detected in the pectin of Arabidopsis roots exposed to the combination of osmotic and heat stress, where suberisation is also described to be induced (Chapter III).

Also, other TFs that are exclusively upregulated in Osmotic treatments in the SD zone, may also be interesting candidate regulators. It is the case of *QsBBM*, a *PLETHORA* (*PLT*) family member, downregulated in response to Heat and combined Heat and Osmotic treatments (Fig. **9b**). PLT factors are described as necessary in root apical meristem to maintain cell division and prevent cell differentiation (Aida *et al.*, 2004; Galinha *et al.*, 2007; Horstman *et al.*, 2014, 2017), and particularly BBM is pointed as a master regulator to maintain the root stem cell niche and as an upstream regulator of totipotency (Boutilier *et al.*, 2002; Galinha *et al.*, 2007; Passarinho *et al.*, 2008; Horstman *et al.*, 2017).

Together, the transcriptome results indicate that the Osmotic treated roots, in the SD zone, maybe at the initial stage of the molecular signalling for the suberization process to occur, justifying the increased detection of suberized cells, although not in a significant number, when compared with the reduction detected for the Heat and combined H+O treatments.

Although it is accepted that that PEG induced water stress, without toxic effects in plants, we considered important the further study of other drought induction strategies, as mannitol, or water withdraw, to strengthen the observed effects.

Antagonistic Regulation by ABA and GA signalling in Heat and Osmotic stress

The combined H+O also induced several ABA related genes in the SD zone of the taproots, similar to what was observed for the Osmotic treatment alone. However, in combined Heat ad Osmotic, we also identified a strong upregulation of *QsCYP707A4*, a gene putatively involved in ABA degradation (Kushiro *et al.*, 2004) (Fig. **9a**). Thus, we may speculate that during combined Heat and Osmotic treatment (as compared to Osmotic treatment) ABA levels are reduced due to the upregulation of QsCYP707A4, with impact on ABA mediated signalling responses. Contrastingly, other genes with putative role in cell wall formation and remodelling were upregulated in the combined Heat and Osmotic treatment (Fig. **8a**). More particularly, the upregulation of *QsFLA11*, which may impact cellulose synthesis and deposition (MacMillan *et al.*, 2010), as well as *QsFRA8* and *QsGUT2* that contribute for the biosynthesis of glucuronoxylan (Zhou *et al.*, 2005; Brown *et al.*, 2009; Wu *et al.*, 2009), may induce structural changes in the matrix of secondary cell walls that are formed in the SD zone throughout H+O treatment, being a distinct adaptation when compared to Heat or Osmotic treatments. Overall, despite some overlap in the transcriptomic profiles described for Heat and Osmotic

treatments, combined H+O treatment results in adaptive response not simply related to an additive effect of both stresses.

In summary, in this study, we verified that fully mature root zones from cork oak root may be particularly influenced by heat and osmotic stress through the balance between the GA and ABA signalling. Heat stress influences the root development in SD conceivably by downregulation of GA signalling, leading to an overall slowdown of secondary growth, particularly regarding phellem differentiation. Contrariwise, Osmotic treatment may induce ABA signalling cascades which could be associated with an accumulation of suberized phellem cells. Interestingly, despite the common downregulation of GA and upregulation of ABA, combined Heat and Osmotic treatment appears to affect the development in a particular way, by specific modulation of genes involved in secondary cell development that were not detected in the individual treatments. GA and ABA hormones have been described as antagonists in the mediation of several plant developmental processes as well as environmental threats (Urano *et al.*, 2017; Shu *et al.*, 2018; Liu & Hou, 2018). Particularly in secondary development, hormonal zonation contributes for tissue-specific developmental processes, with GA contributing for xylem development (Immanen *et al.*, 2016) and ABA described recently as putative regulator in phellem development (Lopes *et al.*, 2019; Chapter II). External stresses applied to cork oak seedlings appear to influence the balance and distribution of the antagonistic pair ABA and GA, leading to distinct cell differentiation and particularly secondary cell wall alterations in SD zone, depending on the applied stress. This work also provides a preliminary functional assessment of multiple cork oak genes regulated at specific developmental stages and in response to stress. The functional associations were mostly driven from knowledge available from model plants, and further work on this cork model may provide additional cues on species-specific regulation.

6. Acknowledgments

Ana Rita Leal performed this experimental work with the collaborations of Pedro Barros, Helena Sapeta, Joana Belo and Diogo Lucas. Pedro Barros, M. Margarida Oliveira and Tom Beckman helped to design and discuss the research experiments and results.

7. Bibliography

Aida M, Beis D, Heidstra R, Willemsen V, Blilou I, Galinha C, Nussaume L, Noh Y-S, Amasino R, Scheres B. **2004**. The PLETHORA Genes Mediate Patterning of the Arabidopsis Root Stem Cell Niche. *Cell* **119**: 109–120.

Ali A, Pardo JM, Yun DJ. **2020**. Desensitization of ABA-Signaling: The Swing From Activation to Degradation. *Frontiers in Plant Science* **11**: 1–7.

Almeida T, Pinto G, Correia B, Santos C. **2013**. QsMYB1 expression is modulated in response to heat and drought stresses and during plant recovery in Quercus suber. *Plant Physiology et Biochemistry* **73**: 274–281.

Andersen TG, Barberon M, Geldner N. **2015**. Suberization-the second life of an endodermal cell. *Current Opinion in Plant Biology* **28**: 9–15.

APCOR - Associação Portuguesa de Cortiça.

Barberon M. **2017**. The endodermis as a checkpoint for nutrients. *New Phytologist* **213**: 1604–1610.

Barberon M, Vermeer JEM, De Bellis D, Wang P, Naseer S, Andersen TG, Humbel BM, Nawrath C, Takano J, Salt DE, *et al.* 2016. Adaptation of Root Function by Nutrient-Induced Plasticity of Endodermal Differentiation. *Cell* **164**: 447–459.

Bindea G, Mlecnik B, Hackl H, Charoentong P, Tosolini M, Kirilovsky A, Fridman W-H, Pagès F, Trajanoski Z, Galon J. **2009**. ClueGO: a Cytoscape plug-in to decipher functionally grouped gene ontology and pathway annotation networks. *Bioinformatics* **25**: 1091–1093.

Bjelica A, Haggitt ML, Woolfson KN, Lee DPN, Makhzoum AB, Bernards MA. **2016**. Fatty acid ω-hydroxylases from Solanum tuberosum. *Plant Cell Reports* **35**: 2435–2448.

Boher P, Serra O, Soler M, Molinas M, Figueras M. **2013**. The potato suberin feruloyl transferase FHT which accumulates in the phellogen is induced by wounding and regulated by abscisic and salicylic acids. *Journal of Experimental Botany* **64**: 3225–3236.

Bolger AM, Lohse M, Usadel B. **2014**. Trimmomatic: a flexible trimmer for Illumina sequence data. *Bioinformatics* **30**: 2114–2120.

Boutilier K, Offringa R, Sharma VK, Kieft H, Ouellet T, Zhang L, Hattori J, Liu CM, Van Lammeren AAM, Miki BLA, *et al.* 2002. Ectopic expression of BABY BOOM triggers a conversion from vegetative to embryonic growth. *Plant Cell* **14**: 1737–1749.

Brown DM, Zhang Z, Stephens E, Dupree P, Turner SR. **2009**. Characterization of IRX10 and IRX10-like reveals an essential role in glucuronoxylan biosynthesis in Arabidopsis. *Plant Journal* **57**: 732–746.

Brundrett MC, Kendrick B, Peterson CA. **1991**. Efficient Lipid Staining in Plant Material with Sudan Red 7B or Fluoral Yellow 088 in Polyethylene Glycol-Glycerol. *Biotechnic & Histochemistry* **66**: 111–116.

Capote T, Barbosa P, Usié A, Ramos AM, Inácio V, Ordás R, Gonçalves S, Morais-Cecílio L. **2018**. ChIP-Seq reveals that QsMYB1 directly targets genes involved in lignin and suberin biosynthesis pathways in cork oak (Quercus suber). *BMC Plant Biology* **18**: 1–19.

Caritat A, Gutiérrez E, Molinas M. **2000**. Influence of weather on cork-ring width. : 893–900.

Costa A, Pereira H, Oliveira A. **2002**. Influence of climate on the seasonality of radial growth of cork oak during a cork production cycle. *Annals of Forest Science* **59**: 429–437.

Crang R, Lyons-Sobaski S, Wise R. **2018**. *Plant Anatomy*. Cham: Springer International Publishing.

Dobin A, Davis CA, Schlesinger F, Drenkow J, Zaleski C, Jha S, Batut P, Chaisson M, Gingeras TR. **2013**. STAR: ultrafast universal RNA-seq aligner. *Bioinformatics* **29**: 15–21.

Doblas VG, Geldner N, Barberon M. **2017**. The endodermis, a tightly controlled barrier for nutrients. *Current Opinion in Plant Biology* **39**: 136–143.

Efetova M, Zeier J, Riederer M, Lee CW, Stingl N, Mueller M, Hartung W, Hedrich R, Deeken R. **2007**. A central role of abscisic acid in drought stress protection of Agrobacterium-induced tumors on Arabidopsis. *Plant Physiology* **145**: 853–862.

Evert RF. **2006**. *Esau's Plant Anatomy*. Hoboken, NJ, USA: John Wiley & Sons, Inc.

Fakult M. **2020**. The Evolution of C4 Photosynthesis. : 341–370.

Felipo-Benavent A, Úrbez C, Blanco-Touriñán N, Serrano-Mislata A, Baumberger N, Achard P, Agustí J, Blázquez MA, Alabadí D. **2018**. Regulation of xylem fiber differentiation by gibberellins through DELLA-KNAT1 interaction. *Development* **145**: dev164962.

Franke R, Höfer R, Briesen I, Emsermann M, Efremova N, Yephremov A, Schreiber L. **2009**. The DAISY gene from Arabidopsis encodes a fatty acid elongase condensing enzyme involved in the biosynthesis of aliphatic suberin in roots and the chalaza-micropyle region of seeds. *Plant Journal* **57**: 80–95.

Fujita Y, Fujita M, Satoh R, Maruyama K, Parvez MM, Seki M, Hiratsu K, Ohme-Takagi M, Shinozaki K, Yamaguchi-Shinozaki K. **2005**. AREB1 is a transcription activator of novel ABRE-dependent ABA signaling that enhances drought stress tolerance in Arabidopsis. *Plant Cell* **17**: 3470–3488.

Fujita Y, Nakashima K, Yoshida T, Katagiri T, Kidokoro S, Kanamori N, Umezawa T, Fujita M, Maruyama K, Ishiyama K, *et al.* 2009. Three SnRK2 protein kinases are the main positive regulators of abscisic acid signaling in response to water stress in arabidopsis. *Plant and Cell Physiology* **50**: 2123–2132.

Fujita Y, Yoshida T, Yamaguchi-shinozaki K. **2013**. Pivotal role of the AREB / ABF-SnRK2 pathway in ABRE-mediated transcription in response to osmotic. : 15–27.

Galinha C, Hofhuis H, Luijten M, Willemsen V, Blilou I, Heidstra R, Scheres B. **2007**. PLETHORA proteins as dose-dependent master regulators of Arabidopsis root development. *Nature* **449**: 1053–1057.

Ginzberg I, Barel G, Ophir R, Tzin E, Tanami Z, Muddarangappa T, De Jong W, Fogelman E. **2009**. Transcriptomic profiling of heat-stress response in potato periderm. *Journal of Experimental Botany* **60**: 4411–4421.

Graça J. **2015**. Suberin: the biopolyester at the frontier of plants. *Frontiers in Chemistry* **3**: 1–11.

Han X, Mao L, Lu W, Wei X, Ying T, Luo Z. **2019**. Positive Regulation of the Transcription of AchnKCS by a bZIP Transcription Factor in Response to ABA-Stimulated Suberization of Kiwifruit. *Journal of Agricultural and Food Chemistry* **67**: 7390–7398.

He Z, Wu J, Sun X, Dai M. **2019**. The Maize Clade A PP2C Phosphatases play critical roles in multiple abiotic stress responses. *International Journal of Molecular Sciences* **20**.

Horstman A, Li M, Heidmann I, Weemen M, Chen B, Muino JM, Angenent GC, Boutiliera K. **2017**. The BABY BOOM transcription factor activates the LEC1-ABI3-FUS3-LEC2 network to induce somatic embryogenesis. *Plant Physiology* **175**: 848–857.

Horstman A, Willemsen V, Boutilier K, Heidstra R. **2014**. AINTEGUMENTA-LIKE proteins: Hubs in a plethora of networks. *Trends in Plant Science* **19**: 146–157.

Immanen J, Nieminen K, Smolander O-P, Kojima M, Alonso Serra J, Koskinen P, Zhang J, Elo A, Mähönen AP, Street N, *et al.* 2016. Cytokinin and Auxin Display Distinct but Interconnected Distribution and Signaling Profiles to Stimulate Cambial Activity. *Current Biology* **26**: 1990–1997.

Kim SY. **2014**. *Abscisic Acid: Metabolism, Transport and Signaling* (D-P Zhang, Ed.). Dordrecht: Springer Netherlands.

Kosma DK, Murmu J, Razeq FM, Santos P, Bourgault R, Molina I, Rowland O. **2014**. AtMYB41 activates ectopic suberin synthesis and assembly in multiple plant species and cell types. *Plant Journal* **80**: 216–229.

Kreszies T, Eggels S, Kreszies V, Osthoff A, Shellakkutti N, Baldauf JA, Zeisler-Diehl V V., Hochholdinger F, Ranathunge K, Schreiber L. **2020**. Seminal roots of wild and cultivated barley differentially respond to osmotic stress in gene expression, suberization, and hydraulic conductivity. *Plant, Cell & Environment* **43**: 344–357.

Kreszies T, Shellakkutti N, Osthoff A, Yu P, Baldauf JA, Zeisler-Diehl V V., Ranathunge K, Hochholdinger F, Schreiber L. **2019**. Osmotic stress enhances suberization of apoplastic barriers in barley seminal roots: analysis of chemical, transcriptomic and physiological responses. *New Phytologist* **221**: 180–194.

Kushiro T, Okamoto M, Nakabayashi K, Yamagishi K, Kitamura S, Asami T, Hirai N, Koshiba T, Kamiya Y, Nambara E. **2004**. The Arabidopsis cytochrome P450 CYP707A encodes ABA 8′-hydroxylases: Key enzymes in ABA catabolism. *EMBO Journal* **23**: 1647–1656.

Lauw A, Oliveira V, Lopes F, Pereira H. **2018**. Variation of cork quality for wine stoppers across the production regions in Portugal. *European Journal of Wood and Wood Products* **76**: 123–132.

Leal AR, Barros PM, Parizot B, Sapeta H, Nick V, Tonni Grube A, Tom B, Oliveira MM. **2020**. Phellem translational landscape throughout secondary development in Arabidopsis roots. *Chapter 2*: 3–29.

Lee SB, Jung SJ, Go YS, Kim HU, Kim JK, Cho HJ, Park OK, Suh MC. **2009**. Two Arabidopsis 3-ketoacyl CoA synthase genes, KCS20 and KCS2/DAISY, are functionally redundant in cuticular wax and root suberin biosynthesis, but differentially controlled by osmotic stress. *Plant Journal* **60**: 462–475.

Leide J, Hildebrandt U, Hartung W, Riederer M, Vogg G. **2012**. Abscisic acid mediates the formation of a suberized stem scar tissue in tomato fruits. *New Phytologist* **194**: 402–415.

Liu X, Hou X. **2018**. Antagonistic Regulation of ABA and GA in Metabolism and Signaling Pathways. *Frontiers in Plant Science* **9**.

Liu C, Yu H, Rao X, Li L, Dixon RA. **2021**. Abscisic acid regulates secondary cell-wall formation and lignin deposition in Arabidopsis thaliana through phosphorylation of NST1. *Proceedings of the National Academy of Sciences* **118**: e2010911118.

Lopes ST, Sobral D, Costa B, Perdiguero P, Chaves I, Costa A, Miguel CM. **2019**. Phellem versus xylem: genome-wide transcriptomic analysis reveals novel regulators of cork formation in cork oak. *Tree Physiology*: 1–39.

Lu T, Zhang G, Wang Y, He S, Sun L, Hao F. **2019**. Genome-wide characterization and expression analysis of PP2CA family members in response to ABA and osmotic stress in Gossypium. *PeerJ* **2019**: 1–24.

Lulai EC, Suttle JC, Pederson SM. **2008**. Regulatory involvement of abscisic acid in potato tuber wound-healing. *Journal of Experimental Botany* **59**: 1175–1186.

MacMillan CP, Mansfield SD, Stachurski ZH, Evans R, Southerton SG. **2010**. Fasciclin-like arabinogalactan proteins: Specialization for stem biomechanics and cell wall architecture in Arabidopsis and Eucalyptus. *Plant Journal* **62**: 689–703.

Magalhães AP, Verde N, Reis F, Martins I, Costa D, Lino-Neto T, Castro PH, Tavares RM, Azevedo H. **2016**. RNA-seq and gene network analysis uncover activation of an ABA-

dependent signalosome during the cork oak root response to drought. *Frontiers in Plant Science* **6**: 1–17.

Mertz R a, Brutnell TP. **2014**. Bundle sheath suberization in grass leaves: multiple barriers to characterization. *Journal of experimental botany* **65**: 3371–3380.

Oliveira V, Lauw A, Pereira H. **2016**. Sensitivity of cork growth to drought events: insights from a 24-year chronology. *Climatic Change* **137**: 261–274.

Passarinho P, Ketelaar T, Xing M, Van Arkel J, Maliepaard C, Hendriks MW, Joosen R, Lammers M, Herdies L, Den Boer B, *et al.* 2008. BABY BOOM target genes provide diverse entry points into cell proliferation and cell growth pathways. *Plant Molecular Biology* **68**: 225–237.

Pereira H. **2007**. *Cork: Biology, Production and Uses*. Elsevier.

Pereira H. **2013**. Variability of the Chemical Composition of Cork. **8**: 2246–2256.

Pereira H. **2016**. The Rationale behind Cork Properties : A Review of Structure and Chemistry.

Pereira H, Graça J, Baptista C. **1992**. The Effect of Growth Rate on the Structure and Compressive Properties of Cork. *IAWA Journal* **13**: 389–396.

Pfaffl MW. **2001**. A new mathematical model for relative quantification in real-time RT-PCR. *Nucleic acids research* **29**: 16–21.

R Foundation for Statistical Computing. 2018. *R: a Language and Environment for Statistical Computing.*

Ramos AM, Usié A, Barbosa P, Barros PM, Capote T, Chaves I, Simões F, Abreu I, Carrasquinho I, Faro C, *et al.* 2018. The draft genome sequence of cork oak. *Scientific Data* **5**: 1–12.

Reid KE, Olsson N, Schlosser J, Peng F, Lund ST. **2006**. An optimized grapevine RNA isolation procedure and statistical determination of reference genes for real-time RT-PCR during berry development. *BMC plant biology* **6**: 27.

Saez A, Apostolova N, Gonzalez-Guzman M, Gonzalez-Garcia MP, Nicolas C, Lorenzo O, Rodriguez PL. **2004**. Gain-of-function and loss-of-function phenotypes of the protein phosphatase 2C HAB1 reveal its role as a negative regulator of abscisic acid signalling. *Plant Journal* **37**: 354–369.

Schindelin J, Arganda-Carreras I, Frise E, Kaynig V, Longair M, Pietzsch T, Preibisch S, Rueden C, Saalfeld S, Schmid B, *et al.* 2012. Fiji: an open-source platform for biological-image analysis. *Nature Methods* **9**: 676–682.

Schreiber L, Franke R, Hartmann K-D, Ranathunge K, Steudle E. **2005**. The chemical composition of suberin in apoplastic barriers affects radial hydraulic conductivity differently in the roots of rice (Oryza sativa L. cv. IR64) and corn (Zea mays L. cv. Helix). *Journal of Experimental Botany* **56**: 1427–1436.

Shu K, Zhou W, Chen F, Luo X, Yang W. **2018**. Abscisic acid and gibberellins antagonistically mediate plant development and abiotic stress responses. *Frontiers in Plant Science* **9**: 1–8.

Silva SP, Sabino MA, Fernandes EM, Correlo VM, Boesel LF, Reis RL. **2005**. Cork: properties, capabilities and applications. *International Materials Reviews* **50**: 345–365.

Uno Y, Furihata T, Abe H, Yoshida R, Shinozaki K, Yamaguchi-Shinozaki K. **2000**. Arabidopsis basic leucine zipper transcription factors involved in an abscisic acid-dependent signal transduction pathway under drought and high-salinity conditions. *Proceedings of the National Academy of Sciences of the United States of America* **97**: 11632–11637.

Urano K, Maruyama K, Jikumaru Y, Kamiya Y, Yamaguchi-Shinozaki K, Shinozaki K. **2017**. Analysis of plant hormone profiles in response to moderate dehydration stress. *The Plant Journal* **90**: 17–36.

Vishwakarma K, Upadhyay N, Kumar N, Yadav G, Singh J, Mishra RK, Kumar V, Verma R, Upadhyay RG, Pandey M, *et al.* 2017. Abscisic acid signaling and abiotic stress tolerance in plants: A review on current knowledge and future prospects. *Frontiers in Plant Science* **8**: 1–12.

Watanabe K, Nishiuchi S, Kulichikhin K, Nakazono M. **2013**. Does suberin accumulation in plant roots contribute to waterlogging tolerance? *Frontiers in Plant Science* **4**: 1–7.

Wei X, Lu W, Mao L, Han X, Wei X, Zhao X, Xia M, Xu C. **2019**. ABF2 and MYB transcription factors dominate feruloyl transferase FHT gene involved in ABA-mediated wound suberization of kiwifruit. *Journal of Experimental Botany*.

Wei X, Mao L, Wei X, Xia M, Xu C. **2020**. MYB41, MYB107, and MYC2 promote ABA-mediated primary fatty alcohol accumulation via activation of AchnFAR in wound suberization in kiwifruit. *Horticulture Research* **7**: 1–10.

Wu AM, Rihouey C, Seveno M, Hörnblad E, Singh SK, Matsunaga T, Ishii T, Lerouge P, Marchant A. **2009**. The Arabidopsis IRX10 and IRX10-LIKE glycosyltransferases are critical for glucuronoxylan biosynthesis during secondary cell wall formation. *Plant Journal* **57**: 718–731.

Wunderling A, Ripper D, Barra-Jimenez A, Mahn S, Sajak K, Targem M Ben, Ragni L. **2018**. A molecular framework to study periderm formation in Arabidopsis. *New Phytologist* **219**: 216–229.

Yadav V, Molina I, Ranathunge K, Castillo IQ, Rothstein SJ, Reed JW. **2014**. ABCG Transporters Are Required for Suberin and Pollen Wall Extracellular Barriers in Arabidopsis. *The Plant Cell* **26**: 3569–3588.

Yoshida T, Fujita Y, Maruyama K, Mogami J, Todaka D, Shinozaki K, Yamaguchi-Shinozaki K. **2015**. Four Arabidopsis AREB/ABF transcription factors function predominantly in gene expression downstream of SnRK2 kinases in abscisic acid signalling in response to osmotic stress. *Plant, Cell and Environment* **38**: 35–49.

Zhang F, Wei Q, Shi J, Jin X, He Y, Zhang Y, Luo Q, Wang Y, Chang J, Yang G, *et al.* 2017. Brachypodium distachyon BdPP2CA6 interacts with BdPYLs and BdSnRK2 and positively regulates salt tolerance in transgenic Arabidopsis. *Frontiers in Plant Science* **8**: 1–15.

Zhou G, Nairn CJ, Wood-jones A, Richardson E a, Zhong R, Pen MJ. **2005**. Arabidopsis Fragile Fiber8 , Which Encodes a Putative Glucuronyltransferase , Is Essential for Normal Secondary Wall Synthesis. *Plant Cell* **17**: 3390–3408.

Zhu A, Ibrahim JG, Love MI. **2019**. Heavy-tailed prior distributions for sequence count data: removing the noise and preserving large differences (O Stegle, Ed.). *Bioinformatics* **35**: 2084–2092.

8. Supplementary information

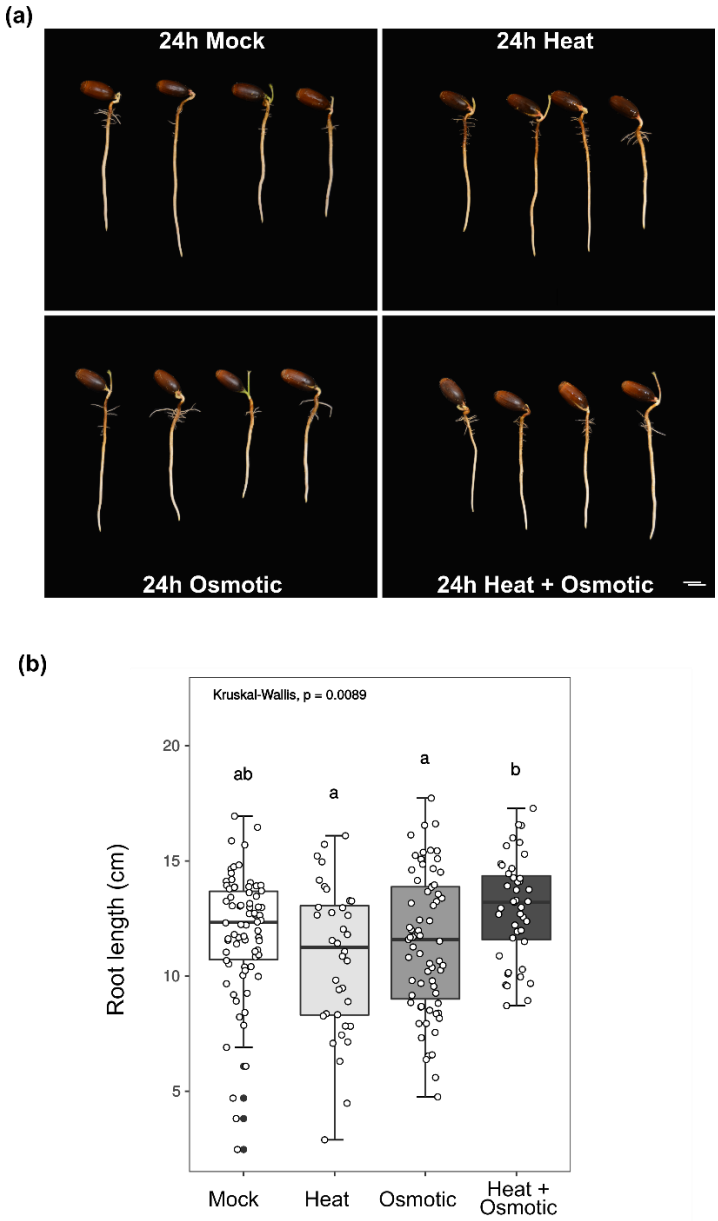

Fig. S1. *(a) Representative cork oak seedlings 24h after application of Mock, Heat, Osmotic and combined Heat and Osmotic treatments. Scale bar: 2cm. (b) Cork oak taproot length measured 24h after application of different treatments. Box plots represent length distribution for n > 20 roots (Mock: n=74; Heat: n=36; Osmotic: n=67; combined Heat ad Osmotic: n=43). Lower case letters represent statistical significance (p < 0.05) determined using Kruskal-Wallis test followed by Dunn's multiple comparison tes*

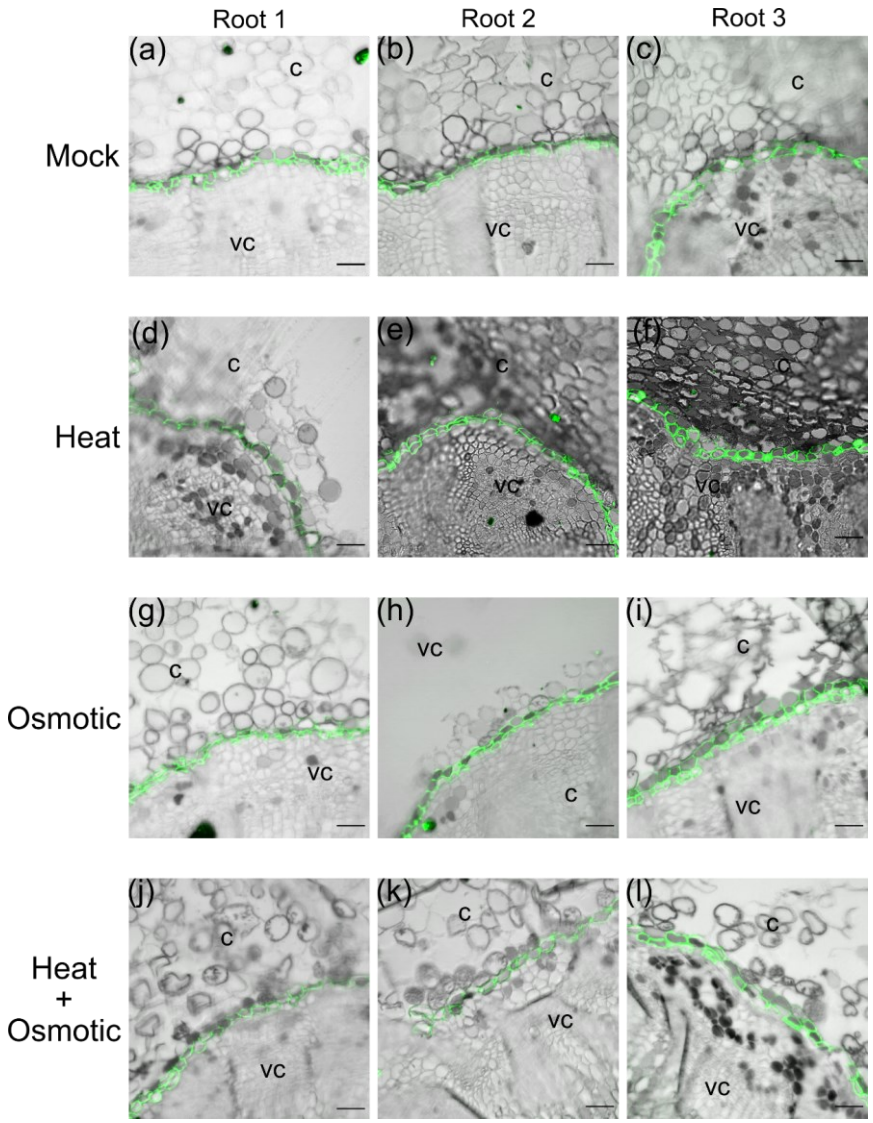

Fig. S2 *Cell-wall suberization in the SD root zones (1cm below root collar) from additional replicate cork oak seedlings, analysed one week after Mock (a-c), Heat (d-f), Osmotic (g-i) and combined Heat and Osmotic (j-l) treatment. Cross sections were stained with FY. Images of 3 independent roots from two independent experiments are represented. C: cortex; VC: vascular cylinder. Scale bar: 50 µm.*

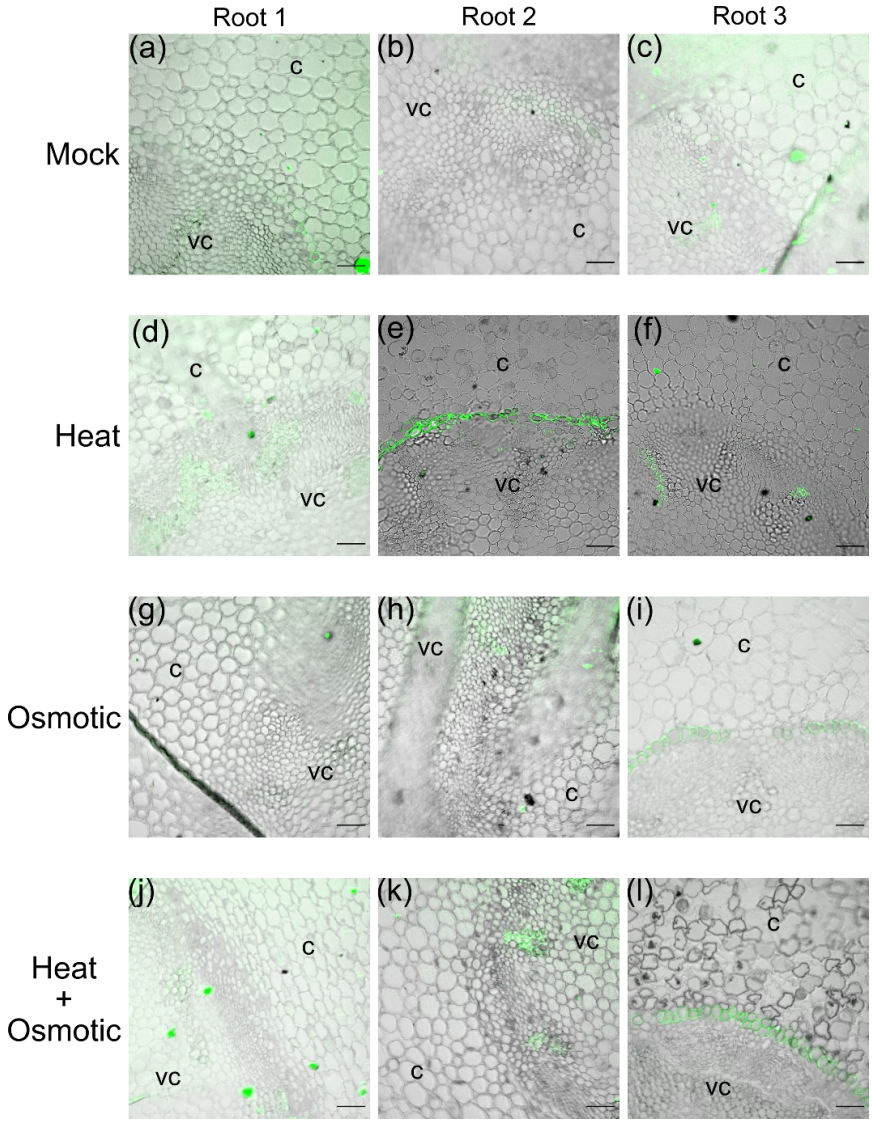

Fig. S3 *Cell-wall suberization in PD root zones (1cm above root tip) from additional replicate cork oak seedlings, analysed one week after Mock (a-c), Heat (d-f), Osmotic (g-i) and combined Heat and Osmotic (j-l) treatment. Cross sections were stained with FY. Images of 3 independent roots from two independent experiments are represented. C: cortex; VC: vascular cylinder. Scale bar: 50 µm.*

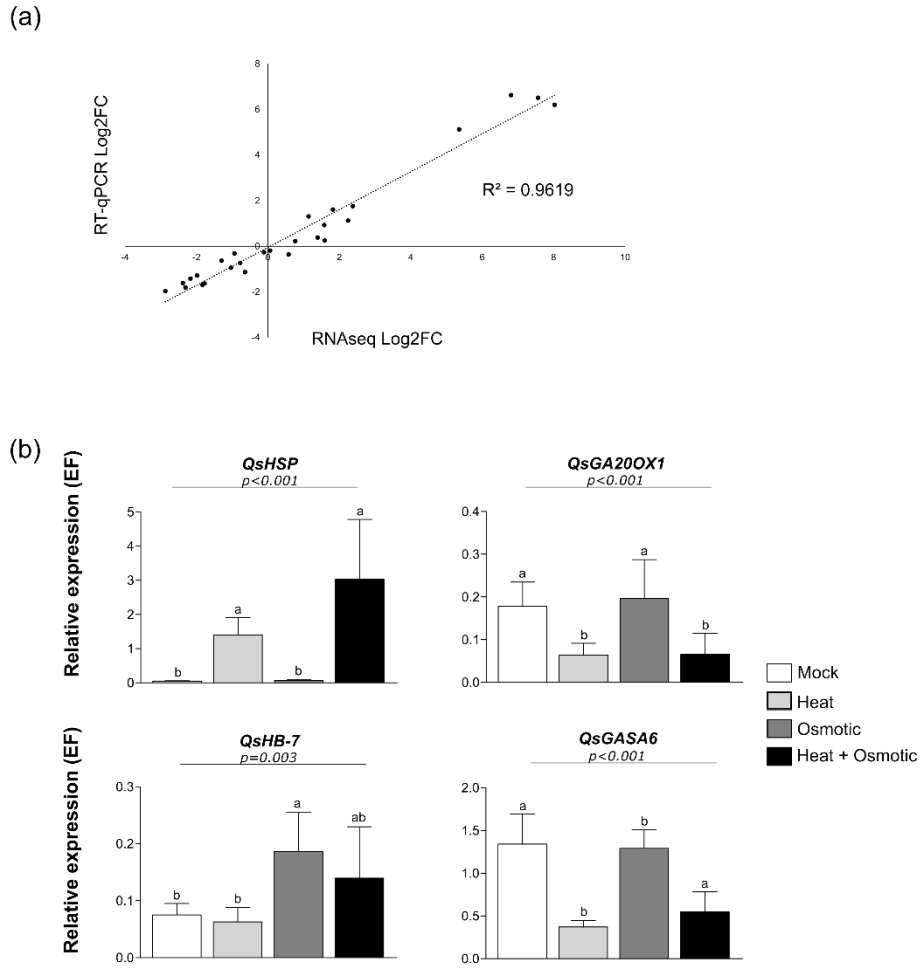

Fig. S4 *RNAseq expression validation by RT-qPCR. Correlation of RNAseq and RT-qPCR expression (Log2FC) of 9 genes (QsAcyl-T; QsBBM; QsCYP707A4; QsGA2OX1; QsGASA6; QsHAI; QsHB-7; QsHSP; QsNAC70, Table S1) with different expression patterns. (a) Relative expression of genes differentially regulated after 24h of stress application in the SD zone. (b) Representative expression profiles of QsHSP, QsHB7, QsGA2OX1 and QsGASA6 analysed by RT-qPCR (TableS1). Relative gene expression was determined using the QsEF as housekeeping gene. Mean expression ± standard deviation (n= 7) collected in two independent experiments is represented. Statistical significance between treatments for each timepoint was assessed using the ANOVA test. Different lower-case letters represent significant differences determined by Tukey's HSD test.*

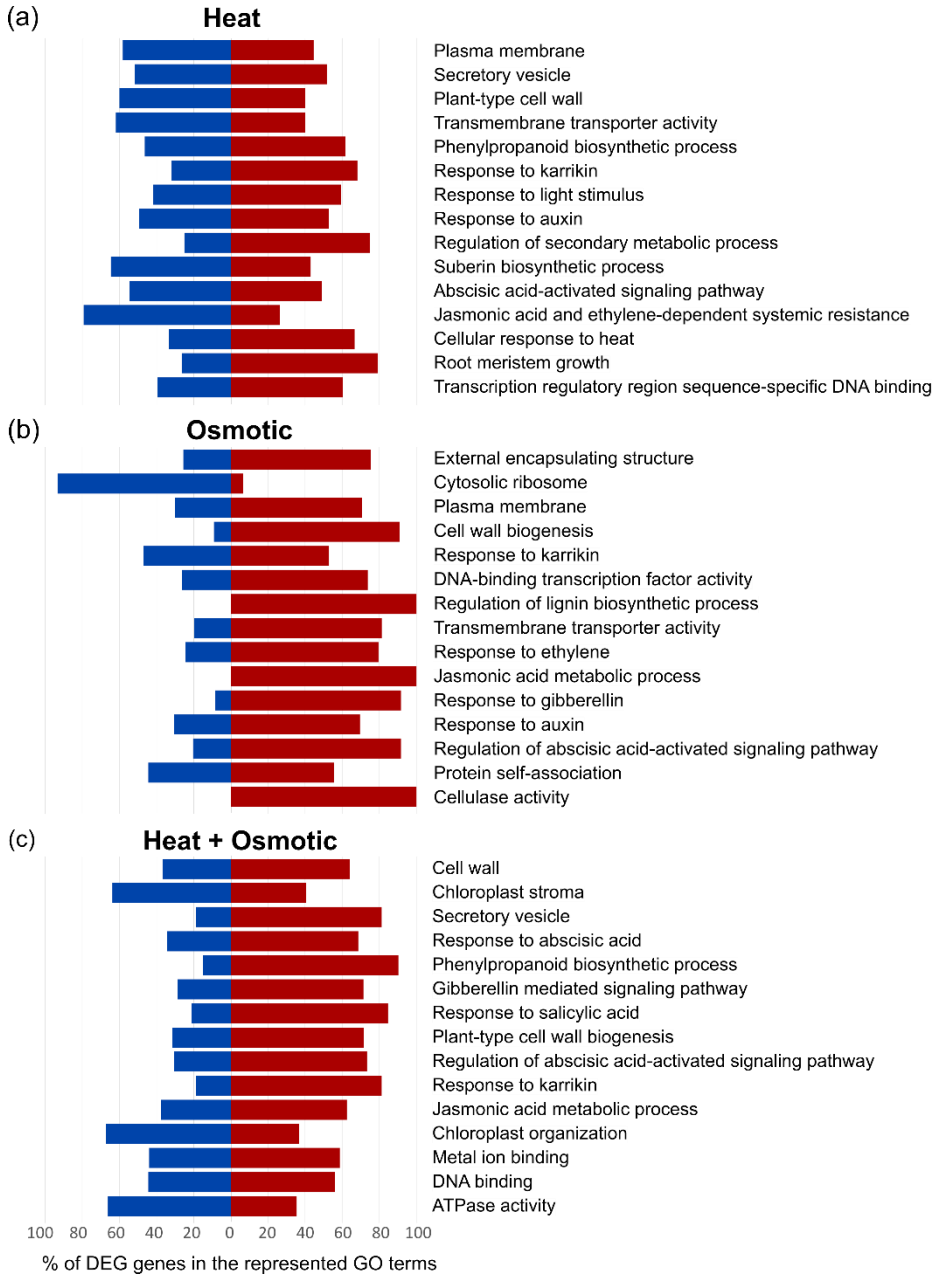

Fig. S5 *Representative GO terms significantly enriched in DEGs for PD zone of cork oak roots after 24h of Heat (a), Osmotic (b) and combined Heat and Osmotic (c) treatments. Coloured bars represent the percentage of upregulated (red) or downregulated (blue) genes enriched in each attributed GO term.*

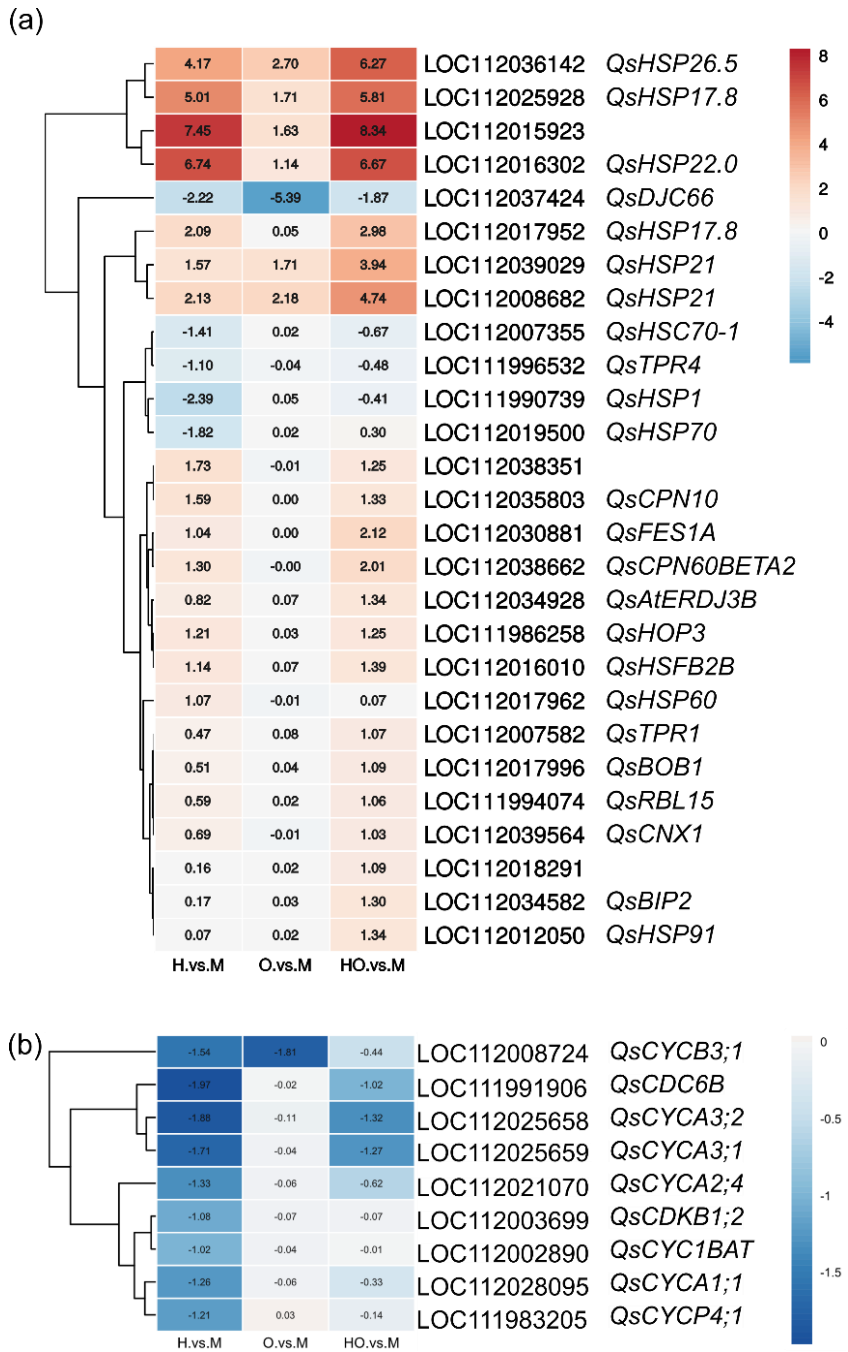

Fig. S6 *Heat map representing the expression profile (Log2FC) of HSP and Cyclins (b) transcripts in Heat (H. vs M), Osmotic (O. vs M) and combined Heat and Osmotic (HO. vs M) treatments in SD zone of cork oak roots.*

Supplemental tables are available by request to the corresponding authors or at:

https://drive.google.com/drive/folders/1ABrAUi7o5UmoANWPgWRaDLyciSfpympU?usp=sharing

Chapter VI

Conclusions and future perspectives

The periderm is a complex structure, organized in three specialized layers: phellogen, phelloderm, and phellem. The phellogen (or cork cambium), is the meristematic layer that dedifferentiates from parenchymatous cells during secondary development. Periderm development occurs through phellogen activity, producing phelloderm cells towards the inside, and phellem cells towards the outside. While phelloderm cells differentiate into parenchyma, phellem cells undergo several differentiation steps, which include cell wall suberization, cell expansion and programmed cell death. Differentiation and development of phellem cells are tightly controlled processes and despite the recent scientific contributions in the domain of plant secondary development, this process is still incompletely understood. This doctoral thesis investigated the development and molecular pattern of phellem ontology in *Arabidopsis thaliana* and *Quercus suber* roots. In addition, we studied how the initial phellem development, and particularly suberization, were affected by heat and osmotic stresses.

We first used specific markers for suberization to follow the phellem onset and development in *Arabidopsis* roots (Chapter II). Based on previous reports that show that secondary development of roots occurs in a gradient pattern, with a more developed region identified closer to the root collar, we have specifically targeted our observations to this root region. In this way we could, for the first time, define the phellem differentiation timeline. Combining the temporal study of suberin deposition, the expression analyses of the specific genes involved in the suberin biosynthetic pathway and morphological studies, we have demonstrated that phellem suberization is initiated at 8 DAG, when the morphological signs of secondary growth are already visible, for both vascular and cork cambium. We demonstrated that phellogen de-differentiates from pericycle cells, which, immediately after periclinal division start to suberize. The mapping of phellem suberization gradient

allowed us to strategically use a suberin biosynthesis marker to assist the sorting of an initial phellem-enriched translatome by TRAP-SEQ. The phellem-enriched specific translatome obtained in this process revealed that the molecular signature of phellem cells is organized in three main domains, namely synthesis and transport of cell wall components, response to stimulus and energy production. Apart from the expected players in phellem differentiation related to suberization, we could also identify new candidate transcripts for suberin monomer transport, such as oleosins and a caleosin, which were never associated with phellem or suberization. This evidence agrees with the hypothesis that suberin monomers are also transported in coated oil bodies. In parallel, in the functional enrichment analysis we found that response to ABA is the most remarkable term related to regulation, reinforcing the already suggested ABA involvement in phellem differentiation. Other interesting phellem-associated regulators are transcripts of *WOX2* and *WOX12*, with functions previously reported in development, and *MYB53*, that is phylogenetically close to other TFs previously described with suberin-related functions. Also noteworthy is the highly expressed phellem-associated *NAC19* that was previously reported in birch suberized phellem cells and in *Arabidopsis* when exposed to dehydration, ABA, or high-salinity conditions. Our network analysis further associated this TF with genes related to cell wall modifications, making it a strong candidate for regulation of cell wall differentiation along phellem development. Also in *Arabidopsis* roots, we found that the combination of heat and osmotic stress severely affected the general suberization pattern (Chapter III). In the stressed plants, a strong induction of the suberin marker *GPAT5*, together with increased suberin deposition were observed in cortex and in epidermal cells of lateral roots, where suberin is usually not found. Also, we detected in newly formed phellem cells, an increased expression of marker genes and enhanced suberin accumulation after imposed stress. The study of the

gene expression pattern of phellem-enriched transcripts, identified by TRAP-SEQ (Chapter II), in plants subjected to the combined heat and osmotic stress, could demonstrate the involvement of these genes in suberization process, not only in normal development of suberized tissues of phellem and/or endodermis, but also its possible contribution in the detected ectopic suberization response.

In parallel, we targeted the development and suberization process of cork oak roots (Chapter IV). Suberin staining in histological cross sections of the root, revealed the first suberized cells already at 8 DAS. Given the position of the first detected suberized cells surrounding the vascular cylinder, we considered these as endodermis cells. At this timepoint, anticlinal divisions were already visible in the layer surrounding the stele, underneath the suberized cell row, likely defining the onset of phellogen activity. Interestingly, the onset of secondary meristem activity in cork oak roots closely overlapped for both vascular and cork cambia (between 6 and 8 DAS). This contrasts with other plant models, where the vascular cambium is recognized to initiate earlier than the phellogen/cork cambium. At 8 DAS, we further performed a comparative transcriptomic analysis using distinct root segments of secondary and primary development, grown in control, osmotic and heat stress conditions. Independently of the treatment, the transcriptomic fingerprint of the two developmental selected zones showed differential expression of genes characterized as markers of primary and secondary development (e.g.: *QsSMB*, *QsFEZ*, *QsPLT2 and QsANT, QsCYCD3;1, QsPXY,* respectively). These results demonstrated the efficiency of the strategy selected to distinguish the molecular pathways typical of each developmental zone. Particularly in the secondary development zone, the transcriptome revealed enriched expression of genes known to be associated with active processes in phellem differentiation, including cell-wall modifications for lignification and suberization. In fact, cork

homologues found enriched in this zone were also identified in *Arabidopsis*, comprising mostly enzymes related to suberization (e.g.: *QsFAR4*, *QsGAPT5*), phenylpropanoid and lipid metabolism (e.g.: *QsLACS2*, *QsKCS2*, *QsCCoAMT*). Furthermore, multiple transcription factors, such as *MYB52*, *MYB39* and *WRKY43*, as well as numerous transcripts related to ABA response were also identified in our both plant models, namely in cork oak secondary development and in *Arabidopsis* phellem-enriched translatome. These results, together with previous reports on targeted transcriptomic studies on other phellem cells, indicate that the key mechanisms controlling phellem development must be conserved across species and organs. Nonetheless, further functional characterization of referred genes will be necessary for the direct association with the phellem cell fate.

When we carefully investigated putative alterations in phellem development and suberization in cork oak roots as result of single and combined heat and osmotic treatments (Chapter V), we found that the applied stresses induced contrasting effects. A positive effect of osmotic stress (over mock, heat, and combined stress) was detected by the upregulation of suberin biosynthesis genes, followed by the development of a higher number of suberized cells. In contrast, whenever heat was applied (independently or in combination with osmotic stress) a negative effect was observed on suberization. The transcriptomic analysis showed the upregulation of ABA biosynthesis, response and signaling genes in the osmotic treatment. These genes include, among others, dehydration responsive genes (*QsLTI65*, *QsHB-7*) and PP2C (protein phosphatases) family members (*QsAHG1* and *QsHAI3*). PP2Cs are part of a well-described signaling cascade together with the PYL ABA receptors and SnRKs homologues, which were also identified as enriched in the SD zone (versus PD) of cork oak roots (Chapter IV). In turn, whenever heat was applied, the QsCYP707A4, a

gene involved in ABA degradation, is upregulated. This allows the speculating that the ABA levels are reduced in response to heat, demonstrating the requirement of ABA on suberization during phellem differentiation. A detailed expression and functional analysis of the regulatory network involving ABA–PYL-PP2C-SnRK2 in SD is however necessary to prove the involvement of this hormone in phellem suberization.

Remarkably, when we investigated more broadly the cell wall alterations, through chemical (ATR-FTIR) and transcriptomic approaches, in both plant models and in control versus stress conditions, we found some elements that could explain how suberin molecules are connected to the primary cell wall. Suberin is covalently bound to the pectin, cellulose, or hemicellulose cell wall components. In our study, the Arabidopsis phellem-enriched translatome is particularly enriched in pectin modulation-related genes, including members of the Pectin lyase-like superfamily protein, the Plant invertase/pectin methylesterase inhibitor superfamily and the Pectinacetylesterase family protein genes. Also, the ATR-FTIR analysis on the Arabidopsis stress samples with increased suberization levels, revealed alterations particularly in spectrum regions attributed to pectin molecules. In addition, transcriptomic analysis of the osmotic SD zone of cork oak roots, which also have increased levels of suberized cells, showed alterations in the expression pattern of pectin related genes (gene homologues also identified in the Arabidopsis phellem translatome). Interestingly, these are not found for the heat and combined treatments of cork oak, where suberization levels are reduced. With the data obtained from the RNA seq analyses in both plant models, together with the results from ATR-FTIR in Arabidopsis stressed roots, we suggest that the main connection of suberin to the cell wall is made through pectin molecules and that the available connections can be controlled

by the methylation and acetylation status of these molecules, particularly in the stress situations. To further test the true involvement of the discussed pathways in the phellem suberization process it would be of high importance to test the function of the putative regulators ABI3, WOX2/12, NAC19, MYB53 and particularly of the signaling cascade ABA–PYL-PP2C-SnRK2. The use of commercially available Arabidopsis knock-out mutants/gain of function and overexpressing lines would be ideal to obtain a preliminary indication of the role of these regulators in the suberization process. Furthermore, making use of targeted induction of a knockdown at the onset of secondary development, we would be able to follow the effects specifically on phellem development by studying the general morphology of the newly formed phellem cells (regarding number and shape), as well as their suberization status. In parallel, with Chip-seq methodology applied to both plant models, we would be able to find possible interactors for the target regulators. This will not enlighten about the specific gene function but would give an idea of the possible interactors and precisely map the binding sites of the regulator. Currently, we are establishing cork oak hairy roots, in order to have a system to test the function and expression specificity of relevant genes identified from this and other studies.

In diverse studies, cork oak is still presented as a difficult plant model, with limitations in the use of acorns, because of the associated genetic variability and irregular germination, mainly associated with long-term storage. In our study we demonstrated that young taproots are a simpler, easier, and faster model to study phellem development in this species, as compared to trunks or shoots. However, the study of root phellem development in the stress situations, as presented here, should be regarded with care, as in nature these stress conditions are unlikely to occur during the cork oak acorn germination. In cork oak forests, acorns germinate at the beginning of winter, when soil is moister, and

temperatures are mild. However, we believe that this model is still more favorable as an agricultural tool, for initial and preliminary studies of cork development. An issue for the cork oak forest production in Portugal is the absence of a national breeding program. In fact, the only selection process in the cork oak amplification by seeds relies on the identified better producing cork oak trees (an identification sometimes empirical). This varies across regions and is highly variable due to open-pollination. With the increasingly available information of the molecular pathways active for phellem differentiation in cork oak, it would be interesting to use, as a tool for genotype selection, candidate genes specifically involved in this differentiation process and known to positively affect cork production and quality.

Despite the fact that the data generated within this project is still preliminary, we believe it may support science-based decisions on the implementation of new practices aiming to promote cork oak faster development, while optimizing water input and ensuring cork quality and properties.

Ana Rita Leal

MSc Biochemistry

https://orcid.org/0000-0001-6608-7661

Work experience	
October 2020 to present	**Oenology laboratory manager assistant** - Barão de Vilar Vinhos S.A., Vila Nova de Gaia Main responsibilities: - Management and coordination of company laboratories; - Analytical management of oenology projects; - Quality control of production processes.
June 2015 to present	**PhD student** - Plant Functional Genomic Lab, Instituto de Tecnologia Química e Biológica António Xavier (ITQB-NOVA), Universidade Nova de Lisboa - Root Development Group, Flemish Institute of Biotechnology, Plant Systems Biology Department (PSB), Ghent University Supervision: **Prof. Dr. Margarida Oliveira** (ITQB) and **Prof. Dr. Tom Beeckman** (PSB) Main developed techniques and methodologies: **- Drought and heat treatments** for *A. thaliana* (in vitro) and *Q. suber* (in soil); **- Histologic evaluation** of roots using microscopy - **DIC, fluorescence, confocal and transmission electron microscopy**; **- Real-time RT-PCR**; **- RNA purification by Translating Ribosome Affinity Purification (TRAP)**; **- RNA-seq data analysis** using the GALAXY platform. - Suberin composition analysis thought **FT-IR**
2013 to 2015	**Research project fellow** Plant Functional Genomic Lab, ITQB-NOVA

	Supervision: **Prof. Dr. Margarida Oliveira** Main developed techniques and methodologies: **- Real-time RT-PCR;** **-Yeast-one-hybrid**. Involved in the workflow are techniques of **gene amplification** and **cloning**, **bacteria and yeast transformation,** growth and selection
2011 to 2013 2009 to 2011	**Research project fellow** **MSc internship** Molecular and Microbial Biotechnology Group, Center for Neuroscience and Cell Biology, Biocant Park, Universidade de Coimbra Supervision: **Dr. Isaura Simões** Main developed techniques and methodologies: **- Heterologous expression of enzymes**. Involved in the workflow are techniques of **gene amplification** and **cloning**, **bacteria transformation,** growth and selection. **- Purification of recombinant enzymes** throughout diverse **chromatography** steps and evaluation of purification yields by **SDS-PAGE** and **Immunoblotting**. - Characterization of **enzymatic specificity** with a proteome-derived specific technique, **PICS - proteomic identification of protease cleavage site**.
Other courses	- Research Skills Development, NOVA Escola Doutoral, Lisboa, Portugal (2018) - Introduction to the analysis of NGS data workshop, VIB, Belgium (2018) - RNA-seq analysis for differential expression workshop, VIB, Belgium (2018) - II Quantitative Fluorescence Microscopy, CNC, Coimbra, Portugal (2016)
Education	
2009 - 2011 2006 - 2009	**Master in Biochemistry** **Bachelor in Biochemistry** Faculdade de Ciências e Tecnologia da Universidade de Coimbra

Publications	
In preparation	**Leal AR**, Barros P, Parizot B, Sapeta H, Vangheluwe N, Andersen TG, Beeckman T & Oliveira MM. (2019) Phellem translational landscape throughout secondary development in *Arabidopsis* roots. *BioRxiv*. DOI: 10.1101/2021.02.08.429142 **(Accepted with minor revisions in *The Plant Journal*)**
Peer-review	**Leal AR,** Sapeta H, Belo J, Beeckman T, Oliveira MM & Barros P (2021) Spatiotemporal development of suberized barriers in cork oak taproots. **(Accepted with minor revisions in *Tree Physiology*)**
	Leal AR, Cruz R, Bur D, Huesgen PF, Faro R, Manadas B, Wlodawer A, Faro C, Simões I. (2016) Enzymatic properties, evidence for in vivo expression, and intracellular localization of shewasin D, the pepsin homolog from Shewanella denitrificans. Scientific Reports. DOI: 10.1038/srep23869
Oral Presentations	**Leal AR**, Vieira N, Reis F, Hardoim PR, Barros PM, Coelho AC, Tavares RM, Lino-Neto T, Lourenço T, Ramalho JC, Dias MC, Saibo N, Oliveira MM, (2015) Searching for cork oak genes involved in the crosstalk between different stresses -the O3FAD –omega 3 fatty acid desnaturase. FV2015, Toledo, Spain, 14th-17th June
Poster	Sapeta H, Barros P, Lucas D, Belo J, **Leal AR** & Oliveira MM. (2021) Impact of different irrigation regimes on the regulation of suberin synthesis and cork development. Plant Biology Europe, Online, 28th June- 1st July
	Barros P, **Leal AR,** Sapeta H, Parizot B, Belo J, Vangheluwe N, Beeckman T & Oliveira MM. (2021) Conserved regulatory networks acting during phellem development in Arabidopsis and cork oak roots. Plant Biology Europe, Online, 28th June- 1st July. **Selected for Extended Elevator Pitch**
	Barros P, **Leal AR**, Belo J, Pais J, Silva Pereira C, Beeckman T, & Oliveira MM. (2019) Decoding the role

of drought and heat stress in cork oak peridermis suberization. IUFRO Tree Biotechnology, North Carolina State University, USA, 24th-28th June, 2019

Leal, AR, Barros P, Parizot B, Belo J, Vangheluwe N, Beeckman T & Oliveira MM. (2019) Revealing the mechanisms underlying peridermis suberization in Arabidopsis and Cork Oak. At the Forefront of Plant Research, Barcelona, Spain, 6th-8th May

Leal AR, Barros P, Parizot B, Belo J, Vangheluwe N, Beeckman T & Oliveira MM. (2019) Understanding the Molecular Regulation of Periderm Suberization in Root Secondary Growth. PADiBa 2019, Bonn, Germany, 28th-30th August. **Best poster presentation award**

ITQB NOVA, Avenida da República, 2780-157 Oeiras, Portugal | Tel +351 214 469 100 | itqb.unl.pt